CHEMICAL REVIEWS

REVIEW

pubs.acs.org/CR

Metal−Organic Frameworks for Separations

Jian-Rong Li, Julian Sculley, and Hong-Cai Zhou*

Department of Chemistry, Texas A&M University, P.O. Box 30012, College Station, Texas 77842-3012, United States

CONTENTS

1. INTRODUCTION

Over the last at least three decades, the science of porous solid materials has become one of the most intense areas of study for chemists, physicists, and materials scientists. These materials have found a large number of applications in many fields, such as adsorption, separation and purification, as well as catalysis.[1,2] Porous solids acting as adsorbents or membrane fillers are playing key roles in separations and purifications of various chemicals that we encounter in our daily activities, directly or indirectly. Explorations of advanced porous materials for these applications are therefore an intense subject of scientific research. Metal−organic frameworks (MOFs), a new class of porous solid materials, emerged approximately two decades ago and have since quickly developed into a fruitful research field.[3−7] Exploring their performances for applications in separations and

Special Issue: 2012 Metal-Organic Frameworks

Received: May 30, 2011
Published: October 06, 2011

purifications is attracting intense interest of researchers working in the fields of chemistry, chemical engineering, materials science, and others. Despite being in its infancy, the research progress in this subject has already shown that MOFs are promising for separation applications.

1.1. General Background on MOFs

MOFs are organic−inorganic hybrid solids with infinite, uniform framework structures built from organic linkers and inorganic metal (or metal-containing cluster) nodes (Figure 1).[3,4,8,9] Because of the lack of a generally accepted definition during the development of this new type of hybrid material, several other parallel appellations have appeared and are being used. Among them, porous coordination polymer (PCP)[10] seems to have been the most widely adopted, followed by porous coordination network (PCN).[11] Others include MCP (microporous coordination polymer),[12] ZMOF (zeolite-like metal−organic framework),[13] ZIF (zeolitic imidazolate framework),[14] MPF (metal peptide framework),[15] MAF (metal azolate frameworks),[16] *meso*MOF (mesoporous metal−organic framework),[17] and bio-MOF or MBioF (metal−biomolecule framework).[18,19] On the other hand, following the tradition of zeolite science, some researchers have also used an acronym of the laboratory in which the material was prepared to name their materials, as for example in the series of MILs (matériauxs de l'Institut Lavoisier),[20] HKUST (Hong-Kong University of Science and Technology),[21] ITQMOF (Instituto de Tecnología Química metal organic framework),[22] SNU (Seoul National University),[23] JUC (Jilin University China),[24] CUK (Cambridge University−KRICT),[25] POST (Pohang University of Science and Technology),[26] and so on. Certainly, using the empirical formula of the material expressing metal, ligands, and their stoichiometry is always popular and used in almost all published papers. In addition, based on the structure of a MOF's net, O'Keeffe and co-workers[27,28] proposed a systematic terminology to classify the known structures. A three-letter symbol, such as "dia", "cub", etc., or its extension ("pcu-a", "cub-d", etc.) has been used to identify a three-dimensional (3D) MOF network with a given geometrical linkage topology. This approach can thus aid in the description and understanding of structures, as well as provide a blueprint for the design of new materials.[29]

Despite some varying opinions, it is generally accepted that the work of Hoskins and Robson[30] reported in 1990, where they introduced a "design" flavor to the construction of 3D MOFs using organic molecular building blocks (ligands) and metal ions, symbolizes a new chapter in the studying of MOFs. After about 10 years, two milestone MOFs, MOF-5 ($Zn_4O(bdc)_3$, bdc = 1,4-benzenedicarboxylate)[31] and HKUST-1 ($Cu_3(btc)_2$, btc = 1,3,5-benzenetricarboxylate)[21] further promoted the development of this field, mainly due to their robust porosity. Shortly thereafter, another representative MOF, MIL-101 ($Cr_3OF(bdc)_3$),[20] with high stability emerged. It is clear that in this decade the rapid development of this field was mainly promoted by the observation of various exciting properties and the promise of potential applications of this type of porous solid materials. Furthermore, the structural flexibility of dynamic MOFs combined with several other unique characteristics has added to the allure of the field, distinguishing them from traditional porous solids.[32,33] It should also be pointed out that MOFs, as porous materials, possess by far the highest surface areas per gram known to date.[34] As a nascent field, the complexity in composition and structures of MOFs is continually increasing, and novel applications are continuously being explored.[35]

1.1.1. From Traditional Porous Solid Materials to MOFs.

Porous materials encompass a very broad range from natural to synthetic, from inorganic to organic, and from crystalline to amorphous. However, until the mid-1990s, only two types of porous solid materials, inorganic and carbon-based materials, were being widely applied in industry. Among porous inorganic solids, the quintessential example is zeolites, a class of crystalline aluminosilicates with interconnected pores of 4−13 Å.[36] In fact, a major part of the global economy currently relies on the use of zeolites in many industrial processes, which reflects the importance of such porous materials in daily life. Activated carbons are amorphous. As compared to zeolites, despite not having uniform structures, activated carbons have higher porosity and specific surface area and occupy a large share of the porous solids market.[37]

Figure 1 presents the general classifications of porous solids (emphasizing MOFs as a type of new organic−inorganic hybrid solid), together with a typical procedure for the construction of MOFs. One of the most significant research motivations for MOFs comes from their porosity, which places them in a new class of porous solid materials with properties often far beyond traditional porous materials. By taking advantage of their regularity, rigidity/flexibility, variety, and designability in both structure and properties, MOFs are being regarded as advanced porous materials capable of reaching or surpassing a number of current technologies. As compared to traditional inorganic porous solids and activated carbon, the number of possibilities of combining inorganic and organic moieties to yield a porous material is staggering and is indeed reflected by the prodigious number of papers on this type of compounds in the last 20 years. Besides adsorption-based properties,[38,39] combining the properties of both inorganic and organic components, MOFs can also display a lot of other unique properties and be useful in areas such as magnetism[40−43] and luminescence.[44]

The crystalline nature of MOFs allows their structures to be easily characterized by single-crystal X-ray diffraction. The associated structural regularity also allows for easy exploration of the relationship between structure and various properties, which in turn may guide the design and synthesis of new, improved MOFs. In fact, a number of adsorption phenomena are directly determined by the regular pore size distribution in a MOF.[45] Molecules confined in a uniform restricted space also afford unique properties that are not realized in the bulk state.[46] Thus, the uniform pore space can be exploited as a molecular reactor to conduct reactions or stabilize reaction intermediates.[47,48]

To some extent, MOFs have a higher degree of designability and adjustability in their structures and functions, when compared to other porous solid materials such as zeolites. This can be attributed to, at least in concept, (a) the synthesis of MOFs is usually carried out at mild conditions, which means that the synthetic conditions are easily controlled; (b) organic ligands can be easily designed and modified using the power of organic synthesis; (c) due to the fixed coordination geometries of both organic ligands and metal ions a certain combination of rigid organic and inorganic building units always produce a specific framework; (d) within a narrow definition of MOFs, using the reticular synthesis approach,[49] researchers can tune the structures and properties of MOFs without changing the connectivity or topology through presynthesis design of ligands, SBUs, and synthetic conditions; and (e) MOFs can be modified at the metal nodes or the organic linker after synthesis.[50−52]

The frameworks of MOFs can be rigid or flexible/dynamic when exposed to certain stimuli. Rigid frameworks are common and have properties similar to most conventional inorganic

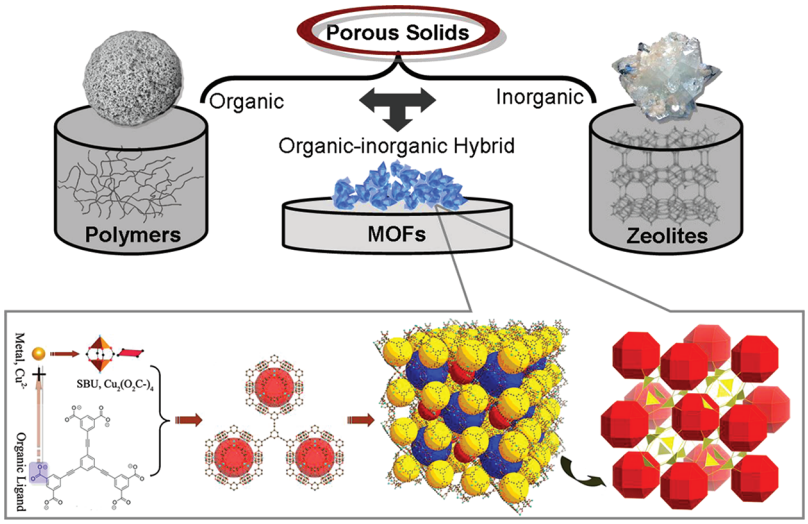

Figure 1. Schematic representations of the general classification of porous solids (top, an example is given in each case: polymers for porous organic solids; zeolites for porous inorganic solids; and MOFs for porous organic−inorganic hybrid solids) and a typical construction procedure of a MOF (bottom).

porous solids, such as zeolites. However, flexible/dynamic frameworks are unique to MOFs and quite interesting due to their uncommon behaviors, especially with regard to adsorptions.[32,33,53−56] Typically, dynamic structural transformations of flexible MOFs take place when guest molecules are removed or readsorbed, while the integrity of the framework is retained during the process. Related to this Review's focus, the structural flexibility of some MOFs can induce highly selective guest adsorption, therefore showing outstanding separation performances, which may be difficult to attain with a rigid porous material.[57]

1.1.2. Design, Synthesis, and Potential Applications of MOFs. The "design" of MOFs has been somewhat controversial, and it is difficult to determine whether or not a final MOF product was rationally designed.[58] Generally and conceptually, based on the fact that MOFs are self-assembled from organic ligands and metal-containing nodes through directional coordination bonds, the shape and/or linkage geometries of both components could be used to predict the formation a desired product.[59] This concept was emphasized in the early stages of this research field. R. Robson and others applied the "node and spacer" approach to generate coordination polymers, where single metal ions usually have a fixed coordination geometry when linked to ligands by a typical coordination bond, and the rigid bridging ligands also offer fixed shapes and linkage geometries.[60] Although, based on this approach the formation of a simple MOF seems to be predictable or controllable to a certain extent, for instance, a diamondoid net can be constructed through the judicious selection of a tetrahedral metal ion (or cluster) and a linear bridging ligand,[30] in reality, it is harder to implement the on-paper design, especially when extending it to more complicated cases (for example, interpenetrated isomers). The debate over whether or not design exists is an ongoing one, and one that becomes particularly complicated in the realm of hybrid solids,[61] materials that encompass mixtures of organic and inorganic moieties in a much broader context (MOFs are only a subcategory). Simply speaking, during the synthesis of MOFs, typically under solvothermal conditions, the formation of desired inorganic clusters (or retaining a single metal ion) is not always controllable. Even in the simple case of a single metal ion acting as node, different coordination geometries and coordination linkages are possible, thus making structure prediction difficult; the effects of solvent molecules must also be considered, as they can sometimes take part in the construction of a MOF.[62] Currently, we refer to MOFs in a narrow sense of materials, which are constructed by linking polyatomic metal-containing clusters (assuming their formations are controllable during synthesis), acting as secondary building units (SBUs), through rigid organic entities through strong covalent bonds; design in this sense seems entirely feasible.[63] Although some metal-based SBUs have been serendipitously "designed", once the synthesis of an SBU is established, it is highly possible to reproduce it in combination with new, similar linkers. This "design" by reticular synthesis, proposed by Yaghi and colleagues, has helped the development of the MOF field and promoted systematic investigation of similar frameworks, which have allowed researchers to carefully investigate the effects of structural modifications on various properties of MOFs.[49] By using this method, again at least in concept, the design and synthesis of a target framework, with specific geometric requirements, can be implemented under precisely controlled synthetic conditions (primarily regarding the SBU formation) and using predesigned ligands with fixed linking geometries. "Design" could also be understood as the capability of researchers to design experiments to produce MOFs of predetermined structural topologies and pore properties, as argued by O'Keeffe,[63] or by designing organic ligands that will result in the construction of the anticipated MOF.[64] On the other hand, in the broader sense of science as a whole, "design" exists everywhere and may hopefully also be admitted to the MOF field.

MOFs are usually synthesized via one-pot self-assembly reactions between ligands and metal salts in solutions between room temperature and 250 °C. Crystalline products, in particular single crystals large enough for single-crystal diffraction, are always desired in MOF synthesis. At near room temperature, the slow evaporation of solvents of a reaction solution or slow diffusion of solvent/solution to control the reaction rate and promote single crystals growth is often adopted. At higher temperature and pressures, generally termed solvothermal approach, reaction times are usually reduced, but single crystalline products are still

dx.doi.org/10.1021/cr200190s |*Chem. Rev.* 2012, 112, 869–932

observed. In these reactions, the resulting products may be more complicated and diverse as compared to those pursued at room temperature. Controlling the reaction rate, by for example adjusting the pH value of the reaction solution, is always important to obtain high-quality crystalline products, and drive the formation of a kinetic over thermodynamic product, although this last area remains largely unstudied. For particularly quick synthesis, microwave-assisted MOF growth has been adopted and has clearly presented several advantages as compared to other synthetic methods.[65] Besides generally used solvents, ionic liquids, usually acting as both solvent and template in the formation of products, also have been used in the synthesis of MOFs; this has been termed ionothermal synthesis of MOFs.[66] In addition, solvent-free synthesis (or green synthesis), which can reduce environmental contamination and potentially be more convenient than using solvent-based synthesis, has also been exploited in the synthesis of MOFs.[67] Apart from the one-pot reactions, a stepwise approach, with a higher level of controllability and construction complexity, by using metal−organic polyhedra (MOPs) as supermolecular building blocks, has also been developed, recently.[59,68,69] A further area of interest is the synthesis of nanoscale MOFs, which have shown some unique properties and functions.[70,71] It should also be pointed out that high-throughput synthesis of MOFs is picking up momentum and aiding in the discovery of new porous materials.[72−74]

Obtaining phase pure products is another noticeable concern in the preparation of MOFs, because structural determination and full characterization require a single polymorph. This is in some cases not easy; for example, frameworks with varying degrees of interpenetration are often difficult to isolate from each other. Furthermore, to reach the full potential of these porous materials a complete activation of samples to produce uniform, empty pores is also an essential but often challenging task, especially for highly porous MOFs. Besides the generally used methods (such as solvent exchange followed by evacuation to remove guest molecules during sample activation), some advanced approaches for the purification (such as "density separation") and activation (such as "supercritical processing") of MOFs have been proposed and carried out, as highlighted in a recent review article.[75] The direct structural characterization of MOFs is usually carried out by single-crystal X-ray diffraction, or powder X-ray diffraction (PXRD) in few cases. The latter is also often used to effectively establish the purity of the harvested crystalline products. Other means including nuclear magnetic resonance (NMR) and thermogravimetric analyses (TGA) can also be used to characterize a MOF's structure.

The regular porosity of MOFs has prompted a myriad of potential applications of them,[35,76−78] in the fields of catalysis,[79−85] H_2 storage,[86−89] CO_2 capture,[90−94] drug delivery,[95−97] biomedical imaging,[71] sensing,[98] and of course chemical separations[81,85,99−104] as highlighted in this Review. The already abundant collection of knowledge and steadily increasing interest in designing new MOFs for specific applications seem to be an indication of the bright and diverse future for these materials.

1.2. Separations with Porous Materials

Separation processes play significant roles in industry and daily life and are used for three primary functions: concentration, fractionation, and purification. These processes usually include distillation, crystallization, extraction, absorption, adsorption, and membrane separations (Figure 2), of which distillation accounts for 90−95% of all processes in the chemical industry.[105]

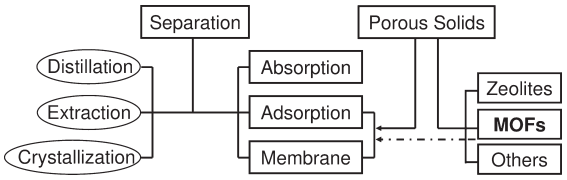

Figure 2. Separation methods and applications of porous solids acting as the supporting medium in separations.

Distillation is however not always feasible because of some inherent limitations, such as the decompositions of some materials at high temperatures that are often required for the system. Adsorption- and membrane-based separations are alternatives, in which a supporting medium, usually a porous material, is required for the separations. A lot of porous materials, including zeolites, carbon and metal−oxide molecular sieves, aluminophosphates, activated carbon, activated alumina, carbon nanotubes, silica gel, pillared clays, inorganic and polymeric resins, porous organic materials, and porous metal−organic composites, have been explored as adsorbents, and some of them have been implemented as membrane (filler) materials, for various separations.[1,105,106] Clearly, MOFs are feasible candidates as medium materials in adsorption and membrane-based separations.

1.2.1. Adsorptive Separations. Adsorptive separations refer to the process by which a mixture is separated based on differences in adsorption/desorption behavior of distinct components in the mixture, and have a wide range of applications throughout a wide range of industries. Several adsorptive separation mechanisms have been proposed, and they are highly dependent on the properties of adsorbates and adsorbents used, as well as the associated interactions. Generally speaking, steric, kinetic, or equilibrium effects or combinations thereof are present in guest adsorption by MOFs. These mechanisms have been explained in several monographs[107,108] and our early review article.[99] In addition, similar to those in zeolites, ion-exchange and reactive adsorption are also possible in some MOFs.

Separation in adsorptive processes is derived from the differences in adsorption behaviors of components of the mixture, which are directly related to the properties of the adsorbent in terms of adsorption equilibria and kinetics.[109,110] The adsorption capacity and selectivity of an adsorbent are the principal properties relevant to adsorptive separation. The former depends on the nature of the adsorbate, the nature of the pores in the adsorbent, and the working conditions (such as temperature and pressures in gas separations, and solvent system in liquid separations). The latter is a more complicated, process-dependent property, although it is still related to the operational environment and the properties of the adsorbent and the adsorbate. For a bulk phase of mixed species, the adsorption selectivity can be simply expressed by $S_{ads} = (q_i/q_j)/(y_i/y_j)$, where q_i and y_i are the mole fraction of species i in the adsorbed and bulk phase, respectively. In addition to acceptable mechanical properties, a promising adsorbent should possess not only good adsorption capacity and selectivity, but also favorable desorption kinetics.

Regeneration of the adsorbent is another important issue in practical separation processes and is directly related to the cost of the processes. In gas-phase adsorption, the adsorbed species are most often removed by changing the temperature and/or the pressure of the system, resulting in temperature swing adsorption (TSA) and pressure swing adsorption (PSA) processes.[107] For liquid systems, a desorbent is required that preferentially displaces

adsorbed species from the adsorbent and can then be easily separated from the adsorbate by other methods.

Experimentally, the separation performance of an adsorbent can be evaluated by several techniques, including adsorption isotherms, pulse testing, breakthrough measurement, and chromatography separation. These methods also allow scientists and engineers to optimize operating parameters for practical mixture separations, although the scalability remains a significant challenge in some cases.[105,108,111]

1.2.2. Membrane Separations. Membrane separations have broad coverage in science and engineering. In a general sense, a membrane is a barrier that selectively allows certain molecules to pass across it.[112] Membrane-based separations have the advantages of low cost, high energy efficiency, ease of processing, excellent reliability, and usually smaller footprints as compared to other technologies, such as distillation and adsorption. When limiting our focus to the subject of MOFs acting as membrane materials for separations (primarily for gas separations), the separation of a mixture is mainly dominated by one (or more) of five separation mechanisms: (1) molecular sieving, (2) Knudson diffusion, (3) surface diffusion, (4) solution diffusion, and (5) capillary condensation. These different mechanisms were developed on the basis of different types of membranes and objects being separated.[112] Detailed descriptions of these mechanisms can be found in an authoritative text edited by Strathmann.[113]

Two parameters, permeance (or flux) (P) and selectivity (α), are usually used to evaluate the performance of a membrane in gas or liquid separations. The first one estimates the transport rate of species through a membrane, while the latter evaluates the ability of the membrane to separate components of a mixture. Experimental evaluations usually involve comparing permeances of pure fluids and mixtures, and therefrom deducing the corresponding ideal selectivity and mixture separation factors. The ideal selectivity is defined as the ratio of permeability coefficients of pure fluid, $\alpha_{A/B} = P_A/P_B$, and can be calculated from pure-fluid measurements. However, for a mixture, the presence of one fluid can influence the transport of the others, therefore deviating from the ideal selectivity. For a binary mixture system, the separation factor is defined as $\alpha^*_{A/B} = (y_A/y_B)/(x_A/x_B)$, where y_A and y_B are the mole fractions of the components in the permeation, and x_A and x_B are their corresponding mole fractions in the feed phase.[114]

Similar to that of adsorptive separation, the efficiency of membrane separations largely depends on the membrane material that is used. In principle, all materials that form sufficiently thin films can be used to create membranes. Polymeric membranes, using organic polymers as membrane materials, are widely studied and being used in industry for gas separations. As compared to other membranes, they are in an advanced stage of development, much cheaper, easily fabricated into commercially useful shapes, stable at high pressures, and easily mass produced. A lot of polymers have been used as membrane materials; among them, cellulose acetate (CA), polysulfone (PSf), and polyimide (PI) are the most widely used for industrial scale applications. Inorganic materials that have been explored for membrane technologies include zeolites, alumina, carbon, ceramic, and others. Their membranes often show better separation performance due to their well-defined, rigid pores. Inorganic members also usually have higher chemical and thermal stability than polymeric membranes. However, high cost, poor mechanical properties (leading to defects), difficult synthesis using templates, and processing difficulties have limited their industrial applications. An alternative approach is to embed these inorganic porous materials, as fillers, into polymeric membranes to obtain hybrid composite membrane, also call mixed-matrix membranes (MMMs). These hybrid membranes are expected to combine the advantages of inorganic porous materials, such as uniform and fixed pore shape and size, with those of organic polymers. However, achieving highly compatible connections between the two phases is a challenging issue.

Clearly, ultrathin separation membranes fabricated by materials with uniform pores are much more desired than other membranes for specific separations because the pore size distribution plays a key role in their separation performance. Despite a long development, however, applications of zeolite membranes are hampered by various aspects, such as their synthesis using a template and limited choice of structure types. MOFs, just like zeolites, satisfy the requirement of well-defined pore size and shape and are therefore promising candidates for advanced membranes. To date, two types of membranes using MOFs as supporting materials have been studied for separations, pure MOF membranes (or thin film) and mixed-matrix membranes with MOFs acting as fillers in organic polymers.

1.2.3. Selective Adsorption and Separation in MOFs. As a new class of porous materials, the investigation of MOFs for selective adsorption and separation not only greatly extended the scope of MOF applications, but it could probably lead to answers of some crucial problems in separation science and related technologies.[115] As briefly discussed above, in either adsorptive separation or membrane separation, the selection of supporting materials is the key. The materials that are used decide not only the final separation performances but also in a broader context, long-term capital cost and application across fields. With the large variety of MOFs that are available, one can expect these novel porous materials to be capable of increasing selectivity, improving energy efficiency, and reducing the costs of separation processes. In addition, the ability to rationally fine-tune structures and pore properties of MOFs at the molecular level may create unique interactions with guest molecules and thus achieve unusual chemico-physical properties for adsorptions, thereby leading to solutions of some specific scientific and engineering challenges in separations. For example, enantio-separation by zeolites is a challenge that has not been overcome as of now, but could potentially be achieved by homochiral MOF adsorbents and membranes. Homochiral MOFs can not only be more easily synthesized from predesigned homochiral ligands or framework constructions than zeolites, but a number of postsynthetic modifications to existing structures can induce framework chirality in a much broader range than what is possible with zeolites.

For adsorptive separations, to date, most reports have focused on selective adsorptions, which are certainly very important for evaluating the materials for their potential separation performance and for screening promising candidates.[99] However, practical separations of a mixture involve more variables than evaluations from single-component measurements. Because of various reasons, coadsorption, diffusion, and breakthrough experiments remain largely unexplored to date, although the reported examples have been increasing. For membrane separations, only very limited MOF members have been tested, although a lot of other MOFs are highly desirable, and computational simulations can help tremendously in scanning these materials. In both separation options, many more scientific investigations are conducted for adsorption or separation of

gases and other chemicals in the gas phase, while liquid separations are limited.[94,99,102]

1.3. Scope and Structure of This Review

To some extent, the separations of chemicals with MOFs have not reached the level of any practical applications to date; only scientific explorations for so-called potential applications have been performed. In most cases, only selective adsorption was tested, suggesting a possible application in separations. In this Review, we present a summary and recommendation of experimental results pertaining to the use of MOFs as separation medium for both gases and liquids. Despite our best efforts and ambitions, we can never cover all of the results in this rapidly growing research area, particularly unpublished results from the industrial arena. It should also be pointed out that despite the importance of computational simulations and large number of published papers, including several excellent review articles,[94,101,116−119] we do not attempt to give an in-depth discussion of these results, but instead compare them with experimental results when applicable. For the selective adsorption and separation in MOFs, readers are also directed to several additional review articles.[81,85,99,100,102,104]

Because of the absence of a standardized nomenclature for MOFs, we name all discussed MOFs, upon their initial appearance in this Review, by their empirical formulas expressing the metal, ligand, and their stoichiometry in the repetitive unit. Following the empirical formula, a code, used in the original literature, is given, and may be used in the subsequent discussion to refer to this MOF. From a structural point of view, we limit the range of MOFs to those infinite structures assembled by strong bonds (including coordination bonds) linked in at least two dimensions (2D); the MOFs discussed here thus contain metal−organic complexes with a 3D or 2D extended structure. Notwithstanding the selective adsorption and separation properties have been observed in some other lower dimensional metal−organic complexes including porous molecular complexes (metal−organic cages, polyhedra, cubes, and rings) and coordination polymers with a one-dimensional (1D) structure (these molecules, chains, or tubes are connected by weak interactions such as hydrogen bonds and π---π stacking to form stable porous supramolecular networks in the solid state),[120−123] they are not included in this Review, except for some specific examples.

Following a brief introduction of MOFs and adsorptive and membrane-based separations, this Review has been structured into three parallel parts referring to different separations, as well as a discussion focusing on the designs and implementations of MOFs for separations (as the fourth part), ending with a conclusion and outlook. The first part outlines the research progress in gas-phase selective adsorptions and separations including gases and small molecules in the vapor phase. The second part discusses liquid-phase selective adsorptions and separations. The third part examines membrane-based separations using MOF materials, including MOF thin films and mixed-matrix membranes with MOFs acting as fillers. All three sections are further organized by the chemicals that are being separated according to their composition, structure, and properties. The fourth part highlights the design of MOFs at the molecular level for their potential applications in separations, as well as general concerns connected to practical applications.

With this Review, we want to present the possibilities and potentials of MOFs as adsorbents or membrane materials for the separation of chemicals, as well as give directions on the requirements to convert them into practical separation-related applications. This Review will also focus on understanding the relationship between the structure and properties of MOFs as the separation medium, as well as the design of new MOFs for separations that are of interest.

2. MOFS FOR GAS-PHASE ADSORPTIVE SEPARATIONS

Separation of gas mixtures based on the differences in adsorption capacity is being widely used in various living and production-related activities, for example, gas drying, air separation, synthesis gas production, carbon dioxide capture, pollution control, etc.[107,124] With the urgent demand for green and particularly energy saving separation procedures, adsorptive separation is becoming increasingly more important in gas-phase separations, especially for light gases. The development and synthesis of new adsorbents is therefore gaining momentum, with MOFs showing great promise.[115] The first review on the subject of selective gas adsorption and separations by MOFs appeared in early 2009 and primarily focused on the examples reported until that time (mainly light gas separations) and the insights gained from these early papers in the field.[99] In that review article, some basic adsorption and separation-related knowledge was presented. In the 3 years that followed, there has been considerable progress in this topic, and a lot of important results and investigations into the observed phenomenon have been reported. In this part of the Review, we attempt to give a comprehensive review not only updating the reader on the last 3 years, but also highlighting and building upon previous reviews in this field. This part will also tackle a fairly new area of MOFs used for separations, that of vapor-phase separations, which encompasses techniques such as GC to separate important liquid compounds. Investigations into selective adsorptions of vapors can also provide valuable information that will aid in the evaluation of potential materials for liquid-phase separations.[102]

2.1. Selective Adsorptions and Separations of Gases

Efficient separations of light gases (H_2, N_2, O_2, CO_2, and CH_4) are becoming increasingly important from energetic, biological, and environmental standpoints. Selective adsorption and separation of light gases is among the most attractive areas of research in MOFs for separation applications. In fact, a large number of MOFs have displayed selective adsorption behavior for small gas molecules, and a small fraction of these MOFs has also been tested for the separation of mixed gases by, for example, breakthrough experiments or gas chromatography. It has also been shown that the modification of the structures and pore properties of MOFs at the molecular level can tune their selective adsorption and separation performance. Although the path to practical separations from the current selective adsorptions and even breakthrough experiments in a lab is laden with obstacles and the route has not yet been clearly laid out, both experimental measurements and theoretical molecular simulations have demonstrated that some MOFs hold great potential for the separation of light gases in an industrial setting.

2.1.1. Carbon Dioxide (CO_2). One of the primary issues of our time is the discussion, observation, and investigation of global climate change and the need to reduce greenhouse gas emissions. CO_2, being one of the predominant greenhouse gases, has been heavily targeted by scientists, politicians, and the media because of clear-cut increases in global emissions since the dawn

dx.doi.org/10.1021/cr200190s |Chem. Rev. 2012, 112, 869–932

Table 1. Selected MOFs Showing Selective Adsorption or Separation of CO_2 over Other Light Gases

gas	MOFs
CO_2/N_2	$Cu_3(btc)_2$ (HKUST-1),[126−131] Cu(dhbc)$_2$(bipy),[132] $Cr_3O(H_2O)_2F(ntc)_{1.5}$ (MIL-102),[133] Cu(fma)(bpee)$_{0.5}$,[134] Co_3(2,4-pdc)$_2(OH)_2$ (CUK-1),[25,135] Co(6-mna) (CUK-2),[25] $Cd_3(OH)_2(aptz)_4(H_2O)_2$,[136] Zn(bdc)(bipy)$_{0.5}$ (MOF-508),[137] [Ni(cyclam)]$_2$(mtb),[138] Al(OH)(1,4-ndc),[139] $Ln_4Co_3(pyta)_6$,[140] Zn(dtp),[141] Zn_2(tcom)(bipy),[142] Zn(cbim)$_2$ (ZIF-95),[143] Zn_{20}(cbim)$_{39}$(OH) (ZIF-100),[143] Zn(bim)(nim) (ZIF-68),[144] Zn(cbim)(nim) (ZIF-69),[144] Zn(im)$_{1.13}$(nim)$_{0.87}$ (ZIF-70),[144] Zn(nbim)(nim) (ZIF-78),[144] Zn(mbim)(nim) (ZIF-79),[144] Zn(bbim)(nim) (ZIF-81),[144] Zn(cnim)(nim) (ZIF-82),[144] Ni_2(dpce)(bptc) (SNU-M10),[145] Ni_2(dpcb)(bptc) (SNU-M11),[145] Zn(3,5-pydc)(DMA),[146] $H_3[(Cu_4Cl)_3(BTTri)_8]$,[147] $H_3[(Cu_4Cl)_3(BTTri)_8](en)_{1.25}$,[147] Mg_2(dhtp) (CPO-27-Mg),[148] Ni_2(dhtp) (CPO-27-Ni)[148] Cu_2(*cis*-chdc)$_2$(bpee),[149] Cu_2(imta)(DMSO)$_{2-x}$,[150] Zn_2(bttb)(x)$_2$ (x = nothing, DMF, or py-CF_3),[151,152] Cd_2(pzdc)$_2$(bhbpb),[153] $CoNa_2$(1,3-bdc)$_2$,[154] Zn(dmtz)(HCO_2),[155] Zn(dmtz)F,[155] Co_2(ad)$_2$(OAc)$_2$ (bio-MOF-11),[156,157] $Co_4(OH)_2$(dcdd)$_3$,[158] Co(dcdd),[158] Co(dcdd)(py)$_2$,[158] Cu(Hoxonic)(bipy)$_{0.5}$,[159] Al(OH)(bpydc) (MOF-253),[160] MOF-253·0.97Cu$(BF_4)_2$,[160] Zn(bchp),[161] $Zn_2(H_2O)_2$(BenzTB) (DUT-10(Zn)),[162] Zn(dabco)(3,3′-tpdc),[163] Zn_2(tcom),[164] Mg(3,5-pydc),[165] Cu_2(pzdc)$_2$(bptz) (CPL-11),[166] Zn(2,7-ndc)(bipy),[167] Zn(mim)$_2$ (ZIF-8),[168] Zn_2(tcpbda)(bpta) (SNU-31′),[169] $NH_4[Cu_3(OH)$(4-cpz)$_3]$,[170] $Fe_3[(Fe_4Cl)_3(btt)_8(MeOH)_4]_2$ (Fe-BTT),[73] $Zn_3(OH)$(dcbdc)$_{2.5}$(DMF)$_{4-x}$,[171] [Fe(Tp)(CN)$_3$]$_2$Co,[172] Cd_2(tzc)$_2$,[173] Zn_2(bmebdc)$_2$(bipy),[174] Cu(inaip),[175] Zn_2(atz)$_2$(ox),[176] Mn$(HCO_2)_2$,[177] Er_2(pda)$_3$,[178] Cu(F-pymo)$_2$,[179] Zn_4O(bmebdc),[180] Zn_4O(bmpbdc)$_3$,[180] Zn_2(bmebdc)$_2$(dabco),[180] Zn_2(bmpbdc)$_2$(dabco),[180] Co(mdpt24)$_2$ (MAF-26),[16] Cu_2(tcom) (SNU-21),[181] Cu_2I_2(bttp4),[182] CuBr(bttp4),[182] Ni_3(bfhc)$_3$(btc)$_2$,[183] Cu_5(tz)$_9(NO_3)$,[184] Co(Htib),[185] Cd_2(hfidp),[186] Cd_2(azpy)(2,3-pydc)$_2$,[187] [Zn_2(tctc)]Cl,[188] Zn(bdc)(dabco)$_{0.5}$,[189] Zn(bdc-OH)(dabco)$_{0.5}$,[189] $Al_4(OH)_2(OCH_3)_4$(2-NH_2-bdc)$_3$,[190] and $Al_3O(X)$(2-NH_2-bdc)$_3$ (X = OH or Cl, NH_2-MIL-101(Al))[191]
CO_2/CH_4	HKUST-1,[126,128,129,131,192−195] Cu(dhbc)$_2$(bipy),[132] MIL-53(Cr, Al),[196−199] V(O)(bdc) (MIL-47),[196] $Al_{12}O(OH)_{18}(H_2O)_3(Al_2(OH)_4)(btc)_6$ (MIL-96),[200] Cu(fma)(bpee)$_{0.5}$,[134] Zn(adc)(bpee)$_{0.5}$,[201] Zn(pur)$_2$ (ZIF-20),[202] Co_3(2,4-pdc)$_2(OH)_2$ (CUK-1),[25,135] $H_2[Ni_3O(H_2O)_3$(tatb)$_2]$,[203] $Zn_3(OH)$(*p*-cdc)$_{2.5}$,[204] $Zn_3(OH)$(*p*-cdc)$_{2.5}$(DMF)$_2$,[204] Zn_2(2,6-ndc)$_2$(dpni),[205] Zn(bdc)(bipy)$_{0.5}$ (MOF-508),[137] [Ni(cyclam)]$_2$(mtb),[138] Zn(cbim)$_2$ (ZIF-95),[143] Zn_{20}(cbim)$_{39}$(OH) (ZIF-100),[143] Zn_2(cnc)$_2$(dpt),[206] Zn(bim)(nim) (ZIF-68),[144] Zn(cbim)(nim) (ZIF-69),[144] Zn(im)$_{1.13}$(nim)$_{0.87}$ (ZIF-70),[144] Zn(nbim)(nim) (ZIF-78),[144] Zn(mbim)(nim) (ZIF-79),[144] Zn(bbIm)(nim) (ZIF-81),[144] Zn(cnim)(nim) (ZIF-82),[144] Mg_2(dhtp) (CPO-27-Mg or Mg-MOF-74),[148,207,208] CPO-27-Ni,[148] Mg(tcpbda) (SNU-25),[209] $Co_4(H_2O)_4$(mtb)$_2$ (SNU-15′),[210] Ni_2(dpce)(bptc) (SNU-M10),[145] Ni_2(dpcb)(bptc) (SNU-M11),[145] Zn(3,5-pydc)(DMA),[146] Al(OH)(2-NH_2-bdc) (Amino-MIL-53(Al)),[211] Cu(bipy)$_2$$(BF_4)_2$ (ELM-11),[212] Cu_2(imta)(DMSO)$_{2-x}$,[150] Zn_2(bttb)(x)$_2$ (x = nothing, DMF, or py-CF_3),[151,152] Cu_2(Hbtb)$_2$,[213] $(H_3O)[Zn_7(OH)_3(bbs)_6]$ (UoC-1′),[214] $Co_4(OH)_2$(dcdd)$_3$,[158] Co(dcdd),[158] Co(dcdd)(py)$_2$,[158] Cu(Hoxonic)(bipy)$_{0.5}$,[159] Zn(bdc)(ted)$_{0.5}$,[215] Cu(bdc-OH),[216] Zn(bchp),[161] Zn(5-NO_2-ip)$_{1-x}$(5-MeO-ip)$_x$(bipy),[217] $(In_3O)(OH)$(adc)$_2$(in)$_2$,[218] $(In_3O)(OH)$(adc)$_2$(NH_2in)$_2$,[218] Cu(1,4-ndc),[219] Zn_2(tcom),[164] Zn(mim)$_2$ (ZIF-8),[168] Zn_2(tcpbda)(bpta) (SNU-31′),[169] Zn_2(bpndc)$_2$(bipy) (SNU-9),[220] Cu_2(bdcppi) (SNU-50′),[221] A[$Cu_3(OH)$(4-cpz)$_3$] (A = NH_4 or Et_3NH),[170] $Zn_3(OH)$(dcbdc)$_{2.5}$(DMF)$_{4-x}$,[171] Cu(tip),[222] Zn_5(bta)$_6$(tda)$_2$,[223] $Zn_4(OH)_2$(1,2,4-btc)$_2$,[224] Zn_2(bmebdc)$_2$(bipy),[174] Mn$(HCO_2)_2$,[177] Zn_4O(bmebdc),[180] Zn_4O(bmpbdc)$_3$,[180] Zn_2(bmebdc)$_2$(dabco),[180] Zn_2(bmpbdc)$_2$(dabco),[180] Ni_2(pbmp),[225] Cu(bdc-OH)(bipy),[226] Zn(bdc-OH)(dabco)$_{0.5}$,[227] Cd_2(hfidp),[186] Cd_2(azpy)(2,3-pydc)$_2$,[187] [Zn_2(tctc)]Cl,[188] Zn(bdc)(dabco)$_{0.5}$,[189] Zn(bdc-OH)(dabco)$_{0.5}$,[189] $Al_4(OH)_2(OCH_3)_4$(2-NH_2-bdc)$_3$,[190] and NH_2-MIL-101(Al)[191]
CO_2/O_2	HKUST-1,[126,127] Cu(dhbc)$_2$(bipy),[132] Zn(bim)(nim) (ZIF-68),[144] Zn(cbim)(nim) (ZIF-69),[144] Zn(im)$_{1.13}$(nim)$_{0.87}$ (ZIF-70),[144] Zn(nbim)(nim) (ZIF-78),[144] Zn(mbim)(nim) (ZIF-79),[144] Zn(bbIm)(nim) (ZIF-81),[144] Zn(cnim)(nim) (ZIF-82),[144] Cd_2(pzdc)$_2$(bhbpb),[153] Zn_2(tcpbda)(bpta) (SNU-31′),[169] [Zn_2(tctc)]Cl,[188] Zn(bdc)(dabco)$_{0.5}$,[189] and Zn(bdc-OH)(dabco)$_{0.5}$[189]
CO_2/H_2	Zn_2(tcom)(bipy),[142] Ni_2(dpce)(bptc) (SNU-M10),[145] Ni_2(dpcb)(bptc) (SNU-M11),[145] Zn(3,5-pydc)(DMA),[146] $CoNa_2$(1,3-bdc)$_2$,[154] Zn(dabco)(3,3′-tpdc),[163] Cu(1,4-ndc),[219] Zn_2(tcpbda)(bpta) (SNU-31′),[169] Cu_2I_2(bttp4),[182] CuBr(bttp4),[182] Ni_3(bfhc)$_3$(btc)$_2$,[183] Zn_4O(btb)$_2$ (MOF-177),[228] $Be_{12}(OH)_{12}$(btb)$_4$ (Be-BTB),[228] Co(bdp),[228] $H_3[(Cu_4Cl)_3(BTTri)_8]$,[228] Mg-MOF-74,[228] and Cd_2(azpy)(2,3-pydc)$_2$[187]
CO_2/CO	Zn(bim)(nim) (ZIF-68),[72,229] Zn(cbim)(nim) (ZIF-69),[72,229] Zn(im)$_{1.13}$(nim)$_{0.87}$ (ZIF-70),[72] Zn(cbim)$_2$ (ZIF-95),[143] Zn_{20}(cbim)$_{39}$(OH) (ZIF-100),[143] HKUST-1,[195,230] MTV-MOF-5-EI,[231] MTV-MOF-5-EHI,[231] [Zn_2(tctc)]Cl,[188] Zn(bdc)(dabco)$_{0.5}$,[189] and Zn(bdc-OH)(dabco)$_{0.5}$[189]
CO_2/Ar	CUK-1,[135] Zn(3,5-pydc)(DMA),[146] Zn_2(atz)$_2$(ox),[176] Er_2(pda)$_3$,[178] and Cd_2(azpy)(2,3-pydc)$_2$[187]

of the Industrial Era. Reducing anthropogenic CO_2 emission and lowering the concentration of greenhouse gases in the atmosphere has become one of the most urgent environmental issues in the world. One option for reducing these harmful CO_2 emissions has been termed carbon capture and storage (CCS), which entails the reduction of emissions primarily from large single point sources, such as power plants. In addition, the separation of CO_2 from CH_4 is also an important process in natural gas upgrading. Apart from establishing new technologies, the exploration of advanced capture materials with high separation performance and low capital cost is equally significant for various CO_2-separation-related issues.[90,91,93,125] MOFs have already been demonstrated to be promising materials in the separation of CO_2 from other gases.[94] In fact, selective CO_2 capture from gas mixtures (especially from CO_2/CH_4 and CO_2/N_2) has attracted the most attention.[92,104] Although a relatively comprehensive review has recently summarized the research progresses in this topic, including basic concerns, experimental and computational results, and insights into targeted designs,[94] new results have been added into this rapidly growing area, and several important issues should be highlighted again.

Table 1 is a collection of MOFs that have shown selective adsorption or separation of CO_2 over other gases. Size exclusion and/or different host−guest interactions between gas molecules and the host frameworks can explain the majority of the observed selective adsorption performances.

dx.doi.org/10.1021/cr200190s |*Chem. Rev.* 2012, 112, 869–932

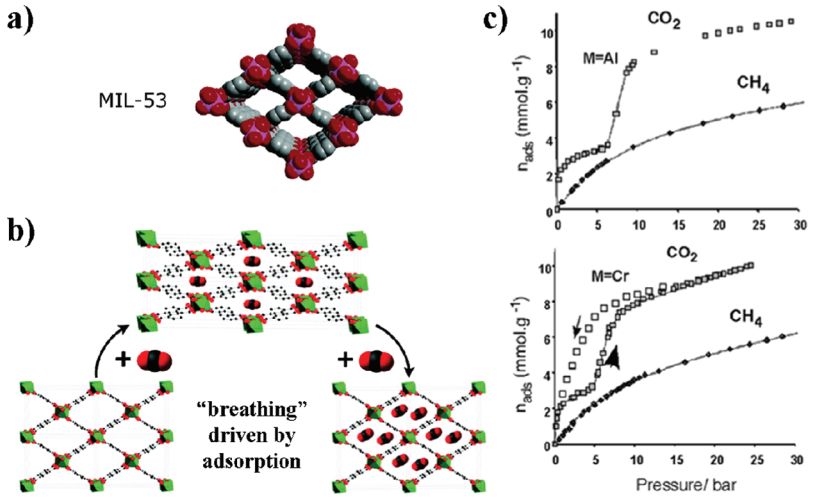

Figure 3. (a) Structure of MIL-53 (space-filling model; metal atoms are shown in pink, carbon atoms in black gray, oxygen atoms in brown; H atoms were omitted for clarity); (b) schematic presentation of the "breathing" of MIL-53 driven by CO_2 adsorption at increasing pressure; and (c) adsorption isotherms of CO_2 and CH_4 on MIL-53 at 304 K. Modified from and reprinted with permission from refs 196 and 236. Copyright 2005 and 2011 American Chemical Society.

The smaller kinetic diameter of CO_2 (3.3 Å) when compared to most other gases (except H_2, He, Ne, H_2O, and NH_3) has established the method of controlling the pore size of a MOF as a highly efficient way of achieving high CO_2 selectivity. This concept of designing a MOF with a pore size between the kinetic diameters of CO_2 and other gases, thus allowing only CO_2 to pass, is easily understood, but designing and synthesizing such a pore in practice is tremendously challenging. In some cases, the actual pore size in a MOF is larger than the sizes of all tested gases; however, only CO_2 adsorption is observed, which is usually attributed to a kinetic sieving effect. For example, $Mn(HCO_2)_2$ has a porous framework structure containing cages with a diameter of about 5.5 Å connected to each other via small windows of about 4.5 Å.[177] This MOF showed almost no N_2 and Ar sorption at 78 K but significant CO_2 uptake at 195 K. The observed selective adsorption can primarily be attributed to the kinetic sieving effect, where the small windows limit the diffusion of larger N_2 and Ar molecules into pores resulting in no adsorption over the diffusion time of the measurement, while smaller CO_2 molecules are allowed to enter into the pore under the given conditions. A similar situation has also been observed in several other MOFs, which selectively adsorb CO_2 over other gases.[143,178,184] This kinetic molecular sieving effect has been widely used in gas separations by using traditional porous materials, such as zeolites in both adsorption- and membrane-based separations.[105] Furthermore, even if all of the tested gases can be adsorbed by a MOF, this diffusion limitation may have a significant effect on the uptake amount of different gases under given conditions. This size-dependent and diffusion-controlled gas selective adsorption has been systematically investigated in a series of ZIFs with incrementally tuned pore sizes.[144]

Alternately, one can take advantage of the comparatively much higher quadrupole moment of CO_2 as compared to other gases, such as N_2, H_2, and CH_4, to facilitate adsorptive separations, which usually leads to stronger adsorbate−adsorbent interactions and correspondingly higher uptake and selective adsorption. The functionalization of pore surfaces by predesigning ligands or through postsynthetic modifications can tune the interaction, thereby improving the selective adsorption capacity for CO_2. This strategy has indeed been widely explored. For example, Long and co-workers[147] functionalized $H_3[(Cu_4Cl)_3(BTTri)_8]$ (H_3BTTri = 1,3,5-tris(1*H*-1,2,3-triazol-5-yl)benzene) by postsynthetic modification with ethylenediamine (en) to obtain $H_3[(Cu_4Cl)_3(BTTri)_8](en)_{1.25}$, in which one of the NH_2 groups of each en is bonded to coordinatively unsaturated Cu(II) sites of the MOF, leaving the other free to interact with guest molecules. It was found that this en-functionalized MOF presents an enhanced heat of adsorption for CO_2 with a maximum value of 90 kJ/mol when compared to its parent MOF (21 kJ/mol), implying a much stronger interaction of CO_2 with the framework. Despite reduction of the CO_2 capacity upon en grafting, the strong interaction between CO_2 and framework endows this MOF with a higher CO_2/N_2 selectivity, especially at low pressure. Through the insertion of metal ions into a stable MOF, the same group also observed the enhanced adsorption selectivity of CO_2 over N_2 in MOF-253·0.97$Cu(BF_4)_2$ as compared to MOF-253 (Al(OH)(bpydc), bpydc = 2,2′-bipyridine-5,5′-dicarboxylate).[160] The selectivity factor of CO_2 over N_2 increases from 2.8 in MOF-253 to 12 in MOF-253·0.97$Cu(BF_4)_2$. The strong interaction between CO_2 molecules with a functionalized pore surface of a MOF has recently also been directly observed and quantified by a single-crystal diffraction method on $Zn_2(atz)_2(ox)$ (Hatz = 3-amino-1,2,4-triazole; ox = oxalate).[176] This MOF has a stable 3D structure with channels, in which the amino groups of the atz ligands stud the pore surface, resulting in a high heat of adsorption of CO_2 and selective adsorption of CO_2 over Ar, H_2, and N_2. High CO_2 adsorption and separation has also been observed in other amine-functionalized MOFs.[156,190,232] Enhanced CO_2 selective adsorptions over N_2 and CH_4 have also been observed in some MOFs with pore surfaces functionalized by acidic open metal sites (or coordinatively unsaturated metal sites (CUMs), Lewis acid sites),[117,128,148,165,207] or other functional groups, such as $-CF_3$,[151] SO_2,[214] and others.[16,189,226,227,231]

Similar to most zeolites, MOFs with charged frameworks have been confirmed as having high CO_2 adsorption capacities and selectivity. Jiang and Babarao[233] by means of molecular simulation demonstrated the high separation ability of gas mixtures (CO_2/H_2, CO_2/CH_4, and CO_2/N_2) in a zeolite-like MOF

dx.doi.org/10.1021/cr200190s |*Chem. Rev.* 2012, 112, 869–932

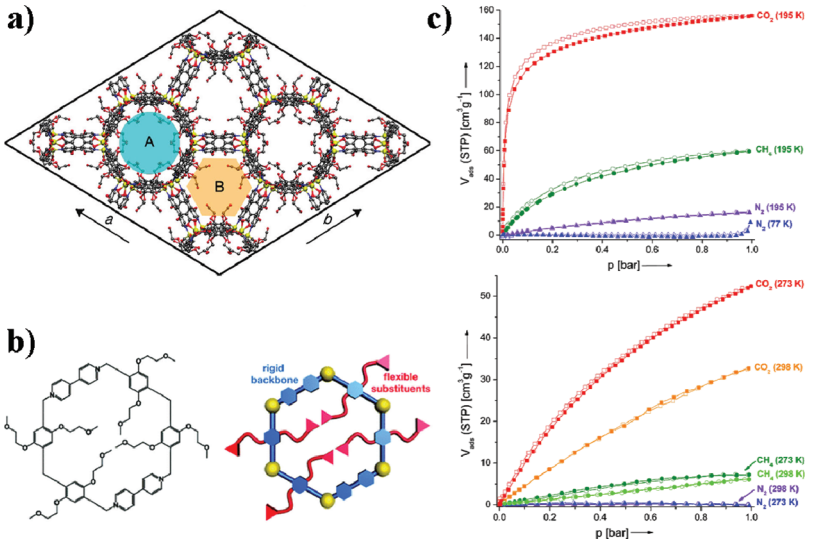

Figure 4. (a) Structure of $Zn_2(bmebdc)_2(bipy)$ showing a unit cell in the *c* direction; (b) sketch of the pore aperture of $Zn_2(bmebdc)_2(bipy)$ (the rigid backbone of the framework is shown in blue, and the flexible alkyl ether substituents are shown in red); and (c) gas adsorption (●) and desorption (○) isotherms on $Zn_2(bmebdc)_2(bipy)$. Reprinted with permission from ref 174. Copyright 2011 American Chemical Society.

(rho-ZMOF), which is composed of an anionic framework and charge-balanced by Na^+ ions. At ambient temperature and pressure, the CO_2 adsorption selectivity is 1800 for the CO_2/H_2, 80 for the CO_2/CH_4, and 500 for the CO_2/N_2 mixture; so far, these results have not been experimentally confirmed.

Another major influence, the guest−host interactions, are sometimes size-dependent (in terms of both framework pores and guest molecules), resulting in a cooperative effect on selective adsorption. This situation is much more evident in flexible MOFs, in which different guest−host interactions can lead to reversible changes in the pore size of a dynamic framework, thereby allowing some molecules to pass though while others are blocked.[33] A thoroughly studied example is the MIL-53 [M(OH)(bdc), M = Al or Cr] series.[92,196,197,234,235] MIL-53 has a stable and reversibly flexible structure with 1D channels functionalized by hydroxyl groups (Figure 3a). A stepwise adsorption and hysteretic desorption isotherm was observed for CO_2 but not for CH_4 (Figure 3c). Importantly, when the pressure was increased to a certain value, CO_2 uptake was significantly higher than that of CH_4. A "breathing" mechanism, in which the strong interaction of CO_2 molecules with the framework leads to pore shrinkage and reopening at high pressure (CH_4 does not cause this structural change), has been proposed to explain the observed sorption behaviors (Figure 3b).[236] For a CO_2/CH_4 mixture gas separation, it was found that the coadsorption of CO_2 and CH_4 leads to a breathing of MIL-53(Cr) similar to that with pure CO_2.[199] The breathing is mainly controlled by the partial pressure of CO_2, but increasing the CH_4 content decreases the extent of the transformation from the closed to open structure. In the closed form, CH_4 seems to be excluded, and only CO_2 is adsorbed. The selectivity of CO_2 over CH_4 decreased when the pressure increased, suggesting that a pressure swing adsorption process may be feasible in practical separations with this material. Adsorptive separation of a CO_2/CH_4 mixture was also demonstrated to be feasible with MIL-53(Al), where the separation selectivity was affected by total pressure, again related to the breathing of the framework and the specific interaction of CO_2 with the framework.[198] In addition, amine-functionalized MIL-53(Al) showed an enhanced separation of CO_2 from CH_4, and again followed a breathing mechanism.[211] Hydration has also been shown to improve adsorption selectivity for CO_2 over CH_4 in MIL-53(Cr).[197] A similar situation has been observed in SNU-M10, which displayed selective adsorption for CO_2 over CH_4, N_2, and H_2.[145]

Other interesting examples are those flexible MOFs in which the pores open at different pressures, which are dependent on the guest molecules being adsorbed. This phenomenon was first observed by Kitagawa and co-workers in $Cu(dhbc)_2(bipy)$ (dhbc = 2,5-dihydroxybenzoate; bipy = 4,4′-bipyridine).[132] This MOF is composed of 2D sheets, which mutually interdigitated to create 1D channels in a 3D supramolecular framework stabilized by π---π stacking interactions. It showed the selective adsorption for different gases (including CO_2 over other light gases) at different gate-opening pressures that depend on the strength of the guest−host intermolecular interaction. A similar situation was also observed in an analogous system of Cu(2,3-pydc)(bpp) (2,3-pydc = pyridine-2,3-dicarboxylate; bpp = 1,3-bis(4-pyridyl)propane).[237]

Furthermore, the design of pore properties utilizing flexible functional groups is another approach to obtaining MOFs with stimuli-responsive selective adsorption properties.[238] By introducing ethylene glycol side chains into the pores, Kitagawa and co-workers[153] obtained a 3D pillared-layer flexible MOF, $Cd_2(pzdc)_2(bhbpb)$ (pzdc = 2,3-pyrazinedicarboxylate; bhbpb = 2,5-bis(2-hydroxyethoxy)-1,4-bis(4-pyridyl)benzene), with hydrogen-bonded gates at the pore windows. This MOF showed reversible single-crystal-to-single-crystal transformations, in response to the removal and readsorption of guest molecules, and the selective adsorption of CO_2 with pronounced hysteresis and the exclusion of N_2 and O_2 at low temperature. It is interesting to note that CO_2 adsorption only begins at a higher vapor pressure. These observed selective adsorptions can be explained by a gating effect. The gates in this MOF cannot be opened by N_2 and O_2 because the interactions with the framework are too weak to break the hydrogen bonds; the same holds true for CO_2 at low vapor pressure. At a higher vapor pressure of CO_2 (P/P_o = 0.9 at 195 K), the gate opens to allow the uptake of CO_2. The same is true at higher temperature where the gate is opened at a lower relative vapor pressure of CO_2 (P/P_o = 0.07 at 293 K), probably

dx.doi.org/10.1021/cr200190s |*Chem. Rev.* 2012, 112, 869–932

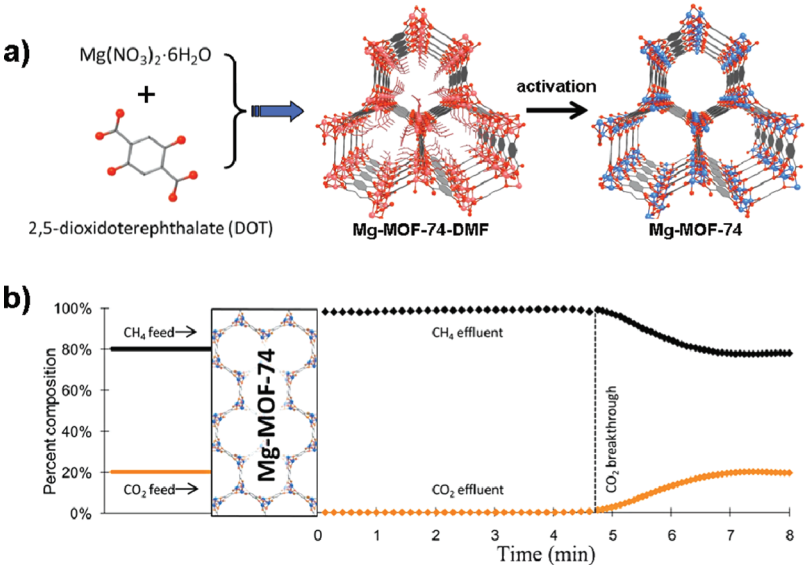

Figure 5. (a) Synthesis, activation, and structure of Mg-MOF-74 (C atoms are shown in gray, O atoms in red, 6-coordinate Mg atoms and terminal ligands in pink, and 5-coordinate Mg atoms in blue; H atoms are omitted for clarity); and (b) breakthrough experiment of Mg-MOF-74 using a 20% mixture of CO_2 in CH_4. Reproduced with permission from ref 207. Copyright 2009 National Academy of Sciences.

due to the increased thermal energy of both the framework and CO_2. On the basis of a similar mechanism, the selective adsorption of CO_2 over N_2 and CH_4 was also observed in Zn_4O(bmebdc) (bmebdc = 2,5-bis(2-methoxyethoxy)-1, 4-benzenedicarboxylate),[180] Zn_4O(bmpbdc)$_3$ (bmpbdc = 2,5-bis(3-methoxypropoxy)benzenedicarboxylate),[180] [Zn_2(bmebdc)$_2$(dabco) (dabco = 1,4-diazabicyclo[2,2,2]octane),[180] and Zn_2(bmpbdc)$_2$(dabco).[180] It was shown that the additional flexible alkyl ether groups in the ligands initiate the structural flexibility of these MOFs and the observed gas sorption selectivity.

The introduction of flexible functional groups into pores to functionalize a gate for selective adsorption has also been achieved in a rigid MOF, Zn_2(bmebdc)$_2$(bipy).[174] As shown in Figure 4a and b, this MOF has a 3D honeycomb-like structure with cylindrical channels that are populated with flexible alkyl ether groups. These flexible substituents in the rigid framework behave as molecular gates to control the entrance of guest molecules, resulting in the highly selective adsorption of CO_2 over N_2 and CH_4 (Figure 4c).

Adsorption dynamics and diffusion are equally as significant as the adsorption equilibrium for separations; however, very limited reports have been documented.[104] Adsorption dynamics of CO_2 in Ni_2(bipy)$_3$(NO_3)$_4$ was first explored by Thomas and co-workers.[239] It was found that the adsorption kinetics obey a linear driving force (LDF) mass transfer model at low surface coverage. The rates of adsorption in the region of the CO_2 isotherm steps are slower than those observed either before or after each step. Recently, Salles and co-workers[240] revealed that CO_2 diffusion in both the closing and the opening structures of MIL-53(Cr) follows a 1D mechanism. They also studied the self- and transport diffusivities of CO_2 in MIL-47.[241] The results showed that self-diffusivity and jump diffusivity monotonously decrease with an increase in loading, whereas transport diffusivity exhibits a slight decrease at low loading followed by a sharp increase at higher loading. In both MOFs, the magnitude of the transport diffusivities is 8−10 m^2/s. In addition, Hernández-Maldonado and García-Ricard[242] evaluated the dynamics of CO_2 adsorption on three forms of Cu_2(pzdc)$_2$(bipy) (pzdc = pyrazine-2,3-dicarboxylate) pretreated at different temperatures, while Lin and co-workers[243] examined the CO_2 diffusion in cubic MOF-5 crystals and revealed that CO_2 diffusion in these crystals is an activated process and the CO_2 loading has almost no effect on the rate of diffusion. Further studies into the adsorption dynamics of CO_2 in MOF-5 (and MOF-177) were also performed by Deng and co-workers.[244]

A technique other than using observed selective adsorption isotherms to evaluate the separation selectivity of CO_2 from a gas mixture is by directly measuring separation by breakthrough experiments or GC. An example of an efficient separation of CO_2 from a mixed CO_2/CH_4 gas stream was demonstrated by a breakthrough measurement using Mg-MOF-74.[148,207] This MOF is highly stable and possesses large pores decorated by CUMs (Figure 5a), which reportedly have strong interactions with CO_2. As shown in Figure 5b, from a 20% mixture of CO_2 in CH_4 the adsorption of CO_2 is substantially preferential over CH_4 with a dynamic capacity of 8.9 wt % CO_2 uptake. Furthermore, this MOF underwent a facile CO_2 release at moderate temperature (80 °C), implying a low regeneration cost, a metric very important to the practical application.

In addition, several ZIFs have also shown high CO_2 separation capacities as demonstrated by breakthrough experiments, including ZIF-68, -69, and -70 for CO_2/CO,[72] ZIF-20 for CO_2/CH_4,[202] and ZIF-95 and -100 for CO_2/CH_4, CO_2/CO, and CO_2/N_2 separations.[143] Breakthrough experiments have also been performed on the MIL-53 series to test their performances in separating CO_2 from CH_4.[198,199,211] Sun and co-workers[190] recently also reported the CO_2/N_2 and CO_2/CH_4 separations on Al_4(OH)$_2$(OCH_3)$_4$(2-NH_2-bdc)$_3$ (2-NH_2-bdc = 2-amino-1,4-benzenedicarboxylate) evaluated by the breakthrough measurements of the gas mixtures. Furthermore, Chen and co-workers[137] examined Zn(bdc)(bipy)$_{0.5}$ (MOF-508) for its performance in the separation and removal of CO_2 from binary CO_2/N_2 and CO_2/CH_4 and ternary CO_2/CH_4/N_2 mixtures by fixed-bed adsorption.

dx.doi.org/10.1021/cr200190s |*Chem. Rev.* 2012, 112, 869–932

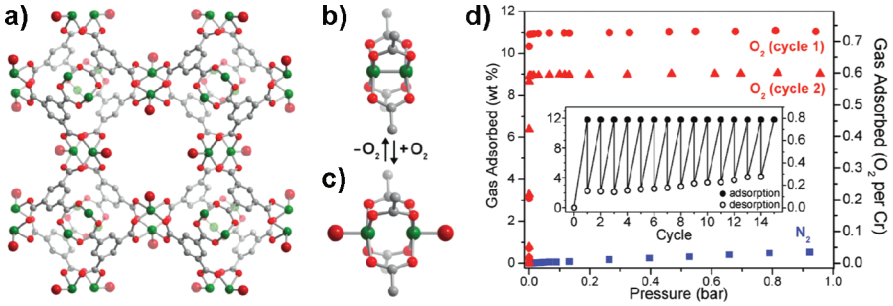

Figure 6. (a) Structure of $Cr_3(btc)_2$ (Cr atoms are shown in green, O atoms in red, and C atoms in gray); (b and c) schematic presentation of the chemical adsorption and desorption of O_2 on the metal sites; and (d) adsorption of O_2 (red symbols) and N_2 (blue squares) by $Cr_3(btc)_2$ at 298 K. Upon evacuation, the O_2 isotherm for a second cycle reveals a slightly reduced capacity, while the isotherm for a third cycle (not shown) is essentially identical to the second (inset: uptake and release of O_2 by a different sample of $Cr_3(btc)_2$ over 15 cycles at 298 K). Reproduced with permission from ref 264. Copyright 2010 American Chemical Society.

Gas chromatography (GC) is an alternative experimental method often used for the evaluation of gas separation performance of an adsorbent, although it has only rarely been adopted for MOFs. Chang and co-workers[135] reported the separation by gas chromatography on CUK-1 of a gas mixture composed of $H_2/O_2/N_2/CH_4/CO_2$ (0.6:2:28:10:27, mol %), which revealed effective separation for these gases. A second example was reported by Navarro and co-workers[170] on an ionic MOF, $A[Cu_3(\mu_3\text{-OH})(\mu_3\text{-4-cpz})_3]$ (4-cpz = 4-carboxypyrazolato; A = NH_4^+ or Et_3NH^+) for $N_2/CH_4/CO_2/C_2H_2$ gas mixture separation. The results revealed that these materials have strong adsorption interactions with CO_2 and C_2H_2, whereas the interactions with N_2 and CH_4 are negligible, thus solidifying the effectiveness of ionic MOFs as a viable option for the separation of CO_2 from N_2 and CH_4.

The effect of humidity on the performance of the MOF-74 series (M = Zn, Ni, Co, or Mg) as adsorbents for CO_2 capture has also been explored by Matzger and co-workers.[245] Mg-MOF-74 demonstrated an exceptional capacity for CO_2 under flow-through conditions with dry flue gas ($5N_2$:$1CO_2$). The effect of humidity on the performance of these MOFs was investigated by $N_2/CO_2/H_2O$ breakthrough experiments at relative humidities (RHs) of 9%, 36%, and 70%. After exposure of the MOFs to the gas stream at 70% RH and subsequent thermal regeneration, only about 16% of the initial CO_2 uptake capacity was recovered for Mg-MOF-74. However, about 60% and 85% were recovered for Ni-MOF-74 and Co-MOF-74, respectively. These results indicated that although Mg-MOF-74 has the highest CO_2 uptake capacity, under the conditions used in this study, Co-MOF-74 may be a more desirable material for CO_2 capture in a practical environment, where water exists in varying quantities in streams of flue gas.

With respect to the CO_2 selective adsorption and separation from N_2 and CH_4, one conclusion that might be drawn from the majority of these investigations is that at room temperature and low pressure the adsorption of N_2 and CH_4 is low for most MOFs, thus leading to another conclusion that increasing the CO_2 uptake capacity (at low pressure) should be a direct method of enhancing the CO_2/N_2 and CO_2/CH_4 separation capacities at conditions relevant to practical carbon capture applications. A MOF with high surface area and heat of adsorption of CO_2 is always desired for these separations. One other important component to this area of research is that of computational simulations, which have been widely used to evaluate CO_2 separations in MOFs, and have produced a lot of publications including several reviews.[90,93,94,117,246,247]

2.1.2. Oxygen (O_2). The separation of O_2 and N_2 from air is an important industrial process, presently carried out by using mainly cryogenic distillation to obtain large volumes of pure products.[111] Other technologies include air separation using polymeric membranes[248,249] or porous zeolites (by a PSA process)[250] at ambient temperatures or using specialized ceramic membranes, suitable for small volumes of specific applications, at high temperature.[251] Cryogenic distillation of air is obviously highly energy-consuming, thus leading to a long-term effort to develop other technologies that might enable this process to be carried out with lower energy costs. Adsorptive and membrane-based separation has already been shown to be energy-saving as compared to distillation, given that proper porous materials are available. However, obtaining a porous material capable of efficiently separating O_2 from air is not easy because of the similarity in its shape to N_2 and size to Ar. MOFs, with highly tailorable pore size, shape, and surface properties, are promising candidates for this task. With the large variety of MOFs already available, one can expect these novel materials to be capable of increasing selectivity for O_2, therefore improving energy efficiency and reducing the costs involved in air separation.

Some MOFs have demonstrated selective adsorption of O_2 over N_2 and other gases. A molecular sieving effect was again believed to be the primary reason for the observed selective adsorption regardless of rigidity or flexibility of the MOF structure. For examples, at low temperature, selective adsorption of O_2 over CO and N_2 has been observed in $Mg_3(2,6\text{-ndc})_3$ (2,6-ndc = 2,6-naphthalenedicarboxylate),[252] $Zn_4O(H_2O)_3(9,10\text{-adc})_3$ (PCN-13, 9,10-adc = 9,10-anthracenedicarboxylate),[253] and $Ln_4(H_2O)(tatb)_{8/3}(SO_4)_2$ (PCN-17, Ln = Yb, Y, Er, or Dy; tatb = 4,4′,4″-*s*-triazine-2,4,6-triyltribenzoate).[254,255] Cu(bdt) (bdt = 1,4-benzeneditetrazolate) revealed adsorption selectivity of O_2 over N_2 and H_2.[256] MOFs showing selective adsorption of O_2 over N_2 at low temperature include CUK-1,[25,135] $[Ni(cyclam)]_2(mtb)$ (cyclam = 1,4,8,11-tetraazacyclotetradecane; mtb = methanetetrabenzoate),[138] Zn(dtp) (H_2dtp = 2,3-di-1*H*-tetrazol-5-ylpyrazine),[141] $Zn_3(OH)(dcbdc)_{2.5}(DMF)_{4-x}$ (dcbdc = 2,5-dichloro-1,4-benzenedicarboxylate; DMF = *N*,*N*-dimethylformamide),[171] $Mn(HCO_2)_2$,[257] SNU-25,[209] SNU-15′,[210] SNU-9,[220] Zn(TCNQ–TCNQ)(bipy) (TCNQ = 7,7,8,8-tetracyano-*p*-quinodimethane),[258] and Cu(bdtri)(DEF) (H_2bdtri = 1,4-benzenedi(1*H*-1,2,3-triazole); DEF = diethylformamide).[259] These MOFs are thus potentially useful for air separation, although further work is required such that these observed selectivities are conducted only at low temperatures.

Explorations of selective adsorption of O_2 over other gases at ambient temperature are more important for evaluating potential

dx.doi.org/10.1021/cr200190s |*Chem. Rev.* 2012, 112, 869–932

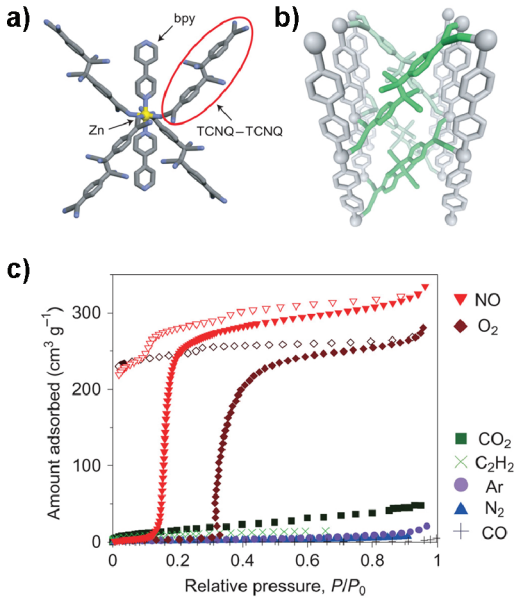

Figure 7. (a and b) Crystal structure of Zn(TCNQ−TCNQ)(bipy): (a) coordination environment of the Zn(II) atom and (b) bipy coordinates to the axial sites of Zn(II) to form 1D chain (gray) and TCNQ dimer (green) coordinates to the equatorial sites of Zn(II) to connect the 1D chains; (c) adsorption isotherms of several gases (N_2, O_2, and CO at 77 K; Ar at 87 K; NO at 121 K; CO_2 and C_2H_2 at 193 K). Filled and open symbols represent adsorption and desorption data, respectively. Reproduced with permission from ref 258. Copyright 2010 Nature Publishing Group.

applications in practical separations. Yang and Li[260] revealed, through low-pressure N_2 and O_2 adsorption measurements at 298 K, that O_2 is adsorbed preferentially over N_2 in MOF-177 with an evaluated selectivity of about 1.8 at 1 atm and 298 K. Notwithstanding the low selectivity at low pressure, it is interesting to note that the adsorption isotherm was linear for O_2, while being strongly concave for N_2, suggesting early adsorption saturation for N_2, but not O_2. This behavior implies that higher selectivities could be achieved at higher pressures. Thus, MOF-177 could be a promising sorbent for air separation at high pressure, such as by a PSA process. Similar selective adsorption of O_2 over N_2 at ambient temperature has also been observed in mesoporous MOF $Zn_4O(bdc)(btb)_{4/3}$ (UMCM-1, H_3btb = 1,3,5-tris(4-carboxyphenyl)benzene)[261]), which gave an O_2/N_2 selectivity of about 1.64 at 298 K and 0.96 bar.[262] However, as the pressure was increased to 24.2 bar, the selectivity decreased to 1.1, contrary to the proposed trend in MOF-177. It should be pointed out that both MOFs have large pore diameters (an order of magnitude larger than the kinetic diameters of O_2 and N_2), thus making a molecular sieving effect hypothesis unreasonable in these cases. The observed selective adsorption is proposed to be a result of preferential adsorption due to a higher magnetic susceptibility of O_2 as compared to N_2; on the other hand, a dynamic effect is also possible. In contrast, HKUST-1, again, with large pore size as compared to O_2 and N_2 but containing unsaturated metal sites displayed adsorption preference for N_2 over O_2 at ambient temperature.[126] The unsaturated metal sites are proposed to be responsible for the stronger interaction with the higher quadrupole moment of N_2 than that of O_2; the mechanism is similar to that observed in zeolites for selective adsorption of N_2 over O_2.[263] These results revealed that adsorption selectivities of N_2 and O_2 in MOFs can be manipulated by the presence or absence of open metal sites. Similarly, the selective adsorption of O_2 over N_2 at room temperature was also observed in $Co_4(OH)_2(dcdd)_3$ (H_2dcdd = 1,12-dihydroxy-carbonyl-1,12-dicarba-*closo*-dodecaborane) and Co(dcdd), both of which contain unsaturated metals sites in their structures.[158] The evaluated O_2/N_2 selectivity in the two MOFs is about 6.5 and 3.5 at low pressure, respectively.

Furthermore, the highly selective adsorption of O_2 over N_2 was observed in rigid $Cr_3(btc)_2$ at 298 K due to the direct bonding of O_2 with the metal sites in the MOF.[264] $Cr_3(btc)_2$ is isostructural with HUKST-1, containing open Cr(II) sites in its framework (Figure 6a). In terms of the uptakes of O_2 at 0.21 bar and N_2 at 0.79 bar, the evaluated O_2/N_2 selectivity factor of 22 is the highest value in MOFs and other porous materials. This record high selectivity can be attributed to the charge transfer interactions of the exposed Cr(II) sites with O_2 but not with N_2 (Figure 6b and c), which have been confirmed by a variety of techniques. It is also important that, despite this strong chemical interaction, most of the adsorbed O_2 can be removed under vacuum at 50 °C. This reversible, selective binding and remarkable loading capacity of O_2 suggests that this MOF is useful in the capture and transport of O_2 (Figure 6d). Similarly, a reversible and selective O_2 chemisorption in a porous metal−organic host material, but not a MOF, was also reported recently.[265]

Similarly, on the basis of the charge transfer interaction between O_2 and the framework, high selective adsorption of O_2 over N_2, Ar, CO, CO_2, and C_2H_2 was also observed in a flexible MOF, Zn(TCNQ−TCNQ)(bipy) at low temperature (Figure 7).[258,266] The mechanism, however, seems to be much more complicated in this flexible MOF than in $Cr_3(btc)_2$. In this case, the charge-transfer interaction of O_2 occurs not with the metal site but with the TCNQ ligand. Additionally, the strong interaction triggered a closed-open structural transformation (gate effect) of this flexible MOF, resulting in the observed selective adsorption. The selective adsorption is thus a result of combining the structural flexibility and electron-donating function of the soft framework. The O_2 adsorption isotherm in this MOF showed a gate-type sorption behavior, that is, no uptake in the low-concentration (or pressure) region but an abrupt increase in adsorption after a threshold concentration (or gate-opening pressure). On the basis of the same mechanism, this MOF is also able to selectively adsorb NO over other gases, which will be discussed below. A similar kinetic gating effect was also observed in flexible Cd(bpndc)(bipy) (bpndc = benzophenone-4,4′-dicarboxylate), which showed the selective adsorption of O_2 over N_2 and Ar at different pressure ranges (that is, each gas has a different gate-opening pressure).[267]

Besides the pressure (or concentration) of adsorbate, the temperature at which gas adsorption is measured can also have an influence on the pore opening or closing. This phenomenon has been observed in several MOF-based mesh-adjustable molecular sieves (MAMSs) developed in the author's group.[268,269] For example, M(bbpdc) (MAMS-2−4, M = Zn, Co, or Cu; bbpdc = 4′-*tert*-butyl-biphenyl-3,5-dicarboxylate)[269] exhibited selective adsorption for O_2 over N_2 and CO at 87 K. Interestingly, at lower temperature (77 K), O_2 cannot be adsorbed at all, but at temperatures above 113 K all of these gases were adsorbed. Another temperature responsive flexible MOF, CPL-11, showed selective adsorption of O_2 over Ar.[166] It was found that an increased measurement temperature clearly leads to enhanced quantities of O_2 adsorbed, but little adsorption of Ar is found, even at high temperatures. This observation was explained as the

dx.doi.org/10.1021/cr200190s |*Chem. Rev.* 2012, 112, 869–932

result of a temperature responsive channel uniformity of the MOF. In addition, the selective adsorption of O_2 over Ar and N_2 was also observed in $Mn(HCO_2)_2$ at a temperature range of 77−140 K.[257] At 77 K, almost no N_2 or Ar was adsorbed, but enhancing the temperature within this range resulted in a decreased O_2 uptake but increased N_2 and Ar uptakes.

Apart from the selective adsorption of O_2 over other gases observed in some MOFs, as discussed above, Morris and co-workers[270] evaluated the kinetic separation of O_2 and N_2 on Cu(mcbdc) (STAM-1, mcbdc = 5-methoxycarbonyl-benzene-1,3-dicarboxylate), which has a 2D structure containing two different channels with hydrophilic and hydrophobic surfaces, respectively. It was found that the adsorption of N_2 in this MOF is significantly slower than that of O_2, which was attributed to a kinetic effect. An analysis based on the normalized kinetic profiles gave an O_2:N_2 selectivity of about 4:1, lower than that (about 20:1) of the best carbon molecular sieves currently used in industry for air separation. It should be mentioned that the PSA process using activated carbon molecular sieves presently used in the separation of O_2 from N_2 in air mainly relies on the kinetic effect: faster diffusion of O_2 than N_2 in the material.[271]

2.1.3. Hydrogen (H_2). H_2 is considered to be one of the best alternative fuels to fossil resources because of its natural abundance, exceptional energy density, and nonpolluting nature when used in fuel cells. MOFs have attracted considerable attention in the hydrogen storage arena in recent years because of their high (and reversible) adsorption capacities.[86,88,272] Alternately, because of their tunable porous structure, MOFs are also promising adsorbents for the purification of H_2, which is another central issue in the hydrogen economy. Although this topic is still in an early stage of development, some MOFs have displayed excellent performance in the selective adsorption and separation of H_2 over other gases. Because H_2 has the smallest size as compared to other gases from which it is usually separated, including CO_2, CO, Ar, N_2, and O_2, molecular sieving effects could be the primary mechanism responsible for the observed selective adsorption of H_2 over the others in MOFs with small pores, except in some special examples where structural transformations take place during gas adsorption.

The hydrogen used in fuel cells is now primarily produced from steam reforming of natural gas. The resulting synthetic gas (syngas) contains CH_4 and CO_2, which must be removed before H_2 can effectively be used.[273] In principle, any porous material with a large enough pore size allowing H_2 and CO_2 to diffuse could be used to selectively adsorb CO_2 over H_2 at temperatures above 195 K because CO_2 is highly polarizable and has a higher quadruple moment as compared to H_2,[99] which results in stronger adsorption interactions between CO_2 and the pore surface of framework as compared to H_2. Some examples have been collected in Table 1. For gate-type flexible MOFs, this strong interaction can also be exploited to open the gate and allow more CO_2 to be adsorbed, whereas H_2 remains excluded. This is the case in Zn(3,5-pydc)(DMA) (3,5-pydc = 3,5-pyridinedicarboxylate; DMA = *N*,*N*′-dimethylacetamide)[146] and $CoNa_2$(1,3-bdc)$_2$.[154] Recently, Long and co-workers[228] tested several representative MOFs including MOF-177, $Be_{12}(OH)_{12}$(btb)$_4$, Co(bdp) (bdp = 1,4-benzenedipyrazolate), $H_3[(Cu_4Cl)_3$(BTTri)$_8]$, and Mg-MOF-74 for their applications in the separation of CO_2 and H_2 via pressure swing adsorption. It is important that these measurements were performed under the conditions (at 313 K and pressures up to 40 bar) close to practical application for H_2 purification and precombustion CO_2 capture. These MOFs showed excellent separation performances with evaluated selectivities, using IAST (ideal adsorbed solution theory[274]), on realistic isotherms for an 80:20 H_2/CO_2 gas mixture (relevant to H_2 purification), between 2 and 860 and the mixed-gas working capacities (under 1 bar purge pressure) as high as 8.6 mol/kg. In particular, Mg-MOF-74 and $H_3[(Cu_4Cl)_3$(BTTri)$_8]$ with a high concentration of CUMs on their pore surfaces showed significant improvements in working capacities over other tested MOFs and several commonly used adsorbents.

Both H_2 and CH_4 usually show weak interactions with framework, but they have different kinetic diameters of 2.8 and 3.8 Å,[99] which suggests that a molecular sieving effect should always be feasible for the selective adsorption and separation of the two gases. This has been observed in $Mn(HCO_2)_2$,[177] and [Ni(cyclam)]$_2$(mtb),[138] at low temperature. Apart from experimental observations, molecular simulations have also been used in the evaluation of the separation performance of MOFs for H_2, CO_2, and CH_4.[193,233,275−277]

Selective adsorption of H_2 over CO (the separation of the two gases is also important for the application of H_2 in fuel cells) was observed in several MOFs with small pores, including Zn(adc)(bpee)$_{0.5}$ (adc = 4,4′-azobenzenedicarboxylate; bpee = bis(4-pyridyl)ethylene),[201] Mg_3(2,6-ndc)$_3$,[252] PCN-17,[254,255] PCN-13,[253] and MAMS-1−4 (at 77 K).[268,269] The adsorption selectivity of these MOFs can be attributed to their small pore size, which discriminates between the two gases.

The selective adsorption of H_2 over N_2 is another important concern because of its potential application for H_2 enrichment from N_2/H_2 exhaust mixtures in ammonia synthesis.[107] Size exclusion and diffusion restricted selective adsorption of H_2 over N_2 was observed in a few MOFs, including Zn(phim)$_2$ (ZIF-11, phim = benzimidazolate),[14] Zn(adc)(bpee)$_{0.5}$,[201] Cu(fma)(bpee)$_{0.5}$,[134] Ln_4Co_3(pyta)$_6$ (pyta = 2,4,6-pyridinetricarboxylate),[140] Zn_3(OH)(dcbdc)$_{2.5}$(DMF)$_{4-x}$,[171] Zn_2(cnc)$_2$(dpt)·G (H_2cnc = 4-carboxycinnamic acid; dpt = 3,6-di-4-pyridyl-1,2,4,5-tetrazine; G = guest molecules),[206] Mg(3,5-pydc) (3,5-pydc = 3,5-pyridinedicarboxylate),[165] [Fe(Tp)(CN)$_3$]$_2$Co (Tp = hydrotris(pyrazolyl)borate),[172] Zn_5Cl_4(bbta)$_3$ (H_2bbta = 1*H*,5*H*-benzo(1,2-*d*:4,5-*d*′)bistriazole),[278] Co(2,6-ndc)(bipy)$_{0.5}$,[279] Cu(F-pymo)$_2$ (F-pymo = 5-fluoropyrimidin-2-olate),[179] PCN-17,[254,255] PCN-13,[253] MAMS-1−4 (at 77 K),[268,269] Mg_3(2,6-ndc)$_3$,[252] $Mn(HCO_2)_2$,[177] [Ni(cyclam)]$_2$(mtb),[138] MAF-26,[16] SNU-15′,[210] Cd_2(tzc)$_2$ (tzc = tetrazolate-5-carboxylate),[173] and Cu_5(tz)$_9$(NO_3) (tz = tetrazolate).[184] It should be pointed out that structural transformation or pore shrinking of MOFs during activation or adsorption probably leads to smaller pore sizes than those observed in the crystal structures determined from the as-synthesized sample. As a result, molecular sieving could still be responsible for the observed selective adsorptions in some MOFs with a "large" pore assessed by crystal structures, especially for some flexible MOFs. In some cases, it is also possible that some solvent molecules remain in the pores even after the activation and partially block the pore opening, resulting in the selective adsorption of smaller H_2 molecule. Another probable explanation for some observed selective adsorption of H_2 over N_2 is that some N_2 molecules interact strongly with polar pore windows, which prevents other N_2 molecules from entering into the pores.[280] This explanation has been proposed to understand the observed selective adsorption of H_2 over N_2 in $Cd_3(OH)_2(aptz)_4(H_2O)_2$ (aptz = 4-aminophenyl-1*H*-tetrazolate), which has a rigid structure with pore size of 5.5 Å.[136] Furthermore, some MOFs, including DUT-10(Zn)[162] and CUK-1,[25] exhibited adsorption selectivity for H_2 over N_2, the origin of which is however not clear.

Observed N_2 uptake is often higher as compared to that of H_2 over a wide range of temperatures in many MOFs with big pores

dx.doi.org/10.1021/cr200190s |*Chem. Rev.* 2012, 112, 869–932

because H_2 usually has weaker interactions with a pore surface than N_2 does. This phenomenon is amplified in Co(bdp)[281] and Zn(3,5-pydc)(DMA),[146] which show an even greater disparity between H_2 and N_2 uptake at 77 K and 1 atm. This phenomenon could be due to the flexible structures of the two MOFs, which are characterized by gate-controlled adsorption properties. The very weak van der Waals interaction of H_2 with framework prevents it from opening the "gate" under the experimental conditions, while N_2 can, due to its higher polarizability.[99]

In addition, the separation of isotopic H_2 and D_2 is highly challenging and cannot be achieved by the traditional molecular sieving technology because they have identical adsorption-based properties. In this case, a quantum molecular sieving process may be useful.[282] Such an effect has been observed in two MOFs, $Zn_3Cu(bdc)_3(Pyen)$ ($PyenH_2$ = 5-methyl-4-oxo-1,4-dihydropyridine-3-carbaldehyde)[283] and $Cu(bipy)_2(CF_3SO_3)_2$.[284]

2.1.4. Gaseous Olefin and Paraffin. The separation of olefin and paraffin, which presently relies on energy-intensive cryogenic distillation-based technologies, is one of the most important separation processes in the petrochemical industry.[285] Adsorptive separation is considered a more energy efficient alternative; however, it still remains a challenge because of the similar molecular properties of olefin and paraffin pairs having the same number of carbon atoms.[286] To date, only a very limited number of zeolites have shown the potential for kinetically separating olefins and paraffins.[287] Other conventional adsorbents such as activated carbon, porous alumina, and silica have not shown a good selectivity. The development of new adsorbents with desired separation performance has thus become a key for the efficient separation of these chemicals.[288] MOFs, as a new type of adsorbent material, have in a short period of time revealed potential in these separations.

Steam cracking of ethane is one of the routes for the ethylene production, in which separation of ethylene and ethane is required. For the first time, Bülow and co-workers[126] showed that HKUST-1 may be useful in the separation of ethylene and ethane mixtures. Sorption isotherms for ethylene and ethane on HKUST-1 measured at 295 K demonstrated the preferential adsorption of ethylene over ethane, particularly in the low pressure range. This adsorption selectivity was proposed to be due to interactions between π-electrons of the double bond in ethylene molecules and partial positive charges of coordinatively unsaturated Cu(II) sites in the framework. This supposition was further supported by the research result from quantum mechanical calculations performed by Nicholson and Bhatia.[289] Besides the electrostatic interactions, their calculations also showed that stronger hydrogen-bonding interactions of ethylene with framework oxygen atoms play an important role in the preferential adsorption. The separation of ethylene/ethane binary mixture on HKUST-1 was also evaluated by grand canonical Monte Carlo simulations.[230] Both computational results suggested a selectivity factor of about 2 for the adsorption of ethylene over ethane at low pressure.

On the contrary, Gascon and co-workers[290] demonstrated that ethane can be selectively adsorbed over ethylene on ZIF-7 ($Zn(bim)_2$, bim = benzimidazolate).[291] This may be the first example of a microporous solid displaying the selective adsorption of paraffins over olefins. Efficient separation of ethane and ethylene by ZIF-7 was further confirmed by breakthrough experiments of the gas mixture. It was proposed that the separation performance of ZIF-7 can be attributed to a gate-opening effect in which specific opening pressures control the uptake and release of different gas molecules. The opening pressure is usually determined by the interaction between guest molecules and the pore (or its window's) surface. In this case, the adsorption process was believed to be dominated by the interaction between the adsorbate gases and the benzene rings in the narrow ZIF-7 windows, which are also capable of selectively discriminating between the two molecules based on their different shapes. On the basis of the same mechanism, this work also showed that ZIF-7 is capable of separating propane and propylene, which is performed by the cryogenic distillation in industry.[285]

Ethylene and acetylene are widely used as chemical feedstocks in the synthesis of many chemical products, in most of which the high purity of starting materials is a prerequisite.[292] Their similar physical properties render removing acetylene from ethylene a difficult task, and, unfortunately, a small amount of acetylene always forms during the generation of ethylene from natural gas cracking.[292,293] Current separation methods in industry involve costly processes accomplished by the partial hydrogenation of acetylene into ethylene over catalyst[294] or solvent extraction of cracked olefins.[295] Adsorptive separation by porous materials is an alternative technology, but has not been achieved to date.

Chen and co-workers[296] explored the adsorptive separation of ethylene and acetylene in two flexible isostructural MOFs, $Zn_3(cdc)_3[Cu(SalPycy)]$ (cdc = 1,4-cyclohexanedicarboxylate; H_2-SalPycy = 5,5′-(cyclohexane-1,2-diylbis(azan-1-yl-1-ylidene)) bis(methan-1-yl-1-ylidene)bis(3-methylpyridin-4-ol)) and $Zn_3(bdc)_3[Cu(SalPycy)]$, with rationally tuned micropores in a 3D structure. At 195 K, $Zn_3(bdc)_3[Cu(SalPycy)$ adsorbed both gases to give similar isotherms, but with a higher acetylene uptake over ethylene (to give an equilibrium selectivity of 1.6). $Zn_3(cdc)_3[Cu(SalPycy)]$, however, exhibited significantly different sorption behaviors with respect to the two gases, possibly because of its smaller pore size. Acetylene adsorption showed a one-step hysteresis loop with high uptake, whereas only a small amount of ethylene was adsorbed (without an obvious hysteresis). The evaluated selectivity for acetylene over ethylene is 25.5. At 273 and 295 K, both MOFs showed type I sorption isotherms for the two gases, with different uptakes in each one. The acetylene/ethylene selectivities on $Zn_3(cdc)_3[Cu(SalPycy)]$ are 4.1 and 5.2, respectively, again higher than the corresponding selectivities of 1.5 and 1.9 on $Zn_3(bdc)_3[Cu(SalPycy)]$. These temperature-dependent gas separation capacities of $Zn_3(cdc)_3[Cu(SalPycy)]$ were attributed to both thermodynamically and kinetically controlled framework flexibility. The enhanced selective capacity of $Zn_3(cdc)_3[Cu(SalPycy)]$ as compared to that of $Zn_3(bdc)_3[Cu(SalPycy)]$ was attributed to the smaller pores within the former, which favors its higher size-specific separation of acetylene and ethylene. Further studies also showed that the gas separation characteristics of $Zn_3(cdc)_3[Cu(SalPycy)]$ are mainly attributed to a size-exclusion effect. In addition, $Zn_3(cdc)_3[Cu(SalPycy)]$ also exhibited a high adsorption selectivity toward CO_2 over ethylene, giving a selectivity factor of 21.60 at 195 K.

Similarly, the separation of propylene and propane is also important in industry. The corresponding experiments to test this separation on HKUST-1 were conducted by Chang and co-workers.[297] The adsorption isotherms exhibited a larger amount of propylene adsorption than that of propane over all of the pressure and temperature ranges tested. This preferential affinity to propylene was attributed to its stronger interaction with the open Cu(II) sites in the MOF as compared to propane, which

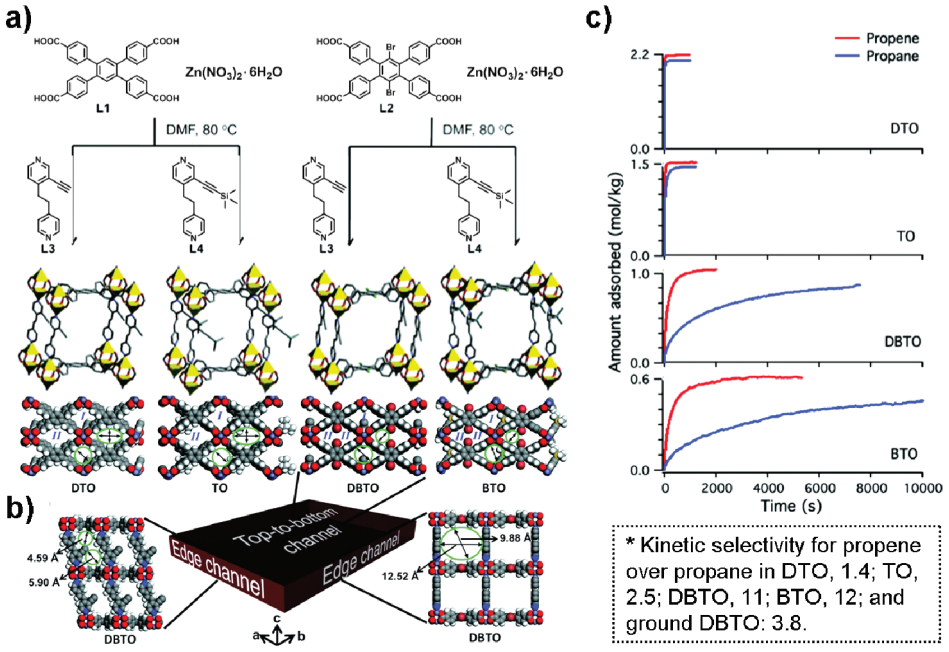

Figure 8. (a) Synthesis and structures of DTO, TO, DBTO, and BTO MOFs (the stick representation of the unit cell and crystal packing diagrams for each MOF are shown (Zn atoms are shown in yellow polyhedra, O atoms in red, Br atoms in green, N atoms in blue, and C atoms in gray; solvent molecules, H atoms, and disordered atoms are omitted for clarity)); (b) crystal packing diagrams of DBTO showing the framework pores along the crystallographic *a* (right) and *b* (left) axes; and (c) time-dependent propene and propane uptake profiles for DTO, TO, DBTO, and BTO MOFs at 0.3 bar and 298 K (top), and kinetic selectivities for the uptake of propene over propane (bottom). Reproduced with permission from ref 304. Copyright 2011 American Chemical Society.

was supported by UV−vis spectra of the guest loaded MOF sample. Calculated separation factors of propylene over propane from the breakthrough curve of a binary mixture ranged from 3.33 (at 313 K) to 5.5 (at 353 K) depending on the measurement temperature. The observed selective adsorption and separation properties of HKUST-1 for propylene and propane gases are consistent with computational results from molecular simulations.[298] Simultaneously, Rodrigues and co-workers[299] also demonstrated similar performances of HKUST-1 in the selective adsorption of propylene over propane from both experimental measurements and molecular simulations.

Preferential adsorption of propylene over propane was also observed in $Fe_3OF_m(OH)_n(btc)_2$ ($m + n < 1$, MIL-100(Fe)[300]), which has a 3D porous framework with coordinatively unsaturated Fe sites.[301] It was found that the sorption affinity for propylene over propane increases at low pressure and is valence-dependent on the Fe centers at low pressure. In the presence of only Fe(III) sites, similar adsorption enthalpies were assessed for propane and propylene. The introduction of Fe(II) sites enhanced the heat of adsorption of propylene at low coverage, while that of propane remained unchanged. Breakthrough experiments gave a separation factor of 28.9 for propylene over propane on the sample activated at 250 °C and 5.1 for that activated at 150 °C. The observed preferential adsorption of propylene on MIL-100(Fe) was ascribed to the role played by unsaturated metal sites that were formed upon the activation of samples, regardless of the different roles for Fe(III) and Fe(II) in the different cases.

Adsorptive separation of isobutene and isobutane on HKUST-1 was tested by Hartmann and co-workers.[302] Adsorption experiments showed a somewhat larger adsorption amount of isobutene as compared to isobutane. It was believed that although the enthalpies of adsorption are only different by about 5 kJ/mol, the strong interaction between the open Cu(II) center and guest molecules dominates the observed differences in adsorption capacity. Separation performance was further evaluated by breakthrough experiments using an equimolar mixture of isobutene and isobutane, which gave a separation factor of 2.1 at 30 °C.

All of the selective adsorptions and separations of gaseous olefin and paraffin on MOFs discussed above are primarily based on adsorption measurements at near equilibrium. Li and co-workers[303] explored, for the first time, the kinetic separation of propylene and propane on three ZIFs, $Zn(2\text{-cim})_2$ (2-cim = 2-chloroimidazolate), $Zn(2\text{-bim})_2$ (2-bim = 2-bromoimidazolate), and ZIF-8. The single-component diffusion studies revealed that the kinetic separation of propene and propane by these MOFs should be feasible on the basis of the observed remarkable difference in diffusion rates of propylene and propane. For example, at 30 °C, the ratio of diffusion rates of propylene and propane through ZIF-8 and $Zn(2\text{-cim})_2$ is 125 and 60, respectively. The effective pore size in these MOFs was believed to be the controlling factor determining the separation capability.

Similarly, Hupp and co-workers[304] studied the kinetic separation of propene and propane in another series of isostructural MOFs shown in Figure 8a. All of these MOFs have single pillared-paddlewheel frameworks with 3D pores. The single crystals of these MOFs were isolated as highly anisotropic rectangular plates. In the direction perpendicular to the largest plane, there are two types of channels ("top-to-bottom" channels), I and II (Figure 8a and b). The aperture of channel II was tuned by 3,6-functionalization of the acid ligands, while functionalization of dipyridine ligands was used to modify the apertures in the other two directions. Both modifications allowed

dx.doi.org/10.1021/cr200190s |*Chem. Rev.* 2012, 112, 869–932

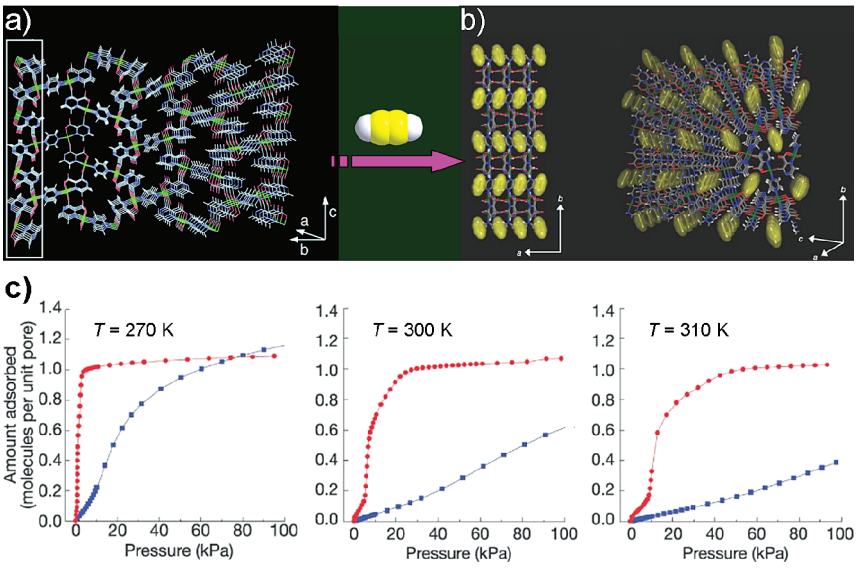

Figure 9. (a) 3D porous pillared-layer structure of $Cu_2(pzdc)_2(pyz)$ (Cu atoms are shown in green, O atoms in red, C atoms in gray, and N atoms in blue); (b) crystal structure of $Cu_2(pzdc)_2(pyz)$ with adsorbed C_2H_2 (yellow) at 170 K from MEM/Rietveld analysis (viewed from different directions); and (c) adsorption isotherms for C_2H_2 (red ●) and CO_2 (blue ■) on $Cu_2(pzdc)_2(pyz)$. Reproduced with permission from refs 46 and 319. Copyright 2002 American Association for the Advancement of Science and 2005 Nature Publishing Group.

the researchers to test the effect of pore apertures on the kinetic separation of propene and propane in this system. The kinetic adsorption selectivity for propene versus propane was qualitatively evaluated from the time-dependent gas uptake profiles (Figure 8c). It was found that DBTO and BTO MOFs showed much higher kinetic selectivities than those of TO and DTO. These differences were explained qualitatively by the thin-rectangular-plate morphology of the MOF crystals, which favors the flow of gas through the "top-to-bottom" channels. On the basis of this understanding, the large kinetic selectivities observed in DBTO and BTO MOFs were attributed to the reduction in the apertures of channels I and II, which efficaciously discriminated the two molecules due to their slight difference in size. This explanation was further supported by the decreased kinetic selectivity observed in a ground sample of DBTO MOF, which reduced the plane of the "top-to-bottom" channels. Overall, these results indicated that controlling diffusion rates in plate-shaped crystals of these MOFs can be achieved by tuning pore apertures of the frameworks and crystal aspect ratios.

2.1.5. Harmful and Unsafe Gases. On the basis of a survey of the literature and our arbitrary definition, harmful or unsafe gases discussed herein include H_2S, SO_2, Cl_2, CNCl, NH_3, NO_x, CO, C_2H_2, ethylene oxide, tetrahydrothiophene, and octane vapor. Most of these gases are released as waste gases from industrial processes into the environment; in some cases, people are even directly exposed to them. Effective capture of these harmful gases is extremely important to the protection of the environment and to those who are at risk. Additionally, the treatment of waste gases, including their separation and capture in nuclear-related industries, is also a significant issue;[305] however, no MOFs have been explored for this application to date.

Yaghi and co-workers[306] tested the adsorption and separation performances of six MOFs, MOF-5, $Zn_4O(2\text{-}NH_2\text{-}bdc)_3$ (IRMOF-3[307]), Zn-MOF-74, MOF-177, HKUST-1, and $Zn_4O(dabb)_3$ (IRMOF-62, dabb = diacetylene-1,4-bis(4-benzoate)[306]), for several harmful gases including SO_2, Cl_2, NH_3, CO, ethylene oxide, and tetrahydrothiophene vapor. Kinetic breakthrough measurements revealed that pore functionality, in particular by active adsorption sites, such as functional groups (NH_2- in IRMOF-3) and open metal sites (in MOF-74 and HKUST-1), played a key role in determining the dynamic adsorption performance of these MOFs. For example, HKUST-1 revealed high efficacy equal to or greater than BPL carbon against all gases tested except Cl_2. It was also found that CO cannot be captured effectively with any of the MOFs that were tested. Furthermore, M-MOF-74 (M = Zn, Co, Ni, or Mg) analogues, all with advantageous open metal sites, were tested to remove toxic gases including NH_3, CNCl, SO_2, and octane vapor (a physically adsorbed compound) from air in both dry and humid conditions by Glover and co-workers.[308] On the basis of experimental breakthrough data, it was found that all of these MOFs are capable of removing toxic gases in dry environments, but failed to do so in humid conditions, where the competitive adsorption of water nearly eliminated the adsorption capacity of all gases except NH_3. NH_3 was adsorbed under all conditions and in fact surpassed the capacities and retention of traditional adsorbent materials. It was also confirmed that the identity of the metal atoms in this series of materials has a significant impact on the loading capability for all chemicals tested in both dry and humid conditions.

The removal of sulfur odorant components from natural gas with HKUST-1 was explored by Mueller and co-workers.[309] A fixed bed breakthrough adsorption experiment of a gas stream of methane odorized with tetrahydrothiophene (THT) at room temperature showed clearly that the sulfur odorant can completely be removed from natural gas by HKUST-1. Control experiments revealed that this MOF has a higher volume specific uptake capacity for THT than two commercially available activated carbon materials, Norit (type RB4) and CarboTech (type C38/4). It was also demonstrated that other electron-rich molecules, including amines, ammonia, water, alcohols, and oxygenates, can be successfully removed from natural gas by adsorption on HKUST-1. The adsorption of these polar molecules induced a color change of the HKUST-1 sample from a deep blue into a light green, which allows for visual detection of contaminants. Furthermore, after removal of the adsorbates by treatment

dx.doi.org/10.1021/cr200190s |*Chem. Rev.* 2012, 112, 869–932

under vacuum or heating, the original color reappeared, indicating practical regeneration of the adsorbent. A further example of harmful gas separation was demonstrated in flexible Zn(bchp) (H_2bcph = 2,2′-bis(4-carboxyphenyl)hexafluoropropane), in which H_2S and SO_2 were selectively adsorbed over N_2, CO_2, and CH_4 at room temperature.[161] The adsorption of H_2S in MIL-53(Al, Cr, Fe), MIL-47, MIL-100(Cr), and MIL-101 also revealed that all of these MOFs are stable toward this corrosive gas and actually have high loading capacities and are easily regenerable, thus making them potential candidates in the purification of natural gas.[310,311]

CO is a notoriously toxic gas because of its strong binding with metal sites of hemachrome. Bearing this in mind, MOFs with similar CUMs in their framework could selectively adsorb CO over other gases, which have comparatively weak interactions with open metal sites, such as N_2, H_2, and CH_4. Although no experimental result has been published to date, molecular simulations have shown that HKUST-1 is quite selective for CO over H_2 and N_2 from their mixtures at 298 K.[312] It was demonstrated that electrostatic interactions between the CO dipole and the partial charges on the open Cu(II) sites dominate the adsorption performances.

NO is a biological signaling molecule and is also interesting in scientific research because of its environmental applications in gas separation and its use in NO_x traps for "lean-burn" engines.[313,314] Two MOFs have shown ultrahigh selectivity for NO over others light gases. One is flexible Cu_2(OH)(sip) (Cu-SIP-3, sip = 5-sulfoisophthalate) reported by Morris and co-workers.[315] This MOF is essentially nonporous in its activated state, but possesses open metal sites in its structure. It was found that Cu-SIP-3 did not adsorb N_2, H_2, CO_2, CO, N_2O, and CH_4 up to 10 bar, even at low temperature. The same is true for NO at very low pressures (<275 mbar); however, above a gate-opening pressure of 275 mbar, this material began to adsorb NO up to 0.88 NO molecules per formula unit at 1 bar. On reduction of the NO pressure, Cu-SIP-3 retained the light gas and showed a large desorption hysteresis, which was attributed to the relatively strong coordination of the gas to CUMs in the structure. It is more interesting that the NO-loaded MOF underwent controllable NO release upon the addition of water as the hydrated phase of the material was formed. On the basis of a similar mechanism, the selective adsorption of NO over Ar, N_2, CO, CO_2, and C_2H_2 was observed in another flexible MOF, Zn(TCNQ−TCNQ)(bipy), reported by Kitagawa and co-workers (see Figure 7).[258] Again, this MOF almost did not adsorb any of the other gases up to the respective saturated vapor pressures at low temperature; however, NO was adsorbed above the gate-opening pressure until saturation at 9 molecules per formula of the MOF took place. The difference in this adsorption is that the NO molecules do not coordinate to the metal sites, but instead interact through charge-transfer with the TCNQ ligands in the MOF. In both cases, the NO−host interaction is strong enough to trigger a structural transformation of MOF frameworks that accounts for the gas uptake.

C_2H_2 is a significant starting material for preparing various fine chemicals[316] and electric materials.[317] It is not only highly reactive but also becomes highly explosive when compressed to over 0.2 MPa at room temperature, even in the absence of oxygen.[318] To obtain high purity C_2H_2, it must be separated from other gases, usually CO_2. Therefore, exploring suitable technologies and looking for associated materials to separate (with high selectivity and low cost) and/or store (with high capacity at safe pressures) C_2H_2 are very important for its production and applications. Kitagawa and co-workers[319] demonstrated the highly selective adsorption of C_2H_2 over CO_2 on Cu_2(pzdc)$_2$(pyz) (pyz = pyrazine),[320] which has a porous structure with 1D channels of 4 × 6 Å in size (Figure 9a). As shown in Figure 9c, adsorption isotherms of C_2H_2 and CO_2 at 270, 300, and 310 K presented evident differences in uptake capacity and isotherm shape, characterized by a steep rise in the low-pressure region and fast saturation with higher uptakes for C_2H_2 as compared to those of CO_2 (low and gradual adsorption). The maximum ratio of the adsorption amount of C_2H_2 to that of CO_2 is 26.0 (at 1.1 kPa and 270 K). X-ray diffraction experiments demonstrated that adsorbed C_2H_2 molecules arranged uniformly in the channels of the MOF and were separated by short intermolecular distances (Figure 9b). Clearly, the pore surface of this MOF, decorated by noncoordinated O atoms of the carboxylate ligands, dominated the C_2H_2 arrangement, where each O atom was hydrogen bonded to one H atom of each C_2H_2 molecule. As a result of this strong interaction, a highly selective adsorption of C_2H_2 over CO_2 as well as probably safe storage of C_2H_2 by this MOF was realized. In addition, this group also reported C_2H_2 adsorption and storage in six other MOFs with a common molecular formula of $M_2(L)_2$(dabco) (M = Cu or Zn; L = bdc, 1,4-naphthalenedicarboxylate (1,4-ndc), and 9,10-adc).[321]

Notwithstanding the absence of any specific interaction except van der Waals forces between the adsorbed C_2H_2 molecules and the walls of the host frameworks, M(HCO$_2$)$_2$ (M = Mg or Mn) also showed selective adsorption of C_2H_2 over CO_2, CH_4, N_2, O_2, and H_2.[322] Interestingly, it was found that as the temperature was increased from 196 to 298 K, the uptake of C_2H_2 only dropped negligibly, whereas the uptake of other gases decreased substantially (CO_2 is the only gas with significant uptake at 298 K, but still far lower than that of C_2H_2). The reason behind this observed adsorption selectivities, although not very clear, was proposed to be due to the slightly larger size of C_2H_2 (5.5 Å) relative to CO_2 (5.3 Å), which provides the former with more-efficient van der Waals interactions with the pore surface of framework. The selective adsorption of C_2H_2 over CO_2 was also observed in Zn_3(cdc)$_3$[Cu(SalPycy)] and Zn_3(bdc)$_3$[Cu(SalPycy)], which were evaluated to give a Henry's law selectivity of 1.10 (195 K), 2.00 (273 K), and 1.89 (295 K) and 1.18 (195 K), 4.74 (273 K), and 8.41 (295 K), respectively.[296] In addition, a reverse C_2H_2/CO_2 selectivity (CO_2 over C_2H_2) was also observed in a gate-type flexible MOF, $CoNa_2$(1,3-bdc)$_2$.[154] The authors attributed this selective adsorption to the host−guest affinity; that is, only CO_2 can utilize its electronegative O atoms to interact with the open Na(I) ions in the framework and consequently open the gates and diffuse into pores of the MOF.

Selective adsorption of C_2H_2 over CH_4 was also observed in Zn_5(bta)$_6$(tda)$_2$ (Hbta = 1,2,3-benzenetriazole; tda = thiophene-2,5-dicarboxylate),[223] Cu(bdc-OH) (bdc-OH = 2-hydroxybenzene-1,4-dicarboxylate),[216] Zn_4(OH)$_2$(1,2,4-btc)$_2$ (1,2,4-btc = benzene-1,2,4-tricarboxylate),[224] and Cu(bdc-OH)(bipy)[226] by Chen and co-workers. The calculated IAST selectivity for an equimolar C_2H_2/CH_4 mixture on Zn_5(bta)$_6$(tda)$_2$ is about 15.5 at 1 atm and 295 K, while the Henry's selectivity obtained from the virial method is 22.3 at 295 K. The Henry's selectivity on Zn_4(OH)$_2$(1,2,4-btc)$_2$, Cu(bdc-OH), and Cu(bdc-OH)(bipy) is 14.7, 9.3, and 55.6, respectively. These adsorption selectivities were attributed to the stronger interactions of C_2H_2 with the host frameworks (particularly those with open metal sites). It should be pointed out that Cu(bdc-OH)(bipy), showing a particularly high adsorption selectivity of 55.6, can be attributed to the

dx.doi.org/10.1021/cr200190s |Chem. Rev. 2012, 112, 869–932

Table 2. Some MOFs Showing Selective Adsorption of Solvent Molecules in the Vapor Phase

MOF	selective adsorption	M[a]
$Cu_2(pzdc)_2(dpyg)$[327]	MeOH over CH_4	A + C
$Co(NCS)_2(3\text{-pia})$[328]	THF, 1,4-dioxane, and Me_2CO over CH_4, cyclopentane, diethylether, propylether, cyclohexane, benzene, pentane, hexane, and heptane	B + C
$Co_2(2,6\text{-ndc})_2(bipyen)$[329]	benzene and cyclohexane over toluene, *m*-, *o*-, and *p*-xylenes, cycloheptatriene, and cyclohexane	A + C B + C
$Cd(pzdc)(bpee)$[330]	H_2O and MeOH over EtOH, THF, and Me_2CO	A
$Cu(2,3\text{-pydc})(bpp)$[237]	MeOH over EtOH	B + C
$Cu(bpe)_{1.5}(1,4\text{-ndc})$[331]	H_2O over N_2, CO_2, and MeOH	A + B
$Zn(tbip)$[332]	dimethylether (DME) over MeOH; MeOH over H_2O	B
Ce(tci) and Pr(tci)[333]	H_2O over MeOH, CO_2, N_2	C
$Ce(tci)(H_2O)$[334]	H_2O and MeOH over MeCN and EtOH	B + C
$Cd(4\text{-btapa})_2(NO_3)_2$[335]	MeOH (298 K) over N_2 (77 K)	B + C
$Zn_2(ip)_2(bipy)_2$[336]	MeOH over EtOH and benzene; EtOH over benzene	A + C B + C
$[Mn(NNdmenH)][Cr(CN)_6]$[337]	H_2O and MeOH over EtOH and CH_3CN	A + C
$Zn(bdc)(ted)_{0.5}$[215,338]	MeOH, EtOH, DME, *n*-hexane, cyclohexane, and benzene over H_2O	B
$[Ni(bpe)_2(N(CN)_2)](N(CN)_2)$[280]	H_2O, EtOH, and Me_2CO (298 K) over N_2, O_2 (77 K), and Xe (195 K)	B + C
Zn(TCNQ−TCNQ)(bipy)[339]	benzene over cyclohexane; 1,4-cyclohexadiene over 1,3-cyclohexadiene	B + C
$Al(OH)(1,4\text{-ndc})$[139]	MeOH and Me_2CO over H_2O and benzene	B + C
Amino-MIL-53 (Al)[340]	benzene over cyclohexane	B + C
Cu(etz)[341]	MeOH, EtOH, and MeCN over H_2O; benzene over cyclohexane	B + C
$Na_2Cu(2,4\text{-pydc})$[342]	H_2O and MeOH over THF and benzene	A + B + C
$Cu(2,5\text{-pydc})$[342]	H_2O and MeOH over THF and benzene	A + B + C
$Gd_2(dhtp)(dhtpH_2)(H_2O)_n$ (n = 4, 5)[343]	H_2O over MeOH, CH_3CN, and EtOH	A + C
$Ag(tmpes)\cdot BF_4$[344]	benzene, toluene, chlorobenzene, bromobenzene, nitrobenzene, 1-bromo-4-fluorobenzene, anisole, ethylbenzene over *n*-hexane, cyclohexane, 1,3-dichlorobenzene, hexafluorobenzene, 4-bromo-1,2-difluorobenzene, and *m*-, *o*-, and *p*-xylenes	A
$Cd(abppt)_2\cdot(ClO_4)_2$[345]	benzene and toluene over *m*-, *o*-, and *p*-xylene; *o*- and *m*-xylene over *p*-xylene	A
$KHo(C_2O_4)_2$[346]	H_2O, MeOH, and CH_3CN over EtOH	A + C
$Zn(SiF_6)(pyz)_2$[347]	MeOH, EtOH, and Me_2CO over *i*-PrOH	A
$Na_2Co(ip)_2$[154]	MeOH, EtOH, and MeCN over Me_2CO	A + C
MIL-53(Cr)[348]	EtOH over H_2O	B + C
$Cu(1,4\text{-ndc})$[219]	MeOH over H_2O and EtOH	A + B + C
MIL-96[349]	*p*-xylene, *m*-xylene, and 1,3,5-trimethylbenzene over 1,3,5-triisopropylbenzene	A
$NH_4[Cu_3(OH)(4\text{-cpz})_3]$[170]	benzene over cyclohexane	A
$Zn_4(OH)_2(1,2,4\text{-btc})_2$[224]	MeOH, EtOH, *n*-PrOH over *i*-PrOH	A
Cu(inaip)[175]	MeOH > EtOH > *n*-BuOH	A
$Cu_2I_2(bttp4)$[182]	benzene over cyclohexane and EtOH	B
$Zn(ip)(bpa)$[350]	benzene over cyclohexane	A + C
$(H_2pip)_{0.5}[VO(cep)]$[351]	H_2O over MeOH and EtOH	A + C
$(H_2dab)[Zn_2(ox)_3]$[352]	H_2O, MeOH and EtOH over MeCN, MeCHO, Me_2CO, Me_2CHOH, PrOH, BuOH, H_2, and N_2	A + B + C

[a] Primary mechanisms involved in the observed selective adsorption: A, size/shape exclusion; B, host−guest interactions (including guest−guest interactions in some cases); C, selective adsorption resulting from guest-adsorption induced structural transformation of the MOF.

combined effect from its small pores (4.1 × 7.8 and 3.7 × 5.1 Å) and the hydroxyl groups on the pore surfaces of the framework. In addition, this group also studied the C_2H_2 storage performance of several MOFs, including HKUST-1, Cu_2(bptc) (MOF-505, bptc = 1,1′-biphenyl-3,3′,5,5′-tetracarboxylate),[323] MOF-508, MIL-53, MOF-5, and ZIF-8.[324,325] Among them, HKUST-1 presented the highest C_2H_2 storage capacity with an uptake of 201 cm^3/g at 295 K and 1 atm, which was believed to be a result of strong interactions of C_2H_2 molecules with the open Cu(II) sites in the framework.

2.1.6. Nobel Gases and Others. Nobel gases, including He, Ne, Ar, Kr, Xe, and Rn, have a lot of important industrial applications. For example, Kr is applied as a filler in the lamp industry, and Xe is used as a narcotic medicinal gas. These gases possess very similar properties and occur naturally as mixtures with other gases; thus, the separation of them is important but challenging. In industry, Ne, Ar, Kr, and Xe are separated from air and He from natural gas by using cryogenic distillation.[111] The separation of noble gases by MOFs as carriers is promising, but largely unexplored. Mueller and co-workers[309] were the first to

dx.doi.org/10.1021/cr200190s |*Chem. Rev.* 2012, 112, 869–932

demonstrate that a simple process of pressure-swing adsorption is feasible in the separation of noble gases by using HKUST-1 as adsorbent. The experimental results showed that HKUST-1 can selectively separate Xe and Kr by a continuous adsorption. It was found that Xe was adsorbed preferentially, while Kr was adsorbed to a much lesser extent. The calculated capacity of HKUST-1 for Xe is more than 60 wt %, almost twice as much as that on a high-surface-area activated carbon.

Apart from the gases discussed above, some other gases have also been investigated in this topic. For examples, Krungleviciute and co-workers[326] tested the kinetic and equilibrium adsorption of CF_4 and Ar on $Co_3(bpdc)_3(bipy)$ (bpdc = biphenyldicarboxylate) and HKUST-1. The presence of kinetic differences in the adsorption and of sterically controlled adsorption sites in the respective frameworks suggested that these two MOFs should, in principle, be usable for the separation of a mixture containing the two gases. Bülow and co-workers[126] reported the selective adsorption of N_2O over N_2 and O_2, and C_2H_4 over CO in HKUST-1 at 295 K. Kitagawa and co-workers[166] revealed that CPL-11 is able to selectively adsorb Xe and CCl_4 over O_2, N_2, and Ar, and Zhou and co-workers[268,269] showed that MAMS-1−4 are capable of selectively adsorbing CH_4 over C_2H_4 at 143 K, C_2H_4 over C_3H_6 at 195 K, and C_3H_6 over iso-C_4H_{10} at 231 K.

2.2. Selective Adsorptions and Separations of Chemicals in the Vapor Phase

Apart from light gases, vapors of various liquid compounds were also tested for their selective adsorption and separations in MOFs. Experimental approaches within this topic include vapor adsorption at room temperature or higher, breakthrough experiments of binary mixtures, gas chromatography (GC), and others. Characterization in each experiment is also diverse, ranging from isotherms to direct TG measurements to evaluate the adsorption capacity.

2.2.1. Small Solvent Molecules. Separation and purification of organic solvents, particularly the removal of water, are of importance in a wide range of applications. Although little work has been reported for an exclusive purpose of special separation, a lot of MOFs have been tested for the adsorption of these small molecules in the vapor phase, and some of them revealed significant adsorption selectivities and separation potential. There are essentially two explanations (or mechanisms), (A) size/shape exclusion and (B) different interactions between sorbates and pore surfaces of MOFs, that can be used to understand the observed preferential adsorption of these solvent vapors in MOFs. In most cases, both mechanisms operate together and complement each other. The flexibility of some MOF frameworks does, however, sometimes complicate the explanation for the observed adsorption performance. In these cases, the adsorption of guest molecules can lead to structural transformations and even changes in the composition of these soft materials, such as opening from no or small pores to large pores, to accommodate guest molecules. We refer to this type of selective inclusion as a third (C) mechanism. Table 2 lists some MOFs that have been examined and shown selective adsorption of various solvent vapors.

Whichever mechanism, the selective adsorption and separation is determined by the properties, including size and shape, of both adsorbate molecules and the pores of the MOF. For the size/shape-based selective adsorption in a rigid MOF, a typical example is the preferential adsorption of benzene over cyclohexane observed in $NH_4[Cu_3(OH)(4\text{-cpz})_3]$.[170] This MOF has a rigid, anionic 3D framework structure containing large cages, which are connected by small windows of 4.5 × 8 Å in size. The NH_4^+ cations reside in the large cages and are exchangeable with other cations. It was found that when this MOF was exposed to benzene/cyclohexane (1:1) mixtures benzene was significantly enriched to give a ratio of 5:1 for benzene/cyclohexane in the adsorbed phase. Even more interesting is that, after exchanging NH_4^+ with larger Et_3NH^+ or $Li(H_2O)_4^+$ cations, the resulting materials displayed a further enhanced preferential uptake for benzene over cyclohexane, with enriched ratios of 8:1 and 12:1, respectively. This increase can be attributed to the greater bulk of the cations and correspondingly resulting smaller pores in the MOF. Thus, this MOF is a viable candidate for the separation of benzene and cyclohexane, which cannot be separated by a distillation process due to their close boiling points of 80.1 and 80.7 °C.

Although some flexible MOFs undergo structural changes during guest adsorption to produce open or closed pores, both forms have definite pore metrics and are therefore still available for size and/or shape selective adsorption. For example, the selective adsorption of H_2O and MeOH over EtOH, THF, and Me_2CO vapors was observed in flexible Cd(pzdc)(bpee) at room temperature.[330] This MOF has a 3D pillared-layer structure containing 1D channels with a window size of 3.5 × 4.5 Å in its as-synthesized state. Despite the framework's flexibility, the adsorption selectivities were mainly attributed to the size constraints of the channels. Similarly, based on vapor phase measurements, the size/shape-dependent selective adsorptions of some small molecule solvents have also been observed in rigid $Zn(SiF_6)(pyz)_2$,[347] $Ag(tmpes)\cdot BF_4$ (tmpes = tetrakis[(4-methylthiophenyl)ethynyl]phenylsilane),[344] $Zn_4(OH)_2(1,2,4\text{-btc})_2$,[224] $Cd(abppt)_2\cdot(ClO_4)_2$ (abppt = 4-amino-3,5-bis(4-pyridyl-3-phenyl)-1,2,4-triazole),[345] and flexible MIL-96[349] and Cu(inaip) (inaip = 5-(isonicotinamido)isophthalate),[175] as shown in Table 2.

Zn(tbip) (tbip = 5-*tert*-butyl isophthalate), on the other hand, is a rigid 3D framework containing close-packed 1D hydrophobic channels, 4.5 Å in size.[332] It was demonstrated that these hydrophobic channels only allow MeOH and DME molecules to be adsorbed while excluding H_2O. Further experiments also showed that DME and MeOH could also be separated by this MOF based on their different uptakes. These selective adsorptions were attributed to the hydrophobic pores in the MOF, which prefer to adsorb hydrophobic guest molecules such as DME. A similar hydrophobic effect has also been observed in $Zn(bdc)(ted)_{0.5}$ (ted = triethylenediamine),[215,338] Cu(etz) (Hetz = 3,5-diethyl-1,2,4-triazole),[341] Al(OH)(1,4-ndc),[139] and $Cu_2I_2(bttp4)$ (bttp4 = benzene-1,3,5-triyltriisonicotinate).[182]

MOFs with hydrophilic pore surfaces, usually decorated by specific functional groups or adsorption sites, prefer to selectively adsorb small, hydrophilic molecules. Active adsorption sites can form favorable interactions, such as coordination, hydrogen bonding, or π---π stacking, with guest molecules. These interactions, in most reported examples, induced a structural transformation of the flexible framework from an amorphous to crystalline or crystalline to crystalline phase. A typical example is Ln(tci) (Ln = Ce or Pr; H_3tci = tris(2-carboxyethyl)isocyanurate),[333] which has a nonporous 3D structure. Upon exposure to water vapor, these MOFs adsorbed water molecules to form a 2D layer structure with some of the adsorbed molecules coordinated to metal atoms, while MeOH vapor was not adsorbed. MOFs showing selective vapor adsorption, combined with a structural transformation induced by H-bonding interactions between adsorbate molecules and the framework, include $Cu_2(pzdc)_2(dpyg)$

dx.doi.org/10.1021/cr200190s |*Chem. Rev.* 2012, 112, 869–932

(dpyg = 1,2-dipyridylglycol),[327] $Co(NCS)_2$(3-pia) (3-pia = *N*-(3-pyridyl)isonicotinamide),[328] Cu(2,3-pydc)(bpp),[237] Ce(tci)(H_2O),[334] (H_2dab)[$Zn_2(ox)_3$],[352] and $Cd(4\text{-btapa})_2(NO_3)_2$ (4-btapa = 1,3,5-benzene-tricarboxylic acid tris[*N*-(4-pyridyl)amide]).[335] Additional examples of MOFs that underwent phase changes induced by other weak interactions (such as π---π and H---π) that lead to the final selective adsorption of different solvent molecules are Zn(TCNQ−TCNQ)(bipy),[339] Co_2(2,6-ndc)$_2$(bipyen) (bipyen = *trans*-1,2-bis(4-pyridyl)ethylene),[329] [Ni(bpe)$_2$(N(CN)$_2$)](N(CN)$_2$) (bpe = 1,2-bis(4pyridyl)-ethane),[280] Zn(TCNQ−TCNQ)(bipy),[266,339] Cu(etz),[341] and MIL-53(Cr).[348]

It should also be pointed out that some structural transformations of MOFs during adsorption are also shape- or size-dependent on the adsorbate molecules. The associated examples showing selective vapor adsorptions include Co_2(2,6-ndc)$_2$(bipyen),[329] $Co(NCS)_2$(3-pia),[328] Cd(pzdc)(bpee),[330] [Mn(NNdmenH)][Cr(CN)$_6$],[337] Gd_2(dhtp)(dhtpH$_2$)(H_2O)$_5$ (H_4dhtp = 2,5-dihydroxyterephthalic acid),[343] Gd_2(dhtp)(dhtpH$_2$)(H_2O)$_4$,[343] KHo-(C_2O_4)$_2$,[346] Zn(ip)(bpa) (ip = isophthalate; bpa = 1,4-bis(4-pyridyl)acetylene),[350] and $Na_2Co(ip)_2$.[154] Furthermore, combining size/shape and host−guest interaction effects, the structural transformation of flexible MOFs has also been observed in the selective adsorption of small solvent molecules in the vapor phase. Some MOFs illustrating this are $Zn_2(ip)_2(bipy)_2$,[336] Na_2Cu-(2,4-pydc) (2,4-pydc = pyridine-2,4-dicarboxylate),[342] Cu(2,5-pydc) (2,5-pydc = pyridine-2,5-dicarboxylate),[342] and Cu(1,4-ndc).[219] The relative selective adsorptions of different molecules for each of the above-mentioned MOFs are given in Table 2. For some examples, although there is no a direct evidence from the original report, structural transformations upon guest selective adsorption, a combination of size/shape and guest−host interaction effects could be responsible for their adsorption behavior. In one particular case, Cu(bpe)$_{1.5}$(1,4-ndc)[331] is capable of selectively adsorbing H_2O over N_2, CO_2, and MeOH. This MOF has a 3-fold-interpenetrated 3D framework composed of interlocking 2D bilayer networks, with a total effective pore size of 2.11 × 1.88 Å. The observed selective adsorptions were explained by the combined effect of guest size and special interactions, which probably induced pore extension.

Besides the selective adsorption of solvent vapor molecules observed in some MOFs, the chromatography separation of solvents in the vapor phase using MOFs as the stationary phase has also been reported. For example, amino-MIL-53(Al) showed an efficient separation for benzene and cyclohexane in using a GC method.[340] The selective adsorptions and separations observed in these MOFs have suggested several very important potential applications in the separation and purification of solvents, for example, benzene and toluene, benzene and cyclohexane, and water and organic solvents, all of which are important in industrial productions.

2.2.2. C8 Alkylaromatic Isomers. C8 alkylaromatic isomeric compounds consisting of *o*-xylene (oX), *m*-xylene (mX), *p*-xylene (pX), and ethylbenzene (EB) are important industrial feedstock chemicals: pX is used to produce polyethylene terephtalate for the polyester industry; oX is used to obtain phthalic anhydride (a plasticizer); mX is used to produce isophthalic acid, used in PET resin blends; and EB is used to produce styrene.[353] Unfortunately, in industry these isomers are always produced as mixtures containg all four components, which must be separated before further use. The separation of these isomers remains a challenge, particularly the separation of pX from mX and EB by, for example, a distillation process, because of their close boiling points. Alternately, fractional crystallization and/or adsorption has been used in industry. Commercially, these four C8 aromatics are currently separated mainly via fractional crystallization;[354] cation exchanged faujasite zeolites are the only adsorbents currently being used in the bulk separation of these isomers.[355]

MOFs are promising adsorbents for the separation of C8 alkylaromatic isomers, although only a limited number have thus far been tested. Experimental exploration of separating C8 alkylaromatic components in the vapor phase with MOFs was first performed by Denayer and co-workers.[356] Breakthrough experiments of their binary mixtures on MIL-47 showed that the separation of these isomers could be achieved with exception of the pX/oX mixture. The selectivities evaluated from the mixed vapor adsorptions follow a trend of oX > pX > mX > EB, which is in agreement with the observations from single-component isotherms. The high selectivities for pX over EB (1.83) and pX over mX (2.07) were achieved in the binary separation at 70 °C. It was also found that the adsorption selectivity increased with an increasing degree of pore filling in each case, indicating that selectivity is pressure dependent. Furthermore, in terms of mX and pX, the selectivity decreased at higher temperature. This temperature dependence was also observed in a quaternary breakthrough experiment containing all isomers. Combining the gas-phase adsorption studies, the authors concluded that the efficient separation of these components at a high pore filling in the vapor phase is a result of differences in packing modes of these molecules in the pores of MIL-47.

As a follow-up study, this group also tested the vapor-phase adsorption and separation of these isomers on MIL-53(Al),[357] a well-studied flexible MOF.[234] It was found that the breathing of its framework, once again, strongly affected the separation of these mixtures. Breakthrough experiments of equimolar oX/EB mixtures revealed that there was no adsorption preference below the "pore-opening" pressure; above it, however, the selectivity increased with increasing pressure (degree of pore filling), resulting in an ultimate separation factor of 6.4 for oX over EB at 110 °C. Similar to MIL-47, high separation performance at high pore filling in the open form of MIL-53(Al) was believed to be a result of different packing modes of the adsorbed molecules in its pores. In addition, the observed dependence of adsorption selectivity on pressure and temperature in MIL-47 and -53(Al) suggests the possibility of using a method, such as PSA or TSA, to optimize the adsorptive separation process when using the two MOFs.

Similarly, Chen and co-workers[358] reported the vapor-phase adsorption and separation of these isomers on Zn(bdc)-(dabco)$_{0.5}$, which has a 3D porous structure with 1D channels of about 7.5 × 7.5 Å interconnected by small windows of 3.8 × 4.7 Å. Single- and multicomponent fixed-bed experiments revealed that the Henry's constant for oX is significantly higher than that of all other components, which have rather close values. In addition, the adsorption affinities were also estimated, to give an order of oX > mX > EB > pX. Binary and quaternary breakthrough experiments also demonstrated that this MOF has the ability to separate oX from other C8 alkylaromatic isomers. High adsorption selectivities were observed for oX over EB and oX over pX in the respective binary mixture measurements, with the evaluated selectivity factors of 1.62 and 1.88, respectively, at 175 °C. The separation selectivity of oX over other components was attributed to stronger interactions between oX molecules and the framework, as well

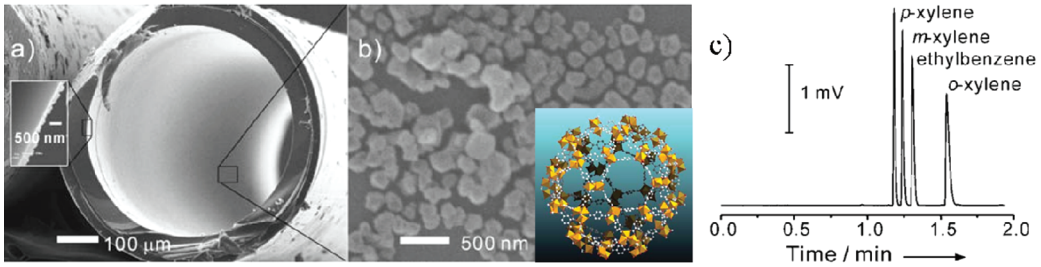

Figure 10. (a) SEM image of the cross section of MIL-101 coated capillary column (inset shows the thickness of the MIL-101 coating), (b) SEM image of MIL-101 microcrystals deposited on the inner wall of the capillary column (inset shows the structure unit of MIL-101); and (c) GC separation of xylene isomers and EB on the MIL-101 coated capillary column (15 m long × 0.53 mm i.d.) at 160 °C under a N_2 flow rate of 3 mL min^{-1}. Reproduced with permission from ref 361. Copyright 2010 Wiley-VCH.

as the differences in pore-filling and molecular packing in the pores.

The vapor-phase adsorption and separation of these isomers on MOF-5[31] and $Zn_3(bdc)_3$ (named MOF-monoclinic)[359] was also explored by Yan and co-workers,[360] by means of pulse GC, static vapor-phase adsorption, and breakthrough adsorption. It was demonstrated that the two MOFs exhibited different selectivity and separation efficiency toward these isomers. Pulse GC revealed that MOF-5 is indeed effective in separating EB from other isomers, whereas $Zn_3(bdc)_3$ showed stronger retention for pX over the other isomers. Binary breakthrough experiment on MOF-5 resulted in an average selectivity of 1.96, 2.34, and 4.14 for EB over oX, mX, and pX, respectively. For $Zn_3(bdc)_3$, the evaluated average selectivity was 2.52 for mX over pX, 5.17 for EB over pX, and 4.55 for oX over pX. Further analysis concluded that the adsorption and separation of these compounds is equilibrium-constant-controlled in MOF-5 and diffusion-dominated in $Zn_3(bdc)_3$.

Furthermore, this group also reported the high-resolution GC separation of C8 alkylaromatic isomers with a MIL-101-coated capillary column (Figure 10a) that was fabricated by a dynamic coating method.[361] MIL-101 is a highly stable, porous MOF with CUMs. It was found that the baseline separation of the four isomers on the capillary column by GC was achieved without the need for temperature programming (Figure 10b). Further experiments showed that the separation selectivity decreased with increasing temperature, whereas column efficiency improved. Moreover, increasing the injected analyte mass resulted in no change in retention time, implying stable separation performance of the column. The excellent separation performance of the MIL-101 coated capillary column was believed to be related to the CUMs and well distributed polarity in the MIL-101 framework. In addition, high-resolution GC separations of other isomer mixtures, including *o*-, *m*-, and *p*-chlorotoluene, 1,3,5-trimethylbenzene, *n*-propylbenzene, and isopropylbenzene, and a mixture of *n*-alkanes with different numbers of carbons, on this MOF-coated capillary column were also demonstrated in this work.

In addition, the selective adsorption of these isomers in the vapor phase has also been observed in several other MOFs. $Co(HCO_2)_2$ having a 3D structure with small apertures exhibited the selective adsorption of EB over pX at 40 °C.[362] $Cd(abppt)_2\cdot(ClO_4)_2$ with a 2D porous structure showed the selective uptake of oX and mX over pX from an equimolar vapor mixture at room temperature.[345] A reverse selectivity, pX over the other isomers, was also reported on In(OH)(oba) (H_2oba = 4,4′-oxybis(benzoic acid)) at room temperature.[363]

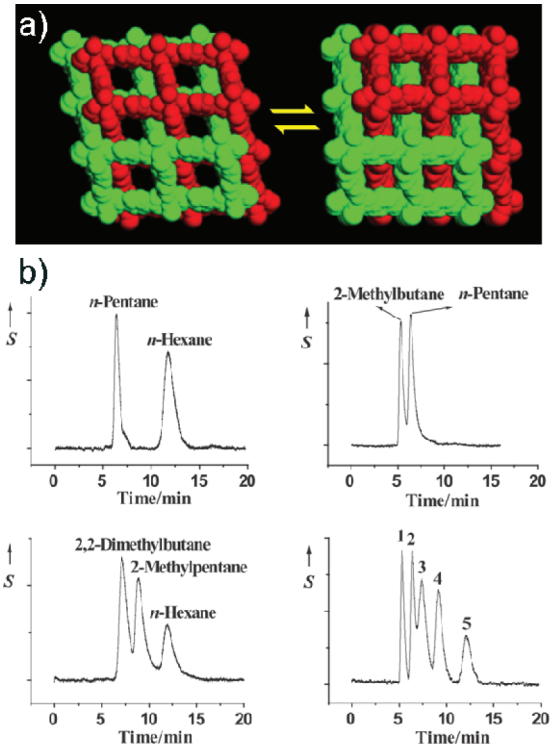

Figure 11. (a) Space-filling representation of the structures of MOF-508 showing the interconversion between the open and dense phases (the two interpenetrating frameworks are shown in red and green); and (b) chromatograms of alkane mixtures separated on a MOF-508 column (bottom right, the alkane mixture containing 2-methylbutane (1), *n*-pentane (2), 2,2-dimethylbutane (3), 2-methylpentane (4), and *n*-hexane (5); *S* = thermal conductivity detector response). Reproduced with permission from ref 366. Copyright 2006 Wiley-VCH.

2.2.3. Aliphatic Isomers. Similar to the separation of alkylaromatic isomers discussed above, the separation of aliphatic isomers is also crucial in industry.[364] As an example, the separation of hexane isomers to boost octane ratings in gasoline has been a very important process in the petroleum industry, which is currently accomplished by cryogenic distillation.[365] Alternative processes, such as adsorption, are expected to lower the energy consumption involved in the distillation. The first example using MOFs to separate aliphatic isomers was reported by Chen and coworkers.[366] They examined the gas-chromatography separation of alkanes (mainly for their isomers) using $Zn(bdc)(bipy)_{0.5}$ (MOF-508) acting as the stationary phase in a column. MOF-508 has a

dx.doi.org/10.1021/cr200190s |*Chem. Rev.* 2012, 112, 869–932

doubly interpenetrated 3D framework with changeable pores based on the movement of single networks with respect to each other, producing open and dense forms (Figure 11a). The framework transformation is reversible and dependent on the uptake and removal of guest molecules. The open structure of this MOF has a cross-section pore size of 4.0 × 4.0 Å. As shown in Figure 11b, this MOF-508 column can efficaciously separate *n*-pentane from *n*-hexane and their respective isomers including 2-methylbutane, and 2-methylpentane and 2,2-dimethylbutane, even from mixtures containing all of these alkanes. The effective GC separation on MOF-508 observed herein was believed to be a result of different interactions between alkane molecules and the pore walls of the framework, which arise from subtle matches of the size and shape of the alkane molecules with the pores.

Following this work, the kinetic separation of hexane isomers by fixed-bed adsorption was studied by the same group on $Zn(bdc)(dabco)_{0.5}$, which has a 3D pillar-layered framework similar to that of MOF-508, but noninterpenetrated.[367] The structure of this MOF contains two types of intersecting channels of about 7.5 × 7.5 Å and 3.8 × 4.0 Å in size. By using the small channels that can exclusively take up linear *n*-hexane while blocking branched isomers, this MOF exhibited extraordinary selectivity. The efficient separation was supported by both pure component and mixed vapor-phase breakthrough experiments. Furthermore, the selective adsorption of linear and monobranched hexane isomers (*n*-hexane and 3-methylpentane) over a dibranched one (2,2-dimethylbutane) has also been observed in $Zn_2(Hbdc)_2(dmtrz)_2$ (Hdmtrz = 3,5-dimethyl-1*H*-1,2,4-triazole), by Zhao and co-workers.[368]

In addition, a pulse chromatography study revealed that flexible amino-MIL-53(Al) is capable of separating C5, C6, and C7 alkane isomers.[340] The selectivity was evaluated to be of 1.7 for *n*-pentane over 2-methylbutane; 2.1, 2.1, 2.3, and 3.4 for *n*-hexane over 2-methylpentane, 3-methylpentane, 2,3-dimethylbutane, and 2,2-dimethylbutane, respectively; and 2.1, 2.4, 2.9, 3.2, and 3.7 for *n*-heptane over 2-methylhexane, 3-methylhexane, 2,3-dimethylpentane, 2,4-dimethylpentane, and 3,3-dimethylpentane, respectively. It was also found that Henry's constants and adsorption enthalpies of iso-alkanes are lower than those of the linear alkanes, suggesting a shape selective effect of this MOF. Prior to this work, an adsorption study of *n*-alkanes in flexible MIL-53, to probe the influence of framework flexibility on the adsorption of nonpolar vapors, was performed.[369] The shape-dependent selective adsorption of linear over branched alkanes was also observed in rigid HKUST-1 for C5, C6, and C7 alkane isomers, evaluated by a similar method.[370] In this report, the preferential adsorption of this MOF toward linear alkanes over their branched isomers was explained as that linear alkanes fit better into the pores of the MOF, resulting in a stronger interaction with the framework. Furthermore, molecular simulation studies were also conducted to evaluate the separation performance of alkane isomers in MOF-5 and $Zn_4O(R_6\text{-bdc})_3$ (IRMOF-6, R_6-bdc = 1,2-dihydrocyclobutabenzene-3,6-dicarboxylate[307]).[371,372]

2.2.4. Others. Apart from the above-discussed vapor-phase selective adsorption and separation of arbitrarily classified and relatively widely explored chemicals on MOFs, there were several reports that dealt with other vapor-phase selective adsorptions. MIL-47 was found to be capable of selectively adsorbing thiophene from CH_4, a process related to natural-gas cleanup.[373] It was demonstrated early, that upon guest adsorption and desorption, the channels of MIL-47 can open and close reversibly, which was induced by the interactions between the guest molecules and the host framework.[374] This selective removal of sulfur-containing molecules from CH_4 can thus be attributed to the noncovalent oriented weak interactions in the packing of thiophene molecules within the channels of the MOF, which are strong enough to open the channels to allow these molecules to be adsorbed.

In another early publication, Li and co-workers[375] reported the adsorptive separation of hydrocarbons in the vapor phase with $Cu(hfipbb)(H_2hfipbb)_{0.5}$ (H_2hfipbb = 4,4′-(hexafluoroisopropylidene)-bis(benzoic acid)). This MOF has a 3D framework structure with hydrophobic channels consisting of large elliptic chambers connected by small necks. It was revealed that this MOF adsorbed methanol, propane, propene, and *n*-butane vapors rapidly, but did not soak up any *n*-pentane, 2-methylpropane, 3-methylbutane, *n*-hexane, and 3-methylpentane at room temperature. This observed selectivity for shorter molecules over longer ones was attributed to the limited chamber length of 7.3 Å in the MOF. This chamber space is slightly longer than the length of *n*-C4 (∼6.9 Å), but shorter than the length of *n*-C5 (8.1 Å). The small neck in the structure was otherwise responsible for the observed adsorption selectivity of normal over branched molecules. The diameter of the neck is approximately 3.2 Å, which is too small to allow branched alkanes with diameters of around 3.9 Å to pass.

Recently, Lang and co-workers[376] reported the adsorptive separation of a solid mixture of naphthalene and anthracene (through sublimation) by $Ni_2(\mu_2\text{-}OH_2)(1,3\text{-bdc})_2(tpcb)$ (tpcb = tetrakis(4-pyridyl)cyclobutane). This MOF has a diamond-type topological framework with 1D channels composed of larger chambers linked by small kite-shaped windows. The effective aperture size of the MOF is approximately 10.0 × 6.4 Å. It was found that at room temperature this MOF can selectively adsorb sublimed naphthalene, which was accompanied by a single-crystal-to-single-crystal transformation, but completely excluded anthracene. Because of the same kinetic diameter of the two molecules, the observed selective adsorption of naphthalene over anthracene can be attributed to suitable guest−host interactions that are indeed shape-dependent on the guest molecules. This has been confirmed by the following single-crystal structural refinement of the guest-loaded MOF. It is also interesting that the adsorbed naphthalene molecules can be easily exchanged with EtOH; after removal of EtOH, the MOF is thus regenerated and thereby reusable.

In addition, some research, although not conducted for the selective adsorption and separation of special chemicals, can offer valuable information for understanding their behaviors in adsorption by MOFs. For example, Jobic and co-workers[377] studied the chain-length dependence of the diffusion of *n*-alkanes in MIL-47, which is closely relevant to the alkane separation processes. Similarly, Stallmach and co-workers[378] explored the self-diffusion of C3 to C6 hydrocarbons adsorbed in the HKUST-1, by means of pulsed field gradient NMR and molecular dynamics (MD) simulations.

3. MOFS FOR LIQUID-PHASE ADSORPTIVE SEPARATIONS

Similar to those in gas-phase separations, MOFs are also attractive candidates as adsorbents for liquid-phase separations. "Liquid phase" in the context of this Review refers to both liquid

chemicals (such as water and commonly used organic solvents) at standard temperature and pressure (STP) and solutions of dissolved solid chemicals. As we know, the separation of liquids, such as various solvents, is usually accomplished by distillation in view of its simple procedure and, to a certain extent, energy efficiency. Exceptions to this rule are in the separation of chemical isomers, where the boiling points of components are too close, or when components of a mixture are unstable or reactive at elevated temperature. In the latter case, distillation under reduced pressure and/or cryogenic conditions is sometimes possible, but dramatically increases energy consumption and therefore cost. Adsorptive separation or membrane-based separation, where molecular shape, size, and some other properties are the key factors, is thus an appealing alternative, because elevated temperatures, used to vaporize the compounds, are not required. For the separation of solid chemical mixtures, recrystallization from a suitable solvent is usually the first choice; however, in cases where components prefer to cocrystallize with each other, such as enantiomers, adsorptive separation has a significant advantage. The same holds true, for small-dose sample separation, especially for purification, where adsorptive separation is always predominant, as a matter of convenience.

Liquid-phase adsorptive separation process includes two main events: adsorption and desorption, with little difference in implementation from gas-phase separation.[105] Adsorption of an adsorbate onto the adsorbent is dictated by the characteristics of the adsorbate−adsorbent interaction. The difference arises during desorption in that a desorbent, which should be a suitable liquid, capable of displacing the adsorbate from the adsorbent, is required. After desorption, the desorbent will be separated from the extracted product usually by fractionation or evaporation, and then recycled back into the system.

Industrial adsorptive separations for liquids are widely adopted and most successful when the species involved have very close boiling points, which make distillation expensive or impossible, or when the species are thermally sensitive at distillation temperatures as mentioned above.[105] In fact, a lot of chemicals have been produced by liquid-phase separation or purification upon selective adsorption on porous materials, such as zeolites, activated carbon, and metal oxides. These applications hold a big market share in the pharmaceuticals, fine chemicals, and petrochemical industries. However, many challenging liquid-phase separations still remain, such as the separation of xylenes or *cis*- and *trans*-olefins. Continuous efforts to find optimal adsorbents and explore new separation feeds have been a steady subject matter in separation science. As compared to the gas phase, less attention has been paid to using MOFs for liquid-phase separations. However, in recent years, there has been an obvious emergence of focused research, some examples of which have been highlighted by Matzger and coworkers[102] in an early review.

Liquid-phase adsorption can, apart from simply investigating the inclusion of different guest molecules into a MOF, provide new insights into the pore properties (size, shape, and surface functions). Early works were primarily focused on the selective binding and inclusion of MOFs with respect to guest molecules. Recently, more and more investigations have transitioned to design MOFs to separate a target mixture, not only by predesigning pore size, shape, and surface properties but also by postmodification of their pores. The selective adsorption and separation of chemical species in the liquid phase by MOFs can be characterized and evaluated by adsorption isotherms, breakthrough experiments, chromatography, crystal structure refinement of the adsorbed state, and a few other methods.

This section summarizes the research progress in liquid selective adsorption/binding and separation by MOFs, with highlights of typical examples. Because we are evaluating the potential application of MOFs as adsorbents for separations, the selective inclusion of liquid solvent molecules or other organic compounds, which act as templates during the synthesis of MOF crystals, is not included in this Review. It should also be pointed out that there have been some reports about the selective accommodation of organic molecules, which is related to the topic of selective catalysis in MOFs.[79,82−84,379] These catalysis-related selective adsorptions are not covered in this Review.

3.1. Selective Adsorptions and Separations of Chemically Different Species

Liquid-phase selective adsorption, inclusion, and separations of chemically different compounds, mainly organic compounds including small solvents and large organic molecules, have been tested on some MOFs. Most of the published results only include selective adsorption but not the separation of a liquid mixture. There is, in fact, nearly infinite potential of inclusion and separation of various organic molecules with porous materials, particularly large organic compounds; however, the related reports for MOFs are very limited. On the basis of the properties of the sorbates and/or the adsorption performance observed, we will discuss the related research progress of the following four groups of chemical species: organic molecules with different functional groups; organic molecules with different shape and size; organosulfur compounds; and ionic species.

3.1.1. Organic Molecules with Different Properties/Functional Groups. One of the advantages of using MOFs as porous materials for adsorption-related applications is the ease of modification of their pore surfaces. This leads to the different adsorption preference for different guest molecules, especially those with special chemical functional groups. These groups can introduce different/preferred interactions with the host frameworks, leading to the so-called selective adsorption. Among various host−guest interactions, π---π stacking, H-bonding, and the coordination with metal sites play important roles in the preferred adsorption and selective recognition. In addition, the hydrophilic−hydrophobic or polar−apolar properties of guest molecules are also at play when contacting the pore surface of a MOF. It should be pointed out that in some cases, the strong interactions between guest molecules and the framework can induce structural change or framework transformation, which consequently affects the selectivity for these guests. These properties based on flexibility of the structure are unique to MOFs and inaccessible to other solid sorbent materials, such as zeolites. The MOFs with this property indeed possess great potential in liquid-phase separations.

The first exploration of MOFs for selective binding of guest molecules in the liquid phase was performed by Yaghi and coworkers[380] on Co(Hbtc)(py)$_2$, which has a sheet structure constructed by Hbtc^{2-} ligands linking Co(II) atoms. These sheets stack to give alternating Co(II)-carboxylate and py (coordinated to Co(II)) layers in its 3D structure. It is important that the py ligands hold these layers together by π---π stacking to create a rigid 3D structure with rectangular channels of 7 × 10 Å in which guest molecules reside. After removal of guest molecules, the channel structure remains unaltered, which allows the guest to be adsorbed by these pores. Adsorption experiments (typically by suspending the guest-free MOF sample in a mixture including several solvents for a given time and then filtrating the

dx.doi.org/10.1021/cr200190s |*Chem. Rev.* 2012, 112, 869–932

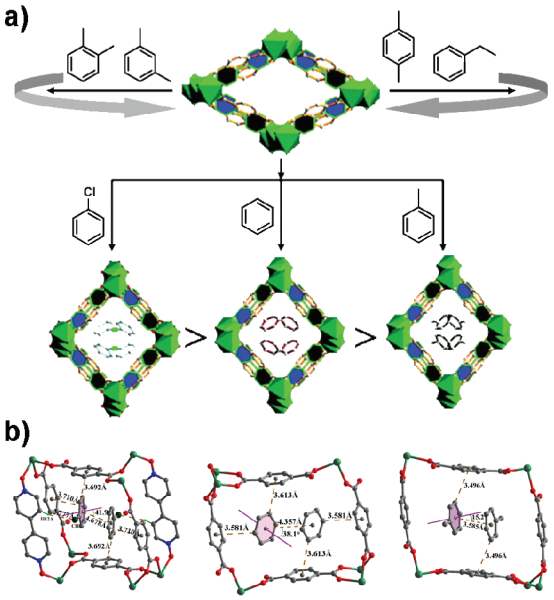

Figure 12. (a) Selective absorptions of C6−C8 aromatics by single crystals of MIL-53(Mn^{II}); and (b) details of noncovalent bondings of guest−guest and guest−linker interactions in guest loaded MIL-53-(Mn^{II}). Reproduced with permission from ref 381. Copyright 2010 American Chemical Society.

solvent and drying the MOF), combined with characterization by IR spectroscopy demonstrated the selective adsorption of aromatic molecules including benzene, nitrobenzene, cyanobenzene, and chlorobenzene over nonaromatic components including acetonitrile, nitromethane, and dichloroethane from their binary mixture. The authors attributed the remarkable selectivity of this MOF toward aromatic molecules to their π-stacking with the btc^{2-} entities within the MOF sheets.

The selective adsorption of C6−C8 aromatics (including benzene, toluene, ethylbenzene, chlorobenzene, and three xylene isomers) in the liquid phase has also been reported by Wang and co-workers[381] on a MIL-53 analogue, $Mn_2(bdc)_2(bpno)$ (MIL-53(Mn^{II}), bpno = 4,4′-bipyridine-*N*,*N*′-dioxide). Single-component adsorptions of benzene, toluene, xylenes, ethylbenzene, and chlorobenzene by MIL-53(Mn^{II}) showed that only C6−C7 molecules could be intercalated into this MOF as confirmed by single-crystal structure determination (Figure 12a). In the case of a two-component mixture of benzene and toluene, only benzene was selectively adsorbed. These observed selective adsorptions were mainly attributed to the different degrees of π---π interactions including those of guest−guest and guest−linker, and other noncovalent interactions (Figure 12b). A higher adsorption selectivity of chlorobenzene over benzene was also observed in this MOF, probably due to C−H---Cl hydrogen bonding between each chlorobenzene and the ligands. In addition, the packing efficiency, where increasing the number of electron-donating substituent groups can lead to an increase of intermolecular repulsions and thus lower packing, may also be a contributing factor in filling guest molecules into the channels of the MIL-53(Mn^{II}).

The presence of CUMs in MOFs and other porous materials has an important influence on the adsorption and inclusion of guest molecules, especially those with potentially coordinating functional groups. The selective binding of guest molecules in liquid phase by MOFs due to the coordination of guest molecules with CUMs was observed early by Yaghi and co-workers[382] on $Zn_2(btc)(NO_3)\cdot$(guest). This MOF possesses a 3D framework structure with open channels that are 14 Å across. After removal of the coordinated guest molecules, the now CUMs in the framework provided a unique environment for promoting the selective binding of special guests into this MOF. The adsorption experiments showed that this material has the ability to bind small nonhindered alcohols, including methanol, ethanol, 1-propanol, isopropyl alcohol, 1-butanol, and *tert*-butyl alcohol, but cannot bind nonalcoholic molecules, including chloroform, 1,2-dichloroethane, acetonitrile, nitrobenzene, cyanobenzene, toluene, acetone, and methyl ethyl ketone. Furthermore, GC results also revealed a high selectivity toward methanol of this material, but little competition was observed among C3 and C4 alcohols and C5 and C7 alcohols. This gave an overall order of alcohol selectivity of C1, C2 > C3, C4 > C5, C7, which is in qualitative agreement with that expected on the basis of a shape and size selective inclusion process. Additionally, the ability of alcohols to form hydrogen bonds with the O atoms of the btc^{2-} ligands and nitrate (NO_3^-) counterions may also play an important role in the selectivity toward the alcohol molecules, which was further supported by the selective binding of DMF.

Selective adsorption of liquid molecules with different functional groups was also observed in another MOF with CUMs, $CoT(p\text{-}CO_2)PPCo_{1.5}$ (PIZA-1, $H_4T(p\text{-}CO_2)PP$ = *meso*-tetra(4-carboxyphenyl)porphine), reported by Suslick and co-workers.[383] As shown in Figure 13a, this MOF has a robust 3D structure with two types of oval-shaped channels of 9 × 7 and 14 × 7 Å in size, and the pore surface was functionalized by two types of CUMs. As shown in Figure 13b. for the series of functionalized *n*-alkanes including hexyl alcohol, thiol, nitrile, aldehyde, bromide, amine, and hexane itself, this MOF exhibited a substantial adsorption of *n*-hexylamine compared to others. The preference for *n*-hexylamine was attributed in part to its increased hydrophobicity and its strong coordinating capability. Sorption of *n*-hexane was also achieved by successive washings of the solid with pyridine solution of hexane with a higher concentration. The authors hypothesized that the accessibility of the interior of PIZA-1 requires the presence of a hydrophilic molecule, such as pyridine, that can then allow the pores to be accessible for hydrophobic molecules (hexane). In addition, the selective adsorption of water from benzene, toluene, and tetrahydrofuran has also been observed, attributed to its strong coordination with CUMs in the MOF.

Similarly, selective adsorption of amines from acetonitrile was observed in $Zn_3(btc)_2$ nanocrystals synthesized using an ultrasonic method.[384] The selectivities were tracked by changes in luminescence of the solid MOF samples. It revealed high selectivity for ethylamine, the adsorption of which led to quenching the luminescence. This selective adsorption of ethylamine from acetonitrile and luminescent sensing was believed to be a result of strong interactions between the amine and CUMs in the MOF. Much larger amines such as *n*-propylamine, *n*-butylamine, and aniline showed no or only a weak effect on the luminescence of the framework, most likely because they blocked diffusion into the channels of the MOF. This MOF thus also exhibited a remarkable selective adsorption of ethylamine from other large amines.

Apart from the observed selective adsorption of liquid molecules with different functional groups in MOFs having CUMs as mentioned above, the same mechanism seems to be at work in the separation of ethyl benzene (EB) and styrene (St) in the liquid

dx.doi.org/10.1021/cr200190s |*Chem. Rev.* 2012, 112, 869–932

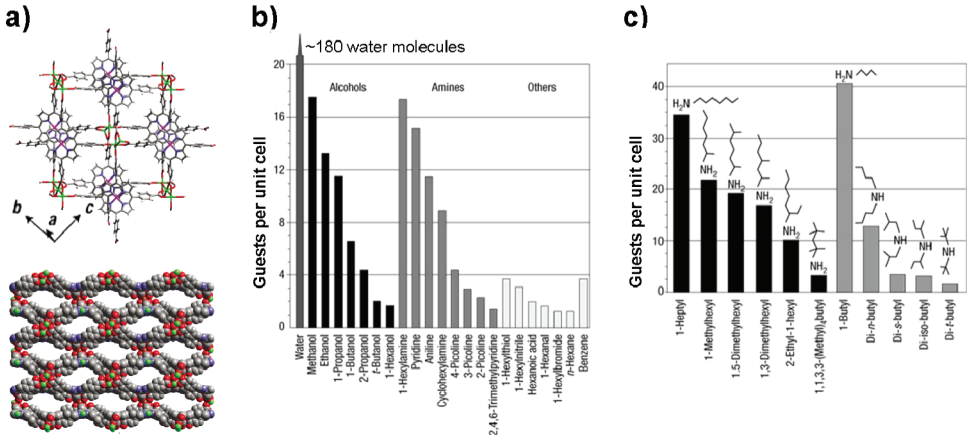

Figure 13. (a) Structure of PIZA-1 showing connectivity (top) and the space-filling view of the network (bottom) (C atoms are shown in gray, O atoms in red, N atoms in blue, Co atoms in purple and green); (b and c) size-, shape-, and functional group-based adsorption selectivity of various guest molecules on PIZA-1. Reproduced with permission from ref 383. Copyright 2002 Nature Publishing Group.

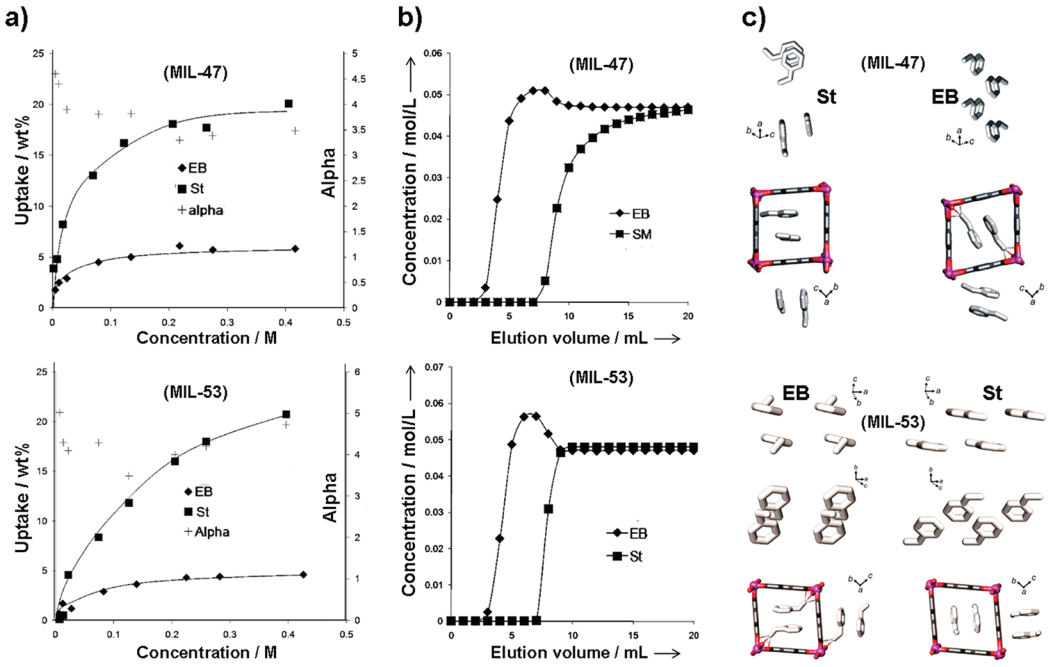

Figure 14. (a) Competitive adsorption of EB and St on MIL-47 and MIL-53 in batch mode (uptake from an equimolar mixture of EB and St in heptane at 298 K as a function of equilibrium liquid-phase concentration of each compound); (b) breakthrough experiments with binary 0.047 M solutions of EB and St in heptane on MIL-47 and MIL-53 at 298 K; and (c) structural refinement of MIL-47 and MIL-53 crystals loaded with St and EB (C atoms are shown in dark gray, O atoms in red, V atoms in pink, and Al atoms in purple; H atoms have been omitted). Reproduced with permission from ref 388. Copyright 2010 American Chemical Society.

phase as demonstrated by Matzger and co-workers.[385] HKUST-1 with open Cu(II) sites was selected as a sorbent to conduct liquid chromatography separation of the two chemicals. The experimental results gave the retention times for EB and St of 35 and 125 min, respectively, and a calculated separation factor of 3.9, indicating a very efficient separation. This separation was proposed to be due to the coordinative interaction of styrene with Cu(II) sites in the stationary phase, on a π-complexation mechanism. To test this hypothesis, the same experiment was performed by using MOF-5 (no CUMs) as the stationary phase. The two components coeluted, showing no separation. This mechanism has also been confirmed by De Vos and co-workers in liquid-phase separations of olefins using HKUST-1, where C5-olefins were separated from corresponding parafins.[386,387] Competitive batch adsorptions showed a preferential uptake of 1-pentene, isoprene, 2-methyl-2-butene, cyclopentene, and piperylene over linear pentane in a binary 1,3,5-triisopropylbenzene solution with an equilibrium bulk-phase concentration in each case.

As most of the readers already know, St is a widely used aromatic monomer for polymerizations in industry, and the separation of EB and St is therefore an industrially important process.[286] St is usually produced by dehydrogenating EB, obtained from petroleum refining, and must be separated from a not fully converted product stream because only pure St can be

dx.doi.org/10.1021/cr200190s |*Chem. Rev.* 2012, 112, 869–932

used in polymerizations. Furthermore, the mixture also contains other impurities, such as toluene and *o*-xylene, which also need to be removed. Because of the fact that the boiling points of St (418 K), EB (409 K), toluene (393 K), and *o*-xylene (418 K) are close, their separation by distillation is a very energy-intensive process, thereby motivating the development of alternative separation techniques including adsorption. An additional difficulty in the separation of St and EB is the size similarity of the two molecules, which is often the property around which adsorption-based separation is centered.

For this challenging separation, De Vos and co-workers[388] have shown that MIL-47 and MIL-53 are capable of separating EB and St in the liquid phase. Both MOFs have a similar 3D structure consisting of chains of metal octahedra connected by ligand linkers to give 1D channels with a diameter of approximately 11 Å (large enough for both molecules).[234,374] There are, however, some differences between them: MIL-53 has hydrophilic pores due to the presence of hydroxyl groups and its structure is known to be flexible; MIL-47, on the other hand, contains only hydrophobic pores and is more rigid as compared to MIL-53. In this work, single-component adsorption experiments showed that the maximal uptake capacities of MIL-47 and MIL-53 are 21 and 24 wt % for St and 16 and 15 wt % for EB, respectively. Competitive adsorption experiments in static conditions proved that both MOFs can discriminate between EB and St with high selectivity, as shown in Figure 14a. The saturation levels are similar at an uptake of 20 and 5 wt % for St and EB on both MOFs. As compared to single-component adsorptions, the maximal uptake of St was not significantly influenced by the presence of EB in the mixture, but that of EB was. The calculated separation factors for MIL-47 and MIL-53 remain constant in each case at a value of approximately 3.6 and 4.1, respectively. Breakthrough experiments (Figure 14b) in dynamic conditions with an equimolar mixture of EB and St (both 0.047 M) in heptane gave average separation factors for St over EB of 2.9 on MIL-47 and 2.3 on MIL-53. Furthermore, the regeneration of the columns can be easily achieved by flushing with pure solvent. Additionally, the combined separation/purification in diluted conditions of a mixture with a more realistic composition that also contains small amounts of toluene and *o*-xylene was also tested on MIL-53. As with the binary experiment, St was preferred over EB, giving a similar average separation factor of 2.2; toluene and *o*-xylene were retained longer on the column. These observations indicated that MIL-53 is capable of removing impurities from the product feed in the first step of the separation process, followed by the separation of EB and St in the second step.

After assessing the potential of MIL-47 and -53 for St and EB separation, they also studied the selective adsorption mechanisms by using temperature-dependent pulse chromatography techniques, vapor-phase adsorption experiments, and Rietveld refinements of the adsorbate-loaded structures. The results showed that the origin of preferential adsorption of St over EB is quite different for the two MOFs (Figure 14c). In the case of MIL-47, diffraction experiments revealed that St molecules were packed inside the pores in a unique, pairwise fashion. This packing of St left available spaces for the coadsorption of EB between the packed St pairs. The coadsorption of EB can further induce a preferential adsorption for St, where entropic effects play a key role. For MIL-53, the origin of the preference for St adsorption was believed to be related to differences in the enthalpy of adsorption for the two molecules, which are based on different degrees of distortion of the framework. In both cases, the ethyl group of EB is rotated out-of-plane and can interact with the framework O atoms. This rotation and interaction induced a significant structural distortion of the more flexible MIL-53, which was coupled with an energy penalty. The structural relaxation resulted in a less negative enthalpy of adsorption for EB in comparison with St, eventually leading to the preferential adsorption of St. This proposed mechanism also answered for the influence of temperature on the separation factors derived from pulse chromatography: separation factors are independent of temperature for MIL-47 but vary with temperature for MIL-53. In addition, the separation of 1- and 2-methylnaphthalene, tested with a breakthrough experiment on the two MOFs, has also been confirmed to be based on a mechanism that involves the reduction of selectivity as loading of adsorbate was increased, which reduced the remaining adsorption sites.[386]

The same group also reported the separation of EB and St by using a silica−HKUST-1 composite as a stationary phase in liquid chromatography.[389] The composite was prepared by embedding HKUST-1 into the pores of silica beads, leading to monodisperse composite spheres with a particle size of 3 μm. By using these composite spheres as the stationary phase, an efficient separation of the mixture was achieved with a resolution of 7.9 and calculated separation factor of 5.2. As compared to pure HKUST-1 as the stationary phase, column backpressure was low and peaks were narrow when using the composite material, while the unmodified silica cannot separate the two compounds. This result thus illustrated the combined effect of the good packing properties of silica and the high separation ability of HKUST-1 on the separation performance. In addition, this silica−MOF composite was also used as the stationary phase to separate *p*-ethyltoluene and *p*-methylstyrene under similar conditions, to give a resolution of 14.

On the basis of a possible entropic effect similar to that proposed in the selective adsorption of St over EB on MIL-47, preferential uptake of diolefins over other olefinic and paraffinic fractions on MIL-96 was also observed.[387] MIL-96 has a 3D structure containing three types of cages, of which only two types are accessible to larger molecules.[200] Single-component liquid-phase adsorption experiments showed that MIL-96 is capable of adsorbing all C5-diolefin isomers (*cis*-piperylene, *trans*-piperylene, and isoprene) from their pentane solution, implying that it can discriminate between C5-diolefins and their paraffinic counterpart, pentane. Competitive batch experiments of binary mixtures also demonstrated that MIL-96 is able to separate C5-diolefins from C5-mono-olefins, including 1-pentene, *cis*-2-pentene, *trans*-2-pentene, 2-methyl-2-butene, and 2-methyl-1-butene, where mono-olefins were not adsorbed at all by MIL-96, while the uptakes of the diolefins were close to the values from the single-compound experiments. These preferential adsorptions were speculated to be a result of entropic effects, which was also partially supported by the almost identical adsorption enthalpies of pentane, 1-pentene, and the dienes at low coverage (measured in the gas phase). The presence of more sp^3-hybridized carbon atoms in mono-olefins and paraffins seems to result in a greater entropic loss due to the loss in degrees of freedom of rotation within the MOF cages. Recently, this group also revealed that $Cu_2(bdc)_2(dabco)$, having a pillared-layer 3D structure with two types of pores of 7.5 × 7.5 Å and 3.8 × 4.7 Å in size, is capable of separating monomethyl-naphthalenes from its mixture containing naphthalene or 1,4-dimethylnaphthalene.[390] It was believed that the specific interactions of the methyl group in

naphthalene with the pore walls of the framework may play an important role in determining the adsorption selectivity.

Besides the above-mentioned examples, preferential adsorptions of small molecules in the liquid phase, mainly due to the formation of H-bonds between guest molecules and the wall of the host frameworks, have also been observed in several other MOFs. Suh and co-workers[391] reported an inclusion study of a 2D MOF, $Ni(C_{10}H_{26}N_6)(btc)_{2/3}$, with various organic guest molecules. Results showed that this material can selectively bind PhOH over PhCl and PhBr due to the formation of host−guest H-bonding interactions. They also reported selective guest binding in another MOF, $Zn_4O(ntb)_2$ (ntb = 4,4′,4″-nitrilotrisbenzate), which has a flexible 3D interpenetrated structure.[392] Inclusion experiments gave a binding affinity sequence of MeOH > pyridine > benzene > dodecane. MeOH possesses the highest affinity, which was attributed to the formation of H-bonds with the carbonyl groups exposed in the channels of the host. This MOF also favored hydrophobic aromatic guests, probably due to the formation of π---π or C−H---π interactions of them with the benzyl rings of the host.

By the same token, Lu and Babb[393] reported the selective inclusion of ethanol over pentane by $Cu(in)_2$ (in = isonicotinate), which has a stable 3D framework structure with 1D helical channels decorated by noncoordinated O atoms of the carboxylate groups. The structure is also expandable by over 8% volume upon guest inclusion. When soaking the material in an ethanol/pentane mixture, only ethanol molecules were included in the structure, which was confirmed by single-crystal X-ray diffraction. The selective inclusion was attributed to the presence of hydrophilic carboxylate groups (available for H-bonding interactions with guest molecules) in the framework.

Similarly, on the basis of the formation of H-bonds, guest selective adsorption in the liquid phase was also observed by Kitagawa and co-workers[335] in a flexible MOF, $Cd(4\text{-btapa})_2\cdot(NO_3)_2$. The crystalline, solvated state of this MOF has a 3D framework structure with channels functionalized by amide groups. There are two types of H-bonding sites: −NH and −C═O moieties in the channels. Selective binding of alcohols inspired by H-bonding interactions was demonstrated by simple component adsorption experiments (immersing the material in various alcohols and then checking inclusions), where short-chain alcohols including methanol, ethanol, *n*-propanol, and *n*-butanol exhibited inclusion with structural transformations of this MOF, as confirmed by PXRD patterns, but *n*-pentane and *n*-pentene were not adsorbed under the same conditions. In addition, the selective uptake of propan-2-ol over cyclohexane into the OH-group functionalized pores of a 3D MOF $(ZnI_2)_3(tpt)_2$(triphenylen-2-ol) (tpt = 2,4,6-tris(4-pyridyl)-1,3,5-triazine), due to the formation of H-bonds, was also demonstrated by Fujita and co-workers.[394]

Selective adsorption of pyridine over 2,6-lutidine in flexible MIL-53(Fe) (Fe(OH,F)(bdc)[395]) was observed by Millange and co-workers,[396] revealing again that H-bonding interactions influenced by sterics of the organic guests play a key role in their adsorption. PXRD experiments showed that the adsorption of pyridine led to the expansion of the MOF structure, along with the formation of H-bonds between pyridine N and framework −OH groups. In contrast, lutidine was coadsorbed with water to give an expanded version of MIL-53(Fe), in which water molecules bridge the N donors of lutidine and the −OH groups through H-bonds. Further investigations showed that when exposed to an aqueous mixture of pyridine and 2,6-lutidine the hydrated MIL-53(Fe) initially took up both guest molecules to give two distinct phases, but the final product is MIL-53(Fe)[2,6-lutidine-H_2O], excluding pyridine entirely.

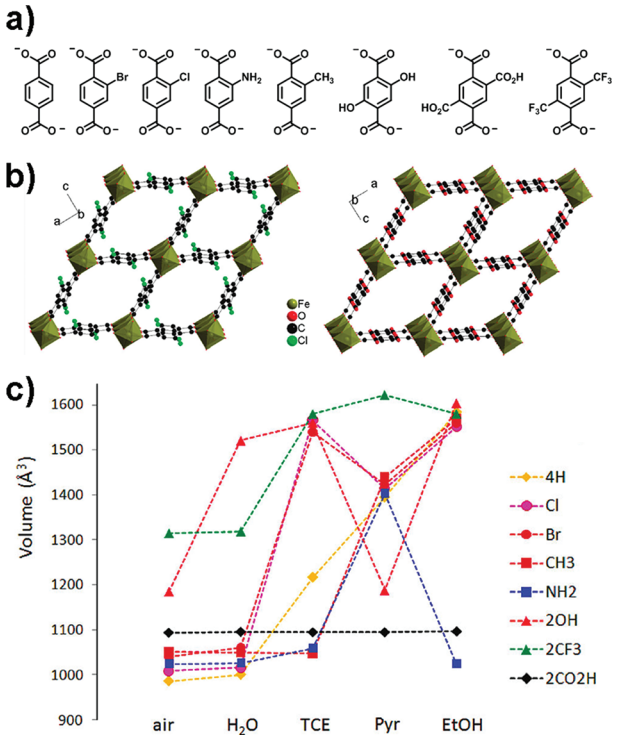

Figure 15. (a) Ligands used in the MIL-53(Fe) type MOFs studied in this work; (b) crystal structures of the as-synthesized MIL-53(Fe)-Cl (left) and MIL-53(Fe)-$(OH)_2$ (right) solids (as representative members); and (c) unit cell volume of the MIL-53(Fe) and its modified analogues in their (air) hydrated form and immersed in various solvents (TCE, 1,1,2,2-tetrachloroethane; Pyr, pyridine; EtOH, ethanol). Reproduced with permission from ref 397. Copyright 2010 American Chemical Society.

Furthermore, a scan of functionalized MIL-53(Fe) MOFs for the adsorption and potential separation of liquid small molecules was performed by Devic and co-workers.[397] In this work, functional groups (−Cl, −Br, $-CF_3$, $-CH_3$, $-NH_2$, −OH, $-CO_2H$) with different polarities, hydrophilicities, and acidities were introduced through predesigned aromatic linkers into the MIL-53(Fe) structure to systematically modify the pore surfaces of the resulting MOFs (Figure 15a and b). These MOFs have a flexible structure similar to MIL-53(Fe) and adopt the narrow pore form in both the hydrated and the dry forms. As shown in Figure 15c, the pore opening of theses MOFs showed different responses to each guest molecule (upon adsorption), which are strongly dependent on the guest−framework affinity in each case. The authors argued that the pore opening of these flexible MOFs triggered by the adsorption of guest molecules was governed by a critical balance between the stability of the narrow and large pore forms and the guest−framework interactions. The evaluated energy cost for opening these structure thus increased in the sequence of MIL-53(Fe)-$(CF_3)_2$ < MIL-53(Fe)-CH_3 < MIL-53(Fe) < MIL-53(Fe)-$(OH)_2$ < MIL-53(Fe)-NH_2 < MIL-53(Fe)-Br < MIL-53(Fe)-Cl.

Even if no distinct special interactions, as discussed above, between adsorbate and pore surface of the frameworks exist, some MOFs are capable of separating polar from apolar organic solvents. An example is $Ca(hfipbb)(H_2hfipbb)_{0.5}(H_2O)$ ($AEPF\text{-}1_{dry}$),

dx.doi.org/10.1021/cr200190s |*Chem. Rev.* 2012, 112, 869–932

reported by Gutiérrez-Puebla and co-workers,[398] which has a dynamic 3D structure with potential open channels. Single-component adsorptions by suspending samples in selected solvents revealed that it could adsorb acetonitrile, acetone, and 1-butanol with an uptake capacity of ca. 90, 70, and 62 mol % adsorbate, respectively. Yet, benzene and toluene showed only limited adsorption, and *n*-hexane and isooctane were not adsorbed at all. Interestingly, the opposite behavior, the selective adsorption of apolar organic solvents over polar ones, was previously reported on a Cu-based MOF tested in the gas phase.[375] Structural refinements also demonstrated the recovery of the solvated phase from AEPF-1_{dry} samples after adsorption treatment at different levels. Furthermore, the selective adsorption from mixtures has also been tested on four equimolar mixtures including acetone/acetonitrile, acetone/1-butanol, acetone/toluene, and acetone/hexane. The results confirmed the selective adsorption of polar over apolar solvents as observed in single-component adsorption experiments.

Preferential adsorption of polar over apolar solvents has also been observed in another flexible MOF, $Fe_3O(CH_3OH)_3Cl(bdc)_3$ (MIL-89), by Serre and co-workers.[399] Their experimental results showed that the adsorption of solvent molecules led to the expansion of the MIL-89 structure. Overall, MIL-89 can adsorb significant amounts of all solvents tested. However, under the same soaking time, the affinity of MIL-89 toward these solvents is different with an order of pyridine > lutidine ≈ dimethylcarbonate > acetonitrile > methanol ≈ nitrobenzene > water ≈ dimethylformamide (DMF) ≈ diethylformamide (DEF) > chloroform ≈ toluene ≈ hexane, which simultaneously also indicated that the swelling behavior of the framework is indeed solvent dependent.

3.1.2. Organic Molecules with Different Shape and Size. Shape and size-based selective adsorption is another popular phenomenon and has been the foundation of adsorptive separation of various molecular sieves and thin film membrane separations. MOFs with easily controllable and adjustable structural metrics of course have great potential for shape and size-based separations in the liquid phase, just as in the gas phase discussed above. In fact, selective adsorptions or separations of liquid chemicals based on different shape or size of components have been demonstrated in some MOFs as discussed below.

Besides the preferential adsorption due to the different functional groups of guest molecules observed in PIZA-1 as discussed above,[383] this MOF also exhibited size and shape selectivity toward organic small molecules. As shown in Figure 13b, by increasing the size of a series of aromatic amines, adsorption results showed a decreased uptake of pyridine > aniline > 2,4,6-trimethylpyridine. The selectivity was also illustrated by comparing the adsorption capacity of cyclohexylamine (8.9 guest molecules per unit cell of host) to that of dicyclohexylamine (2.3 guests per unit cell). The steric influence on the shape selectivity of this MOF (Figure 13c) was also observed in the picoline series (4-picoline >3-picoline > 2-picoline) and a series of butyl-substituted amines (*n*-butylamine > di-*n*-butylamine > di-iso-, di-*s*-, and di-*t*-butylamines). The proposed reason that the bulky organic substituents encroach upon the hydrophilic group resulting in declining adsorption was further supported by the adsorption of simple alcohol molecules, which showed decreasing uptakes in the order of methanol > ethanol > propanol ≫ butanol > hexanol. Direct adsorption comparisons between linear and branched alcohols (for example, 1-propanol vs 3-propanol, and 1-butanol vs *t*-butanol) again proved the correlation between the increased steric hindrance and the decreased adsorption uptake.

Similarly, selective inclusion of alcohol molecules with different size and shape has also been observed in $Zn_2(btc)(NO_3)$.[382] It was found that this MOF can adsorb small nonhindered alcohols including methanol, ethanol, 1-propanol, isopropyl alcohol, 1-butanol, and *tert*-butyl alcohol, but rejected sterically hindered *t*-butylphenol. Finally, the overall order of alcohol inclusion selectivity is C1, C2 > C3, C4 > C5, C7, being directly dependent on their shape and size. A similar situation has also been found in a flexible MOF, $Cd(4\text{-btapa})_2\cdot(NO_3)_2$,[335] which exhibited guest inclusion coupled with structural transformation for short-chain alcohols including methanol, ethanol, *n*-propanol, and *n*-butanol, but not for long-chain alcohols, such as *n*-pentanol and *n*-hexanol. The size selective inclusion of alcohol molecules has also been observed in $Cu(in)_2$.[393] When soaking this MOF in an ethanol/*n*-propanol mixture, only ethanol molecules were adsorbed into its channels. In addition, the selective adsorption of water over methanol, due to their different sizes, from a 1:1 liquid mixture was observed in $Cu(R\text{-gla-Me})(bipy)_{0.5}$ (*R*-gla-Me = *R*-2-methylglutarate).[400] This MOF has a 3D framework structure with narrow pores of about 2.8 × 3.6 Å, which can block the entrance of methanol into its channels, thus making it a potential drying agent.

Size selective adsorption for small aromatic molecules has also been demonstrated in $Ag(tmpes)\cdot BF_4$, which has a 4-fold interpenetrated 3D diamondoid network structure by Xu and co-workers.[344] By combing vapor and liquid-phase experiments of single-component adsorptions, they showed that benzene, toluene, chlorobenzene, 1-bromo-4-fluorobenzene, anisole, and nitrobenezene can be adsorbed by this MOF, whereas *n*-hexane, cyclohexane, 1,3-dichlorobenzene, hexafluorobenzene, 4-bromo-1,2-difluorobenzene, and *p*-xylenes were excluded. Mixture adsorptions also revealed that benzene, the five monosubstituted aromatic molecules, and 1-bromo-4-fluorobenzene can access the pores, but *m*- or *o*-disubstituted aromatics cannot. The separation of benzene and hexafluorobenzene, which is a challenging separation process in industry due to their similar boiling points, could potentially be aided by this MOF. Furthermore, although *p*-xylene, 1-bromo-4-fluorobenzene, and ethylbenzene have the same cross sections as benzene, their sorption behaviors differ markedly: 1-bromo-4-fluorobenzene was easily adsorbed; ethylbenzene was adsorbed slowly; *p*-xylene was not adsorbed at all. These differences suggested that the structural features along the lengthwise direction of the guest molecules become important for their adsorption.

In addition, $Cd(4\text{-btapa})_2(NO_3)_2$,[335] also mentioned above, exhibited selective accommodation of malononitrile over ethyl cyanoacetate and cyano-acetic acid *tert*-butyl ester. It was found that the inclusion amount of malononitrile was 4−5 times larger than those of the other two, implying that malononitrile was most easily introduced into the channels of the MOF. This selective inclusion may be due to the small size of malononitrile and its strong interactions with channel surface induced by hydrogen bonds with the ligand amide groups. Similarly, De Vos and co-workers[401] also demonstrated that HKUST-1 is capable of adsorbing mesitylene and triphenylmethane from hexane, while excluding 1,3,5-triethylbenzene, 1,3,5-triisopropylbenzene, triphenylethylene, and pyrene.

The first example of size-dependent inclusion of large organic dye molecules (in this case, three polycyclic organic dyes, Astrazon Orange R, Nile Red, and Reichardt's dye, were checked) was tested

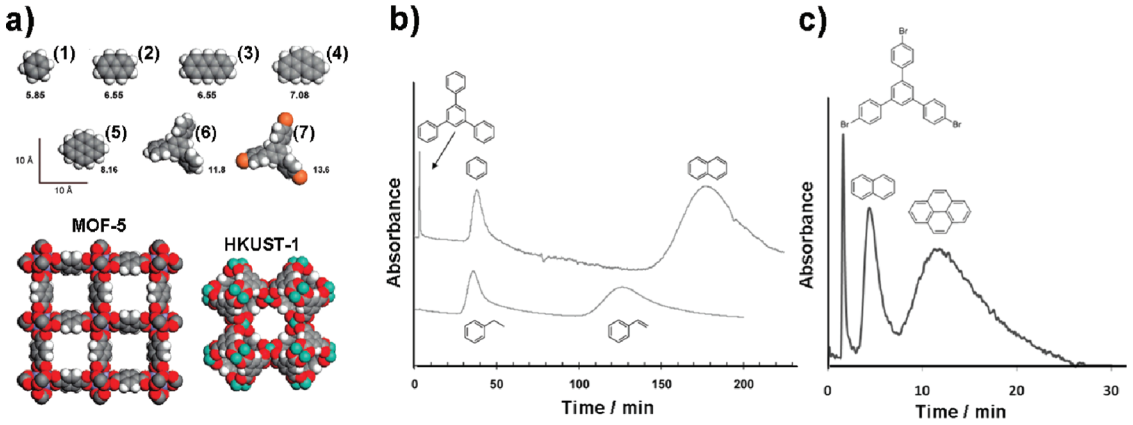

Figure 16. (a) Space-filling representations of the structures of benzene (1), naphthalene (2), anthracene (3), phenanthrene (4), pyrene (5), 1,3,5-triphenylbenzene (6), 1,3,5-tris(4-bromophenyl)benzene (7), MOF-5, and HKUST-1 shown on a common scale to convey the relative sizes of adsorbent and adsorbate. Numbers represent kinetic diameters (Å) (C atoms are shown in gray, H atoms in white, O atoms in red, Br atoms in orange, Cu atoms in turquoise, and Zn atoms in blue); (b) LC separations of organic molecules achieved using Basolite C 300 (HKUST-1) as the stationary phase; and (c) LC separations of large organic molecules achieved using MOF-5 as the stationary phase. Reproduced with permission from ref 385. Copyright 2009 American Chemical Society.

in MOF-177,[402] which has a 3D framework structure with extra-large pores. It was found that the three dyes were adsorbed when soaking the crystals of MOF-177 in their saturated dichloromethane solutions. The uptake of Astrazon Orange R is more than 40 wt %, corresponding to 16 dye molecules in each unit cell; for Nile Red, only two molecules were adsorbed in each unit cell. In the case of the very large molecules of Reichardt's dye, only the outer part of the crystal is penetrated, with an average of only one molecule adsorbing in each unit cell. Another interesting example is the selective inclusion of larger fullerenes over small ones observed in $[Co(SCN)_2]_3(tpt)_4$.[403] When the crystals of this MOF were soaked in a toluene solution containing a 1:1 mixture of C60 and C70, it was found that C70 was enriched in the framework (C60:C70 = 21:79). This MOF also preferentially absorbed other larger fullerenes including C76, C78, C82, and C84, resulting in a ratio relative to C60, which was 2.6−2.7 times higher, upon the adsorption from solution.

Apart from the selective adsorptions discussed above, the shape- or size-based liquid-phase separations of olefins, alkylnaphthalenes, and dichlorobenzenes on MIL-47 and MIL-53 have been tested by De Vos and co-workers[386] by using a combined means of batch, pulse, and breakthrough chromatography experiments. Their results showed that the separation of 1,4-dimethylnaphthalene from naphthalene, 1-methylnaphthalene, and 2-methylnaphthalene isomers, and of *p*- and *m*-dichlorobenzene can be achieved on both MOFs. In all chromatography experiments, the fast elution of 1,4-dimethylnaphthalene points to the size exclusion of the sorbent materials. For dichlorobenzenes, it was found that packing effects dominate the selectivity. In addition, the separation factors measured for 1,4-dimethylnaphthalene from the other compounds in pulse experiments were much larger than the equilibrium-based values measured in batch tests. This is most likely because of steric difficulties of guest molecules to enter the pores, which results in comparatively fast diffusion of 1,4-dimethylnaphthalene.

Liquid chromatography (LC) separations of large hydrocarbons including benzene, ethylbenzene, styrene, naphthalene, anthracene, phenanthrene, pyrene, 1,3,5-triphenylbenzene, and 1,3,5-tris(4-bromophenyl)benzene using HKUST-1 and MOF-5 acting as the stationary phase, respectively, were also studied by Matzger and co-workers.[385] Figure 16a presents the structures and sizes of adsorbates tested in this work. It was found that the column with HKUST-1 (with large square windows of 9 × 9 Å) as the stationary phase exhibited excellent separation performances for benzene, naphthalene, and 1,3,5-triphenyl-benzene (Figure 16b). Additionally, phenanthrene was adsorbed, whereas pyrene eluted rapidly in this column, suggesting that the latter is slightly too large and was excluded from the pores of the adsorbent. These results also indicated that larger molecules were better retained as long as they can access the pores efficiently, but that above a certain size threshold the inability to penetrate/diffuse into the pores led to negligible retention. When a mixture containing benzene, naphthalene, anthracene, phenanthrene, and pyrene passed through a MOF-5 column, the results showed an overall lower retention for all of the chemicals as compared to the HKUST-1 column. When a mixture of 1,3,5-tris(4-bromophenyl)benzene, naphthalene, and pyrene was tested, only naphthalene and pyrene were retained as shown in Figure 16c. These experimental results demonstrated the ability of the two MOFs by acting as size-selective adsorbents for liquid-phase separations, following a behavior similar to gel permeation chromatography (GPC) but with sharp cutoffs at certain molecular dimensions. This was the first demonstration of a molecular sieving effect for the LC separation of large hydrocarbons in MOFs. Similarly, Xu and co-workers[404] also revealed that a mesoporous MOF, Cd(2-NH_2-bdc)(bipy), was effective for size-exclusion-based LC separation of Rhodamine 6G and Brilliant Blue R-250 dyes.

A further, highly interesting example was presented in a single MOF-5 crystal acting as a "column" to efficiently separate mixtures containing several organic dyes.[405] In this work, organic dyes, Pyronin Y (PY), Pyronin B (PB), Thionin (TH), Toluidine Blue O (TBO), Azure A (AA), Brilliant Green (BG), and Methyl Yellow (MY), were passed through a MOF-5 crystal using DMF as the eluent. It was found that the separation performances are directly related to the size and shape of the guest molecules, as well as to their interactions with the pore surface of the framework. Furthermore, the "single-crystal MOF column" can easily be regenerated by simply soaking the used crystal in fresh DMF for period of time. All of these preliminary results have already shown potential in a regime previously inaccessible to other

dx.doi.org/10.1021/cr200190s |*Chem. Rev.* 2012, 112, 869–932

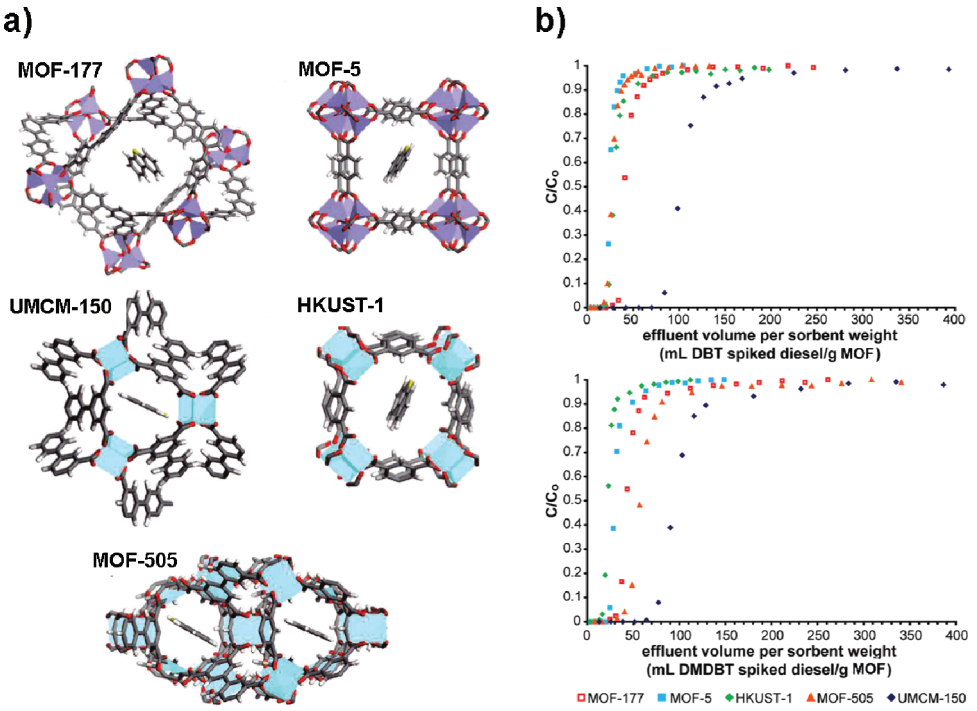

Figure 17. (a) Structures of five MOFs with one molecule of dibenzothiophene added into the pore of each MOF to represent scale; and (b) breakthrough curves for 300 ppmw S dibenzothiophene in ultralow sulfur diesel (ULSD) (top) and 300 ppmw S 4,6-dimethyldibenzothiophene in ULSD (bottom) for each MOF. Reproduced with permission from refs 12 and 407. Copyright 2008 and 2009 American Chemical Society.

porous materials, of using MOFs as adsorbents for the selective inclusion and separation of large organic polycyclic molecules.

3.1.3. Organosulfur Compounds. Sulfur and organosulfur compounds are widely known contaminants in petroleum refining and in fuels (including gasoline, kerosene, diesel, and fuel oil).[105] Desulfurization is understandably a subject of renewed interest because of environmental protection issues, the development of fuel cells that rely on reforming of hydrocarbons to hydrogen, and concerns of catalyst poisoning in petroleum refining. Large organosulfur compounds found in diesel, for example, are indeed difficult to be removed using current industrial processes. In this spectrum, typical organosulfur compounds include mercaptans (RSH), organic sulfides (R−S−R), organic disulfides (R−SS−R), carbon disulfides (S−C−S), thiophene, and substituted thiophenes (benzothiophenes, alkylthiophenes, alylbenzothiophenes, and alkyldibenzothiophenes). The removal of organosulfur compounds from hydrocarbon streams by adsorption has already been implemented in the refining industry by using other porous adsorbents, such as activated carbons and zeolites,[406] but only a very limited number of MOFs have been explored to date.

As pioneers in this subject, Matzger and co-workers[12,407] tested the liquid-phase adsorption of organosulfur compounds and desulfurization in five selected MOFs including $Cu_3(bpt)_2$ (UMCM-150, bpt = biphenyl-3,4′,5-tricarboxylate)[408] MOF-505,[323] HKUST-1,[21] MOF-5,[31] and MOF-177.[402] These MOFs have different pore sizes, shapes, and metal clusters, thus offering a systematic test to determine the key factors impacting adsorption behaviors (Figure 17a). They were first evaluated for the liquid-phase adsorption of benzothiophene (BT), dibenzothiophene (DBT), and 4,6-dimethyldibenzothiophene (DMDBT), typical fuel contaminants.[12] It was found that all of these MOFs exhibited large uptake capacities for the three compounds at high concentrations, even if saturation was not reached in each case. For example, UMCM-150 has an uptake capacity of 40, 83, and 41 g·S/kg for BT, DBT, and DMDBT, respectively. It is worth noting that UMCM-150, MOF-177, and MOF-5 have a larger capacity for DMDBT than BT and DBT at 300 ppmw S (ppm by weight of sulfur), probably due to the fact that the larger guest has more contact with the framework. Pore size was also found to be a factor deciding the adsorption capacity for given compounds; for example, MOF-505 with the smallest pores in this study has an uptake capacity of 38 and 27 g S/kg for BT and DBT, but ∼0 g S/kg for DMDBT, at 300 ppmw S.

In a follow-up study by the same group, these MOFs were tested by breakthrough experiments for evaluating their performance in the removal of DBT and DMDBT from diesel fuel.[407] The experimental results showed that even in the presence of the complex mixture of aromatic compounds found in diesel these MOFs can selectively adsorb organosulfur compounds and are able to desulfurize significant amounts of fuel before the breakthrough point, as shown in Figure 17b. This high selectivity of MOFs for the organosulfur compounds over other aromatic compounds existing in diesel contrasts sharply with activated carbons, which usually have a poor selectivity. For both organosulfur compounds, UMCM-150 presented the best desulfurization performance; MOF-177 is among the worst. These MOFs also outpaced Na(Y) zeolite for the adsorption of DBT and DMDBT, and regardless of the higher adsorption affinities, they could be fully regenerated by washing with commonly used solvents at modest temperatures.

In a similar study, Achmann and co-workers[409] evaluated the capacities of MOF-5, HKUST-1, and $Cu_2(bdc)_2(dabco)$[410] in the removal of sulfur from different thiophene (TPH)- and tetrahydrothiophene (THT)-infused model oils, as well as commercial low-sulfur gasoline and diesel fuels. Their results showed that MOF-5 and $Cu_2(bdc)_2(dabco)$ are indeed not suitable for use in removal of TPH and THT from fuels. However,

dx.doi.org/10.1021/cr200190s |Chem. Rev. 2012, 112, 869–932

HKUST-1 showed a high efficiency for the removal of sulfur from fuels and model oils. Using this MOF, 78 and 86 wt % sulfur content could be removed from TPH- and THT-based model oils, respectively. A decrease of more than 22% of the sulfur content in low-sulfur gasoline could also be achieved by using this material; the sulfur level in diesel fuel could be reduced by 13 wt %. Time-resolved measurements demonstrated that sulfur compound adsorption from these fuels mainly occurred in the first hour after adding the adsorbent, making a fast and efficient sulfur removal possible with this MOF. In addition, Jhung and co-workers[411] have also tested liquid-phase adsorption of BT on MIL-47 and MIL-53(Al, Cr). Their results indicated that the metal ions in these MOFs have a significant effect on the adsorptive desulfurization and MIL-47 presented the highest adsorption capacity. These results have already demonstrated the great potential of MOFs in desulfurization by adsorption. Further work directed toward evaluating other existing MOFs and designing new ones for these special organosulfur compounds, as well as to test other organosulfur compounds in fuels, is still needed.

Apart from sulfur compounds, fossil fuels are also contaminated by other aromatic molecules, including *N*-heterocyclic compounds, such as indole or carbazole. These N-containing compounds compete with sulfur compounds for the catalytic sites during hydro-desulfurization (HDS), which is presently the primary industrial process for the removal of sulfur compounds from fossil fuels.[406] To get deep HDS, these nitrogen contaminants have to be removed, which can be achieved through selective adsorption by porous materials.[107] Recently, De Vos and co-workers[412] tested several MOFs including MIL-100(Fe, Al, Cr), MIL-101, HKUST-1, MOF-74(Ni, Co), MIL-47, and MIL-53 for the selective removal of *N*-heterocyclic aromatic contaminants from simulated fuel feeds. In this work, the adsorptive removal of indole (IND), 2-methylindole (2MI), 1,2-dimethylindole (1,2DMI), carbazole (CBZ), and *N*-methylcarbazole (NMC), as well as of TPH, BT, and DBT from a simulated system with heptane/toluene acting as mixed solvent was examined. It was found that the presence of open metal sites (or CUMs) in the pores of MOFs played a key role in guest adsorption from mixtures. MIL-47 and MIL-53, lacking CUMs, did not show a significant uptake for all tested guests. In contrast, MIL-100(Fe, Al, Cr) and MIL-101 showed a high uptake of N-containing compounds, but weak affinity toward sulfur compounds. For HKUST-1 and MOF-74(Co, Ni), both nitrogen and sulfur compounds were adsorbed. Thus, MIL-100 and MIL-101 are promising candidates for the separation of nitrogen from sulfur compounds. Pearson's hard/soft acid/base concept was used to explain these observed selective adsorptions. As a result, MOFs containing hard Lewis acid sites are the most promising for the selective removal of the nitrogen compounds in fuel feeds, which was further supported by a detailed study on MIL-100(Fe) (the hardness or softness of the open metal sites in this MOF can be tuned[301]). MIL-100(Fe) has been confirmed to be capable of selectively removing only nitrogen compounds in its as-synthesized form (oxidized form) but both sulfur and nitrogen compounds in its partially reduced form. This material can also be easily and fully regenerated after guest adsorption and reused in multiple cycles.

3.1.4. Cations and Anions. Selective exchange and sensing of cations or anions is another important application of porous materials. Some MOFs have been demonstrated to be responsive to different ions, showing selective exchange or recognition from solution.[100] Most of the related publications are indeed directed to the study of sensing chemical species using MOFs.[98]

A typical example of selective cation exchange in MOFs is NaLa(H_4pmtp) (H_8pmtp = 1,4-phenylenbis(methylidyne)tetrakis(phosphonic acid)), reported by Bein and co-workers.[413] This MOF features a flexible anionic framework with a remarkable charge and size selectivity for cations. In aqueous solution, the Na^+ ions in the channels of the structure can be exchanged with other monovalent ions including Li^+, K^+, and Rb^+ having an ionic radii ranging from 0.76 Å (Li^+) to 1.52 Å (Rb^+), while divalent ions (Mg^{2+}, Ca^{2+}, Sr^{2+}, Ba^{2+}, Ni^{2+}, Cu^{2+}, Zn^{2+}, and Mn^{2+}) in the same size range and larger Cs^+ ions were rejected. This charge-dependent selectivity was attributed to the site-specific role of the guest cation, which may affect the equilibrium between the expanded and the contracted forms of the flexible framework. The monovalent cations were located at specific sites in the framework, where they can satisfy their coordination requirements, whereas divalent ions could occupy only one-half of these sites. The size selectivity observed is most likely related to the pore size of the MOF, which is, even in its expanded form, not big enough to accommodate Cs^+ or its hydrate.

The recognition of anions by using Tb(btc) (MOF-76[414]) in methanol solution was explored by Chen and co-workers.[415] MOF-76 has a 3D open framework structure with 1D channels, in which the terminally coordinating solvent molecules partially occupy the pores. After immersing the activated MOF-76 in methanol solutions containing varied amounts of sodium salts with different anions (F^-, Cl^-, Br^-, CO_3^{2-}, and SO_4^{2-}), different quantities of these salts were adsorbed into the pores of the MOF. The adsorption of anions led to an enhanced luminescence, different for each anion, of the MOF in the solid state. Fluoride ion showed the highest enhancement in the luminescent intensity, underlining the potential of MOF-76 for anion sensing. This luminescence enhancement was proposed to be a result of differences in hydrogen-bonding interactions between the anions and terminal OH moieties in the framework of the MOF.

Similarly, luminescent MOF, Tb_2(mucicate)$_3$, also showed an ability in the selective adsorption of different anionic sodium salts from water solution.[416] This MOF has a 2D layer structure connected by hydrogen bonds to form a 3D framework with square channels, in which −OH groups of the mucicate ligands decorated the pore surfaces. With an experimental method similar to that used in MOF-76, different luminescent enhancements of the solid samples were observed upon the adsorption of different anionic salts (sodium salt of I^-, Br^-, Cl^-, F^-, CN^-, CO_3^{2-}, NO_3^-, NO_2^-, SO_4^{2-}, and PO_4^{3-}) from aqueous solutions. Among them, CO_3^{2-} led to the largest enhancement, and NO_3^-, although similar in size to NO_2^-, induced very different intensities, showing the excellent sensing performance of this MOF. These anionic responses were attributed to H-bonding interactions between anions and −OH groups in mucicate ligands. The last two anions in the series showed no significant enhancement under the same experimental conditions, probably due to their larger sizes, which blocked access into the channels of the MOF. Further experiments showed that the cations (Na^+, K^+, and Ca^{2+} in this case) did not have a visible influence on the host's luminescent intensity. In addition, it was also found that the diffusion rates of different ions into the channels are rather similar and the channels showed excellent reversibility.

3.2. Selective Adsorptions and Separations of Structural Isomers

A lot of important chemicals or chemical raw materials coexist with their isomers in natural sources or the early stages of refined

dx.doi.org/10.1021/cr200190s |*Chem. Rev.* 2012, 112, 869–932

products, such as from petroleum and coal. These isomers can be generally classified as structural isomers and stereoisomers. The exceedingly great values for high purities of the individual isomers, coupled with the difficulties arising in the separation of these mixtures due to similarities in boiling and melting points and propensity to cocrystallize, make separation of isomeric compounds one of the most intense and challenging areas of industrial chemical research. An alternative to distillation and recrystallization, adsorption by porous materials, provides an efficient method for the separation of isomers on the basis of their sizes, shapes, chiralities, as well as differences in affinities with pore surfaces of adsorbents. The separations of some structural isomers have been achieved in industry by the selective adsorption or membrane penetration relying on porous materials, such as zeolites.[105] However, the developments of new porous materials are urgently required not only for improving the efficiency of these separations but also for the separation of other isomeric mixtures. MOFs, of course, are promising in the separation of chemical isomers, although only limited studies have been conducted to date.

3.2.1. Aromatic Compounds. Several MOFs have been tested for the separation of aromatic hydrocarbon compounds in the liquid phase, mainly focused on the C8 alkylaromatic isomeric compounds including the three xylene isomers (oX, mX, and pX) and ethylbenzene (EB). In a mixture of these compounds, only oX (bp = 144 °C) can easily be separated from the other isomers by distillation because of the similar boiling points of the remaining compounds (pX, 138 °C; mX, 138−139 °C; and EB, 136 °C).[364]

The liquid-phase adsorption and separation of C8 alkylaromatic compounds using HKUST-1, MIL-53(Al)ht, and MIL-47 was first reported by De Vos and co-workers.[417] Competitive adsorption of a mixture of each of the two C8 isomers in hexane showed that HKUST-1 has low selectivities for the isomeric pairs except of mX over oX, but MIL-53(Al)ht and MIL-47 have much higher selectivities for all C8 compound pairs, particularly, the prominent preference for pX over EB. Moreover, MIL-47 also preferred pX over mX, while MIL-53(Al)ht did not discriminate the two isomers very effectively. Breakthrough experiments gave average selectivities of 2.5 for the separation of pX and mX, and 7.6 for pX and EB. The regeneration of the MIL-47 column can be easily conducted by using hexane as the desorbent. In pulse chromatography experiments of a ternary mixture of EB, mX, and pX using the MIL-47 column, three well-separated peaks were observed as shown in Figure 18. Calculated selectivities for pX versus mX and pX versus EB are 3.1:1 and 9.7:1, respectively. Further experiments, including the measurement of adsorption enthalpies at zero coverage in the gas phase, competitive batch adsorption of binary mixtures from a hexane solution, and the Rietveld refinements of the XRPD patterns of MIL-47 samples with adsorbed guests, revealed that the separation selectivities of MIL-47 are due to the more efficient packing of certain isomers in its pores.

In a following study, they showed that the activation of the MIL-47 sample has an important influence on the adsorption capacity and selectivities of the material to pX and mX isomers.[418] With the departure of uncoordinated terephthalic acid during calcination, the uptakes of both xylenes initially increased and then decreased. The selectivity of pX over mX decreased sharply and then flattened out, indicating that the presence of some terephthalic acid in the pore of MIL-47 enhanced the selectivity between the two isomers. The higher

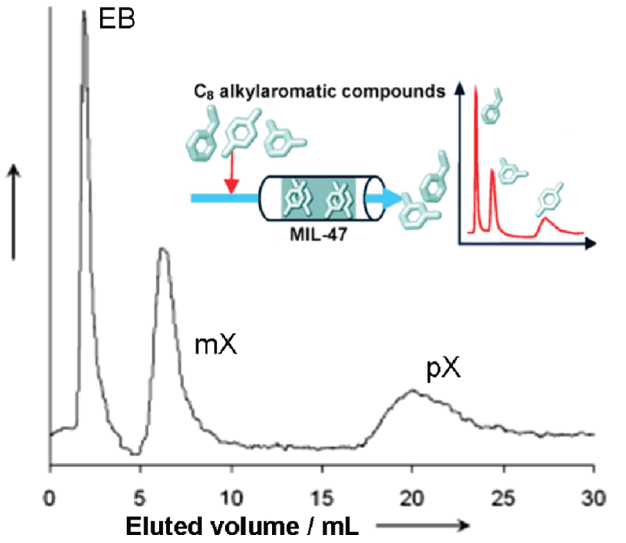

Figure 18. Chromatographic separation of a mixture of EB, mX, and pX on a column packed with MIL-47 in the liquid phase, with hexane as the desorbent at 298 K (inset shows a schematic representation). Reproduced with permission from ref 417. Copyright 2007 Wiley-VCH.

selectivity with the presence of terephthalic acid in the pores was explained as: (1) the partly evacuated framework may be more flexible, therefore allowing an efficient parking of pX, and (2) some specific interactions between xylene molecules and terephthalic acid guests in the pores may lead to the improved selectivity. After removal of all uncoordinated terephthalic acid, the completely activated MIL-47 sample was further tested for the selective adsorption and separation of xylene and other disubstituted aromatic isomers including ethyltoluene, dichlorobenzene, toluidine, and cresol. Pulse chromatography experiments revealed that xylene, dichlorobenzene, and cresol isomers have the same elution order of their respective three isomers: the *m*-isomer eluting first and the *p*-isomer last. This adsorption preference for the *p*-isomer over the *m*-isomer was also observed for the ethyltoluene and toluidine isomers. Selectivities were also confirmed to be phase concentration dependent as supported by the observation that selectivities increased with increased bulk phase concentration for the xylene and dichlorobenzene isomers. Different from those in xylene isomers, molecular packing seems not to be the key factor in determining the *p*/*m* selectivity for ethyltoluene, toluidine, and cresol isomers. In the case of toluidines and cresols, the formation of H-bonds between guest and framework was believed to be the dominant factor. For ethyltoluenes, the large size of the molecule indeed did not allow for efficient packing in the pores. Breakthrough experiment also supported the validity of the *p*- and *m*-dichlorobenzene separation, giving a calculated average selectivity of 5.0. These results showed that the activated MIL-47 is capable of selectively adsorbing the *p*-isomer from *p*−*m* mixtures of these disubstituted aromatics, even though different selectivity mechanisms appear to be at work. The selective adsorption of three dichlorobenzene isomers on HKUST-1 was also reported by the same group.[401] Competitive adsorption tests in batches for each of the two isomers gave adsorption selectivities of 1.4, 6.2, and 9.0 for *m*- over *p*-, *m*- over *o*-, and *p*- over *o*-isomer, respectively. The different affinities were attributed to either the differences in polarity or the steric packing effects of each isomer, or both.

dx.doi.org/10.1021/cr200190s |*Chem. Rev.* 2012, 112, 869–932

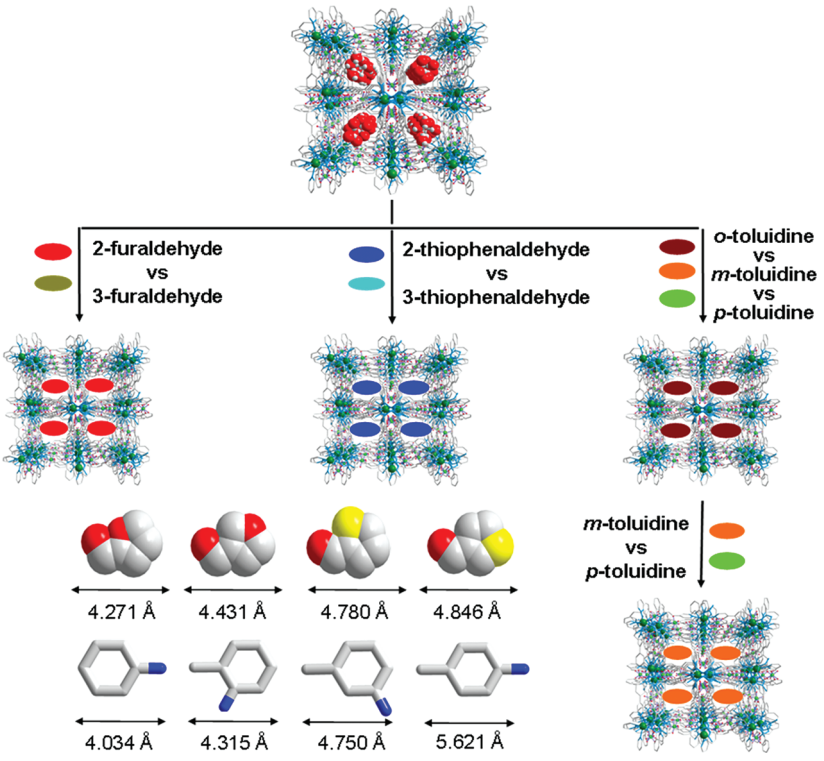

Figure 19. Schematic presentation of separations toward reactive aromatic isomers on a single crystal of $Cd(abppt)_2(ClO_4)_2$ (the guest isomers are shown as ellipses in different colors for clarity; the crystallographic lengths of these guest molecules, which are defined as the longest distances between the non-hydrogen atoms on these guest molecules, are shown). Reproduced with permission from ref 421. Copyright 2010 American Chemical Society.

In a similar study, De Vos and co-workers[419] also tested the selective adsorption and separation of alkylaromatic isomers including xylenes and ethylbenzene, as well as ethyltoluenes and cymenes in the liquid phase in MIL-53(Al) by means of batch, pulse chromatography, and breakthrough experiments. Competitive experiments using binary solutions of C8 isomers in hexane showed that both pretreated MIL-53 (known as MIL-53ht) and pristine MIL-53 samples (MIL-53lt) have a preference for oX, while disfavoring EB, and they did not discriminate between mX and pX in these conditions. These observed selectivities were further confirmed by pulse chromatography experiments, which showed that EB eluted first, followed by pX and mX (as one peak), and oX as the last. Additionally, room-temperature adsorptions isotherms of individual C8 isomer from a hexane solution also confirmed the preferential adsorption of oX. In breakthrough experiments of a binary mixture in hexane, EB broke through before oX, giving a calculated average selectivity of 11.0. The preferred adsorption of oX over mX was also observed, to give a calculated average selectivity of 2.2. For ethyltoluene and cymene isomers, again, a very striking adsorption preference for the *o*-isomer was observed in each case. Breakthrough experiments gave average selectivities of 5.0 and 6.8 for *o*- over *m*-cymene and *o*- over *p*-cymene, respectively. Rietveld refinements of guest-loaded MIL-53 demonstrated that the molecular packing of the adsorbed guests played an important role for adsorption, and the preferences found among the isomers were determined by interactions of the methyl groups with the pore walls. In the case of the *o*-isomer, both methyl groups of each molecule are capable of interacting with the carboxylate groups of framework, while that is impossible for the other isomers. As compared to MIL-53, MIL-47 showed different adsorption preferences, selectivities, and interaction mechanisms. On MIL-47, oX and pX were preferred over mX and EB, and efficient separations of pX and mX as well as of pX and EB were demonstrated, with selectivities of 2.9 and 9.7, respectively. These observed preferential adsorptions for certain xylene isomers in MIL-47 and hypothesized reasons (packing effects) have also been supported by molecular simulations, which gave a preferential order of *o*- > *p*- > *m*-isomer.[420] For ethyltoluene isomers, it was found that *o*- and *p*-ethyltoluene are almost equally preferred by MIL-47 and are more strongly retained than *m*-ethyltoluene. The separation between *m*-ethyltoluene and *o*- or *p*-ethyltoluene can thus be achieved by the selective adsorption of MIL-47. It is clear that despite having almost identical structural topographies, MIL-47 and MIL-53 displayed very different separation performances for alkylaromatic isomers, illustrating once again that tuned framework components, even in very similar structures, can result in a significant change in adsorption and separation properties. Recently, the same group has also shown that $Cu_2(bdc)_2(dabco)$ is capable of separating 1-methylnaphthalene and 2-methylnaphthalene with an evaluated separation factor as high as 2.6, higher than those obtained for reference zeolites.[390]

In addition, the selective adsorption and separation of reactive aromatic isomers, 2-furaldehyde versus 3-furaldehyde, 2-thenaldehyde versus 3-thenaldehyde, and *o*-toluidine versus *m*-toluidine versus *p*-toluidine, in both vapor and liquid phases by $Cd(abppt)_2(ClO_4)_2$ have been reported by Dong and co-workers.[421] This MOF has a 3D framework with 1D amphiphilic channels of 11×11 Å, in which the $-NH_2$ groups are located at corners. Single crystals of the MOF are so robust that the selective adsorption can be characterized by single-crystal X-ray diffraction of the guest-loaded sample. Finally, the diffraction experiments combined by ^1H NMR

dx.doi.org/10.1021/cr200190s |*Chem. Rev.* 2012, 112, 869–932

spectra illustrated selective adsorption of these guest molecules as illustrated in Figure 19. After immersion of the MOF crystals in an equimolar 2-furaldehyde and 3-furaldehyde mixture for 8 days at room temperature, for example, only the 2-furaldehyde isomer was included in the crystals. Similar experiments showed that only 2-substituted isomer in each case was preferentially adsorbed, indicating the guest size and functional group orientation may play a dominant factor in the adsorption. In the case of toluidine isomers, this MOF displayed an adsorption preference for the smaller and more polar isomers, resulting in an affinity sequence of *o*- > *m*- > *p*-toluidine. This work demonstrated for the first time that a MOF is capable of selectively adsorbing reactive aromatic isomers in both the vapor and the liquid phases, based on the size, shape, and polarity differences of the molecules involved.

3.2.2. Aliphatic Compounds. A large number of aliphatic compounds are also very important constituents of raw chemicals in the petroleum and chemical industries. The separation of their isomers is a major component in several industrial processes, such as the separation of linear alkanes from branched isomers in petroleum refining. Some related separations through adsorption have been achieved by using zeolites as adsorbents.[105] MOFs are almost not explored in the liquid-phase separations of aliphatic compound isomers. To date, only one report on experimental results is documented, together with a related report based on computational simulations.[422]

The liquid-phase separation of C5-diolefins including isoprene, *cis*-piperylene, and *trans*-piperylene on MIL-96 was recently reported by De Vos and co-workers.[387] Batch adsorptions showed that this MOF has a strong adsorption preference for *trans*-piperylene over isoprene and *cis*-piperylene. The uptake and degree of pore filling reached the highest values for *trans*-piperylene. It has been evaluated that each A or B cage in the MIL-96 structure accommodated two *trans*-piperylene molecules at maximal uptake, but each cage was loaded with only 0.5 isoprene molecules. The large uptake of *trans*-piperylene was attributed to the efficient packing of the guest molecules in the pores, which was supported by the observed similarities in adsorption enthalpies at a low degree of pore filling and variations in Henry equilibrium constants at low-coverage (with an order of isoprene ≈ *cis*-piperylene > *trans*-piperylene). Competitive batch experiments of all three isomers also showed preferential adsorption for *trans*-piperylene, with an uptake quantity similar to that in single-component adsorption measurements. The uptake of *cis*-piperylene was found to be identical to that for isoprene in the competitive conditions. In breakthrough experiments, the elution order corresponded to the results of the competitive experiments, with *trans*-piperylene being retained a much longer time than the other two isomers. Moreover, the regeneration of the MOF can be easily achieved by flushing the column with pure heptane. These results indicated that MIL-96 is capable of separating *trans*-piperylene and *cis*-piperylene or isoprene isomers in the liquid phase.

3.3. Selective Adsorption and Separations of Stereoisomers

Stereoisomers are isomeric molecules that have the same bond connection and sequence of constituent atoms, but differ only in the 3D orientations of the atoms in space.[423] Stereoisomers include enantiomers where different isomers are nonsuperimposable mirror images of each other and diastereomers (including cis−trans isomers and conformers). As compared to structural isomers, stereoisomers have much closer physical properties, such as nearly identical size, boiling, and melting points. This section summarizes the progress in the research of using MOFs for selective adsorption and separations of stereoisomers, with a central focus on enantioselective separations, that is, enantio-separations (or chiral separations) using homochiral MOFs. It should be pointed out that the asymmetric catalysis using homochiral MOFs is associated with the enantioselective selective adsorption and separation to some extent, but is beyond the scope of this Review. For a full understanding of this MOF-related topic, readers are directed to several excellent reviews that have appeared in recent years.[81,82,85]

3.3.1. Enantiomers (Enantio-separation). Enantio-separation is a major concern particularly in the modern pharmaceutical and agrochemical industries, because, for example, most drugs are only active in a given chirality (optically pure form), with the opposite enantiomer often producing unwanted effects. Methods available to obtain optically pure chemical products include separation of racemates (enantiomeric separation), isolation from natural sources, fermentation, direct synthesis using homochiral starting materials, and synthesis by asymmetric catalysis. Enantiomers usually coexist as racemic mixtures in an achiral environment, thus requiring a chiral reagent for their separation. Doing this, usually, the racemates to be separated are put in a chiral environment where a chiral element (termed chiral selector), capable of interacting enantioselectively, aids in the separation. Several techniques including different chromatographic techniques and electromigration have been developed and used in the separation of enantiomers. To understand these techniques, readers are directed to numerous review papers and specialized monographs,[424,425] bearing in mind that in all of these methods, chiral selectors are prerequisites.

Homochiral materials have already been widely used as chiral selectors in a lot of separation processes; however, porous solids with highly uniform pores, such as zeolites and crystalline inorganic oxides, are not successful because the preparation of these materials in an enantiopure form is very difficult.[105,426] Zeolites, for example, despite considerable efforts, have only rarely been produced in optically pure form.[427,428] More importantly, local chirality, which is more important in separations than topological chirality, is often destroyed during the removal of the templates or activation, resulting in chiral zeolites that may be useless. This situation has prompted the exploration of other homochiral porous solids, such as homochiral MOFs for enantioselective separations.

MOFs are typically synthesized under mild conditions, which allows for the facile construction of homochiral frameworks through the judicious choice of chiral building blocks or by using chiral induction.[429] Clearly, a chiral pore with proper size and shape will give excellent enantioselectivity. To realize this target is much easier in MOFs than in zeolites because of the modular building approach of MOFs. Despite the construction of a large number of homochiral MOFs, only very limited members have thus far been explored in enantioselective adsorption and separations.[81,85]

The first example of enantioselective inclusion of chiral molecules into the well-defined pores of a homochiral MOF was reported by Kim and co-workers,[26] on $Zn_3(\mu_3\text{-}O)(L\text{-}H)_6$ (POST-1, L = (4*S*,5*S*)- or (4*R*,5*R*)-2,2-dimethyl-5-[(4-pyridinylamino)carbonyl]-1,3-dioxolane-4-carboxylic acid). This MOF has a 2D layer structure consisting of edge-sharing hexagons with a trinuclear SBUs at each corner. The 2D layers stack to form a 3D framework with triangular, homochiral channels (that are 13.4 Å per side in length) in the stacking direction. A structurally interesting feature is that part of the pyridyl

dx.doi.org/10.1021/cr200190s |*Chem. Rev.* 2012, 112, 869–932

a)

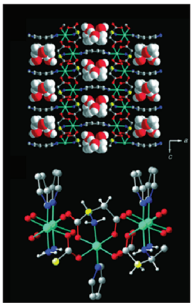

b)

Diol	Extracted *ee* value[b]	Standard *ee* value[c]
1,2-propanediol	5.35	0.16
1,3-butanediol	17.93	0.62
1,2-butanediol	5.07	0.88
2,3-butanediol	1.5[d]	0.5
1,2-pentanediol	13.9[e]	0.34
2,4-pentanediol	24.5	0.00
2-methyl-2,4-pentanediol	53.77	0.46
2,5-hexanediol	3.4[f]	0.0
1,2-hexanediol	5	0.09

Figure 20. (a) Structure of Ni_2(L-asp)$_2$(bipy)·guests; the disordered methanol and water guests that occupy the channels are represented with space-filling spheres (top), and showing the coordination environment of the Ni(II) center (bottom) (Ni atoms are shown in cyan, C atoms in gray (chiral centers in yellow), H atoms in white, N atoms in blue, and O atoms in red); (b) the enantiomeric ee values found for the sorption of small chiral diols by Ni_2(L-asp)$_2$(bipy) at 278 K, as compared to those of the racemic standards (note: [b] For the guest diols recovered by distillation from the MOF, after exposure of it to the liquid diol for 16 h. [c] For the racemic diol standard. [d] Extracted 71.4% meso; standard 65.7% meso. [e] Extracted 45.1% meso; standard 50.7% meso. [f] Extracted 58.5% meso; standard 53.6% meso). Reproduced with permission from ref 435. Copyright 2006 Wiley-VCH.

groups of the ligands are not coordinated to the metal atoms, but are partially protonated and extrude into the channels. The protons in the pyridine groups are indeed exchangeable with other cations such as Na^+ and K^+. The presence of large accessible chiral channels and exchangeable cations in this MOF prompted the exploration of enantioselective inclusion of cationic complexes. It was found that when immersing L-POST-1 in a methanol solution of racemic [Ru(2,2′-bipy)$_3$]Cl$_2$ (2,2′-bipy = 2,2′-bipyridine), 80% of the protons on the free pyridine groups of the framework were exchanged by [Ru(2,2′-bipy)$_3$]$^{2+}$ with a 66% enantiomeric excess in favor of the Δ isomer, which was supported by NMR, UV, and CD spectroscopy measurements.

Another early example in this subject is based on a series of lanthanide bisphosphonates with a common formula of [Ln(debnbp-H$_2$)(debnbp-H$_3$)(H$_2$O)$_4$]·solvent (Ln = La, Ce, Pr, Nd, Sm, Gd, or Tb) constructed by potential chiral ligand, 2,2′-diethoxy-1,1′-binaphthalene-6,6′-bisphosphonic acid (H$_4$debnbp).[430] When homochiral H$_4$debnbp (*R* or *S* isomer) was used in the synthesis, homochiral MOFs were obtained. They have a 2D lamellar structure consisting of elongated rhombohedral grids. These 2D layers stack via interdigitation of the ligand's binaphthyl rings from the adjacent layers to leave void space between layers, where solvent molecules reside. After the removal of free solvents, asymmetric channels of about 12 Å in its largest dimension were created in the stable framework, thus giving rise to a homochiral porous framework with large and accessible channels that are potentially useful in enantioselective separations. An *R*-MOF treated with ammonia was tested in the separation of racemic *trans*-1,2-diaminocyclohexane. At a substrate/host ratio of 1.4, the adsorption gave an enantio-enrichment of 13.6% and 10.0% for *S*,*S*- and *R*,*R*-1,2-diaminocyclohexane at the early and the late fractions, respectively. Despite the low enantioselectivity, these homochiral MOFs are capable of enantio-separation.

Resolution of racemic mixtures of small organic molecules was also observed by Xiong and co-workers[431] in a robust 3D homochiral MOF, Cd(QA)$_2$ (QA = 6′-methoxyl-(8*S*,9*R*)-cinchonan-9-ol-3-carboxylate), which has a diamond-like net containing homochiral open channels. Treating racemic 2-butanol with a powdered sample of this MOF under solvothermal conditions afforded a crystalline sample of ((*S*)-2-butanol)⊂Cd(QA)$_2$ (crystallographically identified). Measured optical rotation of the 2-butanol desorbed from the new MOF sample was identical to the standard of a pure (*S*)-2-butanol, further supporting the selective inclusion. The estimated enantiomeric excess (ee) value was approximately 98.2%. Furthermore, the adsorbed (*S*)-2-butanol can be completely removed upon heating the samples to 210 °C without destroying the framework, suggesting the ability of reversible adsorption with this MOF. Similarly, (*S*)-2-methyl-1-butanol can also be selectively included from its racemic mixture by this homochiral MOF under similar conditions, but with a lower ee value of about 8.4%.

The same group also reported a 2D homochiral Cu(I)-olefin MOF, Cu$_5$Cl$_6$(VB-N-CIN)$_2$·EtOH (VB-N-CIN = 4-vinylbenzylcinchonidinium cation), capable of selectively intercalating the (*R*)-2-butanol isomer from its racemic mixture.[432] In the structure, Cu$_5$Cl$_6$ clusters are linked by the enantiopure chiral ligands to form a layered structure with square grids. Layers stack in an AA arrangement to form a 3D structure with interlayer spaces occupied by noncoordinating ethanol molecules. Under solvothermal conditions, these ethanol guest molecules can be exchanged by other guests. Treating the as-made MOF crystals with racemic 2-butanol, following an experimental method similar to that used in Cd(QA)$_2$ mentioned above, demonstrated that (*R*)-2-butanol isomer was selectively intercalated between layers, with an estimated ee of about 25%.

The resolution of racemic 2-butanol through the similar intercalation was also achieved by another homochiral MOF, [Cu(PPh$_3$)(ppma)$_{1.5}$]·ClO$_4$ (ppma = *N*,*N*′-(2-pyridyl-(4-pyridylmethyl)-amine)), also reported by this group.[433] Interestingly, this homochiral MOF was constructed by an achiral organic ligand through spontaneous resolution during the formation of its single crystals. In its structure, Cu(I) atoms are linked by bridging ligands to form a 2D layer with triangular cavities, where the ClO_4^- ions reside, leading to an absence of pores in the layer. These layers stack in an ABAB packing mode to form a 3D structure, leaving the interlayer space accessible for guest molecules. The enantioselective inclusion of 2-butanol by spontaneous resolution was confirmed by crystal structure determination. The homochiral crystals of the guest loaded MOF were manually separated, and then evacuated to collect enantiopure 2-butanol. The optical rotation of the resolved 2-butanol has a value identical to the standard enantiopure isomer, confirming the enantioselective inclusion. This separation based on spontaneous resolution, although simple in concept, is not economically favorable because the process is

dx.doi.org/10.1021/cr200190s |*Chem. Rev.* 2012, 112, 869–932

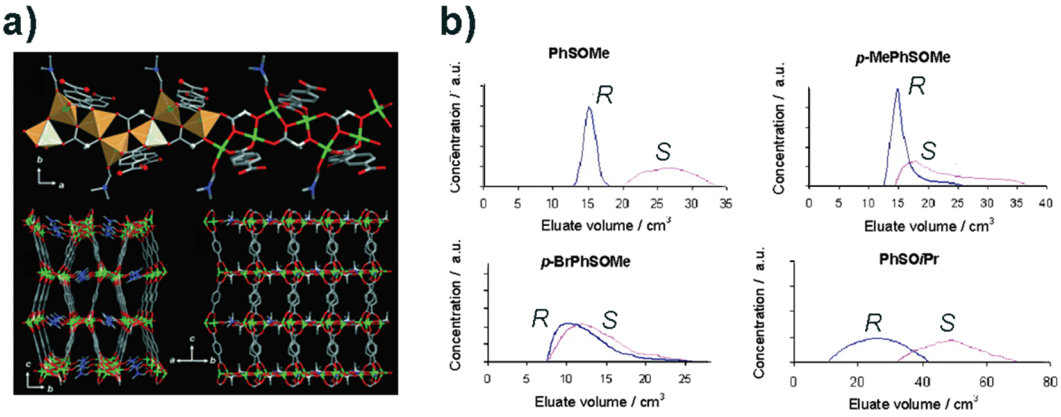

Figure 21. (a) Structure of $Zn_2(bdc)(L\text{-lac})(DMF)$ showing the 1D homochiral chain (top, as both ball-and-stick/polyhedra and wire models; polyhedra represent the Zn coordination environments) and 3D framework viewed from two different directions (bottom) (H atoms and guest molecules are omitted; Zn atoms are shown in green, N atoms in blue, O atoms in red, C atoms in gray; and chiral C atoms in white); and (b) separation of alkyl aryl sulfoxides using $Zn_2(bdc)(L\text{-lac})(DMF)$ as the chiral stationary phase (eluents: for PhSOMe and *p*-MePhSOMe, 12 cm^3 of 0.01 M DMF solution in CH_2Cl_2, then 1% DMF in CH_2Cl_2; for *p*-BrPhSOMe and PhSOPr, 20 cm^3 of 0.01 M DMF solution in CH_2Cl_2, then 1% DMF in CH_2Cl_2. elution rate = 2 cm^3/h). Reproduced with permission from refs 436 and 437. Copyright 2006 Wiley-VCH and 2007 American Chemical Society.

time-consuming and unfeasible on a large scale, as claimed by the authors.

More interestingly, the size-dependent enantioselective adsorption of chiral organic molecules was observed in a homochiral MOF, $Ni_3(btc)_2(3\text{-pic})_6(1,2\text{-pd})_3$ (3-pic = 3-picoline; 1,2-pd = 1,2-propanediol), reported by Rosseinsky and co-workers.[434] This MOF has a 3D structure, in which each btc^{3-} ligand acts as a 3-connected node bridging between three Ni(II) atoms and each Ni(II) atom is linked by two ligands, to generate a 2-fold interpenetrated (10,3)-a topological framework, featuring two types of pores with different diameters of 12 and 14 Å. The coordinated 3-pic and 1,2-pd molecules decorate the surface of the pores. This (10,3)-a net is inherently chiral based on the helical arrangement of network nodes in the same handedness. When an enantiopure 1,2-pd was used in the synthesis of the MOF, a homochiral product was obtained. The framework of this chiral MOF is stable after guest removal and contains 47% free void for the accommodation of guest molecules. It is interesting that the adsorption of racemic mixture of ethyl-3-hydroxybutyrate, menthone, and fenchone by the homochiral MOF in the vapor or liquid phase showed even higher uptakes but no enantioselectivity. However, a larger molecule, binaphthol, was enantioselectively adsorbed by this homochiral MOF (with an evaluated ee value of 8.3%) from a racemic mixture in dichloromethane. Thus, a close match between the dimension of the chiral channel in the MOF and the size of the chiral guest molecule seems to be important in the enantioselective adsorption and separation.

Not only do matching sizes and shapes between guest molecules and pores have significant influences on the enantioselective adsorption of homochiral MOFs, but surface properties also play a significant role. This situation was observed in the enantioselective adsorptions of chiral diols by a homochiral MOF, $Ni_2(L\text{-asp})_2(bipy)\cdot$guests (L-asp = aspartate), again reported by Rosseinsky and co-workers.[435] As shown in Figure 20a, in the structure of this MOF homochiral Ni(L-asp) layers are connected by bipy linkers to afford a 3D pillared framework with 1D channels of 3.8 × 4.7 Å. It is important that chiral carbon atoms, coordinated amine groups, and oxygen atoms of the aspartate ligands project into the channels, which imparts the chiral functionality and active sites of pores in the material. As shown in Figure 20b, the adsorptions of different positional isomers of chiral diols showed different levels of enantioselectivity, with the highest ee value of 53.7% for 2-methyl-2,4-pentanediol. An isomeric homochiral MOF derived from D-aspartate also showed the same degree of enantioselectivity but for the opposite enantiomer in all cases. It is clear that the enantioselectivities achieved herein are guest-geometry dependent. Particularly, the relative positions of the two hydroxyl groups in a diol molecule seem to have a larger impact. In fact, it was revealed that 1,3-disposition of the diol units is favorable in the adsorption selectivity as compared to other positions. For instance, 1,2-butanediol and 2,3-butanediol displayed considerably reduced enantioselectivity as compared to 1,3-butanediol, despite having the same four carbon chain length. Furthermore, the different enantioselective efficiencies of this MOF toward these isomers were demonstrated to be related to different H-bonding interactions between the two −OH groups of each guest molecule and the carboxylate O or amine N atoms on the pore surface of the MOF, which are also geometry-dependent when the guest molecules reside in the confined pore space.

In addition, the enantioselective adsorption and chromatographic resolution of sulfoxides was explored on another amino acid-based homochiral MOF, $Zn_2(bdc)(L\text{-lac})(DMF)$ ($L\text{-}H_2lac$ = L-lactic acid).[436,437] The Zn(II) atoms in this framework are linked by lactate ligands to form 1D homochiral chains, which are further interlinked by bdc^{2-} ligands to form a 3D framework with open pores roughly 5 Å in diameter (Figure 21a). The chiral centers of the L-lactate moieties are exposed to the porous voids to give a homochiral pore environment. It was found that this framework collapses after removal of guest solvent molecules in pores, but withstands the exchange of these free solvent molecules by other guest molecules while in solution.[436] Adsorption experiments of several substituted sulfoxide in CH_2Cl_2 solutions revealed a remarkable uptake capacity toward the sulfoxides with smaller substituents including methylsulfinylbenzene (PhSOMe) and 1-bromo-4-(methylsulfinyl)benzene (4-BrPhSOMe) and an efficacious enantioselective adsorption ability. The evaluated ee was 20% and 27% for the two sulfoxides, respectively, with the *S* enantiomer being in excess. Sulfoxides with larger substituents,

dx.doi.org/10.1021/cr200190s |*Chem. Rev.* 2012, 112, 869–932

including 1-(methylsulfinyl)-4-nitrobenzene (4-NO_2PhSOMe) and benzylsulfinylbenzene (PhSOCH_2Ph), however, were not soaked up. Furthermore, this MOF was also easily regenerable after adsorption and reusable without performance loss.

On the basis of these results, this homochiral MOF, acting as the stationary phase was further tested for the chromatographic separations of sulfoxides.[437] The experimental chromatograms are shown in Figure 21b, from which only PhSOMe demonstrated a clear peak resolution that allowed the complete separation of its enantiomers with a high ee value of about 60%. For the other three sulfoxide isomers, the separations were not so complete. These different separation performances were attributed to both electronic and steric effects of the substituents in the aromatic ring of each sulfoxide molecule. An electron-withdrawing effect of Br− or NO_2− was considered to lower the adsorbate's coordination ability, thereby reducing the enantioselectivity. Although electron-donating substituents could, by this logic, increase the adsorption capacity, the steric hindrance of these additional substituents limited the diffusion of these guest molecules in the pores, resulting in similarly poor enantioseparation. For PhSO*i*-Pr, the incomplete separation as compared to that of PhSOMe may be attributed to the steric crowding from bulkier *i*-Pr substituent of the molecule. In addition, this homochiral MOF also showed remarkable catalytic activity in the oxidization of thioethers to sulfoxides; it can thus be utilized in a one-step reaction-purification system for the synthesis of optically pure sulfoxides.[437]

Furthermore, rationally tuning micropores of homochiral MOFs by ligand modifications for enantiopure selective separation of 1-phenylethyl alcohol (PEA) has also been demonstrated by Chen and co-workers.[296] Two isostructural MOFs, Zn_3-$(cdc)_3$[Cu(SalPycy)] and $Zn_3(bdc)_3$[Cu(SalPycy)] (also mentioned in section 2.1.4 of this Review) containing homochiral pores of about 6.4 Å in diameter were tested in this work. It was found that the two homochiral MOFs can selectively encapsulate *S*-PEA from a racemic *R*/*S*-PEA mixture. For $Zn_3(bdc)_3$[Cu-(SalPycy)], the evaluated ee value was 21.1% in the first use of the fresh sample. It is important that after the adsorption of *S*-PEA the MOF sample kept high crystallinity and could be regenerated by immersion into methanol. The second and third times, regenerated $Zn_3(bdc)_3$[Cu(SalPycy)] gave slightly lower ee values of 15.7% and 13.2%, respectively. Interestingly, Zn_3-$(cdc)_3$[Cu(SalPycy)], with smaller chiral pores as compared to those of $Zn_3(bdc)_3$[Cu(SalPycy)], significantly enhanced the enantioselectivity for the separation of *R*/*S*-PEA. A higher ee value of 64% on the fresh sample was observed. The regenerated $Zn_3(cdc)_3$[Cu(SalPycy)] can also be further used, giving slightly lower ee values of 55.3% and 50.6% after its first and second regenerations, respectively. It is clear that the chiral pores within the two MOFs basically match the size of *S*-PEA, which leads to the observed selective resolution. Also, the smaller pore provided the higher enantioselectivity due to a much more effective chiral identification. In fact, it has been confirmed that the two MOFs are not capable of separating larger alcoholenantiomers, such as 1-(*p*-tolyl)-ethanol, 2-phenyl-1-propanol, and 1-phenyl-2-propanol.

Apart from the experimental explorations discussed above, the computational evaluation of enantioselective adsorption by a homochiral MOF, Cd_3(*R*-ddbb)$_4(NO_3)_6$ (*R*-ddbb = (*R*)-6,6′-dichloro-2,2′-dihydroxy-1,1′-binaphthyl-4,4′-bipyridine), was also performed by Snurr and co-workers.[438] To the best of our knowledge, this is the only example beyond experimental studies in this topic, warranting its inclusion in this section. This MOF, initially synthesized by Wu and Lin,[439] has a 2-fold interpenetrated 3D framework structure containing helical pores of about 13.5 × 13.5 Å in size running in the crystallographic *c*-direction and zigzag pores of about 4.9 × 13.5 Å in the remaining two directions. The separation capabilities of this MOF toward racemic mixtures of (*R*,*S*)-1,3-dimethyl-1,2-propadiene, (*R*,*S*)-1,2-dimethylcyclobutane, and (*R*,*S*)-1,2-dimethylcyclopropane, respectively, were evaluated by grand canonical Monte Carlo simulations. The results showed that this MOF has a remarkable enantioselective adsorption capability for 1,3-dimethyl-1,2-propadiene isomers, giving an ee value of approximately 50%. For the two cyclic compounds, moderate ee values (6% for 1,2-dimethylcyclobutane and 4% for 1,2-dimethylcyclopropane) were calculated. The selective adsorption was further investigated by analyzing adsorption sites, diastereomeric complexes, and adsorption energies. The related results showed that the small zigzag pores in the MOF dominate the enantioselective adsorption, whereas the larger helical pores do not impart any enantioselectivity to these molecules.

Clearly, these reported results have indicated that despite being in an early stage of research, MOFs have great potential in enantioselective separations. In addition, other porous metal−organic materials, including metal−organic supramolecular rings, cages, and other molecular complexes, as well as some 1D structural coordination polymers, also showed potential for the separations of enantiomers.[85] These materials, however, fall outside of the definition of MOFs used by the authors for this particular Review and therefore are not discussed herein.

3.3.2. Cis−Trans Isomers. The separation of *cis*- and *trans*-isomers is another challenging issue, and only very limited progress has been made both in traditional porous sorbents, such as zeolites,[105] and MOFs. MIL-96, as mentioned above, was shown to be capable of separating *cis*-piperylene and *trans*-piperylene in the liquid phase.[387] Single-component adsorption showed that *trans*-piperylene uptake is much higher than that of *cis*-piperylene from their heptane solutions, giving an evaluated pore occupation ratio of 2:0.6 for the two isomers. Competitive batch experiments also confirmed the preferential uptake of *trans*-piperylene from the mixture solution. Furthermore, it was found that the calculated separation factors increase with increasing concentration of the isomer mixture in solution, consistent with the assumption that packing effects determine the selective adsorption. In addition, the regeneration of the MOF adsorbent can be easily achieved by flushing the column with pure heptane.

By contrast, a remarkable adsorption preference of HKUST-1 toward *cis*-olefins over *trans*-olefins was observed by De Vos and co-workers.[386] Several olefins with different chain lengths, including 2-butene, 2-pentene, 2-hexene, 2-heptene, 2-octene, 4-octene, 4-nonene, 5-decene, and methyl-9-octadecenoate, were tested for the adsorption from their binary equimolar mixtures of *cis*- and *trans*-isomers in hexane. The results gave separation factors of *cis*- over *trans*-isomers of 1.9, 4.9, 1.2, 3.4, 6.6, 2.6, 2.1, 4.3, and 2.4, respectively. As discussed in section 3.1.1, the presence of CUMs led to this MOF's ability to concentrate olefins through π-complexation in its pores. It was suggested that after adsorption, a double bond in the cis configuration would be more easily accommodated on the Cu(II) sites for steric reasons. As a representative example, the competitive uptake of *cis*- and *trans*-2-pentene was further investigated as a function of equilibrium bulk-phase concentration. The results indicated that with increased concentration the separation

dx.doi.org/10.1021/cr200190s |*Chem. Rev.* 2012, 112, 869–932

Table 3. H_2 Separation Performances of Some Reported MOF Thin Films and Selected Inorganic Membranes

		observed highest separation factor (ideal separation factor)				
MOF thin film	pore size (Å)	H_2/CO_2	H_2/O_2	H_2/N_2	H_2/CH_4	H_2 perm. (mol m^{-2} s^{-1} Pa^{-1})
HKUST-1[451]	9.0	6.8(4.5)		7.0(4.6)	6(7.8)	1.07×10^{-6}
HKUST-1[452]		(5.1)		(7.5)	(5.7)	
MOF-5[453]	15	KD[a]	KD[a]	KD[a]	KD[a]	4.7×10^{-6}
MMOF[454]	3.2	(4.5)		(23)		4.7×10^{-7}
ZIF-7[455]	3.0	6.5(6.7)		7.7	5.9	4.7×10^{-8}
ZIF-7[456]		13.6		18	14	4.5×10^{-8}
ZIF-8[457]	3.4	(4.5)	(5.8)	(11.6)	11.2	5.1×10^{-8}
ZIF-8[458]				(11.6)	(13.0)	1.7×10^{-7}
ZIF-22[459]	3.0	7.2(8.5)	6.4(7.2)	6.4(7.1)	5.2(6.7)	1.9×10^{-7}
ZIF-90[460]	3.5	7.3(7.2)		11.7(12.6)	16.4(15.9)	2.8×10^{-7}
ZIF-90 (postfunctionalized)[461]	<3.5	15.3(15.7)		15.8(16.6)	18.9(19.3)	2.2×10^{-7}
silicate-1[462]	5.5	(1.84)		(1.72)		7.9×10^{-6}
LTA $AlPO_4$[463]	4.0	7.6(11)	6.1(9)		4.3(7.7)	2.5×10^{-7}
ZSM-5[464]	5.5			(15.5)		9.3×10^{-13}

[a] Knudsen diffusion.

factor decreases, again a cooperative result from the steric hindrance and the strong adsorption through π-complexation of double bonds with the open Cu(II) sites in the framework.

In addition, the selective capture of *cis*-crotononitrile from a mixture with its *trans*-isomer by flexible Mn(pmai)(H_2O) (pmai = 5-(pyridin-4-ylmethylamino)isophthalate) has been confirmed by Bharadwaj and Das.[440] This MOF has a 3D porous structure with water molecules coordinated to metal sites of its pore surface. After immersing crystals of the MOF in a 2:3 mixture of *cis*-crotononitrile and *trans*-crotononitrile for several days, it was found that only the *cis*-isomer was selectively captured, as confirmed by single-crystal X-ray diffraction of the guest loaded MOF. After adsorption, it was found that the coordinated water molecules and free solvent molecules in the as-synthesized crystals were replaced by *cis*-crotononitrile, accompanied by a change of the structural parameters of the MOF. Besides the coordination of *cis*-crotononitrile to metal sites, several other weak interactions between the adsorbed molecules and host framework were also observed. However, even if the crystals are immersed in pure *trans*-crotononitrile for several days, no uptake of the guest molecules was observed, which may be a result of shape mismatches between the *trans*-isomer and the pore or steric hindrance.

4. MOFS FOR MEMBRANE-BASED SEPARATIONS

As with adsorptive separation, distillation, and crystallization, using membranes for separation has its inherent advantages, including high energy efficiency, low cost, ease of processing, and excellent reliability. MOFs, like zeolites, are seen as feasible materials for membrane-based separation due to their well-defined, highly regular pore structures. Although zeolites have been widely studied for membrane technologies, only few successful zeolite membranes have been used for chemical separations in industry.[105] The implementation of zeolite membranes in a broad range of applications is facing serious setbacks and difficulties because of a number of drawbacks not only in the materials themselves (such as the limited range in pore sizes accessible to zeolites) but also in the fabrication of the membranes.[441] For example, organic templates are often used in the synthesis of zeolites, which must be removed, usually by heating at high temperature to burn out the organic molecules, from the final structure to have pores available for separations. This heat treatment sometimes produces cracks in the membrane, leading to low separation performance.[442] MOFs cover a much wider range of pore sizes, shapes, and surface properties than zeolites and are usually synthesized under mild conditions, where solvents, sometimes acting as templates, can easily be removed in most cases. Moreover, the high degree of control over pore functionality (often termed "design" because the modular organic linkers can be prefabricated to nearly any specification) at the molecular level is much easier for MOFs than for zeolites and other inorganic porous solids. MOFs thus present a new class of highly promising membrane materials, overstepping the limitations of zeolites in terms of materials chemistry, at least in principle, although the fabrication of continuous MOF-based membranes also remains a great challenge.

Some MOFs have been tested for their applications in membrane-based separations not only as thin films but also as porous adducts in mixed-matrix membranes; however, the two research subjects are still in an extremely early stage of development. This section discusses the research progress in separations using MOF-based membranes, including thin films (pure MOF membranes) and hybrid membranes (also called mixed-matrix membranes), primarily from experimental results. The fabrications or preparations of these MOF membranes,[443,444] although very important for their subsequent separation applications, are not discussed in detail herein. In addition, several papers have assessed the separation capacities of some MOF-based membranes by computational molecular simulations.[445−450] Again, despite being very important for our fundamental understanding of the separation mechanisms and helpful in designing new materials, an in-depth discussion of these studies is not provided.

4.1. Separations with MOF Thin Films

Crystalline thin films, due to their high permeability and selectivity, have attracted tremendous interest in membrane-based separations, despite the significant fabrication challenges. MOF thin films are very promising for various separations in both the gas and the liquid phases;[444] however, only a limited number of reports have been documented to date.

dx.doi.org/10.1021/cr200190s |*Chem. Rev.* 2012, 112, 869–932

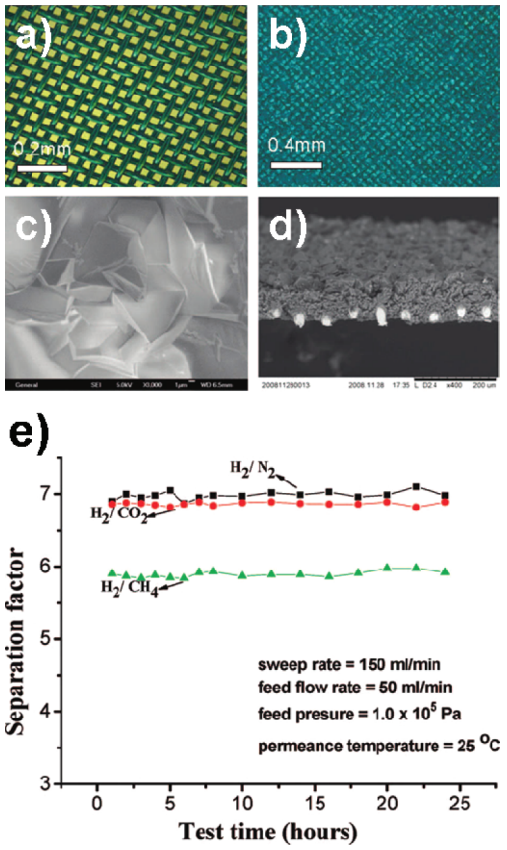

Figure 22. (a and b) Optic micrograph of the copper net and the net-supported HKUST-1 membrane; (c and d) SEM image of the surface and cross section of the membrane, respectively; and (e) plot of H_2/N_2, H_2/CH_4, and H_2/CO_2 separation factors of the copper net supported HKUST-1 membrane with changes in test time. Reprinted with permission from ref 451. Copyright 2009 American Chemical Society.

4.1.1. H_2 Separation. Among those reports testing gas separations using MOF thin films, H_2 separation from other gases is the most popular, possibly due to its importance in application as a new energy source, and the ease of separation and facile measurement. Table 3 summarizes the H_2 separation performances of some reported MOF thin films along with selected inorganic membranes for comparison. For the separation of H_2 from other gases, a MOF with small micropores is considered to be an ideal membrane material. However, some MOF thin films with larger pore openings have also presented excellent separation performance as discussed below.

Using a so-called "twin-copper-source" membrane growth strategy, Zhu and co-workers[451] made a HKUST-1 thin film, where a preoxidized copper net acted as both nucleation sites and support (Figure 22a–d). This resulting membrane is defect-free and has a thickness of about 60 μm. Despite the large pore size of this MOF, the membrane presented an excellent H_2 separation ability from its binary mixture with CO_2, N_2, and CH_4 at room temperature, as shown in Figure 22e. This separation performance is far beyond the Knudsen diffusion behavior, and the permeation flux of H_2 is much higher than those of the other gases in the mixtures, indicating that this membrane has a higher preference for the size selectivity of H_2. It should also be pointed out that the observed separation factors of H_2/N_2 and H_2/CO_2 are higher than the ideal separations factors (Table 3), which were evaluated from single-component gas permeation data. However, for H_2/CH_4, the membrane separation selectivity was lower than the ideal selectivity. These deviations could be diffusion-related, but it is difficult to clarify on the basis of the present set of data. In addition, this MOF thin film also showed an overall better gas permeation performance due to its large pore size. Further experiments also showed that the separation performances are temperature-dependent: the H_2 permeation flux increased and the separation selectivities decreased when the temperature increased from 273 to 343 K. The H_2/N_2 separation factor reached a maximum at 298 K, whereas that of H_2/CO_2 continued to grow until 313 K. The reproducibility and durability of the membrane performances were also shown to be excellent (Figure 22e), highlighting the considerable potential in practical application of this membrane for H_2 separation.

H_2 separation from CO_2, N_2, O_2, and CH_4 by HKUST-1-based membranes was also reported by Jeong and co-workers.[452] They fabricated crack-free MOF membranes on porous α-alumina supports by using a "thermal seeding" secondary growth method. The separation performance of the membranes at different temperatures was evaluated by single gas permeation measurements. The results revealed ideal selectivities of about 3.7, 2.4, and 3.5 at room temperature for H_2 over N_2, CH_4, and CO_2, respectively, which are smaller than the values reported by Zhu and co-workers.[451] This deviation may be due to the effects of the porous supports or nonselective intercrystalline diffusion through grain boundaries. As the temperature was increased, the selectivity of H_2 increased initially and then reached a plateau with maximum ideal selectivities of H_2 over N_2, CH_4, and CO_2 of about 7.5, 5.7, and 5.1, respectively. Regarding permeability, it was found that as temperature was increased the permeance values of all gases generally decreased. Furthermore, the permeance value of CO_2 became larger than those of CH_4 and N_2 with increased temperature, indicating the effect of the affinity between the quadrapolar CO_2 and the framework, in which the accessible Cu(II) sites became vacated when the coordinated solvent molecules were removed at high temperature.

Another popular MOF, MOF-5, has also been fabricated into thin films for H_2 separation. Lai and co-workers[453] made the first continuous and well-intergrown MOF-5 membrane on porous α-alumina supports by in situ solvothermal synthesis. Two as-made MOF-5 membranes with a thickness of 25 and 85 μm were tested for simple gas permeation of H_2, CH_4, N_2, CO_2, and SF_6. The results showed that the diffusion of simple gases through these membranes follows the Knudsen diffusion behavior. A molecular sieving effect was not observed, probably due to the substantially larger pore size of the MOF-5 framework as compared to the tested gas molecules. These observations are comparable to the results from molecular simulations.[447] The similar permeance behaviors of H_2, N_2, CH_4, and CO_2 have also been observed in MOF-5 membranes fabricated by using a microwave-induced rapid seeding and solvothermal secondary growth method.[465] It was found that gas permeances are independent of the trans-membrane pressure drops, indicating that macroscopic defects are insignificant in these membranes.

ZIFs, with high thermal and chemical stability and tunable pore properties, are very promising in membrane-based applications.[14,103] Several ZIF membranes have been made and tested for the separation of H_2 from other gases. Caro and co-workers[457] explored the separation of H_2 from CO_2, N_2, O_2, and CH_4 using a ZIF-8 thin film. ZIF-8 is highly stable and has a sodalite-type porous structure with narrow hydrophobic pores

dx.doi.org/10.1021/cr200190s |Chem. Rev. 2012, 112, 869–932

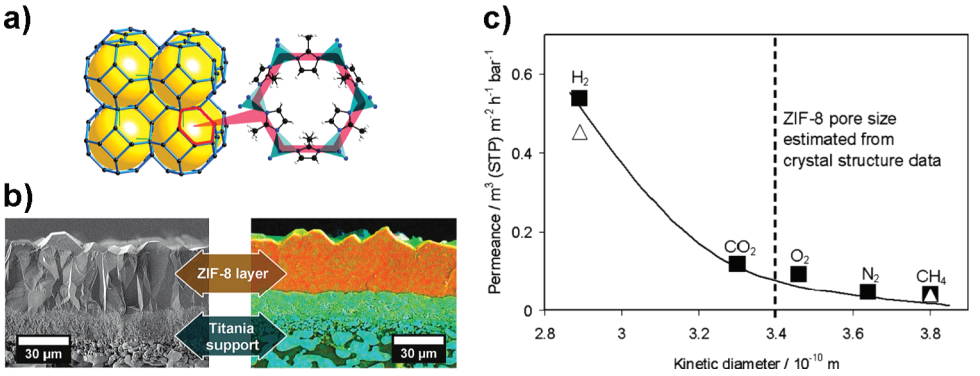

Figure 23. (a) Sodalite topology of ZIF-8 (left) and its narrow opening (right) through which molecules must pass; (b) SEM image of the cross section of a ZIF-8 membrane (left) and EDXS mapping of the sawn and polished ZIF-8 membrane (right, color code: orange, Zn; cyan, Ti); and (c) single (■) and mixed (△) gas permeances for a ZIF-8 membrane versus kinetic diameters of the tested gas molecules. Reprinted with permission from ref 457. Copyright 2009 American Chemical Society.

(with cross sections of about 3.4 Å) in three directions (Figure 23a).[14,466] These features favor a ZIF-8 membrane over zeolites in the separation of H_2 from a mixture steam. A crack-free, dense, polycrystalline ZIF-8 membrane on titania supports (Figure 23b) was fabricated by a microwave-assisted solvothermal process in methanol solution. Methanol easily escaped from the cavities at room temperature, yielding the guest-free, activated ZIF-8 membrane. The volumetric flow rates of the single gases and of a 1:1 mixture of H_2 and CH_4 through the membrane were measured, and the resulting data were used to calculate permeances, which are presented in Figure 23c. It is clear that the calculated permeances are dependent on the molecular size of the tested gases: H_2 permeated the membrane much easier than the other gases. Another interesting observation is that, although the pore size of ~3.4 Å in ZIF-8 (estimated from crystal structure) is smaller than the molecular size of CH_4 (kinetic diameter of 3.8 Å), CH_4 can smoothly pass through the pore network of the membrane, which is supported by the lack of a sharp cutoff in the permeance data for gases above 3.4 Å. This was explained by hypothesizing that the framework is probably flexible enough to allow the pore size to change when gases are passing through.[467] In the case of the H_2/CH_4 mixed-gas permeance, a slight influence of CH_4 on the permeation of H_2 was observed, which is different from the diffusion in some other zeolites, where an immobile component usually reduces the mobility of a more mobile component.[468] The separation factor of H_2 over CH_4 calculated from the permeation data on a 1:1 H_2/CH_4 mixture is 11.2 at room temperature and 1 bar, much higher than the Knudsen separation factor of ~2.8. However, the H_2/CO_2 separation factor of 4.5 is approximately that of the Knudsen separation factor.

H_2 separation by a ZIF-8 membrane was also tested by Jeong and co-workers.[458] They prepared the membranes by a modified method, which they termed "support surface modification and in situ solvothermal growth". On the basis of the single gas permeation experiments, the as-synthesized ZIF-8 membrane showed an ideal selectivity of 11.6 and 13 for H_2/N_2 and H_2/CH_4, respectively, at room temperature and 1 bar, comparable to the values from other groups, mentioned above. Further experiments revealed a decrease in permeance with increased temperature for all of these gases. These results showed that ZIF-8 membranes are indeed capable of separating H_2 from other gases, especially from CH_4.

As mentioned above, ZIF-8 has a pore size of 3.4 Å, larger than the kinetic diameter of CO_2 (3.3 Å), which leads to the observed Knudsen selectivity for H_2/CO_2 separation. To attempt a more effective separation for the two important gases, Caro's group made ZIF-7 (with smaller pore size than ZIF-8) thin film, which indeed presented a high H_2 selectivity over other large gases including CO_2.[455] ZIF-7 has a rigid soladite-type framework structure with a hexagonal arrangement of large cavities that are interconnected by narrow windows of 3.0 Å in size,[291] just between the kinetic diameters of H_2 (2.9 Å) and CO_2 (3.3 Å). Expectedly, this membrane showed a molecular sieving effect for the two gases. The ZIF-7 membrane (about 1.5 μm thick) on a porous alumina support was prepared by a seeded microwave-assisted solvothermal secondary growth method. The membrane was activated at 200 °C for over 40 h, and gas permeation, tested using a Wicke−Kallenbach technique at 200 °C and 1 bar for both single and 1:1 mixed-gas permeations of H_2 and CO_2, showed a clear-cutoff between the two gases. The evaluated H_2/CO_2 ideal selectivity and separation factor were 6.7 and 6.5, respectively, higher than the Knudsen separation factor (ca. 4.7). For 1:1 mixtures of H_2 with N_2 and CH_4, experiments gave a H_2/N_2 and H_2/CH_4 separation factor of 7.7 and 5.9, respectively, both higher than the corresponding Knudsen separation factors (3.7 and 2.8). In addition, it was found that the influences of coexisting gases on the permeances of H_2 in the ZIF-7 membrane are insignificant, as observed in ZIF-8 membrane.

An in-depth investigation of ZIF-7 membranes for potential applications in H_2 separation and purification was performed by the same group.[456] The ZIF-7 membrane in this study presented improved H_2 selectivities and slightly decreased permeances. For the equimolar binary mixtures, calculated H_2/CO_2 ideal selectivity and separation factor were 13.0 and 13.6, and the H_2/N_2 and H_2/CH_4 separation factors were 18.0 and 14.0, respectively. It was found that with a temperature increase, the H_2 permeance increased but CO_2 remained almost constant, which leads to a remarkable increase in the H_2/CO_2 separation factor from 5.4 at 50 °C to 13.6 at 220 °C, and supposedly climbing to 30 at 450 °C. On the other hand, with increased H_2 concentration in the feed mixtures, both H_2 and CO_2 permeances and the separation factor remained nearly unchanged. This observation was believed to be a result of a size-exclusive molecular sieving effect in the system. Additional experiments revealed an outstanding stability of the ZIF-7 membrane under steam, although the addition of the

steam led to a slight decrease of the H_2 permeance, which, however, could be restored after switching off the steam. Consequently, on the basis of their good thermal and hydrothermal stabilities, outstanding separation performances, and broad temperature and feed concentration windows, ZIF-7 membranes could be very promising in practical H_2 purification.

Following these results, the same group modified the fabrication method to obtain *c*-out-of-plane oriented ZIF-7 membranes based on an evolutionary selection (van der Drifts growth) model.[469] The permeation measurement of an equimolar H_2/CO_2 mixture gave a separation factor of 8.4 at 200 °C, close to the average value of the nonoriented ZIF-7 membranes. However, the H_2 permeance of this membrane was only one-tenth that of the randomly oriented one. This difference observed in the two types of ZIF-7 membranes was explained as a result of the anisotropic pore structure of ZIF-7 crystals, which probably resulted in the surface and/or grain boundary resistances associated with the mass transport through polycrystalline layers.[470] In addition, similar to those observed in randomly oriented ZIF-7 membranes, the selectivity of the oriented ZIF-7 membrane for H_2/CO_2 separation increased with the increasing temperature.

Another ZIF, ZIF-22 ($Zn(5\text{-azabenzimidazolate})_2$),[202] having the same pore size in three directions as ZIF-7 has also been used to make membranes for the separation of H_2 from CO_2 and other larger gas molecules.[459] ZIF-22 has an LTA topological framework with high stability and porosity. In this work, a continuous ZIF-22 membrane (about 40 μm thick) was prepared by a newly developed seed-free method, using 3-aminopropyltriethoxysilane (APTES) as a covalent linker to promote nucleation and growth of the ZIF crystals on titania supports under solvothermal conditions. It was found that the measured H_2 permeance of the ZIF-22 membrane was higher than those of the other gases including CO_2, O_2, N_2, and CH_4. Similar to that observed in ZIF-7, a cut off between H_2 and CO_2 was observed, suggesting a molecular sieving effect. On the basis of the single gas permeation data, the calculated ideal separation factors of H_2 from CO_2, O_2, N_2, and CH_4 were 8.5, 7.2, 7.1, and 6.7, respectively. For 1:1 binary mixtures, the evaluated mixture separation factors of H_2/CO_2, H_2/O_2, H_2/N_2, and H_2/CH_4 were 7.2, 6.4, 6.4, and 5.2, respectively. Furthermore, it was found that when the temperature was elevated from 323 to 423 K, the H_2 permeance increased, while the H_2/CO_2 selectivity slightly decreased from 7.2 to 6.5. On the other hand, the H_2 permeance was found to slightly decrease when the partial pressure increased, while the CO_2 permeance increased; accordingly, the H_2/CO_2 selectivity declined from 7.2 to 5.1 when the partial pressure increased from 0.5 to 1.0 bar.

From the same group, a method similar to that used for preparing the ZIF-22 membrane was also adopted to make ZIF-90 ($Zn(ica)_2$, ica = imidazolate-2-carboxyaldehyde[471]) thin films, which also presented the ability to separate H_2 from other gases.[460] ZIF-90 is highly stable and has a sodalite topological framework with small pores (~3.5 Å) in three directions. The ligands in this ZIF provide free aldehyde groups, which allows for the covalent functionalization of ZIF-90 with amine groups. Making use of this feature, ZIF-90 membranes were prepared on Al_2O_3 supports through chemically covalent linkage between ZIF-90 crystals and the support by APTES. A ZIF-90 membrane with a thickness of about 20 μm was tested for H_2 separation from other gases at 200 °C. The results showed that the permeance of H_2 was higher than those of the other gases. The calculated ideal separation factors of H_2 from CO_2, N_2, CH_4, and C_2H_4 were 7.2, 12.6, 15.9, and 63.3, respectively. For the 1:1 binary mixtures, the resulting mixture separation factors for H_2/CO_2, H_2/N_2, H_2/CH_4, and H_2/C_2H_4 were 7.3, 11.7, 15.3, and 62.8, respectively, which are higher than the corresponding Knudsen coefficient (4.7, 3.7, 2.8, and 3.7). It was also confirmed that when the temperature increased from 25 to 225 °C at 1 bar, the H_2 permeance increased, and the H_2/CH_4 mixture separation factor increased from 15.3 to 16.4. In addition, the ZIF-90 membrane exhibited completely reversible separation behavior between 25 and 225 °C and high hydrothermal stability, making it useful in practical separations.

Recently, they also revealed that the covalent postsynthetic functionalization of a ZIF-90 membrane by ethanolamine can enhance the separation ability of H_2 from CO_2 and other gases.[461] After the imine functionalization of an as-prepared ZIF-90 membrane with a thickness of 20 μm, it was found that the resulting membrane was still perfect, with all PXRD peaks matching well with those of the as-prepared one. Similarly, the H_2 permeance in this membrane was much higher than those of the other gases including CO_2, N_2, and CH_4. As compared to the as-prepared ZIF-90 membrane, all single gas permeances decreased slightly because of the constriction of pore aperture after covalent functionalization. The evaluated ideal separation factors of H_2 from CO_2, N_2, and CH_4 were 15.7, 16.6, and 19.3, respectively, higher than those of the pristine ZIF-90 membrane. For the equimolar binary mixtures, the obtained separation factors for H_2/CO_2, H_2/N_2, and H_2/CH_4 were 15.3, 15.8, and 18.9, also higher than those from the as-prepared ZIF-90 membrane. With the increase of the operating temperature from 25 to 225 °C, the mixture separation factor for H_2/CO_2 at 1 bar rose from 8.3 to 16.2. It was also found that this covalent postsynthetic functionalization can control the membrane permeance and selectivity: with longer modification times, the permeance decreased parallel to an increase in selectivity. This functionalized membrane also showed excellent thermal stability and completely reversible separation behavior between 25 and 225 °C, as well as a high stability in the presence of steam.

In addition, penetration selectivities for H_2 over N_2 and CO_2 have also been observed in the thin film (referred to as MMOF membrane by the authors) of $Cu(hfipbb)(H_2hfipbb)_{0.5}$, which has a 3D interpenetrating framework containing cage-like 1D channels narrowing to 3.2 Å at the necks.[454] Because the channels exist only in one direction of the MOF structure, the arraying orientation of the crystals in the membrane is critical for the separation performance. In this work, authors used a seeded growth technique to prepare preferentially oriented and well-intergrown MMOF membranes on surface-modified porous alumina supports. Single gas permeation experiments of the MMOF film with a thickness of about 20 μm showed a moderate selectivity for H_2 over N_2 and CO_2, and very low selectivities for H_2 over He and *n*- over *i*-butane. The ideal selectivity of H_2/N_2 was evaluated to be around 23 at 190 °C. Furthermore, as the temperature increased, permeance values of all gases decreased, in contrast to several MOF membranes discussed above.

Besides the above-discussed MOF thin films that were polycrystalline and fabricated on porous supports, a MOF single-crystal membrane was also tested for H_2 separations by Takamizawa and co-workers.[472] Theoretically, a single-crystal membrane is much more reliable and effective in the precise separations of mixtures compared to a polycrystalline membrane, in which the defects and boundaries between individual crystals always lead to poor separation efficiency and bad reproducibility of the experimental results. In this work, they explored gas

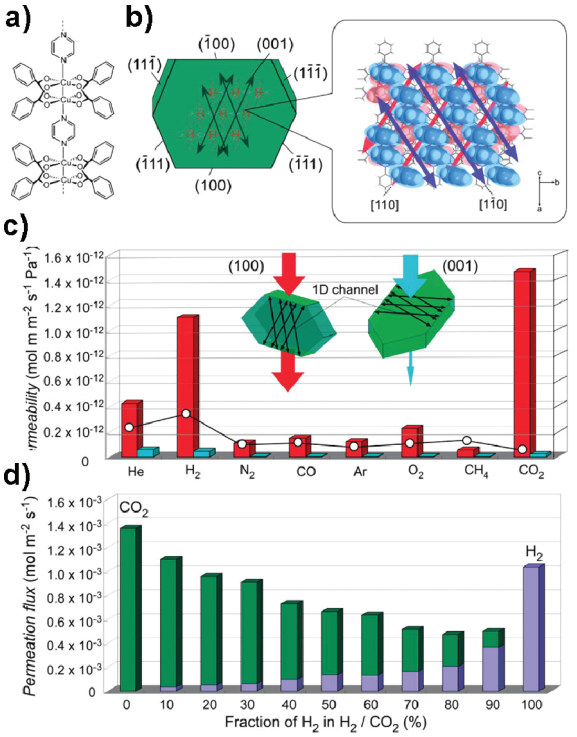

Figure 24. (a) Chemical structure and (b) crystal structure of $Cu_2(bza)_4(pyz)$ showing the determined numbers of the crystal planes and the channel direction; (c) comparison of the permeabilities of the crystal membrane for various gases: (red) along the channels (channel membrane) and (light-blue) perpendicular to the channels (nonchannel membrane) (the inset plot (○) is the calculated permeability based on the Knudsen model); and (d) comparison of the permeation fluxes of H_2 and CO_2 along the channels of gas mixtures with various mixing ratios. Reprinted with permission from ref 472. Copyright 2010 American Chemical Society.

permeation properties of a $Cu_2(bza)_4(pyz)$ (bza = benzoate; pyz = pyrazine)[473] single-crystal membrane. This compound has a 1D chain structure (Figure 24a), not really a MOF according to our definition; however, in the crystal, these chains array in parallel and are held together by π---π interactions to form a stable structure with oriented narrow channels (less than ~4 Å) in two crystallographic directions (Figure 24b). Experimental permeability values showed that passing gas through the single-crystal membrane along the channel direction is 7−60 times faster than that along the direction perpendicular to the channels (Figure 24c). It is interesting that the permeation of H_2 and CO_2 was much faster than that of He, N_2, CO, Ar, O_2, and CH_4, although all of these gases were allowed to penetrate the membrane in the direction of the channels. The calculated selectivities of H_2 over the other gases were 3 (He), 10 (N_2), 7 (CO), 9 (Ar), 5 (O_2), and 19 (CH_4). For a H_2/CO_2 mixture, as shown in Figure 24d, the permeability of H_2 decreased due to the presence of CO_2, while that of CO_2 remained unchanged, suggesting that the CO_2 residing in the channels made it difficult for H_2 to pass. This single-crystal membrane thus exhibited an anisotropic gas permeation behavior, with high permeances for H_2 and CO_2 and high permselectivities for H_2 and CO_2 over other gases.

4.1.2. CO_2 Separation. The separation of CO_2 from other gases is another very important research topic, which is an integral part of carbon capture and natural gas purification, both of which are contemporary global concerns.[93,474] There are a lot of reports regarding CO_2 selective adsorption and adsorptive separation of MOFs;[92,94,104] however, studies exploring CO_2 separation using MOF-based membranes in the spectra of carbon capture (mainly CO_2/N_2 separation) and natural gas purification (mainly CO_2/CH_4 separation) are very limited thus far.

CO_2 separation from N_2 by a MOF thin film was recently reported by Farrusseng and co-workers.[475] They observed high permselectivity of CO_2 over N_2 in humid conditions in a $Zn(mimc)_2$ (SIM-1, Hmimc = 4-methyl-5-imidazolecarboxaldehyde) membrane fabricated on an asymmetric α-alumina tube. It was found that the ideal selectivity of CO_2/N_2, calculated from single gas permeances at 303 K, was 1.1, higher than the Knudsen value of 0.78. For a ternary mixture $CO_2/N_2/H_2O$ (10/87/3 vol%), this membrane presented a CO_2/N_2 separation factor of 4.5 at 324 K and 4 bar. It was thought that surface transport took place in the membrane, which allowed the separation of the two gases by preferential adsorption; that is, the most-adsorbed component reduced the diffusion of the other.

CO_2/CH_4 separation using ZIF-8 membranes, prepared by in situ crystallization on tubular porous α-alumina supports, was reported by Venna and Carreon.[476] In this work, several ZIF-8 membranes with different thicknesses were tested, and they presented high CO_2 permeances and CO_2/CH_4 separation selectivities from ~4 to 7 at 295 K and 139.5 kPa. The evaluated separation index [(CO_2 permeance × (selectivity −1)) × permeate pressure)] of CO_2 over CH_4 ranged from ~6.5 to 10. It was also found that with increasing thickness of the membranes the CO_2 permeance decreased, while the CO_2/CH_4 selectivity and separation index decreased at first but then increased, probably due to cracks in the membranes. The high separation indices were attributed to the small pores of ZIF-8, which favor the diffusion of CO_2 over CH_4.

As a special example, already mentioned above, $Cu_2(bza)_4(pyz)$ single-crystal membranes also exhibited high selectivity toward CO_2 over CO and CH_4, with a calculated selectivity factor of 10 and 25, respectively.[472] In addition, it is also noteworthy that on this membrane the selectivity factor of CO_2 over H_2 evaluated from the mixture gas permeation results was much higher than the permselectivity calculated from single gas penetrations. This reverse selectivity may be useful for removing CO_2 gas from a CO_2/H_2 mixture to concentrate H_2.

4.1.3. Other Gas or Vapor Separations. Apart from the explorations of MOF thin films for the separation of the two above-discussed important gases, Serre and co-workers[477] reported the adsorptions and separations of water and organic solvent vapors by nanoZIF-8 thin films with a tunable thickness. These thin films were prepared by a precisely controlled chemical solution deposition technique. Adsorption measurements of the membranes showed that only organic molecules such as alcohols and THF were adsorbed, but water was not, probably due to the hydrophobic properties of the ZIF-8 framework. Furthermore, the high stability of these membranes was confirmed by running cycles of isopropanol adsorption, which showed no decrease in guest uptakes after several cycles. These ZIF-8 membranes are thus potentially applicable in the vapor-phase separation of organic solvents and water.

4.2. Separations with Mixed-Matrix MOF Membranes

An alternative route to introduce MOFs into membrane-based applications is to incorporate MOFs into polymers to obtain mixed-matrix membranes (MMMs), also called hybrid

dx.doi.org/10.1021/cr200190s |Chem. Rev. 2012, 112, 869–932

Table 4. Light Gas Separation Performances of Selected MMMs with MOFs as Fillers

		observed highest selectivity (ideal selectivity)						
MOF-based MMM	MOF loading	H_2/CO_2	H_2/N_2	H_2/CH_4	CO_2/CH_4	CO_2/N_2	CH_4/N_2	O_2/N_2
Cu-bipy/PSf[483]	5 wt %			(200)			(10)	
$Mn(HCO_2)_2$/PSf[484]	10 wt %		(38)	(14)	(9)	(25.5)		
HKUST-1/PSf[484]	5 wt %		(37.5)		(21.5)	(25)	(32)	
HKUST-1/PI[485]	30 wt %				27.5	27		
HKUST-1/PI-PSf(3:1)[485]	30 wt %				16	23		
MOF-5/Matrimid[486]	30 wt %	2.3(2.7)		(120)	39(45)		CH_4/N_2 0.94 (0.86)	(7.9)
ZIF-8/Matrimid[487]	50% (w:w)	3.5(3.8)	(110)	(490)	89(125)		(2)	(8)
ZIF-9/Ultem[488]	15 wt %				(39)			
ZIF-9/Matrimid[488]	15 wt %				(36)			
ZIF-9/6FDA-DAM[488]	15 wt %				37(28)	(22)		
Cu-BPY-HFS/Matrimid[489]	20 wt %	2.6 (1.7)	(71)	(70)	22.5 (27.6)		1.7 (1.16)	(7)
CuTPA/PVAc[490]	15% (w:w)				(40)	(35)	N_2/CH_4 (1.1)	(6.8)

membranes, which are conceptually comprised of porous material particles (additives or fillers) dispersed in a polymer matrix.[105] This strategy allows for combining the processability of organic polymers with the selective adsorption and diffusion properties of porous materials. The development of polymer membranes is relatively mature, and several products are already being used in industries.[478,479] Although various porous solid materials, including zeolites, carbon molecular sieves, and silica, have been used, as additives in MMMs, a lot of challenges remain in several aspects. For example, by using zeolites to fabricate MMMs, the smooth integration (without breaks) between zeolite particles and organic matrices is very difficult to control.[480,481] Although surface functionalizations of the zeolites help to improve adhesion between the two materials, only a limited number of zeolite structures and compositions can be used, and the chemistry involved is not easy.[36] As alternative materials to zeolites and other porous solids that could be used in MMMs, MOFs possess two distinct advantages: (1) MOFs with countless different structures and compositions can be synthesized; and (2) the organic linkers provide a useful platform for chemical modifications of the surface that can improve their adhesion to polymer matrices, thus making MOFs promising in MMM applications, although only very limited reports can be documented to date.

4.2.1. Gas Separations. The light gas separation performances of selected MMMs with MOFs as fillers are collected in Table 4. The incorporation of MOFs into a polymer matrix to fabricate MMMs for gas separations was for the first time explored by Balkus and co-workers.[482] The tested MMM made from the incorporation of Cu(bpdc)-ted into poly(3-acetoxyethylthiophene) (PAET) showed an improvement in CH_4 permeability and selectivity as compared to a pure polymer membrane.

After that report, Won and co-workers[483] reported the fabrication and gas separation of a $Cu_2(PF_6)(NO_3)(bipy)_4 \cdot 2PF_6$ (Cu-bipy) MMM, in which the MOF was dispersed into amorphous glassy polysulfone (PSf). It was found that the loading amount of the MOF has a significant influence on the uniformity of the resulting MMM membrane. At lower than 5% loading, the MOF was well-dispersed in the polymer matrix and formed membranes with high uniformity. Gas permeation experiments revealed that the MMMs have lower permeabilities than a pure PSf membrane, which was attributed to an increase in the diffusion path length and a decrease in the effective cross-sectional area available for gas transport. However, as expected, the evaluated ideal selectivities of He, H_2, N_2, and O_2 over CH_4 were higher than those from the pure PSf membrane. A significant increase in the H_2/CH_4 and N_2/CH_4 selectivities relative to those of the larger gases was also observed, reportedly a result of a molecular sieving effect contributed by the small pores of the MOF filler. At a 5 wt % loading, the observed ideal selectivity of the MMM for He/CH_4, H_2/CH_4, O_2/CH_4, and N_2/CH_4 was about 230, 200, 20, and 10, respectively.

Gas separations of several MMMs with two different MOFs, HKUST-1 and $Mn(HCO_2)_2$, in polydimethylsiloxane (PDMS) and PSf, were also reported by Car and co-workers.[484] The dependence of gas permeability and diffusion on the presence of the MOFs in the polymer matrices and their loading amounts was observed in these MMMs. HKUST-1/PDMS and HKUST-1/PSf showed high adsorption affinity toward H_2 and CO_2, while $Mn(HCO_2)_2$-based membranes displayed high affinity toward only H_2. It was found that increased loadings reduced the gas solubility, but increased the permeability, suggesting defects of these membranes with interfacial voids. The selectivities were also loading dependent in all cases. For the HKUST-1/PSf membrane, a 5 wt % loading resulted in an increased selectivity for H_2/N_2, H_2/CH_4, CO_2/N_2, and CO_2/CH_4 as compared to pure PSf, but 10 wt % loading gave the opposite results. For the $Mn(HCO_2)_2$/PSf membrane, increased loading led to an increase of the H_2/N_2 selectivity in both 5 and 10 wt % levels, whereas CO_2/CH_4 selectivity decreased under the same conditions. The corresponding behaviors of PDMS-based MMMs might be different from those of the PSf-based ones, but detailed discussions were absent from that report.

A study of HKUST-1-based defect-free asymmetric MMMs (on different polymer matrices) for gas separations was performed by Vankelecom and co-workers.[485] In this work, the incorporation of HKUST-1 into polymer PI Matrimid or PI-PSf (3:1) blend matrices to get target MMMs, HKUST-1/PI and HKUST-1/PI-PSf, respectively, was found to lead to enhanced CO_2/CH_4 and CO_2/N_2 mixed gas selectivities as compared to the pristine polymer membranes. Notably, this trend continued with increased loading amounts of the MOF in both PI and

dx.doi.org/10.1021/cr200190s |Chem. Rev. 2012, 112, 869–932

PI-PSf matrices. The enhanced selectivity contributed by the MOF could be due to either the competitive adsorption of the two gases or a molecular sieving effect. Selectivities for both gas pairs were lower in PI-PSf-based membranes than those in PI-based membranes with the same feed composition. For all membranes and for both gas pairs, a decreased selectivity with increased CO_2 content in the feed gas was also observed, which can be ascribed to a strong interaction between the matrices and CO_2. Furthermore, permeation experiments of mixed gases showed that the CO_2 permeances of these MMMs are greater than those of pure polymer membranes, and increased with increased MOF loading in each case. It was also found that in all cases, the mixed gas selectivities were lower than the ideal gas selectivities, and the deviations increased with increased CO_2 feed concentrations.

Gas separations by MOF-5/Matrimid MMMs were also reported by Musselman and co-workers.[486] Single gas permeation experiments showed that the permeabilities of all gases (H_2, CO_2, O_2, N_2, and CH_4) increased with MOF-5 loading; however, the ideal selectivities remained unchanged due to the proportional permeability increase of all gases. This increased permeability but lack of change in ideal selectivities may be attributed to void defects at the MOF particle/polymer interface. It was also noticed that gas diffusivities of CO_2, O_2, N_2, and CH_4 increased with MOF-5 loading, which was ascribed to the porosity introduced by MOF-5 and the availability of more uniform surfaces for surface diffusion. However, as compared to pure Matrimid, MOF-5/Matrimid MMMs showed almost no significant change in gas solubility with increased MOF-5 loading, attributed to the weak affinity between MOF-5 pore surfaces and these gases. Thus, the increased permeabilities for all gases are a result of the increased diffusivities resulting from the porosity of MOF-5. Furthermore, permeations with mixed gases showed that the selectivity of CH_4/N_2 increased for CH_4, but remained nearly constant for H_2/CO_2 at any loading. This increase in selectivity for CH_4 was attributed to the greater solubility of N_2 as compared to CH_4 in the polymer matrix. This difference in solubility made CH_4 transport mostly diffusion dependent and easy, contributed by the MOF-5 porosity and its uniform pore surfaces.

This group also reported gas separations of Cu-BPY-HFS/Matrimid membranes.[489] Cu-BPY-HFS ($CuSiF_6(bipy)_2$) has a porous 3D framework structure with pores as large as 8 × 8 Å in diameter.[491] It was found that for all gases tested (H_2, N_2, O_2, CH_4, and CO_2), the pure gas permeability increased as the loading increased up to 40%. However, the ideal selectivities of binary gas pairs suffered from different changes with different loading levels. For gas mixtures, as compared to a pure Matrimid membrane, the MMM with a 20% MOF loading showed a 50% enhancement for the CH_4/N_2 selectivity, a 35% decrease for CO_2/CH_4, and almost no change for CO_2/H_2. The observed high selectivity for CH_4 was ascribed to the strong affinity of CH_4 with the MOF and the increased solubility of CH_4 in the membrane induced by the competitive adsorption of CH_4 over N_2 in the mixture.

Several ZIF-based MMMs were also explored by this[487] and other groups[488] for gas separations. Because of the small pore size (3.4 Å) of ZIF-8,[14,466] an evident molecular sieving effect in gas separations was observed in ZIF-8/Matrimid MMMs.[487] It was found that for all tested gases including H_2, N_2, O_2, CO_2, CH_4, and C_3H_8, at low loading of 20% (w/w) ZIF-8, the permeabilities of the MMM were comparable to those of pure Matrimid; however, they began to increase when the ZIF-8 loading was

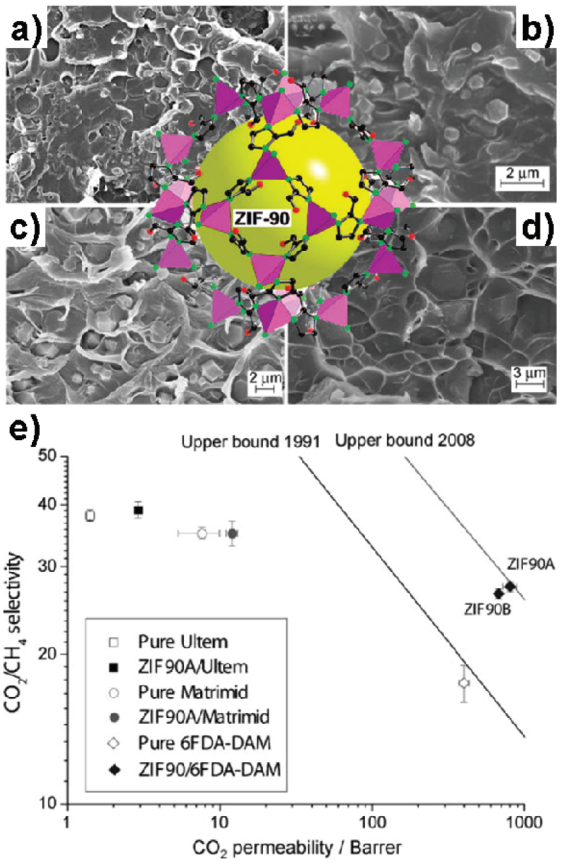

Figure 25. (a−d) SEM images of cross sections of mixed-matrix membranes, ZIF-90A/Ultem, ZIF-90A/Matrimid, ZIF-90A/6FDA-DAM, and ZIF-90B/6FDA-DAM containing ZIF-90 crystals (inset: a cage unit in ZIF-90 structure with ZnN_4 tetrahedra as pink polyhedra and the ligands in ball-and-stick representation); and (e) gas-permeation properties of mixed-matrix membranes containing 15 wt % of ZIF-90 crystals measured with pure gases. The data for pure Ultem and Matrimid are averaged values from the literature. The upper bounds for polymer membrane performance as defined in 1991 and 2008 are shown. Reprinted with permission from refs 488 and 471. Copyright 2010 Wiley-VCH and 2008 American Chemical Society.

enhanced until 40% (w/w), where the permeabilities for all gases were higher than those of Matrimid. As the loading increased to 50% and 60%, the permeabilities decreased as compared to those at 40% loading. These observed phenomena were explained as the initial increase of the distance between polymer chains, creating more polymer free volume that could be used for gas penetration upon the addition of ZIF-8 nanoparticles; however, at higher loadings, the gas diffusion through the pores of the ZIF-8 became dominant, resulting in lower permeabilities. This explanation was also supported by observed higher permeability values for small gases (H_2 and CO_2) than those of larger ones in high ZIF-8 loading MMMs. The ideal selectivities of gas pairs containing small gases, such as H_2/O_2, H_2/CO_2, H_2/CH_4, CO_2/CH_4, CO_2/C_3H_8, and H_2/C_3H_8, showed marked improvement at higher ZIF-8 loading (50%), but almost no change for those pairs containing larger gases, such as O_2/N_2 and CH_4/N_2, demonstrating for the first time, strictly speaking, a molecular sieving effect of ZIF-8 in these MMMs. This effect was further confirmed by control experiments, where as-synthesized ZIF-8 with blocked pores acting as the filler was used. For the gas mixture separations, the observed

dx.doi.org/10.1021/cr200190s |Chem. Rev. 2012, 112, 869–932

selectivities for H_2/CO_2 (1:1) and CO_2/CH_4 (1:9) pairs were almost consistent with the ideal selectivities in the 50% and 60% ZIF-8 loaded MMMs. With respect to H_2/CO_2, this observation was attributed to the lack of competitive adsorption for the two small gases due to their ease of penetration through pores of ZIF-8. However, for CO_2/CH_4, competition exists because high concentrations of the larger CH_4 molecules could block the pore apertures of the MOF. The ability to separate gas mixtures containing small H_2 and CO_2 molecules and the high stability of ZIF-8 itself rank these ZIF-8 MMMs as one of the most promising materials for industrial light gas separations.

Another ZIF, ZIF-90,[471] has also been used as an additive in the fabrication of MMMs for CO_2/CH_4 separation.[488] By adopting a solvent free crystallization method, micrometer-sized ZIF-90 crystals (~2 μm) were synthesized and dispersed within Ultem, Matrimid, or 6FDA-DAM polymers to obtain the corresponding MMMs (Figure 25a−d). At a 15 wt % loading of ZIF-90, the Ultem and Matrimid-based MMMs showed an enhanced CO_2 permeability, without loss of CO_2/CH_4 selectivity as compared to the respective pure polymer membranes (Figure 25e), which was explained by the mismatch between the permeability of ZIF-90 and those of pure polymer matrices. For 6FDA-DAM-based MMMs, substantial enhancements in both CO_2 permeability and CO_2/CH_4 ideal selectivity were observed. For a 1:1 binary CO_2/CH_4 mixture, the ZIF-90/6FDA-DAM membrane showed an evaluated selectivity of 24. On the other hand, the observed CO_2/CH_4 mixed-gas selectivity of the ZIF-90 MMM is higher than the corresponding ideal selectivity, probably due to the selective sorption and diffusion of CO_2 in ZIF-90 crystals. Furthermore, an ideal CO_2/N_2 selectivity of 22 was achieved, which is substantially higher than that (14) of the pure 6FDA-DAM membrane. As compared to other MOF-based MMMs discussed above, ZIF-90/6FDA-DAM membranes seem to fair among the best in the trade-off between permeabilities and selectivities for light gas separations, suggesting again that MOFs with small pores (comparable to the size of the target gas molecule), such as ZIF-90 and ZIF-8, are very promising as highly selective membrane materials for gas separations; this has also been supported by universal computational simulation studies.[450,492,493]

In addition, a 2D MOF, $Cu(bdc)(S)_2$ (S = solvent molecule) has also been used to make MMMs for gas separations.[490] Koros and co-workers dispersed the MOF crystals into poly(vinyl acetate) (PVAc) to create a CuTPA/PVAc MMM with a 15% loading of the filler. This hybrid membrane showed enhanced permeabilities for pure gases, including H_2, CO_2, O_2, N_2, and CH_4, and increased ideal selectivities for He/CH_4, O_2/N_2, N_2/CH_4, CO_2/N_2, and CO_2/CH_4, as compared to the pure PVAc membrane. A marked enhancement of the permeability for CO_2 as compared to other gases was also observed, probably due to a greater solubility of it in the MMM. The selectivity for O_2/N_2 suffered from the lowest enhancement relative to pure PVAc as compared to other gas pairs, probably a result of similar size and shape of the two gases. In contrast, the enhancement of CO_2/CH_4 selectivity was among the most obvious. Furthermore, the diffusivities of the MMM for CO_2, O_2, N_2, and CH_4 were lower than those of pure PVAc membrane, again suggesting that the gas molecules were accessing the MOF pores when penetrating the membrane.

As we can see from the above discussions, MMMs with different MOFs combined with the same polymer matrix or a MOF combined with different matrices display different separation performances. There are therefore numerous MOF/polymer combinations that remain untested. The choice of an appropriate MOF/polymer combination has become one of the great challenges in pursuing MOF-based MMMs for specialized separations. Computation models that can predict the separation properties for this type of composite membranes will as a result play a key role in directing experiments. The only computational exploration, to the best of our knowledge, was published by Keskin and Sholl to explore this type of material for gas separations, by using a combination of atomistic and continuum modeling.[492] The methodology involved in this study is beyond the scope of this Review, but seems to be more important than the resulting separation performances of the investigated systems. As a brief summary of the results, for the Cu(hfipbb)-$(H_2hfipbb)_{0.5}$/Matrimid membrane, the predicted separation selectivity exceeded Robeson's upper bound for CO_2/CH_4 separation. This high selectivity for CO_2 over CH_4 was attributed to the differences in the molecular diffusivities inside the MOF pores. Furthermore, simulation results showed that not every MOF yielded a dramatic improvement in the membrane performance; for example, MOF-5 and HKUST-1 showed a smaller contribution to CO_2/CH_4 separation. Similarly, the excellent performance for one gas pair separation in a given MOF/polymer membrane may be the opposite for another gas pair. This work has opened a door in the computational exploration of this type of hybrid material for separation applications.

4.2.2. Liquid Separations. Apart from exploring gas separations by MOF-based MMMs, liquid separations have also been attempted. In an early report by Jin and co-workers,[494] alcohol/water separation was tested by a pervaporation technique in a MOF-based MMM fabricated by dispersing microcrystals of $Cu_2(bza)_4(pyz)$ (bza = benzoate) into PDMS. The 3 wt % loaded membrane showed enhanced separation selectivities for MeOH and EtOH from a water solution containing 5 wt % alcohol (selectivity factors increased from 2.0 and 2.3 to 6.5 and 6.2, respectively) as compared to pure PDMS. Furthermore, the flux values of the MMM for MeOH and EtOH were slightly higher than those of the pure polymer membrane, indicating that the adsorbed alcohol molecules in the membrane diffused through the MOF crystals without being blocked.

Another example of liquid-phase separations with MOF-based MMMs was reported by Vankelecom and co-workers.[495] In this work, several MMMs with HKUST-1, MIL-47, MIL-53(Al), or ZIF-8 as fillers in a PDMS matrix were fabricated at different loading levels in each case. They were then applied in solvent resistant nanofiltration (SRNF) for the separation of Rose Bengal (RB) from isopropanol (IPA). Additionally, *N*-methyl-*N*-(trimethylsilyl)trifluoroacetamide (MSTFA) was also used to modify these MOF crystals to improve the compatibility between the fillers and the polymer matrix. Overall, the MMMs with unmodified MOF fillers showed an increased permeance for RB as compared to a pure PDMS membrane. It was also found that increasing MOF loading from 5% to 25% resulted in a slight enhancement in permeances in each case, which was attributed to the presence of a larger number of nonselective voids in the high loaded membranes. The MMMs with modified MOF fillers, however, showed almost no change in permeances, even at high loading, but substantially increased retentions for RB in all cases except that with a silylated ZIF-8 filler. The retention of the ZIF-8 MMM was only slightly higher than that of a pure PDMS membrane. The lower retention of the ZIF-8 MMM as compared to those of other membranes may be due to the small pores of ZIF-8, which obstruct IPA transport. The overall increased RB retention

dx.doi.org/10.1021/cr200190s |*Chem. Rev.* 2012, 112, 869–932

in these MMMs was attributed to the size exclusion of the fillers and a reduced swelling of the PDMS.

5. DESIGN AND IMPLEMENTATION OF MOFS FOR SEPARATIONS

As discussed above, a wide variety of MOFs have been tested in a range of potential applications for separations. The majority of these studies revolved around the selective adsorption and separation of gases and vapors. Serendipity's role in these results is often downplayed, and a large number of the observed selective adsorptions or separations are not the consequence of a predesigned material for a particular target, but a result of thorough characterization of the material. The major contribution of all of these results combined are the characteristics and mechanisms involved in separations. Now that the design and consequent synthesis of any particular material has reached the early adolescent stage, the design of a porous material for a specific separation is entirely feasible. Through proper ligand design (including functional moieties) and selection of metal (or metal-containing cluster) one can indeed synthesize a desired MOF with some experimentation of the reaction conditions.[59,63,64,75,496] This concept of precise control at the molecular level is probably the most distinguishing characteristic of MOFs as compared to other sorbent materials. Of course, this control arises not only from the vast number of MOFs that have been synthesized, but from the ongoing work in organic and inorganic synthesis of building blocks. The tuned focus of which application (gas storage, separation, catalysis, etc.) a MOF is being designed for is a fairly recent concept, but is gaining momentum as materials designed for one purpose have significant advantages. On the other hand, the implementation of a separation is also intimately connected to the methods and processes that are adopted; different properties of a selected medium material need to be emphasized and optimized accordingly. Finally, when considering the practical applications of MOFs for separations, several additional issues must also be addressed, including the stability in the final working environments, scale-up, continuous cycling of the materials (i.e., lifetime), associated costs, and process manipulation from an engineering stand point.

5.1. Design at the Molecular Level

In terms of selective adsorption and separation, the design and modification of MOFs at the molecular level can be generally achieved through tuning or controlling their pore size and shape, functionalizing the pore surface, and taking advantage of the structural flexibility of some dynamic MOFs. In fact, the efforts revolving around these issues have led to the rapid development of this field, especially in selective gas adsorption and separation, including CO_2 capture by adsorption[94] and H_2 separation by membranes, as discussed in foregoing sections.[455,456,459,461]

5.1.1. Tailoring Pore Size and Shape. In both adsorptive and membrane-based separations, the pore size and shape of the carrier material is crucial to its performance and is therefore usually the first consideration in selecting the material for a special separation. These two parameters determine not only the strict size/shape exclusion but also the diffusion dynamics of molecules that will be separated. Kinetic separation through differences in diffusion of molecules in a porous material has been used in industry for a portion of all separations, for example, the air separation of a PSA process by using carbon molecular sieves.[497] MOFs, due to their easily controllable synthesis and modification, have great potentials and advantages, as compared to traditional zeolites and other inorganic molecular sieves, in the realm of designing pore size and shape.

First, given that the coordination linkage between metal ions and ligands is predetermined, the size or length of a ligand is the key in the design of a MOF with desired pore size and shape. A short ligand usually leads to a MOF with narrow open channels or small windows that connect big cavities in the framework; both types are desired for the separation of small molecules that are close in size, for example, O_2 and N_2. A typical example is metal formates, $M(HCO_2)_2$ (M = Mg, Mn, Co, or Ni) synthesized under suitable conditions.[177,257,322,362] The three-atom (COO^-) formate moieties link metal atoms to obtain these MOFs having a 3D framework with 1D channels, in which larger cage cavities are connected by small necks. It has been observed that $Mn(HCO_2)_2$ can selectively adsorb H_2 over N_2 and Ar at 78 K, as well as CO_2 over CH_4 at 195 K.[177] In both cases, the uptake capacity of the excluded gases N_2, Ar, and CH_4 was almost zero, suggesting size exclusion by the small pores. Interestingly, a following study revealed that this MOF also has a temperature-triggered gate opening performance for N_2 and Ar adsorption, potentially useful in their separation.[257] $Mg(HCO_2)_2$ and $Mn(HCO_2)_2$ also showed a remarkable selectivity of C_2H_2 adsorption over CO_2, CH_4, N_2, O_2, and H_2 at room temperature.[322]

Similarly, short imidazole-based ligands have been used to construct a large series of ZIFs, which were then tested for selective adsorption and separations (both adsorptive separation and membrane separation). Interestingly, most ZIFs have zeolite-like 3D structures with big cages that are connected by small gates.[103] Porous materials with this type of structure are very promising for separations because large cages in the structure usually endow the material with a high uptake capacity for the component that is adsorbed, while the small gates give rise to a high selectivity. Several members of the ZIF family have shown excellent performance in CO_2 capture as evaluated by single gas adsorption and breakthrough experiments.[144] Research results have also shown that the kinetic separation of propane/propene by some ZIFs is indeed highly probable based on the remarkable differences in their diffusion rates through the small pores of the materials.[303] The effective size of the pores in these ZIFs is believed to be the controlling factor determining the separation capability. Because of their tremendous stability and small pores, several ZIFs have also been used in fabricating membranes for gas separations. Thin films and/or mixed-matrix membranes of ZIF-7,[455,456,458] ZIF-8,[457,458,476,487] ZIF-22,[459] ZIF-90,[460,488] and SIM-1[475] have shown outstanding gas separation performance, especially in separating H_2 from other gases.

A ligand with multiple coordination sites and modes, on the other hand, can also be used to construct a MOF with small pores suitable for gas separation, although the control in synthesis becomes difficult. Two typical examples are Zn(dtp)[141] and Cd(tzc),[173] both of which showed selective adsorption of H_2 and CO_2 over N_2 at low temperature. In the two MOFs, both ligands, 2,3-di-1*H*-tetrazolate-5-ylpyrazine (dtp) and tetrazolate-5-carboxylate (tzc), have multiple atoms available for coordination, which are responsible to the small pores of the resulting frameworks. Ultramicroporous MOFs can also be constructed by using a ligand with bulky noncoordinating species, which occupy a large space of the resulting framework, leaving small pores. For example, PCN-13, based on the 9,10-anthracenedicarboxylate ligand, linked by distorted $Zn_4O(H_2O)_3$ clusters, demonstrated selective adsorption of O_2 and H_2 over N_2 and CO at 77 K.[253]

dx.doi.org/10.1021/cr200190s |*Chem. Rev.* 2012, 112, 869–932

Usually, when a longer ligand is used, the network of the resulting MOF prefers to interpenetrate to stabilize the structure and prevent large vacuous pores from existing. Because of the decreased pore volume, the interpenetration of the framework is believed to be disadvantageous in most MOFs used purely for guest storage, such as CH_4, but can be favorable for separations. A lot of interpenetrated MOFs showed selective adsorptions and separations of gases or vapors due to their reduced pore size; this has been explored largely by Chen and co-workers.[98,201,206,223,279,366] For example, $Zn(adc)(bpee)_{0.5}$ has a paddle-wheel-based pillared layer structure. The triple interpenetration of the frameworks led to a stable material with reduced pores of about 3.4 × 3.4 Å and 3.6 × 3.6 Å along two different directions. As a result, this MOF exhibited highly selective sorption behavior toward H_2 over N_2, H_2 over CO, and CO_2 over CH_4 at low temperature.[201] Another notable example is a series of coordinatively linked interpenetrated MOFs, PCN-17(M) (M = Yb, Dy, Y, or Er), which have a porous structure containing large cages linked by relatively small apertures.[254,255] The framework interpenetration and sulfate bridging in PCN-17 further reduces its pore opening to approximately 3.5 Å, leading to the observed selective adsorption of H_2 and O_2 over N_2 and CO at 77 K.

Rationally tuning the micropores of MOFs by simply changing the length of the bridging ligands for selective adsorption and separation has been demonstrated in several systems. As shown in Figure 26a and b, for example, two homochiral MOFs, $Zn_3(cdc)_3[Cu(SalPycy)]$ and $Zn_3(bdc)_3[Cu(SalPycy)]$ were constructed by a similar procedure. They have similar 3D porous structures with a slightly different pore size resulting from the different bridging ligand lengths (cdc is slightly shorter than bdc).[296] As discussed in sections 2.1.4 and 3.3.1 of this Review, the two MOFs presented different performances in the selective adsorption of C_2H_2 over C_2H_4 and the enantioselective encapsulation of 1-phenylethyl alcohol (PEA). The former MOF, with smaller pores, showed an enhanced separation selectivity of C_2H_2 over C_2H_4 (25.5 vs 1.6) and chiral reorganization of PEA (ee of 64 vs 21) as compared to the latter. The two MOFs also exhibited different sorption behaviors with respect to C_2H_2 and C_2H_4 as shown in Figure 26c. The same group also explored the designs of MOFs for selective adsorption of other gases or vapors through ligand size modifications in series of pillared paddle-wheel MOFs with a common composition of $M(A)(B)_{0.5}$ (where A is a dicarboxylate linker and B is a bidentate N-containing pillar linker).[134,400] Through adjusting A, B, or both, the pore size of these MOFs has been precisely tailored for the selective adsorption of a particular gas. For example, $Cu(fma)(bpee)_{0.5}$ with pore cavities of about 3.6 Å, which are interconnected by pore windows of 2.0 × 3.2 Å, showed selective adsorption of H_2 over N_2, Ar, and CO at 77 K, as well as CO_2 over N_2 at 195 K.[134] $Cu(R\text{-gla-Me})(bipy)_{0.5}$, with pores of about 2.8 × 3.6 Å in size, exhibited exclusive adsorption of water over methanol.[400]

Tuning the pore size and shape of isoreticular MOFs through the introduction of different noncoordinating moieties in ligands is another strategy for optimizing their separation performances. One example is the selective capture of CO_2 in isoreticular ZIFs reported by Yaghi and co-workers.[144] In this work, the authors revealed the precisely controlled metric and functionality of pores in eight ZIFs with a GME topology. Within this series of ZIFs, the pore diameter was varied incrementally from 7.1 to 15.9 Å. Gas adsorptions and dynamic breakthrough experiments showed

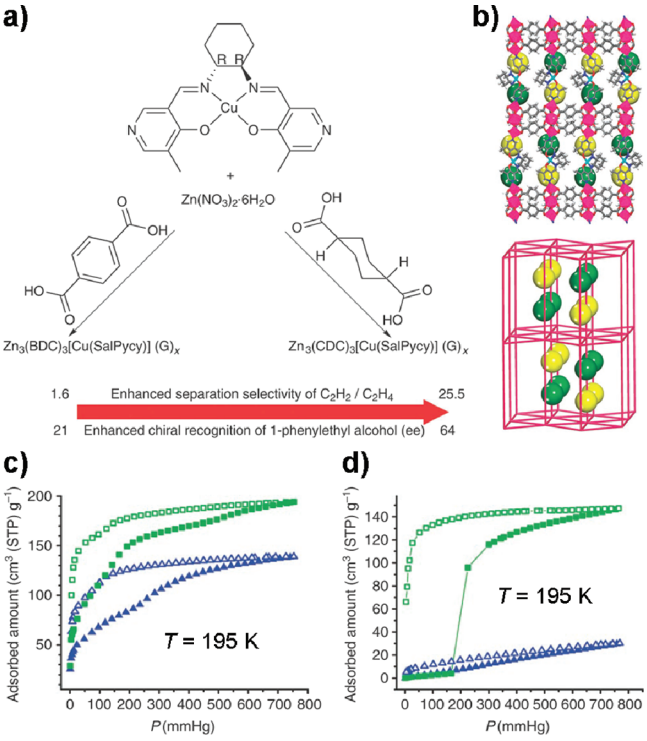

Figure 26. (a) Syntheses and separation capacities of $Zn_3(bdc)_3[Cu(SalPycy)]$ and $Zn_3(cdc)_3[Cu(SalPycy)]$; (b) the 3D pillared framework (top) and hexagonal primitive network topology (bottom) of $Zn_3(cdc)_3[Cu(SalPycy)]$; and (c and d) C_2H_2 (green squares) and C_2H_4 (blue triangles) adsorption on $Zn_3(bdc)_3[Cu(SalPycy)]$ and $Zn_3(cdc)_3[Cu(SalPycy)]$, respectively. Reprinted with permission from ref 296. Copyright 2011 Nature Publishing Group.

that the separation selectivity for CO_2 from CH_4 and N_2 in these ZIFs is dependent on pore size and the functionality of the pore surface. Another example is the observed kinetic separation of propene and propane in a series of isostructural pillared-paddle-wheel MOFs reported by Hupp and co-workers.[304] As discussed in section 2.1.4 of this Review, the two MOFs constructed with the brominated ligand showed similar kinetic selectivities, with a considerably faster uptake of propene than propane, while the other two with the nonbrominated ligand did not show such a large difference in adsorption kinetics of the two gases. Clearly, systematic structural modification of the organic struts in this series of MOFs has allowed researchers to tune the pore size, thereby reaching an effective kinetic separation of propene and propane.

Apart from predesigned ligands and thereby pores, postsynthetic modification of MOFs by introducing bulky groups, not only anchored on ligands (through covalent bonds) but on open metal sites (through coordination), can also be used to tune the pore size and shape, thereby achieving the selective adsorption and separation of guest molecules.[51] A typical example was reported by Suh and co-workers.[169] $[Zn_2(tcpbda)(H_2O)_2]$ (guest) (SNU-30, H_4tcpbda = *N*,*N*,*N*′,*N*′-tetrakis(4-carboxyphenyl)biphenyl-4,4′-diamine), containing large channels, was first synthesized, and then modified by inserting 3,6-di(4-pyridyl)-1,2,4,5-tetrazine (bpta) into its framework pores to obtain $Zn_2(tcpbda)(bpta)$ (SNU-31), in which original large channels are divided by the bpta linkers. In the structure of SNU-31, the bpta ligands are coordinated to Zn(II) atoms by replacing the coordinated

dx.doi.org/10.1021/cr200190s |*Chem. Rev.* 2012, 112, 869–932

water molecules of SNU-30. Interestingly, adsorption experiments showed that the activated sample of SNU-30 presented high uptake capacities for N_2, O_2, H_2, CO_2, and CH_4, while activated SNU-31 only adsorbed CO_2 but hardly any N_2, H_2, O_2, and CH_4 under similar experimental conditions. It should also be pointed out that the crystal structure of as-synthesized SNU-31 indicated that the channel sizes are big enough for these gases to enter, but the channels seem to be contracted after guest removal (upon activation), which is responsible for the observed gas selective adsorption. The fact that only CO_2 was adsorbed in SNU-31 may also be relative to its high quadrupole moment, which may trigger pore opening upon adsorption. Another example is the enhanced separation of H_2 from CO_2 and other gases observed in a covalently postsynthetically functionalizated ZIF-90 membrane, as compared to the unaltered membrane, as discussed above.[461]

For ionic MOFs, the exchange of counterions is an efficient approach to tune their pore size, thereby modifying the selective adsorption and separation performance. This strategy has been demonstrated to be efficient in $A[Cu_3(\mu_3\text{-}OH)(\mu_3\text{-}4\text{-}cpz)_3]$ (A is a cation).[170] The effect of the ion-exchange on the separation selectivity by the adsorption of gases including N_2, CH_4, CO_2, and C_2H_2 and vapors of benzene and cyclohexane was first revealed in this work. Pulse GC experiments of a gas mixture (N_2, CH_4, CO_2, C_2H_2) further showed that the MOFs with NH_4^+ and Et_3NH^+ gave rise to significant interactions with C_2H_2 and CO_2, whereas those with N_2 and CH_4 are negligible. Thus, these MOFs showed excellent performance in the discrimination of C_2H_2/CH_4, CO_2/CH_4, and $C_2H_2/CO_2/CH_4$ mixtures. For the CO_2/CH_4 separation, the Et_3NH^+-MOF showed a slightly reduced capacity for CO_2 as compared to the NH_4^+-based one. These MOFs also showed a significant enrichment of benzene over cyclohexane from their mixture, in which increased selectivity in the Et_3NH^+- and Li^+-based MOFs as compared to NH_4^+-based MOF was observed, which is most likely related to the increased bulk of the Et_3NH^+ and $Li(H_2O)_4^+$ ions. As a further example, cation exchange was adopted to tune the pore size of bio-MOF-1.[498] Different organic ammonium cations in bio-MOF-1 were responsible for different CO_2 adsorption performances observed in this work. It was found that pores with smaller volumes may be better suited for adsorbing CO_2 due to the stronger sorbate/sorbent interactions at temperatures relevant to real-world application, thereby supposedly giving rise to higher separation efficiency for CO_2 from N_2 under similar conditions. Similarly, anion exchange has also been demonstrated to be effective in tuning the pore size of $[Ni(bpe)_2(N(CN)_2)](N(CN)_2)$.[280] It was demonstrated that after $N(CN)_2^-$ was replaced by N_3^-, the resulting MOF presented a higher CO_2 uptake capacity than the original one, a result of increased pore size in the MOF.

One additional method, using mixed ligands to make solid solutions of MOFs, is also a strategy that has been used to modify pore size. There were several reports on this approach;[217,231] however, a clear relationship between the mixture level of the ligands, resulting pore size, and consequent separation performance is difficult to address. Although it is difficult to finely control the pore size by this method, tuning separation properties could be a viable option in some MOF, potentially clearing a new path in this field. In all of these approaches, it is clear that subtle pore control is very important for these kinds of materials to be able to execute highly selective separations.

5.1.2. Tailoring Pore Surface Function. The pore surface properties play another important role in deciding the adsorption and associated separation of guests by porous materials. Pore surface functionalization in a MOF can be reached not only through the design of MOF components and their construction but also through postsynthetic modification. Building active sites that are capable of forming strong interactions with guest adsorbates in MOFs is a central concern, and multiple approaches to modify the surface properties already exist. It should also be pointed out that, for different separation assignments, the properties of target molecules must be considered in figuring out how the modification of pore surfaces of a sorbent will affect the separation.

Open active metal sites located on the pore walls of a MOF provide an approach for the enhanced separation of many chemicals. These active adsorption centers are usually created by the postsynthetic treatment of MOFs, because they are always occupied by a coordinated species, such as a solvent molecule, in the as-synthesized state. A well-studied example, HKUST-1, has demonstrated preferential adsorption of CO_2 over CH_4 and N_2.[128] The adsorption mechanism has been described as coordination of the CO_2 molecule to the Cu(II) center in an end-on fashion. This MOF also showed the ability to remove sulfur odorant components from natural gas due to the presence of the active metal sites.[309] Furthermore, replacing Cu(II) ions in HKUST-1 by chemically more active Cr(II) ions led to a MOF, which exhibited highly selective and reversible O_2 binding, useful in separating O_2 from N_2.[264] This preferred adsorption on an open metal site has also been confirmed in series of isostructural MOFs with a general formula of $[M_2(dhtp)]$ (CPO-27 or MOF-74, M = Ni, Co, Zn, or Mg), for CO_2 separations.[148,207,228] The capability of these materials to remove toxic gas from air has also been demonstrated via fixed-bed breakthrough testing in both dry and humid conditions.[306,308]

Open metal sites in MOFs have also been demonstrated to be useful in the separation of olefin and paraffin. Again, HKUST-1 demonstrated the preferential adsorption of ethylene over ethane,[126] propylene over propane,[297] and isobutene over isobutane.[302] This observed selective adsorption was proposed to be due to the special interaction between the π-electrons of the "double bond" in the olefin molecules and the partial positive charges of open Cu(II) sites in the framework. Preferential adsorption of propylene over propane was also observed in $Fe_3OF_m(OH)_n(btc)_2$ ($m + n < 1$, MIL-100(Fe)) with coordinatively unsaturated iron sites.[301] In addition, these open metal sites in MOFs can be used to selectively adsorb solvent molecules with special functional group, such as water and alcohols via coordination, potentially applicable in the dehydration and purification of organic solvents.[382−384]

By a postsynthetic modification process, the insertion of metal salts into the pores of a MOF has also been demonstrated to be a useful approach to modify its pore surface for enhanced CO_2 binding.[160] Long and co-workers have shown that the selectivity factor for binding CO_2 over N_2 under typical flue gas conditions increased from 2.8 in MOF-253 to 12 in MOF-253·0.97Cu$(BF_4)_2$. The latter MOF was obtained by the postsynthetic treatment of the former with $Cu(BF_4)_2$. The insertion of metal salts was hypothesized to create electric dipoles on the surface of the MOF, which can strongly interact with CO_2. As expected, the heat of adsorption for CO_2 was found to increase from 23 to 30 kJ/mol upon the insertion of $Cu(BF_4)_2$ into the pristine framework.

MOFs with similar framework structures using only different metal ions can result in different separation performances as well.

dx.doi.org/10.1021/cr200190s |Chem. Rev. 2012, 112, 869–932

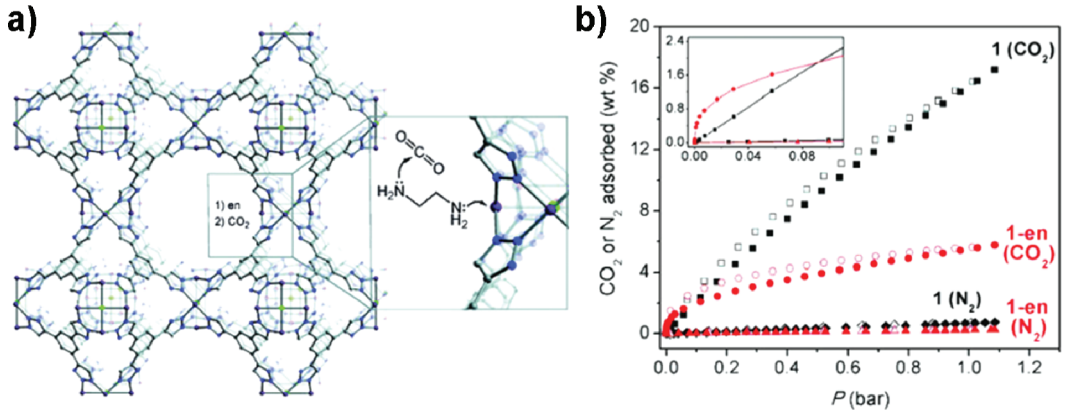

Figure 27. (a) Structure of Cu-BTTri showing surface functionalization of a coordinatively unsaturated Cu(II) site with ethylenediamine (en), followed by attack of an amino group on CO_2; and (b) adsorption−desorption isotherms of CO_2 and N_2 at 298 K in Cu-BTTri (**1**) and Cu-BTTri-en (**1**-en) (the inset shows the increased uptake of CO_2 for Cu-BTTri-en as compared to Cu-BTTri at low pressures). Reproduced with permission from ref 147. Copyright 2009 American Chemical Society.

This has been observed in the selective separation of alkylaromatic isomers by MIL-47 and MIL-53.[417,419] It was determined that the separation of cymene and ethyltoluene isomers with MIL-53 is more effective than that with MIL-47. The pores of MIL-53 seem to be a more suitable environment to accommodate the large ethyltoluene and cymene isomers than those in MIL-47. The observed differences may be attributed to the fact that the presence of different metals in the two MOFs might lead to differences in polarization of the ligand carboxylate groups, which in turn affects the strength of interaction with the guest molecules. The stronger interactions in MIL-53 enabled discrimination of these isomers, resulting in the efficient separations. A similar situation has also been observed in the MOF-74 series for the capture of CO_2[148,207,228,245] and toxic gases.[306,308]

One other useful aspect of open metal sites in MOFs is that they provide a platform to accept functional organic molecules through coordination, which can also be used to modify the pore surface for preferential adsorptions and separations. The prototypical example is the observed enhancement of CO_2 binding by alkylamine-functionalization of a MOF pore reported by Long and co-workers.[147] In this work, the exposed metal sites in $H_3[(Cu_4Cl)_3(BTTri)_8]$ (Cu-BTTri) were coordinated by ethylenediamine (en) by postsynthetically treating to get the en-functionalized MOF (Figure 27a). Despite a reduction in surface area as compared to the parent framework, the en-functionalized MOF presented a higher CO_2 uptake at low pressures as compared to its parent framework, as well as the highest initial heat of adsorption (90 kJ/mol) for any MOF. It is important that the functionalized MOF presented an enhanced selectivity for CO_2 adsorption over N_2 at low pressures (Figure 27b). A second example is the modification of $Zn_2(bttb)(DMF)_2$ (bttb = 4,4′,4″,4‴-benzene-1,2,4,5-tetrayltetrabenzoate) after synthesis by replacing coordinated solvent molecules with highly polar ligand molecules, which resulted in the enhancement of CO_2 adsorption selectivity in the resulting MOFs.[151] As-synthesized $Zn_2(bttb)(DMF)_2$ was postsynthetically treated to obtain first $Zn_2(bttb)$ with open metal sites, and then to produce $Zn_2(bttb)(py\text{-}CF_3)_2$ with metal sites occupied by py-CF_3. It was found that $Zn_2(bttb)(py\text{-}CF_3)_2$ exhibited larger CO_2/N_2 and CO_2/CH_4 selectivities than $Zn_2(bttb)(DMF)_2$ and $Zn_2(bttb)$. This enhanced selectivity was explained by authors as a combination of the highly polar $-CF_3$ groups in $Zn_2(bttb)(py\text{-}CF_3)_2$ that provided stronger attractive forces to CO_2 than N_2 or CH_4 and the more constricted pores of $Zn_2(bttb)(py\text{-}CF_3)_2$, which enhanced the selectivity of the more strongly adsorbed CO_2 due to the increased potential.

Another platform for pore modifications in a MOF is the organic ligand, which can be designed and modified to nearly any specification. Ligand functionalization of MOFs to tune selective adsorption and separation has been widely explored, especially for CO_2 capture.[94] Lewis base functionalization, for example, can enhance CO_2 adsorption due to acid−base interactions between CO_2 (acid) and the basic active centers. This has been realized in a sulfone-functionalized MOF, UoC-1′, which exhibited selective CO_2 adsorption over CH_4, N_2, and H_2.[214] Considering the affinity of amines toward CO_2, amine-functionalized ligands have been combined into several MOFs to enhance the adsorption and selectivity of CO_2. NH_2-MIL-53(Al) presented enhanced CO_2 uptake relative to CH_4 as compared to the parent MIL-53(Al).[211] Similar enhancements were observed in $[Ni_2(NH_2\text{-}bdc)_2(dabco)]$[232] and NH_2-MIL-101(Al),[191] relative to their nonfunctionalized analogues. MOFs with amino-decorated pores showing high and selective CO_2 uptake also include $Co_2(ad)_2(CO_2CH_3)_2$ (bio-MOF-11),[156] $Zn_2(atz)_2(ox)$,[176] amide-decorated $Cu_3(tpbtm)$,[499] and others listed in Table 1. Another notable example is the CO_2 adsorptive separation on a series of isoreticular ZIFs as discussed above.[144] By varying the functional groups in the ligands, the resulting ZIFs have similar structural topologies but different pore surface properties, resulting in different CO_2 adsorption capacities and selectivities.

As discussed in section 2.1.5 of this Review, the functionalization of pore surfaces by noncoordinated O atoms of the ligand has led to the unique selective adsorption of C_2H_2 over CO_2 in $Cu_2(pzdc)_2(pyz)$.[319] The high selectivity toward C_2H_2 was attributed to the formation of H-bonding between C_2H_2 molecules and the surface oxygen moieties of the MOF. The electron-rich pore surface in flexible Zn(TCNQ−TCNQ)(bipy) also led to the effective selective adsorption of O_2 and NO over C_2H_2, Ar, CO_2, N_2, and CO.[258] It was believed that this observed preference arises from the concerted effects of the charge-transfer interactions between TCNQ and these guests and the switchable gate opening and closing of the pores of the framework.

In most cases, the chiral sites located on the pore surface of a MOF decide its performance in enantioselective separation and

dx.doi.org/10.1021/cr200190s |*Chem. Rev.* 2012, 112, 869–932

catalysis. Building a chiral center into pores of MOFs can easily be achieved by the ligand design. As discussed in section 3.3.1 of this Review, the structures of several examples, including homochiral D-POST-1,[26] $Ni_3(btc)_2(3\text{-pic})_6(1,2\text{-pd})_3$,[434] and $Zn_2(bdc)(L\text{-lac})(DMF)$[436,437] exhibiting enantioselective separation toward small chiral molecules by adsorption, are constructed with at least a homochiral organic ligand. Alternately, postsynthetic modification has also been confirmed to be a route to introduce chiral sites into MOF pores by Kim and co-workers.[500] In their work, chiral molecules (*S*)-*N*-(pyridin-3-yl)-pyrrolidine-2-carboxamide and (*S*)-*N*-(pyridin-4-yl)-pyrrolidine-2-carboxamide were anchored to the metal sites in pore walls of MIL-101; the resulting functionalized MOF presented chiral selectivity in catalysis.

Apart from adsorptive separations, enhanced membrane separation performances through tailoring pore surfaces of MOFs has also been observed. ZIF-8,[14,466] ZIF-7,[291] and SIM-1[475] constructed by bridging Zn(II) nodes with 2-methylimidazolate, benzimidazolate, and 4-methyl-5-imidazolecarboxaldehyde, respectively, have the same topology but with different pore sizes and surface properties imparted by the different substituent groups in the imidazolate ligands (on different positions). Their supported thin films showed different selectivities toward the separation of CO_2 from N_2 and CH_4.[455,457,475] Particularly, the SIM-1 membrane revealed an efficient CO_2/N_2 separation, which was ascribed to the polar functional groups and the associated reduced pore size.[475] In contrast to the SIM-1 membrane, the ZIF-8 membrane did not provide a significant CO_2/N_2 separation, due to the very low heat of adsorption of CO_2 in ZIF-8.[246,457] In addition, as discussed above, ion exchange and mixed ligand approaches are applicable to tailor pore surfaces of MOFs for both adsorptive and membrane separations.

5.1.3. Taking Advantage of Structural Flexibility. Most inorganic porous solids, including zeolites and metal oxides, have rigid framework lattices and apertures under typical conditions, although some special examples exhibiting structural flexibility combined with phase transition under higher temperature or pressure have been reported.[501] However, the change of the lattice and aperture in these materials is usually not large because the frameworks are constructed by rigid covalent bonds. In contrast, MOFs are primarily supported by coordination bonds, which are not strong enough to maintain the rigid lattice, in some cases. The possibility of framework/lattice flexibility is thus expected in MOFs, even under mild conditions. In fact, recent developments have shown that a number of special properties in MOFs were associated with their lattice flexibility.[33,502] On the other hand, the introduction of a flexible or stimuli-responsive moiety into a rigid framework is also an attractive and feasible option in MOFs for special properties and functions because of the relative ease associated with tailoring ligands and postmodification.[51,174,180,238] In both cases, the associated flexibility or dynamics of the structure may address an evident response toward guest molecules entering or passing through their pores, or toward other external stimulations, including temperature, pressure, light, and electric fields. It is also important that these flexible MOFs are crystalline and can change their channels reversibly while retaining high regularity, which are unique for MOFs beyond any other porous materials. As compared to rigid MOFs and other porous solids, flexible or stimuli-responsive MOFs have already shown additional advantages in selective adsorption and separation. So far, a lot of flexible MOFs have been synthesized and characterized by adsorption; however, only a minority of them have been explored in separation-related topics.

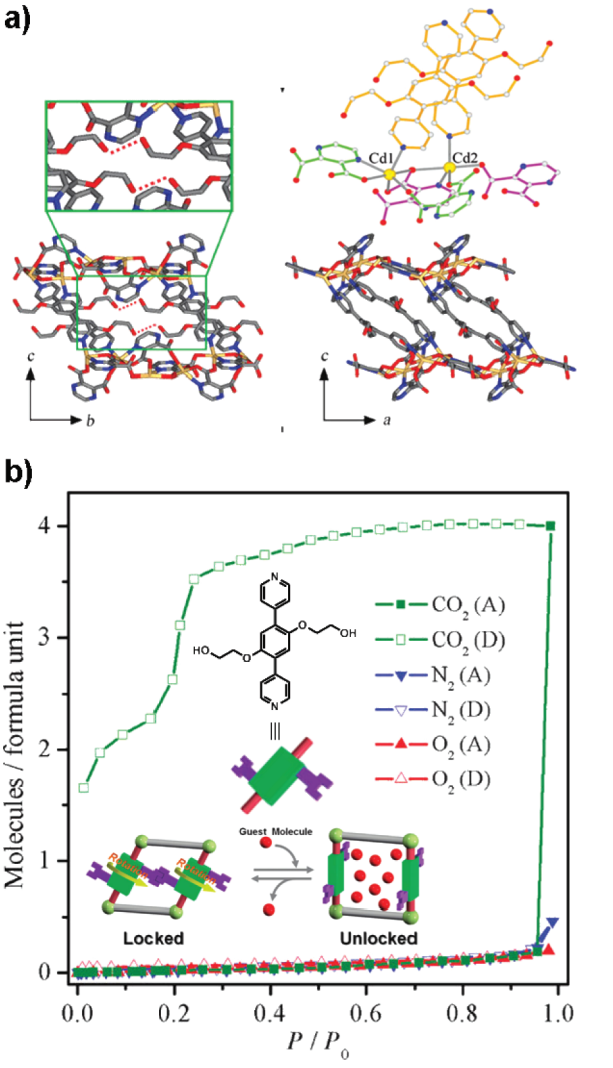

Figure 28. (a) Crystal structure of $Cd_2(pzdc)_2(bhbpb)$ showing the hydrogen bonding and the ligand coordination modes; and (b) adsorption (A) and desorption (D) isotherms of CO_2 (195 K), N_2 (77 K), and O_2 (77 K) on $Cd_2(pzdc)_2(bhbpb)$ (inset: a mode showing the design of pore space via the introduction of a rotational module as a molecular gate with locking/unlocking interactions triggered by guest inclusion). Reproduced with permission from ref 153. Copyright 2009 American Chemical Society.

Among flexible MOFs, the "breathing" MIL-53 series showed responsive behavior to guest adsorption and has been extensively investigated in selective adsorption and separation of gases,[92,196−198,234,235] vapors,[139,340,348] and liquid compounds[386,388,396,397] as discussed in the corresponding sections of this Review. For example, the chromium analogue (MIL-53(Cr)) in its activated state showed a two-step adsorption isotherm for CO_2, whereas that of CH_4 showed a type I isotherm. For the hydrated form, on the other hand, the adsorption of CH_4 became nearly zero, while a gating effect was observed for CO_2.[197] These properties make this MOF an excellent candidate for CO_2 separation. A similar gating phenomenon that can be used for CO_2 separation has been observed in several other flexible MOFs, including SNU-M10[145] and ELM-11.[212] In addition, flexible Zn(TCNQ−TCNQ)(bipy) exhibited the selective adsorption of benzene over cyclohexane at room temperature, as well as O_2 and NO over N_2,

dx.doi.org/10.1021/cr200190s |*Chem. Rev.* 2012, 112, 869–932

CO_2, and Ar at low temperature as discussed in sections 2.1.2 and 2.1.4 of this Review.[258,266]

It has also been demonstrated that a MOF can exhibit selective adsorption toward different gases at different gate-opening pressures, which is decided by the properties of the gas molecules. This type of material provides the possibility of separating several gases by using just one adsorbent. A typical example is $Cu(dhbc)_2(bipy)$,[132] in which the N_2, O_2, CO_2, and CH_4 adsorption isotherms initially showed a flat curve indicative of zero adsorption in the low pressure region, followed by an abrupt increase at a specific gate-opening pressure for each gas. The same abrupt change was observed for the desorption branch as well where the gate closing pressure was clearly different leading to hysteresis. At least theoretically, these gases can be separated by adsorption on this material in different pressure ranges. A second example, Cd(bpndc)(bipy), has different gate-opening pressures for the adsorption of O_2, N_2, and Ar at low temperature.[267]

Apart from the lattice flexibility of MOFs, a flexible or stimuli-responsive species can be introduced into a MOF structure to give an additional dynamic behavior, responsible for the selective adsorption and separation of guest molecules. As discussed in section 2.1.1 of this Review, the modification of pore properties utilizing flexible motifs and functional groups has led to, for example, $Cd_2(pzdc)_2(bhbpb)$ with desirable functions in selective adsorption.[153] As shown in Figure 28, using a rationally designed ligand, a rotatable pillar bearing ethylene glycol side chains was introduced into the flexible framework of the MOF. In this structure, ethylene glycol groups act as a molecular gate with locking/unlocking interactions triggered by guest inclusion. This MOF has no void volume, but can selectively adsorb CO_2 with large hysteresis at higher vapor pressure by means of structural transformation combined with a slipping of its layers and reject N_2 and O_2 (Figure 28b). The inclusion of CO_2 in only the higher vapor pressure region can be viewed as an effect of a molecular gate that is locked by hydrogen bonds, which cannot be broken by CO_2 at low vapor pressure, or at all by the other gases. A second interesting example is Cu(etz) reported by Zhang and Chen.[341] Again, based on the rational design or selection of the ligand, 3,5-diethyl-1,2,4-triazole (Hetz), flexible ethyl groups were introduced into the framework containing a hydrophobic channel system, in which the large cavities are interconnected by small apertures partially obscured with the pendant ethyl groups. It was confirmed that the ethyl-blocked apertures behave as thermoactivated IRIS stops for the guest molecules. Consequently, the gas sorption behavior of Cu(etz) can be controlled by temperature: for instance, N_2 adsorption was only observed at 195 K rather than 77 K. On the basis of the associated flexibility and its hydrophobic pore surface, Cu(etz) exhibited selective inclusion of small organic molecules including MeOH, EtOH, and MeCN, accompanied by framework distortions, but excluded H_2O. More interestingly, this MOF can also separate benzene and cyclohexane in the vapor phase, as its flexible framework lattice can distort to a certain degree so that benzene can diffuse through the flexible apertures but cyclohexane cannot.

Similarly, the flexible motif can also be designed into a rigid lattice of a MOF to exhibit a stimuli-responsive adsorption performance for selective guest uptake and separation. A typical example of $Zn_2(bmebdc)_2(bipy)$ has been described in section 2.1.1 of this Review.[174] Another example is a series of MOFs developed in the author's group, named mesh-adjustable molecular sieves (MAMSs), which showed temperature-dependent gas selective adsorption.[268,269] These MOFs have a graphite-type layer structure containing hydrophobic chambers and hydrophilic channels. The latter channels are occupied by coordinated solvent molecules in their as-synthesized form. Upon careful activation, these MOFs showed different gas selective adsorption performances at different temperatures, probably due to a dynamic gating effect. Recent research also showed that the observed adsorption performances are related to the activation of the samples. The temperature-triggered gate opening effect has also been observed in $Mn(CO_2)_2$ for N_2 and Ar adsorption.[257] The authors claimed that this effect was not due to a structural change of the framework but due to dynamic opening of the pore aperture and/or sufficient kinetic energy of the guest molecules to overcome a diffusion barrier above a critical temperature.

5.2. Implementation and Process for Applications

Despite equivalent importance, studies related to the implementation and complete process of using MOFs for practical applications in separations are largely lacking at this time. Until now, most studies are focusing on the synthesis, structures, and general adsorption/separation properties of these new materials from a scientific research point of view, with few connected to industrial applications.[35,309] For practical separation applications, besides optimizing the separation capacities of the materials, several additional issues must be addressed, including the stability and scale-up of materials, separation process design (adsorptive separation and membrane separation), associated cost, and even environmental impact of these new materials.

5.2.1. Stability of MOFs. The stability of MOFs directly influences the feasibility of their practical applications in a lot of fields including separations. For the sake of discussion, at a clearly defined level, and emphasizing the relationship between stability and associated applications, MOF stability can be arbitrarily divided into framework stability, thermal stability, and chemical stability.

Framework stability in the context of this discussion refers to whether the structure (open lattice) is preserved or collapses after removing guest molecules from the as-synthesized phase or after suffering from changes in environment and/or external stimulation (this intricately involves the thermal and chemical stabilities to some extent). For gas-phase adsorptive separations and membrane separations, the framework stability toward removing guest molecules from its pores is a prerequisite. Solution or liquid-phase separations are, however, a little different, as can be seen with the example of $Zn_2(bdc)(L\text{-}lac)(DMF)$, which prefers to collapse after the removal of all free solvent molecules from the as-synthesized sample, but withstands the exchange of solvent molecules by other guest molecules in solution. Thus, this MOF can be used in the enantioselective adsorption of sulfoxides in solution.[436] Generally speaking, a MOF with small pores or low porosity is stable as is clearly illustrated by the metal formate MOFs that are stable enough to maintain single crystallinity after the complete guest removal at 150 °C.[177] The structure of Zn(tbip) also retained its crystallinity over a prolonged heating at 350 °C.[332] Both MOFs have small pores and showed good gas selective adsorption. With increased pore volume or size, on the other hand, the framework usually suffers in stability.[34,503,504]

Several strategies can be used to enhance framework stability of a highly porous MOF. Using metal clusters as the nodes to construct stable MOFs was recognized at an early stage of the MOF field.[21,31] A lot of MOFs with metal clusters acting as building units have been synthesized and showed framework stability in adsorption-related processes, even those that are highly porous. Recently, metal−organic polyhedra acting as

dx.doi.org/10.1021/cr200190s |Chem. Rev. 2012, 112, 869–932

supramolecular building units were found to be valid in constructing stable MOF with very high porosity.[505,506] In addition, the interpenetration of a network increases the wall thickness and reduces the pore size of a MOF, and has been used to improve the stability of porous MOFs.[254]

It should be pointed out that flexible or dynamic MOFs seem to follow different rules of framework stability. In most cases, after removing guest molecules, the original framework shrinks, which is accompanied by a crystal-to-crystal or crystal-to-amorphous transformation, but the bonding between building components is retained. This reduction or disappearance of porosity in a flexible MOF is different from the collapse of a framework, which usually involves the breaking of bonds.

Thermal stability is a major limitation for many hybrid framework materials; the same situation is true in MOFs. Although some MOFs can be heated to 400 °C or above without losing framework integrity, the majority of them are not stable above 200 °C. A special example of MOF, Li_2(2,6-ndc), with very high thermal stability was reported to be stable to 610 °C.[507] On the other hand, chemical stability, although not widely explored, seems to be a deficiency of MOFs for some separation applications because the coordination bonds between metal nodes and organic ligands are easily broken by reactive chemicals, often as simple as water. This can be averted by using strong bonds, such as those in the highly stable olefin−Cu(I) polymeric compounds.[508]

It must be pointed out that in nature the bond strength and characteristic between metal ions and organic ligands ultimately decide the stability of each MOF. The exceptional chemical and thermal stability of ZIFs has been verified.[14] ZIF-8 and -11 are prototypical examples that have been checked for thermal (decomposition temperature around to 550 °C) and chemical stability. ZIF-11 is stable in water at 50 °C for 7 days and ZIF-8 for 7 days in boiling water and up to 24 h in 0.1 and 8 M aqueous solution of NaOH at 100 °C. In addition, the ZIF-90 membranes also showed high thermal and hydrothermal stabilities.[460] These high thermal and chemical stabilities of ZIFs can be attributed to the much stronger bonds betweenimidazole nitrogen atoms and Zn(II). With carboxylate ligands, Al(III),[160] Cr(III),[509] and Zr(IV)[510] cluster-based MOFs have been revealed to be much more stable than those with other transitional metal ions, with which multi-N-based ligands, such as triazolate[147] and pyrazolate,[511] seem to be better for constructing a stable MOF.

Water stability of MOFs may be much more important in some practical separations, such as the separation of CO_2 from flue gases. Recently, Cychosz and Matzger explored the water stability of several popular MOFs, including MOF-5, -177, -505, HKUST-1, UMCM-150, MIL-101, and ZIF-8.[512] These MOFs containing different metal-cluster SBUs and associated coordination bonds are representative members that were widely studied in the MOF field. It was found that that the stability of the MOFs is related to the metal cluster: the Cr(III) clusters of MIL-101 did not degrade at all and were much more stable than Cu(II) paddlewheel clusters, which are more stable than Zn_4O clusters; the ZIF-8 N−Zn bonds are also more water stable than Zn_4O MOFs. Another noticeable water-stable MOF that was investigated for CO_2 separation is $H_3[(Cu_4Cl)_3(BTTri)_8]$, which is also stable in a solution of 0.001 M HCl.[147] Obviously, the water stability is also directly related to the strength of metal−ligand bonds, including those in the metal clusters, in a MOF. It should also be pointed out that for different target separations and processes, the requirements to the stability of materials are different.

5.2.2. Separation Process and Beyond. Despite a lot of MOFs having been investigated for their potential applications in adsorptive and membrane-based separations, the design and evaluation of the entire separation process using these materials remains almost untouched in both science and engineering aspects.[309] As an exception, the separation of Kr/Xe by pressure swing adsorption, as well as the purification of methane in natural gas, were piloted using some MOF adsorbents.[513,514] Recently, Simmons and co-workers[515] also evaluated the performance of several MOFs including MOF-5, Cu_2(sbtc) (PCN-11, sbtc = *trans*-stilbene-3,3′,5,5′-tetracarboxylate[516]), Cu_2(ebdc) (PCN-16, ebdc = 5,5′-(1,2-ethynediyl)bis(1,3-benzenedicarboxylate)[517]), HKUST-1, ZIF-8, Mg-MOF-74, and Zn-MOF-74 in industrially relevant swing adsorption processes for CO_2 capture. Their results showed that the efficacy of MOFs for CO_2 capture depends dramatically on the process that is adopted. In fact, some MOFs showed significant capture capacity under typical pressure and vacuum swing processes. In particular, MOFs with CUMs offered as high as 9 mmol g^{-1} swing capacity under certain conditions. They concluded that "there is no single ideal compound for CO_2 capture applications and that different materials can perform better or worse depending on the specific process conditions; the performance of a given MOF cannot be determined without also considering the detailed industrial process in which the MOF is to be applied".

For adsorptive separation, depending on the regeneration methods, several adsorption processes can been adopted to achieve gas separations, including (1) vacuum or pressure swing adsorption (VSA or PSA), (2) temperature swing adsorption (TSA), (3) electric swing adsorption (ESA), (4) simulated moving bed (SMB), and (5) purge displacement; however, few evaluations have thus far been reported as mentioned above. MOFs have also been used as a stationary phase for chromatography separations in both gas and liquid phases, but only in a laboratory setting. In terms of membrane separations, the fabrication of a perfect MOF-based membrane (thin film and mixed-matrix membrane) is still challenging, even in the lab.

Different separations require different process and associated technologies. From an exploring and optimizing materials point of view, further laboratory measurements should be carried out under conditions that simulate the process environment. For example, in the case of CO_2 separation from flue gases, the partial pressure of CO_2 is very low, and the stream has a high temperature and contains water and other toxic gases. Although it is very difficult to study the adsorption of multicomponent streams, a binary system is accessible. In addition, a breakthrough experiment may be much more straightforward to evaluate the adsorption and separation performance of a material toward mixed systems. In fact, more and more publications are reporting results using these methods, particularly in CO_2 separation. A typical example is the exploration of the effect of humidity on the performance of the MOF-74 series (M = Zn, Ni, Co, or Mg) as adsorbents for CO_2 capture, as discussed in section 2.1.1 of this Review.[245]

On the other hand, the cost and scale-up in the preparation of MOFs have probably limited their development for practical applications, although efforts have been made.[35] The large-scale syntheses of several MOFs, including Al-terephthalate (Basolite A100), HKUST-1 (Basolite C300), Fe-benzene-1,3,5-tricarboxylate (Basolite F300), ZIF-8 (Basolite Z1200), and Mg-formate (Basolite M050) (Mg-MOF), are being worked on by BASF. BASF has also claimed the success of industrial-scale synthesis

of MOFs for the first time.[518] The easy and cheap synthesis of MOFs will promote the applied research into the entire process, thereby accelerating the development of using MOFs for separations.

6. CONCLUSIONS AND OUTLOOK

Separations play an important role in human activities, which is why they have attracted such wide attention in both scientific research and applied technologies. The exploitation of new materials for separation applications is essential and will continue indefinitely. As a class of newly developed porous solids, MOFs have shown great application potential in various separations, from CO_2 capture to natural gas purification, from H_2 purification to noble-gas separation, from air separation to harmful gas removal, from desulfurization to large-molecule inclusion, and from structural isomer separation to enantio-separations, in both gas-phase and liquid-phase systems. There are several approaches that have been developed to help evaluate a MOF for separation-related applications, from single-component selective adsorption/permeation to the separation of mixtures by adsorptive and membrane separations.

As a relatively comprehensive review, one of the underlying themes of this Review is to demonstrate that MOFs have significant potential for separation-related applications and significant advantages over other porous materials such as zeolites and activated carbon. They are highly crystalline, which allows researchers to investigate and observe pore and surface properties more closely. They are easily tunable by virtue of the fact that they are self-assembled from metal salts and nearly infinitely variable organic ligands, which can be used to introduce functional groups to a pore surface, precisely control pore metrics, and impart the material with a structural flexibility that is unprecedented in other types of materials. MOFs have, over the course of the past decade, made tremendous advances in terms of the understanding of how these materials are assembled and what factors are involved in controlling the synthesis of a predesigned framework; they have given researchers a certain extent of "control" of a material at the molecular level. Systematic investigations, both experimental and computational, into isostructural MOFs have indeed let researchers tease out specific variables and give us a better understanding of what properties are the keys to a targeted application. Clearly, designing a material, particularly at the molecular level, for special separation is becoming feasible in the field of MOF research.

In separation-related topics, particularly in gas adsorptive separations, thus far, MOF researchers have primarily focused on exploring new materials with single adsorption properties, from which selectivities are calculated. The majority of these measurements revolve around PSA, TSA, or other processes and are highly accurate to their own right, but should not be viewed as the best way of characterizing a new adsorbent material for practical separation applications. Mixed gas breakthrough measurements and using column chromatography (both vapor and liquid) for separation measurements are highly valuable tools in understanding these new materials and will aid in determining which ones have long-term promise and applicability. In terms of membrane separations, the development of the manufacturing processes for various membranes that are reproducible and can be made on a large scale is a central issue of future research. Finally, setting up processes and evaluating the scaled-up and practical separations from both approaches must be pursued; collaboration with engineers will be of great value in this arena.

With all that has been learned already and the myriad of MOFs that have been synthesized, it is time to take the materials from a laboratory and test them in the real world. Research over the next decades must also focus more heavily on applying all of this knowledge in industrial scenarios, or at least developing and using multivariable systems to further fine-tune MOFs for eventual applications. Some researchers have already begun to focus on thermally and chemically stable MOFs, on using MOFs that can easily and cheaply be scaled up, and on the total separation process. Much still needs to be learned from the commercial successes, such as the zeolites industry, which has proven that adsorptive materials have a significant role in the enormous and complex separation processes.

By collaborating with engineers and always keeping the complete process in mind, researchers will be able to modify, scale up, and finely tune these materials to be used in a commercial setting. The ultimate goal for MOFs, for example, should not be a calculated selectivity of CO_2 over N_2 or CH_4, using single-component isotherms, but it should be selectively capturing CO_2 from a hot, wet flue gas stream that is also filled with SO_x, NO_x, and other contaminants, without degrading over the course of many years.

ASSOCIATED CONTENT

Supporting Information

ChemDraw structures of some ligands in this Review. This material is available free of charge via the Internet at http://pubs.acs.org.

AUTHOR INFORMATION

Corresponding Author

*E-mail: zhou@mail.chem.tamu.edu.

BIOGRAPHIES

Jian-Rong "Jeff" Li received his Ph.D. in 2005 from Nankai University under the supervision of Prof. Xian-He Bu. Until 2007, he was an assistant professor at Nankai University. In 2004, he was also a research assistant in Prof. Guo-Cheng Jia's group at Hong Kong University of Science & Technology. In 2008, he joined Prof. Hong-Cai Zhou's group as a postdoctoral research associate, first at Miami University and later at Texas A&M University. Since 2010, he has been an assistant research scientist

at Texas A&M University. His recent research interest focuses on metal−organic materials for clean energy-related applications.

Julian Sculley was born in Birkenfeld, Germany in 1987. He received his B.S. (2009) from Virginia Military Institute. After that, he joined Prof. Hong-Cai Zhou's group as a graduate student at Texas A&M University. His research interests include carbon capture related gas separation and postsynthetic modification of porous frameworks to increase sorbent interactions.

Hong-Cai "Joe" Zhou (http://www.chem.tamu.edu/rgroup/zhou/) obtained his Ph.D. in 2000 from Texas A&M University under the supervision of F. A. Cotton. After a postdoctoral stint at Harvard University with R. H. Holm, he joined the faculty of Miami University, Oxford, in 2002. Since the fall of 2008, he has been a professor of chemistry at Texas A&M University. His research interest focuses on gas storage and separations that are relevant to clean energy technologies.

ACKNOWLEDGMENT

We are thankful for financial support from the U.S. Department of Energy (DOE), the National Science Foundation (NSF), the Welch Foundation, and Texas A&M University. Particularly, this Review is based upon work supported by the Advanced Research Projects Agency − Energy (ARPA-E) through the IMPACCT program (AR0000073), NSF on CBET-0930079, and as part of the Center for Gas Separations Relevant to Clean Energy Technologies, an Energy Frontier Research Center funded by the U.S. Department of Energy, Office of Science, Office of Basic Energy Sciences under Award Number DE-SC0001015.

ABBREVIATIONS

6FDA	2,2′-bis-(3,4-dicarboxyphenyl) hexafluoropropane dianhydride
AEPF	alkaline-earth polymer framework
BT	benzothiophene
CA	cellulose acetate
CCS	carbon capture and storage
CPL	coordination pillared layer structure
CUK	Cambridge University−KRICT
CUMs	coordinatively unsaturated metal sites
DBT	dibenzothiophene
DMA	*N*,*N*′-dimethylacetamide
DMDBT	4,6-dimethyldibenzothiophene
DME	dimethylether
DMF	*N*,*N*-dimethylformamide
DMSO	dimethyl sulfoxide
DUT	Dresden University of Technology
EB	ethylbenzene
ee	enantiomeric excess
ELM	elastic layer-structured metal organic framework
ESA	electric swing adsorption
GC	gas chromatography
GPC	gel permeation chromatography
HDS	hydro-desulfurization
HKUST	Hong-Kong University of Science and Technology
IAST	ideal adsorbed solution theory
IND	indole
IPA	isopropanol
IRMOF	isoreticular metal−organic framework
LC	liquid chromatographic
MAFs	metal azolate frameworks
MAMS	mesh-adjustable molecular sieve
MCP	microporous coordination polymer
MD	molecular dynamics
MIL	Matériauxs de l'Institut Lavoisier (Material Institut Lavoisier)
MMM	mixed-matrix membrane
MOF	metal−organic framework
MOP	metal−organic polyhedron
MTV-MOF	multivariate metal−organic framework
mX	*m*-xylene
oX	*o*-xylene
PCN	porous coordination network
PCP	porous coordination polymer
PDMS	polydimethylsiloxane
PI	polyimide
POST	Pohang University of Science and Technology
PSA	pressure swing adsorption
PSf	polysulfone
PVAc	poly(vinyl acetate)
pX	*p*-xylene
PXRD	powder X-ray diffraction
QA	6′-methoxyl-(8*S*,9*R*)-cinchonan-9-ol-3-carboxylate
RB	Rose Bengal

RH	relative humidity
SBU	secondary building unit
SMB	simulated moving bed
SNU	Seoul National University
SRNF	solvent resistant nanofiltration
St	styrene
STP	standard temperature and pressure
TCNQ	7,7,8,8-tetracyano-*p*-quinodimethane
TGA	thermogravimetric analysis
THF	tetrahydrofuran
THT	tetrahydrothiophene
TPH	thiophene
TSA	temperature swing adsorption
ULSD	ultralow sulfur diesel
UMCM	University of Michigan Crystalline Material
Ouch	University of Crete
VB-N-CIN	4-vinylbenzylcinchonidinium cation
ZIF	zeolitic imidazolate framework
ZMOF	zeolite-like metal−organic framework
1,2,4-btc	benzene-1,2,4-tricarboxylate
1,2-pd	1,2-propanediol
1,3-bdc	1,3-benzenedicarboxylate
1,4-ndc	1,4-naphthalenedicarboxylate
2-NH_2-bdc	2-amino-1,4-benzenedicarboxylate
2,2′-bipy	2,2′-bipyridine
2,3-pyrdc	pyridine-2,3-dicarboxylate
2,4-pdc	2,4-pyridinedicarboxylate
2,4-pydc	pyridine-2,4-dicarboxylate
2,5-pydc	pyridine-2,5-dicarboxylate
2,6-ndc	2,6-naphthalenedicarboxylate
2,7-ndc	2,7-naphthalenedicarboxylate
2-bim	2-bromoimidazolate
2-cim	2-chloroimidazolate
3,3′-tpdc	terphenyl-3,3′-dicarboxylate
3,5-pydc	3,5-pyridinedicarboxylate
3-pia	*N*-(3-pyridyl)isonicotinamide
3-pic	3-picoline
4-btapa	1,3,5-benzene-tricarboxylic acid tris-[*N*-(4-pyridyl)amide]
4-cpz	4-carboxypyrazolato
5-MeO-ip	5-methoxyisophthalate
5-NO_2-ip	5-nitroisophthalate
6-mna	6-mercapto-3-pyridinecarboxylate
abppt	4-amino-3,5-bis(4-pyridyl-3-phenyl)-1,2,4-triazole
ad	adeninate
adc	4,4′-azobenzenedicarboxylate
aptz	4-aminophenyl-1*H*-tetrazolate
azpy	4,4′-azopyridine
bbim	5-bromobenzimidazolate
bbpdc	4′-*tert*-butyl-biphenyl-3,5-dicarboxylate
bdc	1,4-benzenedicarboxylate
bdc-OH	2-hydroxybenzene-1,4-dicarboxylate
bdp	1,4-benzenedipyrazolate
BenzTB	*N*,*N*,*N*′,*N*′-benzidinetetrabenzoate
bfhc	3,10-bis(2-fluorobenzyl)-1,3,5,8,10,12-hexaazacyclotetradecane
bhbpb	2,5-bis(2-hydroxyethoxy)-1,4-bis(4-pyridyl)benzene
bim	benzimidazolate
bipy	4,4′-bipyridine
bipyen	*trans*-1,2-bis(4-pyridyl)ethylene
bmebdc	2,5-bis(2-methoxyethoxy)-1,4-benzenedicarboxylate
bmpbdc	2,5-bis(3-methoxypropoxy)benzenedicarboxylate
bpa	1,4-bis(4-pyridyl)acetylene
bpcb	tetrakis(4-pyridyl)cyclobutane
bpe	1,2-bis(4-pyridyl)ethane
bpee	bis(4-pyridyl)ethylene
bpndc	benzophenone-4,4′-dicarboxylate
bpno	4,4′-bipyridine-*N*,*N*′-dioxide
bpp	1,3-bis(4-pyridyl)propane
bpt	biphenyl-3,4′,5-tricarboxylate
bpta	3,6-di(4-pyridyl)-1,2,4,5-tetrazine
bptc	1,1′-biphenyl-3,3′,5,5′-tetracarboxylate
bptz	3,6-bis(4-pyridyl)-1,2,4,5-tetrazine
bpydc	2,2′-bipyridine-5,5′-dicarboxylate
btc	1,3,5-benzenetricarboxylate
btt	1,3,5-benzenetristetrazolate
bttb	4,4′,4″,4‴-benzene-1,2,4,5-tetrayltetrabenzoate
bttp4	benzene-1,3,5-triyltriisonicotinate
bza	benzoate
cbim	5-chlorobenzimidazolate
chdc	1,4-cyclohexanedicarboxylate
H_2cnc	4-carboxycinnamic acid
cnim	4-cyanoimidazolate
cyclam	1,4,8,11-tetraazacyclotetradecane
dabb	diacetylene-1,4-bis(4-benzoate)
dabco, ted	1,4-diazabicyclo[2,2,2]octane
dcbdc	2,5-dichloro-1,4-benzenedicarboxylate
dhbc	2,5-dihydroxybenzoate
dmtz	3,5-dimethyl-1,2,4-triazolate
dpcb	1,4-di(1,3,5,8,12-pentaazacyclotetradecan-3-yl)butane
dpce	1,2-di(1,3,5,8,12-pentaazacyclotetradecan-3-yl)ethane
dpni	*N*,*N*′-di-(4-pyridyl)-1,4,5,8-naphthalene tetracarboxydiimide
dpt	3,6-di-4-pyridyl-1,2,4,5-tetrazine
dpyg	1,2-dipyridylglycol
ebdc	5,5′-(1,2-ethynediyl)bis(1,3-benzenedicarboxylate)
en	ethylenediamine
F-pymo	5-fluoropyrimidin-2-olate
Hatz	3-amino-1,2,4-triazole
H_2bbs	4,4′-bibenzoic acid-2,2′-sulfone
H_2bbta	1*H*,5*H*-benzo(1,2-*d*:4,5-*d*′)bistriazole
H_2bchp	2,2′-bis(4-carboxyphenyl)hexafluoropropane
H_3cep	2-carboxyethylphosphonic acid
H_2dcdd	1,12-dihydroxy-carbonyl-1,12-dicarba-*closo*-dodecaborane
H_2dtp	2,3-di-1*H*-tetrazol-5-ylpyrazine
H_2oba	4,4′-oxybis(benzoic acid)
H_2SalPycy	5,5′-(cyclohexane-1,2-diylbis(azan-1-yl-1-ylidene))bis(methan-1-yl-1-ylidene)bis(3-methylpyridin-4-ol)
H_3btb	1,3,5-tris(4-carboxyphenyl)benzene
H_3BTTri	1,3,5-tris(1*H*-1,2,3-triazol-5-yl)benzene
H_3oxonic	4,6-dihydroxy-1,3,5-triazine-2-carboxylic acid

dx.doi.org/10.1021/cr200190s |*Chem. Rev.* 2012, 112, 869–932

H_3tci	tris(2-carboxyethyl)isocyanurate
H_3tctc	1,4,7-tris(4-carboxybenzyl)-1,4,7-triazacyclononane
H_3tib	1,3,5-tri(1*H*-imidazol-4-yl)benzene
H_4bdcppi	*N*,*N*′-bis(3,5-dicarboxyphenyl)pyromellitic diimide
H_4debnbp	2,2′-diethoxy-1,1′-binaphthalene-6,6′-bisphosphonic acid
H_4dhtp	2,5-dihydroxyterephthalic acid
H_4imta	*N*,*N*′-bis(2,6-dimethyl-3,5-carboxylphenyl)imidazolium chloride
H_4T(p-CO_2)PP	meso-tetra(4-carboxyphenyl)porphine
H_4tcom	tetrakis-[4-(carboxyphenyl)oxamethyl]methane
H_4tcpbda	*N*,*N*,*N*′,*N*′-tetrakis(4-carboxyphenyl)biphenyl-4,4′-diamine
H_8pmtp	1,4-phenylenbis(methylidyne)tetrakis-(phosphonic acid)
Hbta	1,2,3-benzenetriazole
Hdmtrz	3,5-dimethyl-1*H*-1,2,4-triazole
Hetz	3,5-diethyl-1,2,4-triazole
hfidp	4,4′-(hexafluoroisopropylidene)diphthalate
Hmimc	4-methyl-5-imidazolecarboxaldehyde
ica	imidazolate-2-carboxyaldehyde
im	imidazolate
in	isonicotinate
inaip	5-(isonicotinamido)isophthalate
ip	isophthalate
L-asp	L-aspartate
L-H_2lac	L-lactic acid
mbim	5-methylbenzimidazolate
mcbdc	5-methoxycarbonyl-benzene-1,3-dicarboxylate
mdpt24	3-(3-methyl-2-pyridyl)-5-(4-pyridyl)-1,2,4-triazolate
mim	2-methylimidazolate
mtb	methanetetrabenzoate
NH_2in	3-aminoisonicotinate
nim	2-nitroimidazolate
ntc	naphthalene-1,4,5,8-tetracarboxylate
ox	oxalate
pbmp	*N*,*N*′-piperazinebismethylenephosphonate
p-cdcH_2	1,12-dihydroxydicarbonyl-1,12-dicarba-*closo*-dodecaborane
pda	1,4-phenylendiacetate
phim	benzimidazolate
pip	piperazine
pmai	5-(pyridin-4-ylmethylamino)isophthalate
ppma	*N*,*N*′-(2-pyridyl-(4-pyridylmethyl)-amine)
pur	purinate
py	pyridine
PyenH_2	5-methyl-4-oxo-1,4-dihydro-pyridine-3-carbaldehyde
pyta	2,4,6-pyridinetricarboxylate
pyz	pyrazine
pzdc	2,3-pyrazinedicarboxylate
R_6-bdc	1,2-dihydrocyclobutabenzene-3,6-dicarboxylate
R-ddbb	(*R*)-6,6′-dichloro-2,2′-dihydroxy-1,1′-binaphthyl-4,4′-bipyridine
R-gla-Me	*R*-2-methylglutarate
sbtc	*trans*-stilbene-3,3′,5,5′-tetracarboxylate
sip	5-sulfoisophthalate
tatb	4,4′,4″-*s*-triazine-2,4,6-triyltribenzoate
tbip	5-*tert*-butyl isophthalate
tda	thiophene-2,5-dicarboxylate
ted	triethylenediamine
tip	5-(1*H*-tetrazol-1-yl)isophthalate
tmpes	tetrakis[(4-methylthiophenyl)ethynyl]phenylsilane
Tp	hydrotris(pyrazolyl)borate
tpt	2,4,6-tris(4-pyridyl)-1,3,5-triazine
tz	tetrazolate
tzc	tetrazolate-5-carboxylate

Codes of a Majority of Important MOFs

AEPF-1_{dry}	$Ca(hfipbb)(H_2hfipbb)_{0.5}(H_2O)$[398]
Amino-MIL-53(Al)	$Al(OH)(2\text{-}NH_2\text{-}bdc)$[519]
bio-MOF-11	$Co_2(ad)_2(OAc)_2$[156]
COP-27-M	$M_2(dhtp)$ (M = Mg, Ni)[148]
CPL-11	$Cu_2(pzdc)_2(bptz)$[166]
Cu-BTTri	$HCu[(Cu_4Cl)_3(BTTri)_8]$[147]
CUK-1	$Co_3(2,4\text{-}pdc)_2(OH)_2$[25]
CUK-2	$Co(6\text{-}mna)$[25]
Cu-SIP-3	$Cu_2(OH)(sip)$[315]
DUT-10(Zn)	$Zn_2(H_2O)_2(BenzTB)$[162]
ELM-11	$Cu(bipy)_2(BF_4)_2$[212]
Fe-BTT	$Fe_3[(Fe_4Cl)_3(btt)_8(MeOH)_4]_2$[73]
HKUST-1	$Cu_3(btc)_2$[21]
IRMOF-3	$Zn_4O(2\text{-}NH_2\text{-}bdc)_3$[307]
IRMOF-6	$Zn_4O(R_6\text{-}bdc)_3$[307]
IRMOF-62	$Zn_4O(dabb)_3$[306]
MAF-26	$Co(mdpt24)_2$[16]
MAMS-2−4	M(bbpdc) (M = Zn, Co, Cu)[269]
MIL-100(Al, Cr)	$M_3OX(btc)_2$ (M = Al, Cr; X = F, OH)[520,521]
MIL-100(Fe)	$Fe_3OF_m(OH)_n(btc)_2$ ($m + n \leq 1$)[300]
MIL-101(Cr)	$Cr_3OF(bdc)_3$[20]
MIL-102	$Cr_3O(H_2O)_2F(ntc)_{1.5}$[133]
MIL-47	$V(O)(bdc)$[374]
MIL-53	M(OH)(bdc) (M = Cr, Al)[234,235]
MIL-53(Al)ht	MIL-53(Al) activated at high temperature[235]
MIL-53(Fe)	Fe(OH,F)(bdc)[395]
MIL-53(Mn^{II})	$Mn_2(bdc)_2(bpno)$[381]
MIL-89	$Fe_3O(CH_3OH)_3Cl(bdc)_3$[399]
MIL-96	$Al_{12}O(OH)_{18}(H_2O)_3(Al_2(OH)_4)(btc)_6$[200]
M-MOF-74	$M_2(dhtp)$ (M = Zn, Ni, Co, Mg)[414,522−524]
MOF-177	$Zn_4O(btb)_2$[402]
MOF-253	$Al(OH)(bpydc)$[160]
MOF-5	$Zn_4O(bdc)_3$[31]
MOF-505	$Cu_2(bptc)$[323]
MOF-508	$Zn(bdc)(bipy)_{0.5}$[366]
MOF-76	$Tb(btc)$[414]
NH_2-MIL-101(Al)	$Al_3O(X)(2\text{-}NH_2\text{-}bdc)_3$ (X = OH, Cl)[191]
PCN-11	$Cu_2(sbtc)$[516]
PCN-13	$Zn_4O(H_2O)_3(9,10\text{-}adc)_3$[253]
PCN-16	$Cu_2(ebdc)$[517]
PCN-17	$Ln_4(H_2O)(tatb)_{8/3}(SO_4)_2$ (Ln = Yb, Y, Er, Dy)[254,255]
PIZA-1	CoT(*p*-CO_2)P$Co_{1.5}$[383]
POST-1	$Zn_3(\mu_3\text{-}O)(L\text{-}H)_6$ (L = (4*S*,5*S*)- or (4*R*,5*R*)-2,2-dimethyl-5-[(4-pyridinylamino)carbonyl]-1,3-dioxolane-4-carboxylic acid))[26]

dx.doi.org/10.1021/cr200190s |*Chem. Rev.* 2012, 112, 869–932

SIM-1	$Zn(mimc)_2$[475]
SNU-15′	$Co_4(H_2O)_4(mtb)_2$[210]
SNU-21	$Cu_2(tcom)$[181]
SNU-25	$Mg(tcpbda)$[209]
SNU-30	$[Zn_2(tcpbda)(H_2O)_2](guest)$[169]
SNU-31	$[Zn_2(tcpbda)(bpta)](guest)$[169]
SNU-50′	$Cu_2(bdcppi)$[221]
SNU-M10	$Ni_2(dpce)(bptc)$[145]
SNU-M11	$Ni_2(dpcb)(bptc)$[145]
STAM-1	$Cu(mcbdc)$[270]
UMCM-1	$Zn_4O(bdc)(btb)_{4/3}$[261]
UMCM-150	$Cu_3(bpt)_2$[408]
UoC-1′	$(H_3O)[Zn_7(OH)_3(bbs)_6]$[214]
ZIF-100	$Zn_{20}(cbim)_{39}(OH)$[143]
ZIF-11	$Zn(phim)_2$[14]
ZIF-20	$Zn(pur)_2$[202]
ZIF-22	$Zn(5\text{-azabenzimidazolate})_2$[202]
ZIF-68	$Zn(bim)(nim)$[144]
ZIF-69	$Zn(cbim)(nim)$[144]
ZIF-7	$Zn(bim)_2$[14]
ZIF-70	$Zn(im)_{1.13}(nim)_{0.87}$[144]
ZIF-78	$Zn(nbim)(nim)$[144]
ZIF-79	$Zn(mbim)(nim)$[144]
ZIF-8	$Zn(mim)_2$[14]
ZIF-81	$Zn(bbim)(nim)$[144]
ZIF-82	$Zn(cnIm)(nIm)$[144]
ZIF-90	$Zn(ica)_2$[471]
ZIF-95	$Zn(cbim)_2$[143]

REFERENCES

(1) Schuth, F.; Sing, K. S. W.; Weitkamp, J. *Handbook of Porous Solids*; Wiley-VCH: New York, 2002.
(2) Valtchev, V.; Mintova, S.; Tsapatsis, M. *Ordered Porous Solids: Recent Advances And Prospects*; Elsevier B.V.: Oxford, 2009.
(3) James, S. L. *Chem. Soc. Rev.* **2003**, *32*, 276.
(4) Rowsell, J. L. C.; Yaghi, O. M. *Microporous Mesoporous Mater.* **2004**, *73*, 3.
(5) Natarajan, S.; Mahata, P. *Chem. Soc. Rev.* **2009**, *38*, 2304.
(6) Long, J. R.; Yaghi, O. M. *Chem. Soc. Rev.* **2009**, *38*, 1213.
(7) Meek, S. T.; Greathouse, J. A.; Allendorf, M. D. *Adv. Mater.* **2011**, *23*, 249.
(8) Ferey, G. *Chem. Soc. Rev.* **2008**, *37*, 191.
(9) Papaefstathiou, G. S.; MacGillivray, L. R. *Coord. Chem. Rev.* **2003**, *246*, 169.
(10) Kitagawa, S.; Kitaura, R.; Noro, S. *Angew. Chem., Int. Ed.* **2004**, *43*, 2334.
(11) Ma, S. Q.; Zhou, H. C. *J. Am. Chem. Soc.* **2006**, *128*, 11734.
(12) Cychosz, K. A.; Wong-Foy, A. G.; Matzger, A. J. *J. Am. Chem. Soc.* **2008**, *130*, 6938.
(13) Liu, Y. L.; Kravtsov, V. C.; Larsen, R.; Eddaoudi, M. *Chem. Commun.* **2006**, 1488.
(14) Park, K. S.; Ni, Z.; Cote, A. P.; Choi, J. Y.; Huang, R. D.; Uribe-Romo, F. J.; Chae, H. K.; O'Keeffe, M.; Yaghi, O. M. *Proc. Natl. Acad. Sci. U.S.A.* **2006**, *103*, 10186.
(15) Mantion, A.; Massuger, L.; Rabu, P.; Palivan, C.; McCusker, L. B.; Taubert, A. *J. Am. Chem. Soc.* **2008**, *130*, 2517.
(16) Lin, J. B.; Zhang, J. P.; Chen, X. M. *J. Am. Chem. Soc.* **2010**, *132*, 6654.
(17) Fang, Q. R.; Makal, T. A.; Young, M. D.; Zhou, H. C. *Comments Inorg. Chem.* **2010**, *31*, 165.
(18) An, J.; Geib, S. J.; Rosi, N. L. *J. Am. Chem. Soc.* **2009**, *131*, 8376.
(19) Imaz, I.; Rubio-Martinez, M.; An, J.; Sole-Font, I.; Rosi, N. L.; Maspoch, D. *Chem. Commun.* **2011**, *47*, 7287.
(20) Ferey, G.; Mellot-Draznieks, C.; Serre, C.; Millange, F.; Dutour, J.; Surble, S.; Margiolaki, I. *Science* **2005**, *309*, 2040.
(21) Chui, S. S. Y.; Lo, S. M. F.; Charmant, J. P. H.; Orpen, A. G.; Williams, I. D. *Science* **1999**, *283*, 1148.
(22) Harbuzaru, B. V.; Corma, A.; Rey, F.; Atienzar, P.; Jorda, J. L.; Garcia, H.; Ananias, D.; Carlos, L. D.; Rocha, J. *Angew. Chem., Int. Ed.* **2008**, *47*, 1080.
(23) Park, H. J.; Suh, M. P. *Chem.-Eur. J.* **2008**, *14*, 8812.
(24) Qiu, S. L.; Zhu, G. S. *Coord. Chem. Rev.* **2009**, *253*, 2891.
(25) Humphrey, S. M.; Chang, J. S.; Jhung, S. H.; Yoon, J. W.; Wood, P. T. *Angew. Chem., Int. Ed.* **2007**, *46*, 272.
(26) Seo, J. S.; Whang, D.; Lee, H.; Jun, S. I.; Oh, J.; Jeon, Y. J.; Kim, K. *Nature* **2000**, *404*, 982.
(27) Ockwig, N. W.; Delgado-Friedrichs, O.; O'Keeffe, M.; Yaghi, O. M. *Acc. Chem. Res.* **2005**, *38*, 176.
(28) O'Keeffe, M.; Peskov, M. A.; Ramsden, S. J.; Yaghi, O. M. *Acc. Chem. Res.* **2008**, *41*, 1782.
(29) Batten, S. R.; Neville, S. M.; Turner, D. R. *Coordination Polymers: Design, Analysis and Application*; The Royal Society of Chemistry: Cambridge, 2009.
(30) Hoskins, B. F.; Robson, R. *J. Am. Chem. Soc.* **1990**, *112*, 1546.
(31) Li, H.; Eddaoudi, M.; O'Keeffe, M.; Yaghi, O. M. *Nature* **1999**, *402*, 276.
(32) Bradshaw, D.; Claridge, J. B.; Cussen, E. J.; Prior, T. J.; Rosseinsky, M. J. *Acc. Chem. Res.* **2005**, *38*, 273.
(33) Horike, S.; Shimomura, S.; Kitagawa, S. *Nat. Chem.* **2009**, *1*, 695.
(34) Furukawa, H.; Ko, N.; Go, Y. B.; Aratani, N.; Choi, S. B.; Choi, E.; Yazaydin, A. O.; Snurr, R. Q.; O'Keeffe, M.; Kim, J.; Yaghi, O. M. *Science* **2010**, *329*, 424.
(35) Czaja, A. U.; Trukhan, N.; Muller, U. *Chem. Soc. Rev.* **2009**, *38*, 1284.
(36) Xu, R.; Pang, W.; Yu, J.; Huo, Q.; Chen, J. *Chemistry of Zeolites and Related Porous Materials: Synthesis and Structure*; John Wiley and Sons, Inc.: Singapore, 2007.
(37) Bansal, R. C.; Goyal, M. *Activated Carbon Adsorption*; Taylor & Francis Group CRC Press: Boca Raton, FL, 2005.
(38) Ma, S. Q. *Pure Appl. Chem.* **2009**, *81*, 2235.
(39) Lin, X.; Champness, N.; Schröder, M. Hydrogen, Methane and Carbon Dioxide Adsorption in Metal−Organic Framework Materials. In *Functional Metal-Organic Frameworks: Gas Storage, Separation and Catalysis*; Schröder, M., Ed.; Springer: Berlin/Heidelberg, 2010. *Top. Curr. Chem.* **2010**, *293*, 35.
(40) Roques, N.; Mugnaini, V.; Veciana, J. Magnetic and Porous Molecule-Based Materials. In *Functional Metal-Organic Frameworks: Gas Storage, Separation and Catalysis*; Schröder, M., Ed.; Springer: Berlin/Heidelberg, 2010. *Top. Curr. Chem.* **2010**, *293*, 207.
(41) Huang, Y. G.; Jiang, F. L.; Hong, M. C. *Coord. Chem. Rev.* **2009**, *253*, 2814.
(42) Kurmoo, M. *Chem. Soc. Rev.* **2009**, *38*, 1353.
(43) Zeng, Y. F.; Hu, X.; Liu, F. C.; Bu, X. H. *Chem. Soc. Rev.* **2009**, *38*, 469.
(44) Allendorf, M. D.; Bauer, C. A.; Bhakta, R. K.; Houk, R. J. T. *Chem. Soc. Rev.* **2009**, *38*, 1330.
(45) Kitagawa, S.; Matsuda, R. *Coord. Chem. Rev.* **2007**, *251*, 2490.
(46) Kitaura, R.; Kitagawa, S.; Kubota, Y.; Kobayashi, T. C.; Kindo, K.; Mita, Y.; Matsuo, A.; Kobayashi, M.; Chang, H. C.; Ozawa, T. C.; Suzuki, M.; Sakata, M.; Takata, M. *Science* **2002**, *298*, 2358.
(47) Uemura, T.; Yanai, N.; Kitagawa, S. *Chem. Soc. Rev.* **2009**, *38*, 1228.
(48) Kawamichi, T.; Haneda, T.; Kawano, M.; Fujita, M. *Nature* **2009**, *461*, 633.
(49) Yaghi, O. M.; O'Keeffe, M.; Ockwig, N. W.; Chae, H. K.; Eddaoudi, M.; Kim, J. *Nature* **2003**, *423*, 705.
(50) Wang, Z. Q.; Cohen, S. M. *Chem. Soc. Rev.* **2009**, *38*, 1315.
(51) Tanabe, K. K.; Cohen, S. M. *Chem. Soc. Rev.* **2011**, *40*, 498.
(52) Song, Y. F.; Cronin, L. *Angew. Chem., Int. Ed.* **2008**, *47*, 4635.
(53) Uemura, K.; Matsuda, R.; Kitagawa, S. *J. Solid State Chem.* **2005**, *178*, 2420.
(54) Bureekaew, S.; Shimomura, S.; Kitagawa, S. *Sci. Technol. Adv. Mater.* **2008**, 9.
(55) Serre, C. *Actual. Chim.* **2008**, 15.

(56) Halder, G. J.; Kepert, C. J. *Aust. J. Chem.* **2006**, *59*, 597.
(57) Kuznicki, S. M.; Bell, V. A.; Nair, S.; Hillhouse, H. W.; Jacubinas, R. M.; Braunbarth, C. M.; Toby, B. H.; Tsapatsis, M. *Nature* **2001**, *412*, 720.
(58) Jansen, M.; Schon, J. C. *Angew. Chem., Int. Ed.* **2006**, *45*, 3406.
(59) Perry, J. J.; Perman, J. A.; Zaworotko, M. J. *Chem. Soc. Rev.* **2009**, *38*, 1400.
(60) Robson, R. *J. Chem. Soc., Dalton Trans.* **2000**, 3735.
(61) Ferey, G. *Dalton Trans.* **2009**, 4400.
(62) Li, C. P.; Du, M. *Chem. Commun.* **2011**, *47*, 5958.
(63) O'Keeffe, M. *Chem. Soc. Rev.* **2009**, *38*, 1215.
(64) Zhao, D.; Timmons, D. J.; Yuan, D.; Zhou, H.-C. *Acc. Chem. Res.* **2011**, *44*, 123.
(65) Klinowski, J.; Paz, F. A. A.; Silva, P.; Rocha, J. *Dalton Trans.* **2011**, *40*, 321.
(66) Parnham, E. R.; Morris, R. E. *Acc. Chem. Res.* **2007**, *40*, 1005.
(67) Garay, A. L.; Pichon, A.; James, S. L. *Chem. Soc. Rev.* **2007**, *36*, 846.
(68) Li, J. R.; Timmons, D. J.; Zhou, H. C. *J. Am. Chem. Soc.* **2009**, *131*, 6368.
(69) Zaworotko, M. J. *Nat. Chem.* **2009**, *1*, 267.
(70) Carne, A.; Carbonell, C.; Imaz, I.; Maspoch, D. *Chem. Soc. Rev.* **2011**, *40*, 291.
(71) Della Rocca, J.; Liu, D.; Lin, W. *Acc. Chem. Res.* **2011**, DOI: 10.1021/ar200028a.
(72) Banerjee, R.; Phan, A.; Wang, B.; Knobler, C.; Furukawa, H.; O'Keeffe, M.; Yaghi, O. M. *Science* **2008**, *319*, 939.
(73) Sumida, K.; Horike, S.; Kaye, S. S.; Herm, Z. R.; Queen, W. L.; Brown, C. M.; Grandjean, F.; Long, G. J.; Dailly, A.; Long, J. R. *Chem. Sci.* **2010**, *1*, 184.
(74) Wollmann, P.; Leistner, M.; Stoeck, U.; Grunker, R.; Gedrich, K.; Klein, N.; Throl, O.; Grahlert, W.; Senkovska, I.; Dreisbach, F.; Kaskel, S. *Chem. Commun.* **2011**, *47*, 5151.
(75) Farha, O. K.; Hupp, J. T. *Acc. Chem. Res.* **2010**, *43*, 1166.
(76) Kuppler, R. J.; Timmons, D. J.; Fang, Q. R.; Li, J. R.; Makal, T. A.; Young, M. D.; Yuan, D. Q.; Zhao, D.; Zhuang, W. J.; Zhou, H. C. *Coord. Chem. Rev.* **2009**, *253*, 3042.
(77) Zou, R.; Abdel-Fattah, A. I.; Xu, H.; Zhao, Y.; Hickmott, D. D. *CrystEngComm* **2010**, *12*, 1337.
(78) Ma, S. Q.; Zhou, H. C. *Chem. Commun.* **2010**, *46*, 44.
(79) Wang, Z.; Chen, G.; Ding, K. L. *Chem. Rev.* **2009**, *109*, 322.
(80) Isaeva, V. I.; Kustov, L. M. *Pet. Chem.* **2010**, *50*, 167.
(81) Kim, K.; Banerjee, M.; Yoon, M.; Das, S. Chiral metal−organic porous materials: Synthetic strategies and applications in chiral separation and catalysis. In *Functional Metal−Organic Frameworks: Gas Storage, Separation and Catalysis*; Schröder, M., Ed.; Springer: Berlin/Heidelberg, 2010. *Top. Curr. Chem.* **2010**, *293*, 115.
(82) Ma, L. Q.; Abney, C.; Lin, W. B. *Chem. Soc. Rev.* **2009**, *38*, 1248.
(83) Corma, A.; Garcia, H.; Xamena, F. X. L. *Chem. Rev.* **2010**, *110*, 4606.
(84) Farrusseng, D.; Aguado, S.; Pinel, C. *Angew. Chem., Int. Ed.* **2009**, *48*, 7502.
(85) Liu, Y.; Xuan, W. M.; Cui, Y. *Adv. Mater.* **2010**, *22*, 4112.
(86) Zhao, D.; Yuan, D. Q.; Zhou, H. C. *Energy Environ. Sci.* **2008**, *1*, 222.
(87) Hu, Y. H.; Zhang, L. *Adv. Mater.* **2010**, *22*, E117.
(88) Murray, L. J.; Dinca, M.; Long, J. R. *Chem. Soc. Rev.* **2009**, *38*, 1294.
(89) Dinca, M.; Long, J. R. *Angew. Chem., Int. Ed.* **2008**, *47*, 6766.
(90) Hedin, N.; Chen, L. J.; Laaksonen, A. *Nanoscale* **2010**, *2*, 1819.
(91) Choi, S.; Drese, J. H.; Jones, C. W. *ChemSusChem* **2009**, *2*, 796.
(92) Ferey, G.; Serre, C.; Devic, T.; Maurin, G.; Jobic, H.; Llewellyn, P. L.; De Weireld, G.; Vimont, A.; Daturi, M.; Chang, J.-S. *Chem. Soc. Rev.* **2011**, *40*, 550.
(93) D'Alessandro, D. M.; Smit, B.; Long, J. R. *Angew. Chem., Int. Ed.* **2010**, *49*, 6058.
(94) Li, J. R.; Ma, Y.; McCarthy, M. C.; Sculley, J.; Yu, J.; Jeong, H. K.; Balbuena, P. B.; Zhou, H. C. *Coord. Chem. Rev.* **2011**, *255*, 1791.
(95) Horcajada, P.; Serre, C.; Vallet-Regi, M.; Sebban, M.; Taulelle, F.; Ferey, G. *Angew. Chem., Int. Ed.* **2006**, *45*, 5974.
(96) Huxford, R. C.; Della Rocca, J.; Lin, W. B. *Curr. Opin. Chem. Biol.* **2010**, *14*, 262.
(97) Horcajada, P.; Serre, C.; Ferey, G.; Couvreur, P.; Gref, R. *M. S. Med. Sci.* **2010**, *26*, 761.
(98) Chen, B. L.; Xiang, S. C.; Qian, G. D. *Acc. Chem. Res.* **2010**, *43*, 1115.
(99) Li, J. R.; Kuppler, R. J.; Zhou, H. C. *Chem. Soc. Rev.* **2009**, *38*, 1477.
(100) Custelcean, R.; Moyer, B. A. *Eur. J. Inorg. Chem.* **2007**, 1321.
(101) Liu, D. H.; Zhong, C. L. *J. Mater. Chem.* **2010**, *20*, 10308.
(102) Cychosz, K. A.; Ahmad, R.; Matzger, A. J. *Chem. Sci.* **2010**, *1*, 293.
(103) Phan, A.; Doonan, C. J.; Uribe-Romo, F. J.; Knobler, C. B.; O'Keeffe, M.; Yaghi, O. M. *Acc. Chem. Res.* **2010**, *43*, 58.
(104) Keskin, S.; van Heest, T. M.; Sholl, D. S. *ChemSusChem* **2010**, *3*, 879.
(105) Kulprathipanja, S. *Zeolites in Industrial Separation and Catalysis*; Wiley-VCH Verlag GmbH & Co.: KGaA, Weinheim, 2010.
(106) Loureiro, J. M.; Kartel, M. T. *Combined and Hybrid Adsorbents: Fundamentals and Applications*; Springer: Netherlands, 2006.
(107) Yang, R. T. *Adsorbents: Fundamentals and Applications*; Wiley & Sons: Hoboken, NJ, 2003.
(108) Keller, J. U.; Staudt, R. *Gas Adsorption Equilibria, Experimental Methods and Adsorptive Isotherms*; Springer Science + Business Media, Inc.: Boston, 2005.
(109) Ruthven, D. M. *Principles of Adsorption and Adsorption Processes*; John Wiley & Sons: New York, 1984.
(110) Seader, J.; Henley, M. *Separation Process Principles*; Wiley: New York, 1998.
(111) Kerry, F. G. *Industrial Gas Handbook: Gas Separation and Purification*; CRC Press: Boca Raton, FL, 2007.
(112) Ockwig, N. W.; Nenoff, T. M. *Chem. Rev.* **2007**, *107*, 4078.
(113) Strathmann, H. *Membranes and Membrane Separation Processes*; Wiley-VCH Verlag GmbH & Co. KGaA: New York, 2000.
(114) Yampolskii, Y.; Pinnau, I.; Freeman, B. D. *Materials Science of Membranes for Gas and Vapor Separation*; John Wiley & Sons Ltd.: New York, 2006.
(115) Snurr, R. Q.; Hupp, J. T.; Nguyen, S. T. *AIChE J.* **2004**, *50*, 1090.
(116) Duren, T.; Bae, Y. S.; Snurr, R. Q. *Chem. Soc. Rev.* **2009**, *38*, 1237.
(117) Xiang, Z. H.; Cao, D. P.; Lan, J. H.; Wang, W. C.; Broom, D. P. *Energy Environ. Sci.* **2010**, *3*, 1469.
(118) Krishna, R.; van Baten, J. M. *Phys. Chem. Chem. Phys.* **2011**, *13*, 10593.
(119) Jiang, J. W.; Babarao, R.; Hu, Z. Q. *Chem. Soc. Rev.* **2011**, *40*, 3599.
(120) Taylor, T. J.; Bakhmutov, V. I.; Gabbaï, F. P. *Angew. Chem., Int. Ed.* **2006**, *45*, 7030.
(121) Otsubo, K.; Wakabayashi, Y.; Ohara, J.; Yamamoto, S.; Matsuzaki, H.; Okamoto, H.; Nitta, K.; Uruga, T.; Kitagawa, H. *Nat. Mater.* **2011**, *10*, 291.
(122) An, J. Y.; Fiorella, R. P.; Geib, S. J.; Rosi, N. L. *J. Am. Chem. Soc.* **2009**, *131*, 8401.
(123) Li, J. R.; Zhou, H. C. *Nat. Chem.* **2010**, *2*, 893.
(124) Sircar, S. *Ind. Eng. Chem. Res.* **2006**, *45*, 5435.
(125) Tagliabue, M.; Farrusseng, D.; Valencia, S.; Aguado, S.; Ravon, U.; Rizzo, C.; Corma, A.; Mirodatos, C. *Chem. Eng. J. (Lausanne)* **2009**, *155*, 553.
(126) Wang, Q. M.; Shen, D. M.; Bulow, M.; Lau, M. L.; Deng, S. G.; Fitch, F. R.; Lemcoff, N. O.; Semanscin, J. *Microporous Mesoporous Mater.* **2002**, *55*, 217.
(127) Yang, Q. Y.; Xue, C. Y.; Zhong, C. L.; Chen, J. F. *AIChE J.* **2007**, *53*, 2832.
(128) Liang, Z. J.; Marshall, M.; Chaffee, A. L. *Energy Fuels* **2009**, *23*, 2785.
(129) Liang, Z. J.; Marshall, M.; Chaffee, A. L. In *Greenhouse Gas Control Technologies 9*; Gale, J., Herzog, H., Braitsch, J., Eds.; Elsevier: Amsterdam, The Netherlands, 2009; Vol. 1.
(130) Xue, C. Y.; Yang, Q. Y.; Zhong, C. L. *Mol. Simul.* **2009**, *35*, 1249.

(131) Yazaydin, A. O.; Benin, A. I.; Faheem, S. A.; Jakubczak, P.; Low, J. J.; Willis, R. R.; Snurr, R. Q. *Chem. Mater.* **2009**, *21*, 1425.
(132) Kitaura, R.; Seki, K.; Akiyama, G.; Kitagawa, S. *Angew. Chem., Int. Ed.* **2003**, *42*, 428.
(133) Surble, S.; Millange, F.; Serre, C.; Duren, T.; Latroche, M.; Bourrelly, S.; Llewellyn, P. L.; Ferey, G. *J. Am. Chem. Soc.* **2006**, *128*, 14889.
(134) Chen, B.; Ma, S.; Zapata, F.; Fronczek, F. R.; Lobkovsky, E. B.; Zhou, H.-C. *Inorg. Chem.* **2007**, *46*, 1233.
(135) Yoon, J. W.; Jhung, S. H.; Hwang, Y. K.; Humphrey, S. M.; Wood, P. T.; Chang, J. S. *Adv. Mater.* **2007**, *19*, 1830.
(136) Zou, Y.; Hong, S.; Park, M.; Chun, H.; Lah, M. S. *Chem. Commun.* **2007**, 5182.
(137) Bastin, L.; Barcia, P. S.; Hurtado, E. J.; Silva, J. A. C.; Rodrigues, A. E.; Chen, B. *J. Phys. Chem. C* **2008**, *112*, 1575.
(138) Cheon, Y. E.; Suh, M. P. *Chem.-Eur. J.* **2008**, *14*, 3961.
(139) Comotti, A.; Bracco, S.; Sozzani, P.; Horike, S.; Matsuda, R.; Chen, J.; Takata, M.; Kubota, Y.; Kitagawa, S. *J. Am. Chem. Soc.* **2008**, *130*, 13664.
(140) Li, C. J.; Lin, Z. J.; Peng, M. X.; Leng, J. D.; Yang, M. M.; Tong, M. L. *Chem. Commun.* **2008**, 6348.
(141) Li, J. R.; Tao, Y.; Yu, Q.; Bu, X. H.; Sakamoto, H.; Kitagawa, S. *Chem.-Eur. J.* **2008**, *14*, 2771.
(142) Thallapally, P. K.; Tian, J.; Kishan, M. R.; Fernandez, C. A.; Dalgarno, S. J.; McGrail, P. B.; Warren, J. E.; Atwood, J. L. *J. Am. Chem. Soc.* **2008**, *130*, 16842.
(143) Wang, B.; Cote, A. P.; Furukawa, H.; O'Keeffe, M.; Yaghi, O. M. *Nature* **2008**, *453*, 207.
(144) Banerjee, R.; Furukawa, H.; Britt, D.; Knobler, C.; O'Keeffe, M.; Yaghi, O. M. *J. Am. Chem. Soc.* **2009**, *131*, 3875.
(145) Choi, H. S.; Suh, M. P. *Angew. Chem., Int. Ed.* **2009**, *48*, 6865.
(146) Chun, H.; Seo, J. *Inorg. Chem.* **2009**, *48*, 9980.
(147) Demessence, A.; D'Alessandro, D. M.; Foo, M. L.; Long, J. R. *J. Am. Chem. Soc.* **2009**, *131*, 8784.
(148) Dietzel, P. D. C.; Besikiotis, V.; Blom, R. *J. Mater. Chem.* **2009**, *19*, 7362.
(149) Gurunatha, K. L.; Maji, T. K. *Inorg. Chem.* **2009**, *48*, 10886.
(150) Lee, J. Y.; Roberts, J. M.; Farha, O. K.; Sarjeant, A. A.; Scheidt, K. A.; Hupp, J. T. *Inorg. Chem.* **2009**, *48*, 9971.
(151) Bae, Y. S.; Farha, O. K.; Hupp, J. T.; Snurr, R. Q. *J. Mater. Chem.* **2009**, *19*, 2131.
(152) Farha, O. K.; Mulfort, K. L.; Hupp, J. T. *Inorg. Chem.* **2008**, *47*, 10223.
(153) Seo, J.; Matsuda, R.; Sakamoto, H.; Bonneau, C.; Kitagawa, S. *J. Am. Chem. Soc.* **2009**, *131*, 12792.
(154) Zhang, J. P.; Ghosh, S. K.; Lin, J. B.; Kitagawa, S. *Inorg. Chem.* **2009**, *48*, 7970.
(155) Zhu, A. X.; Lin, J. B.; Zhang, J. P.; Chen, X. M. *Inorg. Chem.* **2009**, *48*, 3882.
(156) An, J.; Geib, S. J.; Rosi, N. L. *J. Am. Chem. Soc.* **2010**, *132*, 38.
(157) Chen, Y. F.; Jiang, J. W. *ChemSusChem* **2010**, *3*, 982.
(158) Bae, Y. S.; Spokoyny, A. M.; Farha, O. K.; Snurr, R. Q.; Hupp, J. T.; Mirkin, C. A. *Chem. Commun.* **2010**, *46*, 3478.
(159) Barea, E.; Tagliabue, G.; Wang, W. G.; Perez-Mendoza, M.; Mendez-Linan, L.; Lopez-Garzon, F. J.; Galli, S.; Masciocchi, N.; Navarro, J. A. R. *Chem.-Eur. J.* **2010**, *16*, 931.
(160) Bloch, E. D.; Britt, D.; Lee, C.; Doonan, C. J.; Uribe-Romo, F. J.; Furukawa, H.; Long, J. R.; Yaghi, O. M. *J. Am. Chem. Soc.* **2010**, *132*, 14382.
(161) Fernandez, C. A.; Thallapally, P. K.; Motkuri, R. K.; Nune, S. K.; Sumrak, J. C.; Tian, J.; Liu, J. *Cryst. Growth Des.* **2010**, *10*, 1037.
(162) Grunker, R.; Senkovska, I.; Biedermann, R.; Klein, N.; Klausch, A.; Baburin, I. A.; Mueller, U.; Kaskel, S. *Eur. J. Inorg. Chem.* **2010**, 3835.
(163) Gu, J. M.; Kwon, T. H.; Park, J. H.; Huh, S. *Dalton Trans.* **2010**, *39*, 5608.
(164) Kishan, M. R.; Tian, J.; Thallapally, P. K.; Fernandez, C. A.; Dalgarno, S. J.; Warren, J. E.; McGrail, B. P.; Atwood, J. L. *Chem. Commun.* **2010**, *46*, 538.
(165) Mallick, A.; Saha, S.; Pachfule, P.; Roy, S.; Banerjee, R. *J. Mater. Chem.* **2010**, *20*, 9073.
(166) Matsuda, R.; Tsujino, T.; Sato, H.; Kubota, Y.; Morishige, K.; Takata, M.; Kitagawa, S. *Chem. Sci.* **2010**, *1*, 315.
(167) Nakagawa, K.; Tanaka, D.; Horike, S.; Shimomura, S.; Higuchi, M.; Kitagawa, S. *Chem. Commun.* **2010**, *46*, 4258.
(168) Nune, S. K.; Thallapally, P. K.; Dohnalkova, A.; Wang, C. M.; Liu, J.; Exarhos, G. J. *Chem. Commun.* **2010**, *46*, 4878.
(169) Park, H. J.; Cheon, Y. E.; Suh, M. P. *Chem.-Eur. J.* **2010**, *16*, 11662.
(170) Procopio, E. Q.; Linares, F.; Montoro, C.; Colombo, V.; Maspero, A.; Barea, E.; Navarro, J. A. R. *Angew. Chem., Int. Ed.* **2010**, *49*, 7308.
(171) Xue, M.; Zhang, Z. J.; Xiang, S. C.; Jin, Z.; Liang, C. D.; Zhu, G. S.; Qiu, S. L.; Chen, B. L. *J. Mater. Chem.* **2010**, *20*, 3984.
(172) Zhang, Y. J.; Liu, T.; Kanegawa, S.; Sato, O. *J. Am. Chem. Soc.* **2010**, *132*, 912.
(173) Zhong, D. C.; Zhang, W. X.; Cao, F. L.; Jiang, L.; Lu, T. B. *Chem. Commun.* **2011**, *47*, 1204.
(174) Henke, S.; Fischer, R. A. *J. Am. Chem. Soc.* **2011**, *133*, 2064.
(175) Chen, M.-S.; Chen, M.; Takamizawa, S.; Okamura, T.-a.; Fan, J.; Sun, W.-Y. *Chem. Commun.* **2011**, *47*, 3787.
(176) Vaidhyanathan, R.; Iremonger, S. S.; Shimizu, G. K. H.; Boyd, P. G.; Alavi, S.; Woo, T. K. *Science* **2010**, *330*, 650.
(177) Dybtsev, D. N.; Chun, H.; Yoon, S. H.; Kim, D.; Kim, K. *J. Am. Chem. Soc.* **2004**, *126*, 32.
(178) Pan, L.; Adams, K. M.; Hernandez, H. E.; Wang, X. T.; Zheng, C.; Hattori, Y.; Kaneko, K. *J. Am. Chem. Soc.* **2003**, *125*, 3062.
(179) Navarro, J. A. R.; Barea, E.; Rodriguez-Dieguez, A.; Salas, J. M.; Ania, C. O.; Parra, J. B.; Masciocchi, N.; Galli, S.; Sironi, A. *J. Am. Chem. Soc.* **2008**, *130*, 3978.
(180) Henke, S.; Schmid, R.; Grunwaldt, J.-D.; Fischer, R. A. *Chem.-Eur. J.* **2010**, *16*, 14296.
(181) Kim, T. K.; Suh, M. P. *Chem. Commun.* **2011**, *47*, 4258.
(182) Yang, R.; Li, L.; Xiong, Y.; Li, J. R.; Zhou, H. C.; Su, C. Y. *Chem.-Asian J.* **2010**, *5*, 2358.
(183) Meng, X. R.; Zhong, D. C.; Jiang, L.; Li, H. Y.; Lu, T. B. *Cryst. Growth Des.* **2011**, *11*, 2020.
(184) Zhong, D. C.; Lu, W. G.; Jiang, L.; Feng, X. L.; Lu, T. B. *Cryst. Growth Des.* **2010**, *10*, 739.
(185) Chen, S. S.; Chen, M.; Takamizawa, S.; Wang, P.; Lv, G. C.; Sun, W.-Y. *Chem. Commun.* **2011**, *47*, 4902.
(186) Hou, L.; Shi, W.-J.; Wang, Y.-Y.; Guo, Y.; Jin, C.; Shi, Q.-Z. *Chem. Commun.* **2011**, *47*, 5464.
(187) Kanoo, P.; Mostafa, G.; Matsuda, R.; Kitagawa, S.; Kumar Maji, T. *Chem. Commun.* **2011**, *47*, 8106.
(188) Ortiz, G.; Brandès, S.; Rousselin, Y.; Guilard, R. *Chem.-Eur. J.* **2011**, *17*, 6689.
(189) Zhao, Y.; Wu, H.; Emge, T. J.; Gong, Q.; Nijem, N.; Chabal, Y. J.; Kong, L.; Langreth, D. C.; Liu, H.; Zeng, H.; Li, J. *Chem.-Eur. J.* **2011**, *17*, 5101.
(190) Si, X.; Jiao, C.; Li, F.; Zhang, J.; Wang, S.; Liu, S.; Li, Z.; Sun, L.; Xu, F.; Gabelica, Z.; Schick, C. *Energy Environ. Sci.* **2011**, DOI: 10.1039/C1EE01380G.
(191) Serra-Crespo, P.; Ramos-Fernandez, E. V.; Gascon, J.; Kapteijn, F. *Chem. Mater.* **2011**, *23*, 2565.
(192) Yang, Q. Y.; Zhong, C. L. *ChemPhysChem* **2006**, *7*, 1417.
(193) Yang, Q. Y.; Zhong, C. L. *J. Phys. Chem. B* **2006**, *110*, 17776.
(194) Cavenati, S.; Grande, C. A.; Rodrigues, A. E. *Ind. Eng. Chem. Res.* **2008**, *47*, 6333.
(195) Hamon, L.; Jolimaitre, E.; Pirngruber, G. D. *Ind. Eng. Chem. Res.* **2010**, *49*, 7497.
(196) Bourrelly, S.; Llewellyn, P. L.; Serre, C.; Millange, F.; Loiseau, T.; Ferey, G. *J. Am. Chem. Soc.* **2005**, *127*, 13519.
(197) Llewellyn, P. L.; Bourrelly, S.; Serre, C.; Filinchuk, Y.; Ferey, G. *Angew. Chem., Int. Ed.* **2006**, *45*, 7751.
(198) Finsy, V.; Ma, L.; Alaerts, L.; De Vos, D. E.; Baron, G. V.; Denayer, J. F. M. *Microporous Mesoporous Mater.* **2009**, *120*, 221.

(199) Hamon, L.; Llewellyn, P. L.; Devic, T.; Ghoufi, A.; Clet, G.; Guillerm, V.; Pirngruber, G. D.; Maurin, G.; Serre, C.; Driver, G.; van Beek, W.; Jolimaitre, E.; Vimont, A.; Daturi, M.; Ferey, G. *J. Am. Chem. Soc.* **2009**, *131*, 17490.
(200) Loiseau, T.; Lecroq, L.; Volkringer, C.; Marrot, J.; Férey, G.; Haouas, M.; Taulelle, F.; Bourrelly, S.; Llewellyn, P. L.; Latroche, M. *J. Am. Chem. Soc.* **2006**, *128*, 10223.
(201) Chen, B. L.; Ma, S. Q.; Hurtado, E. J.; Lobkovsky, E. B.; Zhou, H. C. *Inorg. Chem.* **2007**, *46*, 8490.
(202) Hayashi, H.; Cote, A. P.; Furukawa, H.; O'Keeffe, M.; Yaghi, O. M. *Nat. Mater.* **2007**, *6*, 501.
(203) Ma, S. Q.; Wang, X. S.; Manis, E. S.; Collier, C. D.; Zhou, H. C. *Inorg. Chem.* **2007**, *46*, 3432.
(204) Bae, Y. S.; Farha, O. K.; Spokoyny, A. M.; Mirkin, C. A.; Hupp, J. T.; Snurr, R. Q. *Chem. Commun.* **2008**, 4135.
(205) Bae, Y. S.; Mulfort, K. L.; Frost, H.; Ryan, P.; Punnathanam, S.; Broadbelt, L. J.; Hupp, J. T.; Snurr, R. Q. *Langmuir* **2008**, *24*, 8592.
(206) Xue, M.; Ma, S. Q.; Jin, Z.; Schaffino, R. M.; Zhu, G. S.; Lobkovsky, E. B.; Qiu, S. L.; Chen, B. L. *Inorg. Chem.* **2008**, *47*, 6825.
(207) Britt, D.; Furukawa, H.; Wang, B.; Glover, T. G.; Yaghi, O. M. *Proc. Natl. Acad. Sci. U.S.A.* **2009**, *106*, 20637.
(208) Bao, Z.; Yu, L.; Ren, Q.; Lu, X.; Deng, S. *J. Colloid Interface Sci.* **2011**, *353*, 549.
(209) Cheon, Y. E.; Park, J.; Suh, M. P. *Chem. Commun.* **2009**, 5436.
(210) Cheon, Y. E.; Suh, M. P. *Chem. Commun.* **2009**, 2296.
(211) Couck, S.; Denayer, J. F. M.; Baron, G. V.; Remy, T.; Gascon, J.; Kapteijn, F. *J. Am. Chem. Soc.* **2009**, *131*, 6326.
(212) Kanoh, H.; Kondo, A.; Noguchi, H.; Kajiro, H.; Tohdoh, A.; Hattori, Y.; Xu, W. C.; Moue, M.; Sugiura, T.; Morita, K.; Tanaka, H.; Ohba, T.; Kaneko, K. *J. Colloid Interface Sci.* **2009**, *334*, 1.
(213) Mu, B.; Li, F.; Walton, K. S. *Chem. Commun.* **2009**, 2493.
(214) Neofotistou, E.; Malliakas, C. D.; Trikalitis, P. N. *Chem.-Eur. J.* **2009**, *15*, 4523.
(215) Chen, Y. F.; Lee, J. Y.; Babarao, R.; Li, J.; Jiang, J. W. *J. Phys. Chem. C* **2010**, *114*, 6602.
(216) Chen, Z. X.; Xiang, S. C.; Arman, H. D.; Li, P.; Tidrow, S.; Zhao, D. Y.; Chen, B. L. *Eur. J. Inorg. Chem.* **2010**, 3745.
(217) Fukushima, T.; Horike, S.; Inubushi, Y.; Nakagawa, K.; Kubota, Y.; Takata, M.; Kitagawa, S. *Angew. Chem., Int. Ed.* **2010**, *49*, 4820.
(218) Gu, X. J.; Lu, Z. H.; Xu, Q. *Chem. Commun.* **2010**, *46*, 7400.
(219) Kanoo, P.; Gurunatha, K. L.; Maji, T. K. *J. Mater. Chem.* **2010**, *20*, 1322.
(220) Park, H. J.; Suh, M. P. *Chem. Commun.* **2010**, *46*, 610.
(221) Prasad, T. K.; Hong, D. H.; Suh, M. P. *Chem.-Eur. J.* **2010**, *16*, 14043.
(222) Zhang, S.-M.; Chang, Z.; Hu, T.-L.; Bu, X.-H. *Inorg. Chem.* **2010**, *49*, 11581.
(223) Zhang, Z. J.; Xiang, S. C.; Chen, Y. S.; Ma, S. Q.; Lee, Y.; Phely-Bobin, T.; Chen, B. L. *Inorg. Chem.* **2010**, *49*, 8444.
(224) Zhang, Z. J.; Xiang, S. C.; Rao, X. T.; Zheng, Q. A.; Fronczek, F. R.; Qian, G. D.; Chen, B. L. *Chem. Commun.* **2010**, *46*, 7205.
(225) Miller, S. R.; Pearce, G. M.; Wright, P. A.; Bonino, F.; Chavan, S.; Bordiga, S.; Margiolaki, I.; Guillou, N.; Feerey, G.; Bourrelly, S.; Llewellyn, P. L. *J. Am. Chem. Soc.* **2008**, *130*, 15967.
(226) Chen, Z.; Xiang, S.; Arman, H. D.; Mondal, J. U.; Li, P.; Zhao, D.; Chen, B. *Inorg. Chem.* **2011**, *50*, 3442.
(227) Chen, Z.; Xiang, S.; Arman, H. D.; Li, P.; Zhao, D.; Chen, B. *Eur. J. Inorg. Chem.* **2011**, 2227.
(228) Herm, Z. R.; Swisher, J. A.; Smit, B.; Krishna, R.; Long, J. R. *J. Am. Chem. Soc.* **2011**, *133*, 5664.
(229) Hou, X. J.; Li, H. Q. *J. Phys. Chem. C* **2010**, *114*, 13501.
(230) Wang, S. Y.; Yang, Q. Y.; Zhong, C. L. *Sep. Purif. Technol.* **2008**, *60*, 30.
(231) Deng, H. X.; Doonan, C. J.; Furukawa, H.; Ferreira, R. B.; Towne, J.; Knobler, C. B.; Wang, B.; Yaghi, O. M. *Science* **2010**, *327*, 846.
(232) Arstad, B.; Fjellvåg, H.; Kongshaug, K.; Swang, O.; Blom, R. *Adsorption* **2008**, *14*, 755.
(233) Babarao, R.; Jiang, J. W. *J. Am. Chem. Soc.* **2009**, *131*, 11417.
(234) Serre, C.; Millange, F.; Thouvenot, C.; Nogues, M.; Marsolier, G.; Louer, D.; Ferey, G. *J. Am. Chem. Soc.* **2002**, *124*, 13519.
(235) Loiseau, T.; Serre, C.; Huguenard, C.; Fink, G.; Taulelle, F.; Henry, M.; Bataille, T.; Ferey, G. *Chem.-Eur. J.* **2004**, *10*, 1373.
(236) Neimark, A. V.; Coudert, F. o.-X.; Triguero, C.; Boutin, A.; Fuchs, A. H.; Beurroies, I.; Denoyel, R. *Langmuir* **2011**, *27*, 4734.
(237) Maji, T. K.; Mostafa, G.; Matsuda, R.; Kitagawa, S. *J. Am. Chem. Soc.* **2005**, *127*, 17152.
(238) Deng, H. X.; Olson, M. A.; Stoddart, J. F.; Yaghi, O. M. *Nat. Chem.* **2010**, *2*, 439.
(239) Fletcher, A. J.; Cussen, E. J.; Prior, T. J.; Rosseinsky, M. J.; Kepert, C. J.; Thomas, K. M. *J. Am. Chem. Soc.* **2001**, *123*, 10001.
(240) Salles, F.; Jobic, H.; Ghoufi, A.; Llewellyn, P. L.; Serre, C.; Bourrelly, S.; Ferey, G.; Maurin, G. *Angew. Chem., Int. Ed.* **2009**, *48*, 8335.
(241) Salles, F.; Jobic, H.; Devic, T.; Llewellyn, P. L.; Serre, C.; Ferey, G.; Maurin, G. *ACS Nano* **2010**, *4*, 143.
(242) Garcia-Ricard, O. J.; Hernandez-Maldonado, A. J. *J. Phys. Chem. C* **2010**, *114*, 1827.
(243) Zhao, Z. X.; Li, Z.; Lin, Y. S. *Ind. Eng. Chem. Res.* **2009**, *48*, 10015.
(244) Saha, D.; Bao, Z. B.; Jia, F.; Deng, S. G. *Environ. Sci. Technol.* **2010**, *44*, 1820.
(245) Kizzie, A. C.; Wong-Foy, A. G.; Matzger, A. J. *Langmuir* **2011**, *27*, 6368.
(246) Yazaydin, A. O.; Snurr, R. Q.; Park, T. H.; Koh, K.; Liu, J.; LeVan, M. D.; Benin, A. I.; Jakubczak, P.; Lanuza, M.; Galloway, D. B.; Low, J. J.; Willis, R. R. *J. Am. Chem. Soc.* **2009**, *131*, 18198.
(247) Keskin, S. *J. Phys. Chem. C* **2011**, *115*, 800.
(248) Coombe, H. S.; Nieh, S. *Energy Convers. Manage.* **2007**, *48*, 1499.
(249) Robeson, L. M. *Curr. Opin. Solid State Mater. Sci.* **1999**, *4*, 549.
(250) Sircar, S.; Myers, A. *Handbook of Zeolite Science and Technology*; CRC Press: Boca Raton, FL, 2003.
(251) Hashim, S. M.; Mohamed, A. R.; Bhatia, S. *Adv. Colloid Interface Sci.* **2010**, *160*, 88.
(252) Dinca, M.; Long, J. R. *J. Am. Chem. Soc.* **2005**, *127*, 9376.
(253) Ma, S. Q.; Wang, X. S.; Collier, C. D.; Manis, E. S.; Zhou, H. C. *Inorg. Chem.* **2007**, *46*, 8499.
(254) Ma, S. Q.; Wang, X. S.; Yuan, D. Q.; Zhou, H. C. *Angew. Chem., Int. Ed.* **2008**, *47*, 4130.
(255) Ma, S. Q.; Yuan, D. Q.; Wang, X. S.; Zhou, H. C. *Inorg. Chem.* **2009**, *48*, 2072.
(256) Dinca, M.; Yu, A. F.; Long, J. R. *J. Am. Chem. Soc.* **2006**, *128*, 8904.
(257) Kim, H.; Samsonenko, D. G.; Yoon, M.; Yoon, J. W.; Hwang, Y. K.; Chang, J. S.; Kim, K. *Chem. Commun.* **2008**, 4697.
(258) Shimomura, S.; Higuchi, M.; Matsuda, R.; Yoneda, K.; Hijikata, Y.; Kubota, Y.; Mita, Y.; Kim, J.; Takata, M.; Kitagawa, S. *Nat. Chem.* **2010**, *2*, 633.
(259) Demessence, A.; Long, J. R. *Chem.-Eur. J.* **2010**, *16*, 5902.
(260) Li, Y.; Yang, R. T. *Langmuir* **2007**, *23*, 12937.
(261) Koh, K.; Wong-Foy, A. G.; Matzger, A. J. *Angew. Chem., Int. Ed.* **2008**, *47*, 677.
(262) Mu, B.; Schoenecker, P. M.; Walton, K. S. *J. Phys. Chem. C* **2010**, *114*, 6464.
(263) Rege, S. U.; Yang, R. T. *Ind. Eng. Chem. Res.* **1997**, *36*, 5358.
(264) Murray, L. J.; Dinca, M.; Yano, J.; Chavan, S.; Bordiga, S.; Brown, C. M.; Long, J. R. *J. Am. Chem. Soc.* **2010**, *132*, 7856.
(265) Southon, P. D.; Price, D. J.; Nielsen, P. K.; McKenzie, C. J.; Kepert, C. J. *J. Am. Chem. Soc.* **2011**, *133*, 10885.
(266) Shimomura, S.; Matsuda, R.; Kitagawa, S. *Chem. Mater.* **2010**, *22*, 4129.
(267) Tanaka, D.; Nakagawa, K.; Higuchi, M.; Horike, S.; Kubota, Y.; Kobayashi, L. C.; Takata, M.; Kitagawa, S. *Angew. Chem., Int. Ed.* **2008**, *47*, 3914.
(268) Ma, S.; Sun, D.; Wang, X. S.; Zhou, H. C. *Angew. Chem., Int. Ed.* **2007**, *46*, 2458.
(269) Ma, S. Q.; Sun, D. F.; Yuan, D. Q.; Wang, X. S.; Zhou, H. C. *J. Am. Chem. Soc.* **2009**, *131*, 6445.

(270) Mohideen, M. I. H.; Xiao, B.; Wheatley, P. S.; McKinlay, A. C.; Li, Y.; Slawin, A. M. Z.; Aldous, D. W.; Cessford, N. F.; Düren, T.; Zhao, X.; Gill, R.; Thomas, K. M.; Griffin, J. M.; Ashbrook, S. E.; Morris, R. E. *Nat. Chem.* **2011**, *3*, 304.
(271) Reid, C. R.; O'koye, I. P.; Thomas, K. M. *Langmuir* **1998**, *14*, 2415.
(272) Rowsell, J. L. C.; Yaghi, O. M. *Angew. Chem., Int. Ed.* **2005**, *44*, 4670.
(273) Hufton, J. R.; Mayorga, S.; Sircar, S. *AIChE J.* **1999**, *45*, 248.
(274) Myers, A. L.; Prausnitz, J. M. *AIChE J.* **1965**, *11*, 121.
(275) Babarao, R.; Eddaoudi, M.; Jiang, J. W. *Langmuir* **2010**, *26*, 11196.
(276) Jiang, J. W. *AIChE J.* **2009**, *55*, 2422.
(277) Liu, Y. H.; Liu, D. H.; Yang, Q. Y.; Zhong, C. L.; Mi, J. G. *Ind. Eng. Chem. Res.* **2010**, *49*, 2902.
(278) Biswas, S.; Grzywa, M.; Nayek, H. P.; Dehnen, S.; Senkovska, I.; Kaskel, S.; Volkmer, D. *Dalton Trans.* **2009**, 6487.
(279) Chen, B. L.; Ma, S. Q.; Hurtado, E. J.; Lobkovsky, E. B.; Liang, C. D.; Zhu, H. G.; Dai, S. *Inorg. Chem.* **2007**, *46*, 8705.
(280) Maji, T. K.; Matsuda, R.; Kitagawa, S. *Nat. Mater.* **2007**, *6*, 142.
(281) Choi, H. J.; Dinca, M.; Long, J. R. *J. Am. Chem. Soc.* **2008**, *130*, 7848.
(282) Beenakker, J. J. M.; Borman, V. D.; Krylov, S. Y. *Chem. Phys. Lett.* **1995**, *232*, 379.
(283) Chen, B.; Zhao, X.; Putkham, A.; Hong, K.; Lobkovsky, E. B.; Hurtado, E. J.; Fletcher, A. J.; Thomas, K. M. *J. Am. Chem. Soc.* **2008**, *130*, 6411.
(284) Noguchi, D.; Tanaka, H.; Kondo, A.; Kajiro, H.; Noguchi, H.; Ohba, T.; Kanoh, H.; Kaneko, K. *J. Am. Chem. Soc.* **2008**, *130*, 6367.
(285) Eldridge, R. B. *Ind. Eng. Chem. Res.* **1993**, *32*, 2208.
(286) *Kirk-Othmer Encyclopedia of Chemical Technology*; John Wiley & Sons, Inc.: New York, 2008.
(287) Palomino, M.; Cantin, A.; Corma, A.; Leiva, S.; Rey, F.; Valencia, S. *Chem. Commun.* **2007**, 1233.
(288) Safarik, D. J.; Eldridge, R. B. *Ind. Eng. Chem. Res.* **1998**, *37*, 2571.
(289) Nicholson, T. M.; Bhatia, S. K. *J. Phys. Chem. B* **2006**, *110*, 24834.
(290) Gücüyener, C.; van den Bergh, J.; Gascon, J.; Kapteijn, F. *J. Am. Chem. Soc.* **2010**, *132*, 17704.
(291) Huang, X. C.; Zhang, J. P.; Chen, X. M. *Chin. Sci. Bull.* **2003**, *48*, 1531.
(292) Downie, N. A. *Industrial Gases*; Kluwer Academic Publishers: New York, 2002.
(293) Roberts, L. R. *Encyclopedia of Chemical Process and Design*; Marcel Dekker, Inc.: New York, 1976; Vol. 1.
(294) Bos, A. N. R.; Westerterp, K. R. *Chem. Eng. Process.: Process Intensification* **1993**, *32*, 1.
(295) Weissermel, K.; Arpe, H.-J. *Industrial Organic Chemistry*, 4th ed.; Wiley-VCH: New York, 2003.
(296) Xiang, S. C.; Zhang, Z.; Zhao, C.-G.; Hong, K.; Zhao, X.; Ding, D. R.; Xie, M. H.; Wu, C. D.; Das, M. C.; Gill, R.; Thomas, K. M.; Chen, B. *Nat. Commun.* **2011**, *2*, 204, doi: 10.1038/ncomms1206.
(297) Yoon, J. W.; Jang, I. T.; Lee, K. Y.; Hwang, Y. K.; Chang, J. S. *Bull. Korean Chem. Soc.* **2010**, *31*, 220.
(298) Jorge, M.; Lamia, N.; Rodrigues, A. E. *Colloids Surf., A* **2010**, *357*, 27.
(299) Lamia, N.; Jorge, M.; Granato, M. A.; Paz, F. A. A.; Chevreau, H.; Rodrigues, A. E. *Chem. Eng. Sci.* **2009**, *64*, 3246.
(300) Horcajada, P.; Surble, S.; Serre, C.; Hong, D.-Y.; Seo, Y.-K.; Chang, J.-S.; Greneche, J.-M.; Margiolaki, I.; Ferey, G. *Chem. Commun.* **2007**, 2820.
(301) Yoon, J. W.; Seo, Y. K.; Hwang, Y. K.; Chang, J. S.; Leclerc, H.; Wuttke, S.; Bazin, P.; Vimont, A.; Daturi, M.; Bloch, E.; Llewellyn, P. L.; Serre, C.; Horcajada, P.; Greneche, J. M.; Rodrigues, A. E.; Ferey, G. *Angew. Chem., Int. Ed.* **2010**, *49*, 5949.
(302) Hartmann, M.; Kunz, S.; Himsl, D.; Tangermann, O.; Ernst, S.; Wagener, A. *Langmuir* **2008**, *24*, 8634.
(303) Li, K. H.; Olson, D. H.; Seidel, J.; Emge, T. J.; Gong, H. W.; Zeng, H. P.; Li, J. *J. Am. Chem. Soc.* **2009**, *131*, 10368.
(304) Lee, C. Y.; Bae, Y.-S.; Jeong, N. C.; Farha, O. K.; Sarjeant, A. A.; Stern, C. L.; Nickias, P.; Snurr, R. Q.; Hupp, J. T.; Nguyen, S. T. *J. Am. Chem. Soc.* **2011**, *133*, 5228.
(305) Izumi, J. *Handbook of Zeolite Science and Technology*; CRC Press: New York, 2003.
(306) Britt, D.; Tranchemontagne, D.; Yaghi, O. M. *Proc. Natl. Acad. Sci. U.S.A.* **2008**, *105*, 11623.
(307) Eddaoudi, M.; Kim, J.; Rosi, N.; Vodak, D.; Wachter, J.; O'Keeffe, M.; Yaghi, O. M. *Science* **2002**, *295*, 469.
(308) Grant Glover, T.; Peterson, G. W.; Schindler, B. J.; Britt, D.; Yaghi, O. *Chem. Eng. Sci.* **2011**, *66*, 163.
(309) Mueller, U.; Schubert, M.; Teich, F.; Puetter, H.; Schierle-Arndt, K.; Pastre, J. *J. Mater. Chem.* **2006**, *16*, 626.
(310) Hamon, L.; Serre, C.; Devic, T.; Loiseau, T.; Millange, F.; Ferey, G.; De Weireld, G. *J. Am. Chem. Soc.* **2009**, *131*, 8775.
(311) Hamon, L.; Vimont, A.; Serre, C.; Devic, T.; Ghoufi, A.; Maurin, G.; Loiseau, T.; Millange, F.; Daturi, M.; Ferey, G.; De Weireld, G. *Characterization of Porous Solids VIII - Proceedings of the 8th International Symposium of the Characterization of Porous Solids - R. Soc. Chem.* **2009**, *318*, 25.
(312) Karra, J. R.; Walton, K. S. *Langmuir* **2008**, *24*, 8620.
(313) Keefer, L. K. *Nat. Mater.* **2003**, *2*, 357.
(314) Wheatley, P. S.; Butler, A. R.; Crane, M. S.; Fox, S.; Xiao, B.; Rossi, A. G.; Megson, I. L.; Morris, R. E. *J. Am. Chem. Soc.* **2005**, *128*, 502.
(315) Xiao, B.; Byrne, P. J.; Wheatley, P. S.; Wragg, D. S.; Zhao, X. B.; Fletcher, A. J.; Thomas, K. M.; Peters, L.; Evans, J. S. O.; Warren, J. E.; Zhou, W. Z.; Morris, R. E. *Nat. Chem.* **2009**, *1*, 289.
(316) Stang, P.; Diederich, F. *Modern Acetylene Chemistry*; VCH Publishers: New York, 1995.
(317) Chien, J. C. W. *Polyacetylene: Chemistry, Physics, and Material Science*; Academic Press: New York, 1984.
(318) O'Neil, M. J.; et al. *The Merck Index*, 14th ed.; Merck & Co., Inc.: Rahway, NJ, 2006.
(319) Matsuda, R.; Kitaura, R.; Kitagawa, S.; Kubota, Y.; Belosludov, R. V.; Kobayashi, T. C.; Sakamoto, H.; Chiba, T.; Takata, M.; Kawazoe, Y.; Mita, Y. *Nature* **2005**, *436*, 238.
(320) Kondo, M.; Okubo, T.; Asami, A.; Noro, S.; Yoshitomi, T.; Kitagawa, S.; Ishii, T.; Matsuzaka, H.; Seki, K. *Angew. Chem., Int. Ed.* **1999**, *38*, 140.
(321) Tanaka, D.; Higuchi, M.; Horike, S.; Matsuda, R.; Kinoshita, Y.; Yanai, N.; Kitagawa, S. *Chem.-Asian J.* **2008**, *3*, 1343.
(322) Samsonenko, D. G.; Kim, H.; Sun, Y. Y.; Kim, G. H.; Lee, H. S.; Kim, K. *Chem.-Asian J.* **2007**, *2*, 484.
(323) Chen, B. L.; Ockwig, N. W.; Millward, A. R.; Contreras, D. S.; Yaghi, O. M. *Angew. Chem., Int. Ed.* **2005**, *44*, 4745.
(324) Xiang, S. C.; Zhou, W.; Gallegos, J. M.; Liu, Y.; Chen, B. L. *J. Am. Chem. Soc.* **2009**, *131*, 12415.
(325) Hu, Y. X.; Xiang, S. C.; Zhang, W. W.; Zhang, Z. X.; Wang, L.; Bai, J. F.; Chen, B. L. *Chem. Commun.* **2009**, 7551.
(326) Krungleviciute, V.; Lask, K.; Migone, A. D.; Lee, J. Y.; Li, J. *AIChE J.* **2008**, *54*, 918.
(327) Kitaura, R.; Fujimoto, K.; Noro, S.; Kondo, M.; Kitagawa, S. *Angew. Chem., Int. Ed.* **2002**, *41*, 133.
(328) Uemura, K.; Kitagawa, S.; Kondo, M.; Fukui, K.; Kitaura, R.; Chang, H. C.; Mizutani, T. *Chem.-Eur. J.* **2002**, *8*, 3586.
(329) Choi, E. Y.; Park, K.; Yang, C. M.; Kim, H.; Son, J. H.; Lee, S. W.; Lee, Y. H.; Min, D.; Kwon, Y. U. *Chem.-Eur. J.* **2004**, *10*, 5535.
(330) Maji, T. K.; Uemura, K.; Chang, H. C.; Matsuda, R.; Kitagawa, S. *Angew. Chem., Int. Ed.* **2004**, *43*, 3269.
(331) Maji, T. K.; Ohba, M.; Kitagawa, S. *Inorg. Chem.* **2005**, *44*, 9225.
(332) Pan, L.; Parker, B.; Huang, X. Y.; Olson, D. H.; Lee, J.; Li, J. *J. Am. Chem. Soc.* **2006**, *128*, 4180.
(333) Ghosh, S. K.; Zhang, J. P.; Kitagawa, S. *Angew. Chem., Int. Ed.* **2007**, *46*, 7965.
(334) Ghosh, S. K.; Bureekaew, S.; Kitagawa, S. *Angew. Chem., Int. Ed.* **2008**, *47*, 3403.
(335) Hasegawa, S.; Horike, S.; Matsuda, R.; Furukawa, S.; Mochizuki, K.; Kinoshita, Y.; Kitagawa, S. *J. Am. Chem. Soc.* **2007**, *129*, 2607.

(336) Horike, S.; Tanaka, D.; Nakagawa, K.; Kitagawa, S. *Chem. Commun.* **2007**, 3395.
(337) Kaneko, W.; Ohba, M.; Kitagawa, S. *J. Am. Chem. Soc.* **2007**, *129*, 13706.
(338) Lee, J. Y.; Olson, D. H.; Pan, L.; Emge, T. J.; Li, J. *Adv. Funct. Mater.* **2007**, *17*, 1255.
(339) Shimomura, S.; Horike, S.; Matsuda, R.; Kitagawa, S. *J. Am. Chem. Soc.* **2007**, *129*, 10990.
(340) Couck, S.; Remy, T.; Baron, G. V.; Gascon, J.; Kapteijn, F.; Denayer, J. F. M. *Phys. Chem. Chem. Phys.* **2010**, *12*, 9413.
(341) Zhang, J. P.; Chen, X. M. *J. Am. Chem. Soc.* **2008**, *130*, 6010.
(342) Gurunatha, K. L.; Maji, T. K. *Eur. J. Inorg. Chem.* **2009**, 1592.
(343) Gurunatha, K. L.; Mohapatra, S.; Suchetan, P. A.; Maji, T. K. *Cryst. Growth Des.* **2009**, *9*, 3844.
(344) Huang, G.; Yang, C.; Xu, Z. T.; Wu, H. H.; Li, J.; Zeller, M.; Hunter, A. D.; Chui, S. S. Y.; Che, C. M. *Chem. Mater.* **2009**, *21*, 541.
(345) Liu, Q. K.; Ma, J. P.; Dong, Y. B. *Chem.-Eur. J.* **2009**, *15*, 10364.
(346) Mohapatra, S.; Hembram, K. P. S. S.; Waghmare, U.; Maji, T. K. *Chem. Mater.* **2009**, *21*, 5406.
(347) Uemura, K.; Maeda, A.; Maji, T. K.; Kanoo, P.; Kita, H. *Eur. J. Inorg. Chem.* **2009**, 2329.
(348) Bourrelly, S.; Moulin, B.; Rivera, A.; Maurin, G.; Devautour-Vino, S.; Serre, C.; Devic, T.; Horcajada, P.; Vimont, A.; Clet, G.; Daturi, M.; Lavalley, J. C.; Loera-Serna, S.; Denoyel, R.; Llewellyn, P. L.; Ferey, G. *J. Am. Chem. Soc.* **2010**, *132*, 9488.
(349) Lee, J. S.; Jhung, S. H. *Microporous Mesoporous Mater.* **2010**, *129*, 274.
(350) Hijikata, Y.; Horike, S.; Sugimoto, M.; Sato, H.; Matsuda, R.; Kitagawa, S. *Chem.-Eur. J.* **2011**, *17*, 5138.
(351) Kanoo, P.; Ghosh, A. C.; Maji, T. K. *Inorg. Chem.* **2011**, *50*, 5145.
(352) Sadakiyo, M.; Yamada, T.; Kitagawa, H. *J. Am. Chem. Soc.* **2011**, *133*, 11050.
(353) Minceva, M.; Rodrigues, A. E. *AIChE J.* **2007**, *53*, 138.
(354) Mowry, J. R. *Handbook of Petroleum Refining Processes*; McGraw-Hill: New York, 1986.
(355) Méthivier, A. In *Zeolites for Cleaner Technologies*; Guisnet, M., Gilson, J.-P., Eds.; Imperial College Press: London, 2002.
(356) Finsy, V.; Verelst, H.; Alaerts, L.; De Vos, D.; Jacobs, P. A.; Baron, G. V.; Denayer, J. F. M. *J. Am. Chem. Soc.* **2008**, *130*, 7110.
(357) Finsy, V.; Kirschhock, C. E. A.; Vedts, G.; Maes, M.; Alaerts, L.; De Vos, D. E.; Baron, G. V.; Denayer, J. F. M. *Chem.-Eur. J.* **2009**, *15*, 7724.
(358) Nicolau, M. P. M.; Barcia, P. S.; Gallegos, J. M.; Silva, J. A. C.; Rodrigues, A. E.; Chen, B. L. *J. Phys. Chem. C* **2009**, *113*, 13173.
(359) Edgar, M.; Mitchell, R.; Slawin, A. M. Z.; Lightfoot, P.; Wright, P. A. *Chem.-Eur. J.* **2001**, *7*, 5168.
(360) Gu, Z. Y.; Jiang, D. Q.; Wang, H. F.; Cui, X. Y.; Yan, X. P. *J. Phys. Chem. C* **2010**, *114*, 311.
(361) Gu, Z. Y.; Yan, X. P. *Angew. Chem., Int. Ed.* **2010**, *49*, 1477.
(362) Li, K. H.; Olsan, D. H.; Lee, J. Y.; Bi, W. H.; Wu, K.; Yuen, T.; Xu, Q.; Li, J. *Adv. Funct. Mater.* **2008**, *18*, 2205.
(363) Jin, Z.; Zhao, H.-Y.; Zhao, X.-J.; Fang, Q.-R.; Long, J. R.; Zhu, G.-S. *Chem. Commun.* **2010**, *46*, 8612.
(364) *Ullmann's Encyclopedia of Industrial Chemistry*, 6th ed.; electronic release, 2000.
(365) Sohn, S. W. In *Handbook of Petroleum Refining Processes*, 3rd ed.; Meyers, R. A., Ed.; McGraw-Hill: New York, 2004.
(366) Chen, B. L.; Liang, C. D.; Yang, J.; Contreras, D. S.; Clancy, Y. L.; Lobkovsky, E. B.; Yaghi, O. M.; Dai, S. *Angew. Chem., Int. Ed.* **2006**, *45*, 1390.
(367) Barcia, P. S.; Zapata, F.; Silva, J. A. C.; Rodrigues, A. E.; Chen, B. L. *J. Phys. Chem. B* **2007**, *111*, 6101.
(368) Ling, Y.; Chen, Z.-X.; Zhai, F.-P.; Zhou, Y.-M.; Weng, L.-H.; Zhao, D.-Y. *Chem. Commun.* **2011**, *47*, 7197.
(369) Trung, T. K.; Trens, P.; Tanchoux, N.; Bourrelly, S.; Llewellyn, P. L.; Loera-Serna, S.; Serre, C.; Loiseau, T.; Fajula, F.; Ferey, G. *J. Am. Chem. Soc.* **2008**, *130*, 16926.
(370) Finsy, V.; De Bruyne, S.; Alaerts, L.; De Vos, D.; Jacobs, A.; P.; Baron, G. V.; Denayer, J. F. M. In *Studies in Surface Science Catalysis*; Ruren Xu, Z. G. J. C., Wenfu, Y., Eds.; Elsevier: New York, 2007; Vol. 170.
(371) Jiang, J. W.; Sandler, S. I. *Langmuir* **2006**, *22*, 5702.
(372) Zhang, L.; Wang, Q.; Wu, T.; Liu, Y. C. *Chem.-Eur. J.* **2007**, *13*, 6387.
(373) Wang, X. Q.; Liu, L. M.; Jacobson, A. J. *Angew. Chem., Int. Ed.* **2006**, *45*, 6499.
(374) Barthelet, K.; Marrot, J.; Riou, D.; Férey, G. *Angew. Chem., Int. Ed.* **2002**, *41*, 281.
(375) Pan, L.; Olson, D. H.; Ciemnolonski, L. R.; Heddy, R.; Li, J. *Angew. Chem., Int. Ed.* **2006**, *45*, 616.
(376) Liu, D.; Lang, J.-P.; Abrahams, B. F. *J. Am. Chem. Soc.* **2011**, *133*, 11042.
(377) Jobic, H.; Rosenbach, N.; Ghoufi, A.; Kolokolov, D. I.; Yot, P. G.; Devic, T.; Serre, C.; Ferey, G.; Maurin, G. *Chem.-Eur. J.* **2010**, *16*, 10337.
(378) Wehring, M.; Gascon, J.; Dubbeldam, D.; Kapteijn, F.; Snurr, R. Q.; Stallmach, F. *J. Phys. Chem. C* **2010**, *114*, 10527.
(379) Lee, J.; Farha, O. K.; Roberts, J.; Scheidt, K. A.; Nguyen, S. T.; Hupp, J. T. *Chem. Soc. Rev.* **2009**, *38*, 1450.
(380) Yaghi, O. M.; Li, G. M.; Li, H. L. *Nature* **1995**, *378*, 703.
(381) Xu, G. H.; Zhang, X. G.; Guo, P.; Pan, C. L.; Zhang, H. J.; Wang, C. *J. Am. Chem. Soc.* **2010**, *132*, 3656.
(382) Yaghi, O. M.; Davis, C. E.; Li, G. M.; Li, H. L. *J. Am. Chem. Soc.* **1997**, *119*, 2861.
(383) Kosal, M. E.; Chou, J. H.; Wilson, S. R.; Suslick, K. S. *Nat. Mater.* **2002**, *1*, 118.
(384) Qiu, L. G.; Li, Z. Q.; Wu, Y.; Wang, W.; Xu, T.; Jiang, X. *Chem. Commun.* **2008**, 3642.
(385) Ahmad, R.; Wong-Foy, A. G.; Matzger, A. J. *Langmuir* **2009**, *25*, 11977.
(386) Alaerts, L.; Maes, M.; van der Veen, M. A.; Jacobs, P. A.; De Vos, D. E. *Phys. Chem. Chem. Phys.* **2009**, *11*, 2903.
(387) Maes, M.; Alaerts, L.; Vermoortele, F.; Ameloot, R.; Couck, S.; Finsy, V.; Denayer, J. F. M.; De Vos, D. E. *J. Am. Chem. Soc.* **2010**, *132*, 2284.
(388) Maes, M.; Vermoortele, F.; Alaerts, L.; Couck, S.; Kirschhock, C. E. A.; Denayer, J. F. M.; De Vos, D. E. *J. Am. Chem. Soc.* **2010**, *132*, 15277.
(389) Ameloot, R.; Liekens, A.; Alaerts, L.; Maes, M.; Galarneau, A.; Coq, B.; Desmet, G.; Sels, B. F.; Denayer, J. F. M.; De Vos, D. E. *Eur. J. Inorg. Chem.* **2010**, 3735.
(390) Maes, M.; Schouteden, S.; Hirai, K.; Furukawa, S.; Kitagawa, S.; De Vos, D. E. *Langmuir* **2011**, *27*, 9083.
(391) Choi, H. J.; Lee, T. S.; Suh, M. P. *J. Inclusion Phenom. Macrocyclic Chem.* **2001**, *41*, 155.
(392) Lee, E. Y.; Jang, S. Y.; Suh, M. P. *J. Am. Chem. Soc.* **2005**, *127*, 6374.
(393) Lu, J. Y.; Babb, A. M. *Chem. Commun.* **2002**, 1340.
(394) Kawano, M.; Kawamichi, T.; Haneda, T.; Kojima, T.; Fujita, M. *J. Am. Chem. Soc.* **2007**, *129*, 15418.
(395) Millange, F.; Serre, C.; Guillou, N.; Férey, G.; Walton, R. I. *Angew. Chem., Int. Ed.* **2008**, *47*, 4100.
(396) Millange, F.; Guillou, N.; Medina, M. E.; Ferey, G.; Carlin-Sinclair, A.; Golden, K. M.; Walton, R. I. *Chem. Mater.* **2010**, *22*, 4237.
(397) Devic, T.; Horcajada, P.; Serre, C.; Salles, F.; Maurin, G.; Moulin, B.; Heurtaux, D.; Clet, G.; Vimont, A.; Greneche, J. M.; Le Ouay, B.; Moreau, F.; Magnier, E.; Filinchuk, Y.; Marrot, J.; Lavalley, J. C.; Daturi, M.; Ferey, G. *J. Am. Chem. Soc.* **2010**, *132*, 1127.
(398) Platero-Prats, A. E.; de la Peña-O'Shea, V. A.; Snejko, N.; Monge, Á.; Gutiérrez-Puebla, E. *Chem.-Eur. J.* **2010**, *16*, 11632.
(399) Serre, C.; Surble, S.; Mellot-Draznieks, C.; Filinchuk, Y.; Ferey, G. *Dalton Trans.* **2008**, 5462.
(400) Chen, B. L.; Ji, Y. Y.; Xue, M.; Fronczek, F. R.; Hurtado, E. J.; Mondal, J. U.; Liang, C. D.; Dai, S. *Inorg. Chem.* **2008**, *47*, 5543.
(401) Alaerts, L.; Thibault-Starzyk, F.; Séguin, E.; Denayer, J. F. M.; Jacobs, P. A.; De Vos, D. E. In *Studies in Surface Science Catalysis*; Ruren Xu, Z. G. J. C., Wenfu, Y., Eds.; Elsevier: New York, 2007; Vol. 170.

(402) Chae, H. K.; Siberio-Perez, D. Y.; Kim, J.; Go, Y.; Eddaoudi, M.; Matzger, A. J.; O'Keeffe, M.; Yaghi, O. M. *Nature* **2004**, *427*, 523.
(403) Inokuma, Y.; Arai, T.; Fujita, M. *Nat. Chem.* **2010**, *2*, 780.
(404) Jiang, H. L.; Tatsu, Y.; Lu, Z. H.; Xu, Q. *J. Am. Chem. Soc.* **2010**, *132*, 5586.
(405) Han, S. B.; Wei, Y. H.; Valente, C.; Lagzi, I.; Gassensmith, J. J.; Coskun, A.; Stoddart, J. F.; Grzybowski, B. A. *J. Am. Chem. Soc.* **2010**, *132*, 16358.
(406) Yang, R. T.; Hernández-Maldonado, A. J.; Yang, F. H. *Science* **2003**, *301*, 79.
(407) Cychosz, K. A.; Wong-Foy, A. G.; Matzger, A. J. *J. Am. Chem. Soc.* **2009**, *131*, 14538.
(408) Wong-Foy, A. G.; Lebel, O.; Matzger, A. J. *J. Am. Chem. Soc.* **2007**, *129*, 15740.
(409) Achmann, S.; Hagen, G.; Hammerle, M.; Malkowsky, I.; Kiener, C.; Moos, R. *Chem. Eng. Technol.* **2010**, *33*, 275.
(410) Seki, K.; Mori, W. *J. Phys. Chem. B* **2002**, *106*, 1380.
(411) Khan, N. A.; Jun, J. W.; Jeong, J. H.; Jhung, S. H. *Chem. Commun.* **2011**, *47*, 1306.
(412) Maes, M.; Trekels, M.; Boulhout, M.; Schouteden, S.; Vermoortele, F.; Alaerts, L.; Heurtaux, D.; Seo, Y.-K.; Hwang, Y. K.; Chang, J.-S.; Beurroies, I.; Denoyel, R.; Temst, K.; Vantomme, A.; Horcajada, P.; Serre, C.; De Vos, D. E. *Angew. Chem., Int. Ed.* **2011**, *50*, 4210.
(413) Plabst, M.; McCusker, L. B.; Bein, T. *J. Am. Chem. Soc.* **2009**, *131*, 18112.
(414) Rosi, N. L.; Kim, J.; Eddaoudi, M.; Chen, B. L.; O'Keeffe, M.; Yaghi, O. M. *J. Am. Chem. Soc.* **2005**, *127*, 1504.
(415) Chen, B. L.; Wang, L. B.; Zapata, F.; Qian, G. D.; Lobkovsky, E. B. *J. Am. Chem. Soc.* **2008**, *130*, 6718.
(416) Wong, K. L.; Law, G. L.; Yang, Y. Y.; Wong, W. T. *Adv. Mater.* **2006**, *18*, 1051.
(417) Alaerts, L.; Kirschhock, C. E. A.; Maes, M.; van der Veen, M. A.; Finsy, V.; Depla, A.; Martens, J. A.; Baron, G. V.; Jacobs, P. A.; Denayer, J. E. M.; De Vos, D. E. *Angew. Chem., Int. Ed.* **2007**, *46*, 4293.
(418) Alaerts, L.; Maes, M.; Jacobs, P. A.; Denayer, J. F. M.; De Vos, D. E. *Phys. Chem. Chem. Phys.* **2008**, *10*, 2979.
(419) Alaerts, L.; Maes, M.; Giebeler, L.; Jacobs, P. A.; Martens, J. A.; Denayer, J. F. M.; Kirschhock, C. E. A.; De Vos, D. E. *J. Am. Chem. Soc.* **2008**, *130*, 14170.
(420) Castillo, J. M.; Vlugt, T. J. H.; Calero, S. *J. Phys. Chem. C* **2009**, *113*, 20869.
(421) Liu, Q. K.; Ma, J. P.; Dong, Y. B. *J. Am. Chem. Soc.* **2010**, *132*, 7005.
(422) Dubbeldam, D.; Galvin, C. J.; Walton, K. S.; Ellis, D. E.; Snurr, R. Q. *J. Am. Chem. Soc.* **2008**, *130*, 10884.
(423) Davankov, V. A. *Pure Appl. Chem.* **1997**, *69*, 1469.
(424) Subramanian, G. *Chiral Separation Techniques: A Practical Approach*, 3rd ed.; Wiley-VCH Verlag GmbH & Co. KGaA: New York, 2007.
(425) Stalcup, A. M. *Annu. Rev. Anal. Chem.* **2010**, *3*, 341.
(426) Morris, R. *Top. Catal.* **2010**, *53*, 1291.
(427) Yu, J.; Xu, R. *J. Mater. Chem.* **2008**, *18*, 4021.
(428) Yu, J.; Xu, R. *Acc. Chem. Res.* **2010**, *43*, 1195.
(429) Morris, R. E.; Bu, X. H. *Nat. Chem.* **2010**, *2*, 353.
(430) Evans, O. R.; Ngo, H. L.; Lin, W. B. *J. Am. Chem. Soc.* **2001**, *123*, 10395.
(431) Xiong, R. G.; You, X. Z.; Abrahams, B. F.; Xue, Z. L.; Che, C. M. *Angew. Chem., Int. Ed.* **2001**, *40*, 4422.
(432) Xie, Y. R.; Wang, X. S.; Zhao, H.; Zhang, J.; Weng, L. H.; Duan, C. Y.; Xiong, R. G.; You, X. Z.; Xue, Z. L. *Organometallics* **2003**, *22*, 4396.
(433) Song, Y. M.; Zhou, T.; Wang, X. S.; Li, X. N.; Xiong, R. G. *Cryst. Growth Des.* **2006**, *6*, 14.
(434) Bradshaw, D.; Prior, T. J.; Cussen, E. J.; Claridge, J. B.; Rosseinsky, M. J. *J. Am. Chem. Soc.* **2004**, *126*, 6106.
(435) Vaidhyanathan, R.; Bradshaw, D.; Rebilly, J. N.; Barrio, J. P.; Gould, J. A.; Berry, N. G.; Rosseinsky, M. J. *Angew. Chem., Int. Ed.* **2006**, *45*, 6495.
(436) Dybtsev, D. N.; Nuzhdin, A. L.; Chun, H.; Bryliakov, K. P.; Talsi, E. P.; Fedin, V. P.; Kim, K. *Angew. Chem., Int. Ed.* **2006**, *45*, 916.
(437) Nuzhdin, A. L.; Dybtsev, D. N.; Bryliakov, K. P.; Talsi, E. P.; Fedin, V. P. *J. Am. Chem. Soc.* **2007**, *129*, 12958.
(438) Bao, X. Y.; Broadbelt, L. J.; Snurr, R. Q. *Mol. Simul.* **2009**, *35*, 50.
(439) Wu, C.-D.; Lin, W. *Angew. Chem., Int. Ed.* **2007**, *46*, 1075.
(440) Das, M. C.; Bharadwaj, P. K. *J. Am. Chem. Soc.* **2009**, *131*, 10942.
(441) Gascon, J.; Kapteijn, F. *Angew. Chem., Int. Ed.* **2010**, *49*, 1530.
(442) denExter, M. J.; vanBekkum, H.; Rijn, C. J. M.; Kapteijn, F.; Moulijn, J. A.; Schellevis, H.; Beenakker, C. I. N. *Zeolites* **1997**, *19*, 13.
(443) Zacher, D.; Shekhah, O.; Woll, C.; Fischer, R. A. *Chem. Soc. Rev.* **2009**, *38*, 1418.
(444) Shekhah, O.; Liu, J.; Fischer, R. A.; Woll, C. *Chem. Soc. Rev.* **2011**, *40*, 1081.
(445) Keskin, S.; Liu, J. C.; Johnson, J. K.; Sholl, D. S. *Microporous Mesoporous Mater.* **2009**, *125*, 101.
(446) Keskin, S.; Sholl, D. S. *J. Phys. Chem. C* **2007**, *111*, 14055.
(447) Keskin, S.; Sholl, D. S. *Ind. Eng. Chem. Res.* **2009**, *48*, 914.
(448) Keskin, S. *J. Phys. Chem. C* **2010**, *114*, 13047.
(449) Xue, C. Y.; Zhou, Z.; Liu, B.; Yang, Q. Y.; Zhong, C. L. *Mol. Simul.* **2009**, *35*, 373.
(450) Haldoupis, E.; Nair, S.; Sholl, D. S. *J. Am. Chem. Soc.* **2010**, *132*, 7528.
(451) Guo, H. L.; Zhu, G. S.; Hewitt, I. J.; Qiu, S. L. *J. Am. Chem. Soc.* **2009**, *131*, 1646.
(452) Guerrero, V. V.; Yoo, Y.; McCarthy, M. C.; Jeong, H. K. *J. Mater. Chem.* **2010**, *20*, 3938.
(453) Liu, Y. Y.; Ng, Z. F.; Khan, E. A.; Jeong, H. K.; Ching, C. B.; Lai, Z. P. *Microporous Mesoporous Mater.* **2009**, *118*, 296.
(454) Ranjan, R.; Tsapatsis, M. *Chem. Mater.* **2009**, *21*, 4920.
(455) Li, Y. S.; Liang, F. Y.; Bux, H.; Feldhoff, A.; Yang, W. S.; Caro, J. *Angew. Chem., Int. Ed.* **2010**, *49*, 548.
(456) Li, Y. S.; Liang, F. Y.; Bux, H. G.; Yang, W. S.; Caro, J. *J. Membr. Sci.* **2010**, *354*, 48.
(457) Bux, H.; Liang, F. Y.; Li, Y. S.; Cravillon, J.; Wiebcke, M.; Caro, J. *J. Am. Chem. Soc.* **2009**, *131*, 16000.
(458) McCarthy, M. C.; Varela-Guerrero, V.; Barnett, G. V.; Jeong, H. K. *Langmuir* **2010**, *26*, 14636.
(459) Huang, A. S.; Bux, H.; Steinbach, F.; Caro, J. *Angew. Chem., Int. Ed.* **2010**, *49*, 4958.
(460) Huang, A. S.; Dou, W.; Caro, J. *J. Am. Chem. Soc.* **2010**, *132*, 15562.
(461) Huang, A.; Caro, J. *Angew. Chem., Int. Ed.* **2011**, *50*, 4979.
(462) Algieri, C.; Bernardo, P.; Golemme, G.; Barbieri, G.; Drioli, E. *J. Membr. Sci.* **2003**, *222*, 181.
(463) Huang, A. S.; Liang, F. Y.; Steinbach, F.; Gesing, T. M.; Caro, J. *J. Am. Chem. Soc.* **2010**, *132*, 2140.
(464) Geus, E. R.; Denexter, M. J.; Vanbekkum, H. *J. Chem. Soc., Faraday Trans.* **1992**, *88*, 3101.
(465) Yoo, Y.; Lai, Z. P.; Jeong, H. K. *Microporous Mesoporous Mater.* **2009**, *123*, 100.
(466) Huang, X. C.; Lin, Y. Y.; Zhang, J. P.; Chen, X. M. *Angew. Chem., Int. Ed.* **2006**, *45*, 1557.
(467) Fairen-Jimenez, D.; Moggach, S. A.; Wharmby, M. T.; Wright, P. A.; Parsons, S.; Düren, T. *J. Am. Chem. Soc.* **2011**, *133*, 8900.
(468) Fernandez, M.; Karger, J.; Freude, D.; Pampel, A.; van Baten, J. M.; Krishna, R. *Microporous Mesoporous Mater.* **2007**, *105*, 124.
(469) Li, Y. S.; Bux, H.; Feldhoff, A.; Li, G. L.; Yang, W. S.; Caro, J. *Adv. Mater.* **2010**, *22*, 3322.
(470) Newsome, D. A.; Sholl, D. S. *J. Phys. Chem. B* **2005**, *109*, 7237.
(471) Morris, W.; Doonan, C. J.; Furukawa, H.; Banerjee, R.; Yaghi, O. M. *J. Am. Chem. Soc.* **2008**, *130*, 12626.
(472) Takamizawa, S.; Takasaki, Y.; Miyake, R. *J. Am. Chem. Soc.* **2010**, *132*, 2862.
(473) Takamizawa, S.; Nakata, E.; Yokoyama, H. *Inorg. Chem. Commun.* **2003**, *6*, 763.

(474) Plasynski, S. I.; Litynski, J. T.; McIlvried, H. G.; Srivastava, R. D. *Crit. Rev. Plant Sci.* **2009**, *28*, 123.
(475) Aguado, S.; Nicolas, C.-H.; Moizan-Basle, V.; Nieto, C.; Amrouche, H.; Bats, N.; Audebrand, N.; Farrusseng, D. *New J. Chem.* **2011**, *35*, 41.
(476) Venna, S. R.; Carreon, M. A. *J. Am. Chem. Soc.* **2010**, *132*, 76.
(477) Demessence, A.; Boissiere, C.; Grosso, D.; Horcajada, P.; Serre, C.; Ferey, G.; Soler-Illia, G.; Sanchez, C. *J. Mater. Chem.* **2010**, *20*, 7676.
(478) Maier, G. *Angew. Chem., Int. Ed.* **1998**, *37*, 2961.
(479) *Polymer Membranes for Gas and Vapor Separation*; American Chemical Society: Washington, DC, 1999.
(480) Trzpit, M.; Soulard, M.; Patarin, J.; Desbiens, N.; Cailliez, F.; Boutin, A.; Demachy, I.; Fuchs, A. H. *Langmuir* **2007**, *23*, 10131.
(481) Husain, S.; Koros, W. J. *J. Membr. Sci.* **2007**, *288*, 195.
(482) Yehia, H.; Pisklak, T. J.; Ferraris, J. P.; B., K. J., Jr.; Musselman, I. H. *Polym. Prepr.* **2004**, *45*, 35.
(483) Won, J. G.; Seo, J. S.; Kim, J. H.; Kim, H. S.; Kang, Y. S.; Kim, S. J.; Kim, Y. M.; Jegal, J. G. *Adv. Mater.* **2005**, *17*, 80.
(484) Car, A.; Stropnik, C.; Peinemann, K.-V. *Desalination* **2006**, *200*, 424.
(485) Basu, S.; Cano-Odena, A.; Vankelecom, I. F. J. *J. Membr. Sci.* **2010**, *362*, 478.
(486) Perez, E. V.; Balkus, K. J.; Ferraris, J. P.; Musselman, I. H. *J. Membr. Sci.* **2009**, *328*, 165.
(487) Ordoñez, M. J. C.; Balkus, K. J.; Ferraris, J. P.; Musselman, I. H. *J. Membr. Sci.* **2010**, *361*, 28.
(488) Bae, T. H.; Lee, J. S.; Qiu, W. L.; Koros, W. J.; Jones, C. W.; Nair, S. *Angew. Chem., Int. Ed.* **2010**, *49*, 9863.
(489) Zhang, Y. F.; Musseman, I. H.; Ferraris, J. P.; Balkus, K. J. *J. Membr. Sci.* **2008**, *313*, 170.
(490) Adams, R.; Carson, C.; Ward, J.; Tannenbaum, R.; Koros, W. *Microporous Mesoporous Mater.* **2010**, *131*, 13.
(491) Noro, S.; Kitagawa, S.; Kondo, M.; Seki, K. *Angew. Chem., Int. Ed.* **2000**, *39*, 2082.
(492) Keskin, S.; Sholl, D. S. *Energy Environ. Sci.* **2010**, *3*, 343.
(493) Sheffel, J. A.; Tsapatsis, M. *J. Membr. Sci.* **2009**, *326*, 595.
(494) Takamizawa, S.; Kachi-Terajima, C.; Kohbara, M. A.; Akatsuka, T.; Jin, T. *Chem.-Asian J.* **2007**, *2*, 837.
(495) Basu, S.; Maes, M.; Cano-Odena, A.; Alaerts, L.; De Vos, D. E.; Vankelecom, I. F. J. *J. Membr. Sci.* **2009**, *344*, 190.
(496) Eddaoudi, M.; Moler, D. B.; Li, H. L.; Chen, B. L.; Reineke, T. M.; O'Keeffe, M.; Yaghi, O. M. *Acc. Chem. Res.* **2001**, *34*, 319.
(497) Shirley, A. I.; Lemcoff, N. O. *Adsorption* **2002**, *8*, 147.
(498) An, J.; Rosi, N. L. *J. Am. Chem. Soc.* **2010**, *132*, 5578.
(499) Zheng, B.; Bai, J.; Duan, J.; Wojtas, L.; Zaworotko, M. J. *J. Am. Chem. Soc.* **2010**, *133*, 748.
(500) Banerjee, M.; Das, S.; Yoon, M.; Choi, H. J.; Hyun, M. H.; Park, S. M.; Seo, G.; Kim, K. *J. Am. Chem. Soc.* **2009**, *131*, 7524.
(501) Lee, Y.; Hriljac, J. A.; Vogt, T.; Parise, J. B.; Edmondson, M. J.; Anderson, P. A.; Corbin, D. R.; Nagai, T. *J. Am. Chem. Soc.* **2001**, *123*, 8418.
(502) Ferey, G.; Serre, C. *Chem. Soc. Rev.* **2009**, *38*, 1380.
(503) Yuan, D. Q.; Zhao, D.; Sun, D. F.; Zhou, H. C. *Angew. Chem., Int. Ed.* **2010**, *49*, 5357.
(504) Wang, X. S.; Ma, S. Q.; Sun, D. F.; Parkin, S.; Zhou, H. C. *J. Am. Chem. Soc.* **2006**, *128*, 16474.
(505) Liu, X. F.; Park, M.; Hong, S.; Oh, M.; Yoon, J. W.; Chang, J. S.; Lah, M. S. *Inorg. Chem.* **2009**, *48*, 11507.
(506) Zhao, D.; Yuan, D.; Sun, D.; Zhou, H.-C. *J. Am. Chem. Soc.* **2009**, *131*, 9186.
(507) Banerjee, D.; Kim, S. J.; Parise, J. B. *Cryst. Growth Des.* **2009**, *9*, 2500.
(508) Ye, Q.; Wang, X. S.; Zhao, H.; Xiong, R. G. *Chem. Soc. Rev.* **2005**, *34*, 208.
(509) Hong, D. Y.; Hwang, Y. K.; Serre, C.; Ferey, G.; Chang, J. S. *Adv. Funct. Mater.* **2009**, *19*, 1537.
(510) Cavka, J. H.; Jakobsen, S.; Olsbye, U.; Guillou, N.; Lamberti, C.; Bordiga, S.; Lillerud, K. P. *J. Am. Chem. Soc.* **2008**, *130*, 13850.
(511) Choi, H. J.; Dinca, M.; Dailly, A.; Long, J. R. *Energy Environ. Sci.* **2010**, *3*, 117.
(512) Cychosz, K. A.; Matzger, A. J. *Langmuir* **2010**, *26*, 17198.
(513) Mueller, U.; Hesse, M.; Puetter, H.; Schubert, M.; Mirsch, D. Patent EP, 1674555, 2005.
(514) Mueller, U.; Hesse, M.; Puetter, H.; Kamieth, M.; Schierle-Arndt, K. Patent WO 2006072573 A2, 2006.
(515) Simmons, J. M.; Wu, H.; Zhou, W.; Yildirim, T. *Energy Environ. Sci.* **2011**, *4*, 2177.
(516) Wang, X.-S.; Ma, S.; Rauch, K.; Simmons, J. M.; Yuan, D.; Wang, X.; Yildirim, T.; Cole, W. C.; López, J. J.; Meijere, A. d.; Zhou, H. C. *Chem. Mater.* **2008**, *20*, 3145.
(517) Sun, D. F.; Ma, S. Q.; Simmons, J. M.; Li, J. R.; Yuan, D. Q.; Zhou, H. C. *Chem. Commun.* **2010**, *46*, 1329.
(518) http://www.basf.com/group/pressrelease/P-10-428, 2010.
(519) Ahnfeldt, T.; Gunzelmann, D.; Loiseau, T.; Hirsemann, D.; Senker, J. R.; Férey, G.; Stock, N. *Inorg. Chem.* **2009**, *48*, 3057.
(520) Volkringer, C.; Popov, D.; Loiseau, T.; Férey, G. R.; Burghammer, M.; Riekel, C.; Haouas, M.; Taulelle, F. *Chem. Mater.* **2009**, *21*, 5695.
(521) Ferey, G.; Serre, C.; Mellot-Draznieks, C.; Millange, F.; Surble, S.; Dutour, J.; Margiolaki, I. *Angew. Chem., Int. Ed.* **2004**, *43*, 6296.
(522) Dietzel, P. D. C.; Morita, Y.; Blom, R.; Fjellvag, H. *Angew. Chem., Int. Ed.* **2005**, *44*, 6354.
(523) Dietzel, P. D. C.; Panella, B.; Hirscher, M.; Blom, R.; Fjellvag, H. *Chem. Commun.* **2006**, 959.
(524) Caskey, S. R.; Wong-Foy, A. G.; Matzger, A. J. *J. Am. Chem. Soc.* **2008**, *130*, 10870.